DOE/NV/10461--T43

EVALUATION OF THE GEOLOGIC RELATIONS AND SEISMOTECTONIC STABILITY OF THE YUCCA MOUNTAIN AREA NEVADA NUCLEAR WASTE SITE INVESTIGATION (NNWSI)

PROGRESS REPORT

30 SEPTEMBER 1993

CENTER FOR NEOTECTONIC STUDIES

MACKAY SCHOOL OF MINES

UNIVERSITY OF NEVADA, RENO

Table of Contents

Annual Progress Report----General Task
Prepared by Steven G. Wesnousky

October 1, 1992 to September 30, 1993

Introduction

This report provides a summary of progress for the project "Evaluation of the Geologic Relations and Seismotectonic Stability of the Yucca Mountain Area, Nevada Nuclear Waste Site Investigation (NNWSI)." A similar report was previously provided for the period of 1 October 1991 to 30 September 1992. The report initially covers the activities of the General Task and is followed by sections that describe the progress of the other ongoing Tasks which are listed below.

Task 1:	Quaternary Tectonics
Task 3.	Mineral Deposits, Volcanic Geology
Task 4:	Seismology
Task 5:	Tectonics
Task 8:	Basinal Studies

General Task

Staff

Steven G. Wesnousky, Project Director; Craig H. Jones, Research Associate; Gloria Sutherland, Secretary (until August 1993); Nina Petrenko, Secretary (from September 1993)

Administrative Activities

The General Task continued the (1) coordination and oversight of the research of Tasks 1, 3, 5, and 8, the (2) oversight of budgets and (3) the collation and preparation of required monthly reports. As well, Dr. Wesnousky has continued to represent NWPO at meetings with the National Academy of Sciences, the Nuclear Regulatory Commission, and the Department of Energy.

Steven G. Wesnousky attended the following meetings for NWPO:

Feb. 9, 1993, Office of Nuclear Projects, Mineral County, Affected Counties meeting, Hawthorne, NV 99415 (presentation given).

May 25 and 26, 1993, DOE/NRC site visit to Yucca Mountain to review neotectonic studies.

June 8, 1993, DOE-NRC Technical Exchange on Integration of Geophysics at Las Vegas.

Technical Activities

Technical activities have been divided between research activities and review of technical reports.

Technical Reports Reviewed:

Jan. 25, 1993, provide review of Yucca Mountain Study Plan 8.3.1.17.4.5 regarding study of Detachment faults.
Sept. 29, 1993, DOE topical report outline 'Methodology for seismic Hazards Assessment at Yucca Mountain.'

Research Activities:

Projects Completed:

Seismometers were deployed in the high Sierra Nevada of southern California in 1988. Teleseisms and regional earthquake arrival times recorded by this network were used to examine the crustal and upper mantle structure beneath the southern Sierra. The results are proving quite controversial: While extension in the upper crust has accommodated over 250 km of motion in the Basin and Range, it appears from this work (when placed in context for the entire region) that the downward continuation of that deformation actually lies under the Sierra Nevada to the west. This deformation is inferred to have warmed and thinned the anti-buoyant mantle lithosphere, thus causing the Sierra Nevada to rise. Such a model has important implications in the Yucca Mountain area, because Death Valley's deformation lies only a few miles to the southwest. Understanding the lithosphere-scale tectonics of the region should improve the framework for systematically examining the Yucca Mountain site. Such work compliments the earlier study of Dr. Zhang, who described, without providing a tectonic explanation, the evolution of faulting in the Death Valley area through time. The work has been accepted for publication in the Journal of Geophysical Research and is currently in press.

Jones, C. H., H. Kanamori, and S. W. Roecker, Missing Roots and Mantle "Drips:" Regional P_n and Teleseismic Arrival Times in the Southern Sierra Nevada and Vicinity, California, *J. Geophys. Res., in press.*

Dr. Jones combined with other scientists representing other subdisciplines to write a single paper that attempts to integrate geological, geochemical, and geophysical observation. Dr. Jones has been responsible for the geophysical study and the overall compilation and preparation of the manuscript. Although the paper contains considerable review, new work in the geophysical section explores the variation in the style of deformation through the Basin and Range by taking seismic velocity profiles of the crust that have been obtained in the past few years and converting them into density structures. Armed with the density of the crust, one can infer how much of the variation in elevation seen through the Basin and Range is due to variations in density in the crust; what remains is probably due to variations in the mantle. Results of this study that bear on Yucca Mountain directly are that to the north, extensional deformation in the mantle probably lies under the central part of the Basin and Range, while to the south, deformation in the upper mantle lies under the western flank of the Basin and Range. This implies that a major lithospheric boundary lies near the Yucca Mountain area; this boundary might be responsible for the diffuse band of seismicity that crosses the Basin and Range at this latitude. These results will be important when interpreting results from a 3-d velocity structure study discussed below. Some additional work might be started in the coming year to expand this analysis to the entire western U.S. and quantify the uncertainties in the techniques used will be quite useful in evaluating the inferences from this study. The work was published in

Jones, C. H., Wernicke, B.P.; Farmer, G.L.; Walker, J.D.; Coleman, D.S., McKenna. L.W., and F.V. Perry, Variations across and along a major continental rift: and interdisciplinary study of the Basin and Range Province, western USA, *Tectonophysics*, 213, 57-96, 1992.

Ongoing Projects:

Paleomagnetic samples have been gathered in Miocene sediments near Lake Mead in order to understand the mechanics that accompany the creation of "oroflexes," which are great bends in the earth's crust adjacent to large strike-slip faults. These bends are best understood through paleomagnetic work, which can constrain the exact amount of bending. Earlier work by Nelson and Jones documented the presence of an oroflex in the Las Vegas Range northwest of Las Vegas; that study lacked the spatial resolution to understand the mechanical underpinnings of the deformation and also could not constrain the age of deformation. The present study should solve both problems, for the young sediments in the Lake Mead area are well exposed and have not been as deformed as the sedimentary rocks in the Las Vegas Range. Although the study is still proceeding, data to date do clearly show that the oroflex does extend to the southeast and formed within the past 15-20 m.y.. This same structure or one analogous to it might extend into Yucca Mountain, where similar paleomagnetic rotations have been observed by USGS scientists over the past few years. Completion of this work should provide insight into structures that might be present in Yucca Mountain itself, including, possibly, the presence of large, subhorizontal decollements. Data collected in the past year have led to the presentation of this work at professional meetings (see below).

Dr. Jones is collaborating with Dr. Steven Roecker (Rensselaer Polytechnic Institute) and Dr. Joan Gomberg (USGS Golden) on the seismic velocity structure of southern Nevada. The dataset is being used to determine a 3-dimensional velocity structure for southern Nevada. In addition, the Little Skull Mountain earthquake sequence from the summer of 1992 should provide additional constraints on the velocity structure in the immediate vicinity of Yucca Mountain. The determination of the lateral variations in seismic velocity will both improve the locations of earthquakes in the area and provide insight into lateral changes in earth structure reflecting subsurface geology.

Dr. Wesnousky and Dr. Jones have been investigating the physical parameters that control the partitioning of slip between a vertical fault. The work has resulted in development of a simple physical framework to examine the implications of such partitioned fault systems to (1) the relative strength of faults, (2) variations in regional stress fields both in space and time, (3) potential pitfalls in interpreting the stress field from focal mechanism data, (4) the mechanics of low-angle faulting, and (5) variations in slip rate along fault strike. A manuscript was published in*Science* during 1992. We are currently focusing our attention on the Basin and Range.Within the Basin and Range, several faults exhibit similar behavior: one large, vertical fault will tend to be strike-slip, while an adjacent fault might have oblique-slip on its dipping surface. Such fault systems include the Death Valley and Owens Valley fault systems. The latter fault system has been inferred to have slipped in different ways at different times in the past because of changes in the stress field in the Owens Valley area. We have found by extending our analysis to this area that this conclusion is unwarranted; this style of faulting is compatible with a single stress system. Implications from this work include

evaluating the likely amount of variation in the stress field both in space and time; as such, it will have implications for evaluating the potential for changes in the stress regime and changes in the activity of faulting in the Yucca Mountain area. Our preliminary results have been presented at both the Fall 1992 American Geophysical Union meeting in San Francisco and the 1993 Cordilleran Section Meeting of the Geological Society of America meeting in Reno (see below).

Principally funded by other sources but of important consequence to understanding the tectonic framework and style of earthquake faulting in the Basin and Range, Steven G. Wesnousky and Ph.D. student John Caskey have been reinvestigating both the slip distribution and the distributed pattern of faulting associated with the M7 Dixie Valley and Fairview Peak earthquakes within the Nevada Seismic Belt. Mapping has been assisted by 1:12000 low-sun angle photographs taken during the 1960's. As well, trenches have been excavated across the Fairview Peak fault trace and are currently under study to place constraints on the recurrence behavior of the fault zone. The implications of the observations resulting from this effort will necessarily be taken into account in the development of seismic hazard models and determinations in the Yucca Mountain region. Initial results of mapping were presented at the 1993 Cordilleran Section Meeting of the Geological Society of America meeting in Reno (see below).

Meetings and Abstracts:

1992 Annual Meeting of the American Geophysical Union

Wesnousky, S.G., and C.H. Jones, Implications Regarding the Temporal and Spatial Variation of Stress in the Southwestern Basin and Range from Observations of Slip Partitioning, *DOS supplement, Program and Abstracts,* Dec 7-11, 1992, p. 560.

Yu, Guang, S.G. Wesnousky, and G. Ekstrom, Slip Partitioning along Major Plate Boundaries, *DOS supplement, Program and Abstracts,* Dec 7-11, 1992, p. 570.

1993 Cordilleran Section of the Geological Society of America

Michetti, A., and S.G. Wesnousky, Holocene Surface Faulting Along the West flank of the Santa Rosa Range (Nevada-Oregon) and the Possible Northern Extension of the Central Nervada Seismic Belt,*Geol. Soc. Am. Abstr. Progs., 25* (5), 1993

Caskey, J., S. Wesnousky, P. Zhang, and D.B. Slemmons, Reinvestigation of Fault Trace Complexity and Slip Distribution for the 16 December 1954 Fairview Peak (Ms=7.2) and Dixie Valley (Ms=6.8) Earthquakes, Central Nevada, *Geol. Soc. Am. Abstr. Progs., 25* (5), 1993.

Hirabayashi, C.K., Rockwell, T.K., and S.G. Wesnousky, Late Quaternary Activity of the San Miguel Fault, Northern Baja California, Mexico, *Geol. Soc. Am. Abstr. Progs., 25* (5), 1993.

Jones, C.H. and S. Wesnousky, Implications Regarding the Temporal and Spatial Variation of Stress in the Southwestern Basin and Range from Observations of Slip Partitioning , *Geol. Soc. Am. Abstr. Progs., 25* (5), 1993.

Jones, C. H., and S. G. Wesnousky, Implications regarding the temporal and spatial variation of stress in the southwestern Basin and Range from observations of slip partitioning,*Geol. Soc. Am. Abstr. Progs., 25* (5), 1993.

Jones, C. H., Isostasy and its implications for the structure of the Sierra Nevada,*Geol. Soc. Am. Abstr. Progs., 25* (5), 1993.

Jones, C. H., P. H. Molnar, S. W. Roecker, R. B. Smith, and D. Hatzfeld, Possible expression of low-angle normal faulting in the seismicity of the Hansel Valley–Pocatello Valley region, Utah and Idaho,*Geol. Soc. Am. Abstr. Progs., 25* (5), 1993.

Sheehan, A. F., G. A. Abers, A. L. Lerner-Lam, and C. H. Jones, Crustal thickness variations across the Rocky Mountain Front from teleseismic reciever functions, *Geol. Soc. Am. Abstr. Progs., 25* (5), 1993.

PROGRESS REPORT

Task 1 Quaternary Tectonics

1 October 1992 to September 1993

John W. Bell
Principal Investigator

Craig M. dePolo
Co- Investigator

SUMMARY OF ACTIVITIES CONDUCTED DURING THE CONTRACT PERIOD

During the contract period, the following activities were conducted by Task 1:

* J.W. Bell planned and scheduled the low-sun-angle photography of the Little Skull Mountain area. Photographs were taken in the later part of 1992 and early 1993. This photography covers the area of the 1992 Little Skull earthquake and recent seismic activity along the southwestern part of the Rock Valley fault zone. A student from the Center for Neotectonic Studies will be analyzing these photographs and mapping faults from them in the upcoming year.

* J.W. Bell and R.I. Dorn collected and dated rock varnish samples from the 1932 Cedar Mountain earthquake area for ^{14}C AMS and cation-ratio analysis. Dr. Dorn's report briefly discusses the results and some field complications with the samples. These samples further constrain the allostratigraphy in this area, which has correlations to the Yucca Mountain region. These studies complete the rock varnish research being conducted in the Cedar Mountain area. Dr. Dorn's report is included in Appendix A.

* C.M. dePolo, J.W. Bell, and S. Foreman collected samples for thermoluminescence dating from the 1932 Cedar Mountain earthquake area. These samples suggest ages for the penultimate and triultimate events along the Monte Cristo Valley fault zone. The samples that yielded the best age estimates came from Trench 6 in Monte Cristo Valley (see figure below). This trench lies along one of the main traces of the 1932 surface rupturing, in an area where the vertical displacement is up to 50 cm and a nearby stream is ponded by bedrock after surface rupture events similar in size to those of 1932. Sample F93-NV1 is of the upper 1 cm of a buried Av deposit/horizon (see figure). Although this horizon has at least two potential interpretations (an Av soil horizon or silt deposited because of tectonic ponding of the stream), in both cases it immediately underlies a colluvial deposit thought to be related to the scarp from the penultimate event; thus the age of this Av deposit should be close to this event. Foreman states about this sample,

> The fine-silt fraction yielded TL age estimates by the total and partial bleach methods, respectively of 12.6 ± 1.1 and 10.6 ± 1.0 ka. The concordancy of the total and partial bleach analyses indicates that this sediment was well light exposed prior to deposition and the resultant ages are probably finite estimates. The best estimate for tectonic burial of this horizon is 11 ± 2 ka.

Sample F93-NV6 is from the distal part of a colluvial wedge formed from the triultimate event (see figure). Foreman states about this sample,

> The fine-silt fraction yielded the total bleach age of 25.1 ± 4.0 ka. This may be a maximum estimate for the time of faulting.

At this time, final potassium content estimates of the samples have yet to be considered in the estimates, thus they are still preliminary. Nevertheless, we can make some preliminary

inferences from these data.

The preliminary preferred estimates suggest an earthquake about 11 kyr prior to 1932, and one 14 kyr prior to that. Mixing the maximum and minimum age estimates from the penultimate and the triultimate event yields the shortest interseismic interval of 8 kyr and the longest of 20 yr. Considering natural variability, these the ages of these three events suggest a fairly regular frequency of earthquake occurrence. Steve Foreman's results are in Appendix B.

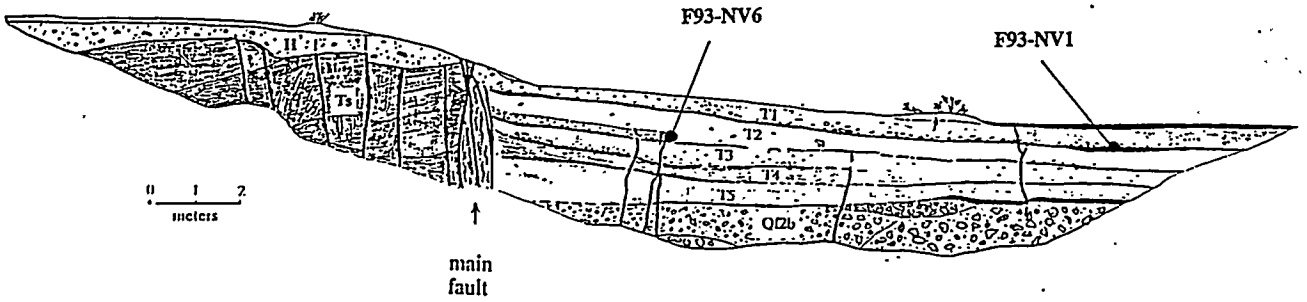

Trench log of the south wall of Trench 6 in Monte Cristo Valley. Units T1 through T5, generally sandy silts, are tectonically ponded behind coseismic scarps at the main fault. H = Holocene colluvium, Ts = Tertiary sediments, and Qf2b = late Pleistocene gravels. The thin black units on the right side of the trench log are ponded due to faulting of adjacent stream. Thermoluminescent dating locations are shown.

* J.W. Bell completed mapping of the northern part of Crater Flat for the surficial geologic map "Geologic Map of Portions of the Bare Mountain SE and Bare Mountain NE Quadrangles." This map has been reviewed and is being revised for publication by the Nevada Bureau of Mines and Geology.

* J.W. Bell and C.M. dePolo co-led a field trip examining the Walker Lane belt, that focused for over a third of its extent on the 1932 Cedar Mountain earthquake. C.M. dePolo gave a one hour lecture on the earthquake, and the next day was spent traveling north to south along in the earthquake area, including a 3 km hike along the ruptures. This gave representatives from the USGS, the DOE, the NRC, the U.S. Bureau of Reclamation, Los Alamos National Laboratories, and several consulting companies related to the Yucca Mountain project, such as Geomatrix and Woodward-Clyde Consultants, a chance to view the work going on in the Cedar Mountain area first hand.

* C.M. dePolo and J.W. Bell convened a symposium with A.R. Ramelli and M. Machette on "Latest Pleistocene and Holocene faulting in the Basin and Range province" at the joint meeting of the Rocky Mountain and Cordilleran sections of the Geological Society of America (GSA), held in Reno, Nevada. This symposium brought together several experts on the neotectonics of the Basin and Range province, and using a regional framework, focused on contemporary analyses of faults, segmentation, fault slip rates, and the timing of earthquake events along individual faults. A listing of the symposium title and authors is given in Appendix C.

* J.W. Bell gave a paper at the GSA meeting in Reno titled, "Behavior of late Quaternary and historical faults in the western Basin and Range province." Data presented deemphasized the importance of the Central Nevada seismic belt as a long term feature, and supports clustered earthquake behavior along faults. Consequently, low rates of historical seismicity at the Yucca Mountain site are not indicators of low seismotectonic activity, rather they fit the behavior of faults and regions alternating between periods of activity and nonactivity. Bell's abstract is presented in Appendix D.

* C.M. dePolo presented a paper at the GSA meeting in Reno titled, "Analysis of the seismic hazard of faults in Nevada." A preliminary study was presented in which major faults throughout Nevada were analyzed for their seismic potential. The abstract is presented in Appendix D.

* J.W. Bell and C.M. dePolo attended a field review of the DOE tectonics program at Yucca Mountain visiting trenches along the Paintbrush Canyon, the Solitario, and the Stagecoach Road faults, and viewed the fractured rock in the portal for the exploratory shaft.

* J.W. Bell and C.M. dePolo reviewed the DOE study plan 8.3.1.17.4.3 "Quaternary faulting within 100 km of Yucca Mountain, including the Walker Lane."

* C.M. dePolo's note on the "The maximum background earthquake for the Basin and Range province, western North America" has been accepted with minor revisions by the Bulletin of the Seismological Society of America. This paper implies (although it is not stated within the text) that in the study of Yucca Mountain, probabilistic analyses using background earthquake data should represent earthquakes at least as large as magnitude 6.5 and that in a deterministic analysis, a fault with surface rupture should be assigned a minimum magnitude of 6.5 or 6.6, irrespective of smaller magnitudes estimated from surface parameters.

* The first of a series of papers on the 1932 Cedar Mountain earthquake was completed and submitted to "Geology." The paper is titled "Distributed surface faulting from the 1932 Cedar Mountain earthquake, west-central Nevada: seismic hazard implications for the Basin and Range province" and emphasizes the need for considering distributed earthquakes in seismotectonic analyses in the Basin and Range province. Although this notion should not be particularly a new one at this point in time, this paper makes the case using the 1932 Cedar Mountain earthquake, and reminding people of other distributed earthquakes from this province.

The implications for Yucca Mountain are clear. Faulting within Yucca Mountain should be considered as a system and modeled as failing as a system during an earthquake. This means considering potentially larger surface rupture parameters, and consequently larger corresponding earthquake magnitudes, than if considering individual faults. This manuscript is in Appendix E.

* C.M. dePolo, A.R. Ramelli, and A. Michetti conducted a brief field survey of the May 17, 1993 Eureka Valley earthquake area (M_L 6.1). Small cracks were found that had as much as a few millimeters of vertical displacement, and were at the base of northeast-trending Holocene fault scarps. Over 4 km of fracturing was found. These cracks may have been primary, secondary, or sympathetic; although a first-motion nodal plane is northeast striking and the preliminary epicenter downdip, a well-constrained aftershock pattern will be needed to further pursue a primary nature for these fractures. Fracturing in epicentral areas that is non-primary is common and is an equal hypothesis for the fractures seen in the field. A car-sized mound of dirt in the area, for example, showed spectacular shattered ridge effects. The information we gathered including the location of the fracturing was given to scientists with the U.S. Geological Survey as a starting point for their field studies of the event. This event appears to be barely at or below the threshold level of surface faulting.

* J.W. Bell and F.F. Peterson resubmitted the manuscript "Late Quaternary geomorphology and soils in Crater Flat, next to Yucca Mountain, southern Nevada: a reinterpretation" to the Geological Society of America Bulletin.

* J.W. Bell, C.M. dePolo, and several other authors submitted a paper titled "Aseismic slip on an extensional Basin and Range fault: evidence for tectonic creep" to the Journal of Geophysical Research. This paper details our observations of a 1 km long crack that aseismically occurred in 1988 in eastern Carson Valley. Trenching studies confirm this crack soles into a fault plane. Several other possible causes for this crack, such as subsidence, are ruled out through observations. Small swarms of shallow earthquakes occurred in adjacent areas, such as the Virginia City area, in the following year. A possible scenario is that a mild tectonic pulse may have come into the area. This was expressed as a crack, either shallowly or deeply seated, in the eastern Carson Valley area, and as triggering small earthquakes elsewhere. The crack clearly occurred over a short period of time, was aseismic, and occurs directly along a well-developed Holocene fault zone. Such phenomena are not reported in the literature for the Basin and Range province, or other extensional areas that we are aware of, although there is hearsay of similar occurrences. This paper is presented in Appendix F.

APPENDIX A

REPORT ON VARNISH SAMPLES COLLECTED FROM MONTE CRISTO VALLEY AREA

for

YUCCA MOUNTAIN PROJECT

as part of the

Investigation of J.W. Bell

by

Ronald I. Dorn, Ph.D.
2031 S. Sierra Vista Dr.
Tempe, AZ 85282
(602) 966-4245

February 6, 1993

INTRODUCTION

The purpose of this investigation is to provide rock varnish ages on geomorphic surfaces in the Monte Cristo Valley area, in particular surfaces associated with the Benton Springs and Cedar Mountain faults.

Two sets of samples were collected. The first sampling of rock varnish took place in May of 1990. The second sampling occurred in November of 1992.

The samples in May of 1990 were collected from fourteen different sites:

1-JWB-1-CM-18
1-JWB-1-CM-22
1-JWB-1-CM-33
1-JWB-1-CM-34
1-JWB-1-CM-35
1-JWB-1-BS-9
1-JWB-1-BS-27
1-JWB-1-BS-28
1-JWB-1-BS-34
1-JWB-1-BS-35
1-JWB-1-BS-37
1-JWB-1-BS-39
1-JWB-1-BS-41
1-JWB-1-BS-42

The samples from November of 1992 were collected from seven different sites:

11-mile wash
1-JWB-1-BS-8
1-JWB-1-BS-9
1-JWB-1-BS-10
1-JWB-1-BS-43
1-JWB-1-BS-46
1-JWB-1-BS-75

Two types of rock varnish dating was conducted. (1) Rock varnish cation ratios were measured on samples from all sites. (2) Accelerator radiocarbon dates were submitted for analysis from 8 sites in the first collection and all 7 sites in the second collection. Results are reported here for both rock varnish cation-ratios and rock varnish radiocarbon analyses.

METHODS

Rock varnish samples were collected in the field and assessed in the laboratory according to criteria outlined elsewhere (Dorn, 1989, table 2; Dorn et al., 1990; Krinsley et al.,1990).

Samples for cation-ratio dating were prepared according to the methods outlined in Dorn (1989) and Dorn et al. (1990). However, a different cleaning technique was also instituted for particularly 'dirty' samples. Varnish scrapings were ground up into a fine powder (less than 2 microns), suspended in deionized water, and let settle for a few minutes. The rock contaminants settled out first, leaving the rock varnish behind. The sample contamination assessment procedures in Dorn (1989) were used to assess

contamination after cleaning by this new technique. I estimate the greatest contamination to be about 4% by volume and less than 2% by chemistry in BS 9 (1990 collection) and BS 34 since the underlying rocks that were sampled had minimal amounts of Ca, K, and Ti. The other sites are estimated to have less than 2% contamination by volume and less than 2% contamination by chemistry.

Samples for radiocarbon dating were prepared by the technique in Dorn et al. (1992). These samples were then pretreated as in Dorn et al. (1989), with HF and HCl used to remove loose organics attached to clays and carbonates. The organics were analyzed by accelerator mass spectrometry at the Institute of Geological and Nuclear Science in New Zealand (Lowe et al., 1988).

RESULTS

Table 1 presents a summary of cation ratio measurements from the sites not radiocarbon dated. Table 2 presents radiocarbon dates from 15 sites and their corresponding cation-ratios used in the development of a cation-leaching curve. Table 3 presents cation ratio measurements, reasons why certain analyses were rejected, and cation-ratio age-estimates for sites not radiocarbon dated.

Table 1. Cation-ratio analyses from sites not radiocarbon dated. Results are reported with a 1 sigma error. The sites are ordered from oldest (top) to youngest (bottom).

Site	(K+Ca)/Ti
1-JWB-1-BS-41	Range 3.79 - 4.06, where 3.79 best reflects minimum age of site
1-JWB-1-BS-35	4.40 ± 0.14
1-JWB-1-BS-28	5.48 ± 0.12
1-JWB-1-BS-39	5.52 ± 0.16
1-JWB-1-BS-9 (1990 Collection)	9.27 ± 0.60

Table 2. Cation-ratio and radiocarbon data used in the construction of a cation-leaching curve for the Monte Cristo area.

Site (Year Collected)	Age	Cation	Lab No. of Radiocarbon Date
JWB BS34 (1990)	625 ± 75	9.07 ± 0.20	NZA 1382
JWB BS46 (1992)	823±66	8.95 ± 0.12	NZA 2929
JWB BS10 (1992)	1134±70	8.66 ± 0.16	NZA 2931
JWB BS9 (1992)	1267±71	8.66 ± 0.19	NZA 2930
11-mile wash (1992)	2258±68	8.63 ± 0.07	NZA 2932
JWB BS 75 (1992)	4347±72	7.31 ± 0.21	NZA 2933
JWB CM35 (1990)	5900 ± 90	7.03 ± 0.10	NZA 1380
JWB BS42 (1990)	8000 ± 100	6.82 ± 0.15	NZA 1368
JWB CM33 (1990)	11,250 ± 120	6.59 ± 0.10	NZA 1381
JWB CM18 (1990)	21,940 ± 360	5.56 ± 0.23	NZA 1377
JWB BS37 (1990)	22,170 ± 370	5.50 ± 0.11	NZA 1360
JWB CM22 (1990)	22,740 ± 360	5.50 ± 0.11	NZA 1417
JWB BS 8 (1992)	25, 020 ±270	5.41± 0.09	NZA 2935
JWB BS27 (1990)	25,430 ± 480	5.42 ± 0.09	NZA 1379
JWB BS43 (1992)	>47,000	4.33±0.18	NZA 2934

Figure 1 presents the best estimate for the cation-leaching curve in the Monte Cristo Valley. The cation-ratios and radiocarbon dates align up nicely for the last ~26 ka. However, the use of this calibration beyond ~26 radiocarbon years before present is speculative.

Figure 1. Cation-leaching curve for the Monte Cristo Valley and vicinity. The least-squares regression can be described by the following equation:

$$CR = 16.23 - 2.41\ (\text{Log}_{10}\ \text{Age}) \qquad (1)$$

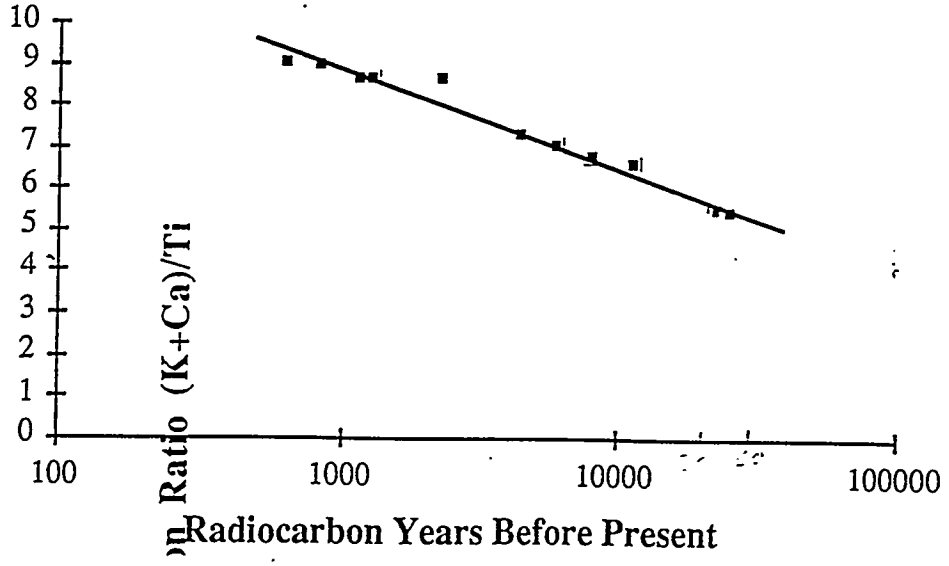

Table 3. Cation-ratio dates, and chemical data associated with unknowns and calibration for cation-leaching curve.

Sites Using Equation CR= 16.11 - 2.41 (Log10 Age)

Sample	Age	CR	Ave ± 1 sigma	Na	Mg	Al	Si	P	K	Ca	Ti	Mn	Fe	Cu	Zn	Ba
& 1-JWB-1-BS9-probe-a	504	9.60	800±400	0.04	* nm	22.77	35.02	nm	2.16	1.87	0.42	2.03	7.18	0.08	0.00	0.03
1-JWB-1-BS9-probe-b	701	9.25		2.13	nm	19.73	39.59	nm	2.14	1.56	0.40	2.20	11.82	0.00	0.07	0.00
1-JWB-1-BS9-probe-c	311	10.10		1.08	nm	20.52	38.80	nm	2.24	1.70	0.39	2.05	9.00	0.16	0.05	0.02
1-JWB-1-BS9-probe-d	976	8.90		0.00	nm	23.05	36.78	nm	2.00	1.65	0.41	1.90	9.75	0.00	0.00	0.03
1-JWB-1-BS9-probe-e	1123	8.76		0.00	nm	19.76	40.31	nm	2.01	1.58	0.41	1.87	14.14	0.00	0.00	0.00
1-JWB-1-BS9-probe-f	1624	8.37		1.98	nm	21.18	30.94	nm	2.07	1.78	0.46	1.85	9.71	0.08	0.00	0.00
1-JWB-1-BS9-probe-g	735	9.20		0.07	nm	27.91	43.54	nm	2.37	1.77	0.45	2.01	1.22	0.00	0.00	0.04
1-JWB-1-BS9-probe-h	1122	8.76		0.68	nm	16.10	31.81	nm	1.79	1.45	0.37	2.23	2.15	0.15	0.09	0.00
1-JWB-1-BS9-probe-i	306	10.12		0.03	nm	21.22	36.33	nm	2.28	1.97	0.42	2.53	13.42	0.00	0.00	0.00
1-JWB-1-BS9-probe-j	1168	8.71		0.01	nm	20.19	39.17	nm	2.01	1.65	0.42	2.00	11.83	0.00	0.00	0.00
1-JWB-1-BS9-probe-k	1088	8.79		0.16	nm	22.00	38.59	nm	1.54	1.80	0.38	2.05	11.86	0.00	0.05	0.00
1-JWB-1-BS9-probe-l	1117	8.76		0.08	nm	19.00	32.13	nm	2.02	1.66	0.42	1.97	8.11	0.00	0.10	0.60
1-JWB-1-BS9-probe-m	319	10.07		0.04	nm	23.41	38.19	nm	1.01	1.71	0.27	1.74	7.82	0.00	0.00	0.00
1-JWB-1-BS9-probe-n	484	9.64		1.01	nm	20.04	37.55	nm	1.97	1.50	0.36	3.04	4.15	0.02	0.06	0.10
1-JWB-1-BS9-probe-o	343	10.00		0.55	nm	19.11	36.20	nm	1.88	1.62	0.35	1.90	6.88	0.27	0.00	0.40
Sample	Age	CR	Ave ± 1 sigma	Na	Mg	Al	Si	P	K	Ca	Ti	Mn	Fe	Cu	Zn	Ba
+ 1-JWB-1-CM34-ICP-a	5194	7.15	5300±800	0.34	1.56	18.35	21.30	1.02	2.34	1.45	0.53	12.06	17.77	nm	nm	0.65
1-JWB-1-CM34-ICP-b	4819	7.23		0.36	1.82	15.76	18.13	1.16	2.81	2.25	0.70	12.30	13.42	nm	nm	0.19
1-JWB-1-CM34-ICP-c	4051	7.41		0.26	1.04	12.04	46.06	1.03	1.38	1.51	0.39	8.20	7.37	nm	nm	0.14
1-JWB-1-CM34-ICP-d	5657	7.06		0.46	0.98	6.85	29.71	1.09	2.42	0.48	0.41	14.35	5.17	nm	nm	0.11
1-JWB-1-CM34-ICP-e	6400	6.93		0.25	2.17	9.48	20.91	0.69	2.50	1.59	0.59	15.74	14.42	nm	nm	0.12
1-JWB-1-CM34-ICP-f	5705	7.05		0.35	1.70	12.44	27.72	1.01	2.44	0.64	0.44	10.95	10.60	nm	nm	0.09
1-JWB-1-CM34-ICP-g	5486	7.09		0.39	1.82	11.89	19.31	1.19	2.40	1.00	0.48	13.22	17.10	nm	nm	0.11
1-JWB-1-CM34-ICP-H-Ca-reject		15.49		0.39	2.36	9.22	17.75	0.90	2.94	7.92	0.70	4.27	12.78	nm	nm	0.13
Sample	Age	CR	Ave ± 1 sigma	Na	Mg	Al	Si	P	K	Ca	Ti	Mn	Fe	Cu	Zn	Ba
1-JWB-1-BS42-ICP-a	6799	6.87	7200±1000	0.56	1.25	12.12	18.51	1.41	2.50	1.69	0.61	15.02	16.08	nm	nm	0.11
1-JWB-1-BS42-ICP-b	8556	6.63		0.19	2.85	10.08	19.40	0.57	1.77	1.08	0.43	11.34	18.24	nm	nm	0.17
1-JWB-1-BS42-ICP-c	5630	7.07		0.45	1.54	25.02	31.80	1.69	2.77	0.98	0.53	7.97	8.25	nm	nm	0.15
1-JWB-1-BS42-ICP-d	7165	6.81		0.23	0.89	15.73	21.36	0.40	3.62	2.37	0.88	7.36	17.78	nm	nm	0.00
1-JWB-1-BS42-ICP-e	7839	6.72		0.38	1.51	7.93	44.21	1.06	1.60	1.08	0.40	5.37	6.58	nm	nm	0.12
1-JWB-1-BS42-ICP-f	7184	6.81		0.19	1.59	17.89	27.69	0.59	1.60	1.94	0.52	6.39	7.68	nm	nm	0.12
1-JWB-1-BS42-ICP-g-Ca-reject		18.62		0.68	0.85	5.89	36.01	1.28	2.08	6.39	0.45	9.10	4.96	nm	nm	0.11

Sample	Age	CR	Ave ± 1 sigma	Na	Mg	Al	Si	P	K	Ca	Ti	Mn	Fe	Cu	Zn	Ba
1-JWB-1-BS39-ICP-a	25840	5.47	25,000±4000	1.60	1.09	14.65	25.21	1.32	2.03	1.58	0.66	12.50	19.76	nm	nm	0.14
1-JWB-1-BS39-ICP-b	22791	5.60		0.59	7.44	6.55	28.86	0.82	1.14	2.89	0.72	11.28	10.30	nm	nm	0.67
1-JWB-1-BS39-ICP-c	29219	5.34		0.59	0.87	16.82	20.30	1.24	1.20	1.15	0.44	9.66	8.07	nm	nm	0.11
1-JWB-1-BS39-ICP-d	29517	5.33		0.46	1.15	9.53	9.03	1.55	2.04	1.69	0.70	14.11	21.72	nm	nm	0.15
1-JWB-1-BS39-ICP-e	22274	5.63		0.56	2.02	22.94	25.02	1.42	1.98	1.40	0.60	5.05	5.18	nm	nm	0.16
1-JWB-1-BS39-ICP-f	20248	5.73		0.55	1.12	22.56	25.23	1.21	1.62	2.20	0.67	5.12	6.16	nm	nm	0.58
1-JWB-1-BS39-ICP-g-MCF reject		2.25		0.78	1.75	21.49	32.44	1.01	0.97	0.72	0.75	13.04	10.36	nm	nm	0.14
1-JWB-1-BS39-ICP-h-Ti reject		1.48		0.57	1.20	28.84	4.90	0.71	0.99	1.60	1.75	5.79	14.13	nm	nm	0.16

Sample	Age	CR	Ave ± 1 sigma	Na	Mg	Al	Si	P	K	Ca	Ti	Mn	Fe	Cu	Zn	Ba
1-JWB-1-BS28-ICP-a	28316	5.37	26,000±3000	2.50	0.95	21.92	30.13	1.84	2.74	1.02	0.70	9.81	6.25	nm	nm	0.00
1-JWB-1-BS28-ICP-b	23862	5.55		0.49	0.77	21.84	23.49	0.92	1.80	1.20	0.54	5.01	5.47	nm	nm	0.15
1-JWB-1-BS28-ICP-c	21525	5.66		1.20	1.20	18.40	39.25	0.78	2.25	1.13	0.60	6.34	7.61	nm	nm	0.13
1-JWB-1-BS28-ICP-d	26420	5.45		0.47	0.90	35.85	17.06	1.63	0.99	1.25	0.41	2.56	4.19	nm	nm	0.10
1-JWB-1-BS28-ICP-e	29126	5.34		5.00	1.10	15.22	12.10	1.66	1.80	1.46	0.61	13.55	8.25	nm	nm	0.12
1-JWB-1-BS28-ICP-f	25458	5.49		0.46	1.54	19.66	41.26	0.62	1.96	1.77	0.68	6.99	2.81	nm	nm	0.13
1-JWB-1-BS28-ICP-g-Ca reject		18.44		0.34	1.49	5.08	16.09	1.05	2.64	8.06	0.58	2.07	14.42	nm	nm	0.10

Sites Beyond Calibration

Sample	Age	CR	Na	Mg	Al	Si	P	K	Ca	Ti	Mn	Fe	Cu	Zn	Ba
1-JWB-1-BS41-ICP-a	128473	3.79	0.28	1.30	17.30	43.15	0.65	1.90	1.16	0.81	7.53	7.15	nm	nm	0.13
1-JWB-1-BS41-ICP-c	123567	3.83	0.41	1.46	15.39	24.49	0.77	1.20	1.40	0.68	7.07	6.09	nm	nm	0.12
1-JWB-1-BS41-ICP-d	119833	3.86	0.22	2.07	31.83	9.65	0.52	1.30	0.41	0.44	1.59	8.09	nm	nm	0.14
1-JWB-1-BS41-ICP-e	114160	3.91	0.29	1.93	18.78	29.97	0.77	1.48	2.04	0.90	7.64	7.66	nm	nm	0.18
1-JWB-1-BS41-ICP-f	112037	3.93	0.44	2.43	18.97	30.91	0.86	1.54	2.00	0.90	7.72	8.20	nm	nm	0.13
1-JWB-1-BS41-ICP-g	102440	4.03	0.47	1.87	16.80	25.95	1.03	1.45	1.66	0.77	8.18	6.29	nm	nm	0.15
1-JWB-1-BS41-ICP-h	101622	4.03	0.33	1.96	22.43	18.16	0.88	2.23	0.68	0.72	3.44	9.29	nm	nm	0.10
1-JWB-1-BS41-ICP-i	99280	4.06	0.46	1.85	18.37	30.85	1.20	1.55	2.23	0.93	8.14	9.12	nm	nm	0.15

Sample	Age	CR	Na	Mg	Al	Si	P	K	Ca	Ti	Mn	Fe	Cu	Zn	Ba
1-JWB-1-BS35-ICP-a	84855	4.22	0.34	1.98	8.31	32.19	0.77	1.21	3.43	1.10	6.85	10.77	nm	nm	0.13
1-JWB-1-BS35-ICP-b	84593	4.23	0.36	1.66	17.20	26.27	1.34	1.31	1.52	0.67	7.60	5.54	nm	nm	0.15
1-JWB-1-BS35-ICP-c	69966	4.43	0.39	1.37	18.03	31.58	1.11	2.57	2.25	1.09	12.81	12.70	nm	nm	0.13
1-JWB-1-BS35-ICP-d	66356	4.48	0.25	2.00	31.32	13.03	0.88	1.44	1.02	0.55	2.24	10.08	nm	nm	0.18
1-JWB-1-BS35-ICP-e	65712	4.49	0.32	2.18	10.15	29.39	0.75	1.14	3.73	1.08	6.63	7.85	nm	nm	0.71
1-JWB-1-BS35-ICP-f	61730	4.56	0.53	1.25	12.12	36.69	1.56	1.54	0.54	0.46	5.84	5.10	nm	nm	0.50
1-JWB-1-BS35-ICP-g-Ti reject		0.97	0.31	2.19	24.75	27.14	0.67	1.96	0.51	2.55	14.97	3.69	nm	nm	0.13

	Age	CR	Na	Mg	Al	Si	P	K	Ca	Ti	Mn	Fe	Cu	Zn	Ba
1-JWB-1-BS-43-a	86620	4.20	0.59	2.04	13.55	20.11	0.46	1.88	2.07	0.94	19.20	9.05	nm	nm	0.09
1-JWB-1-BS-43-b	82752	4.25	1.01	1.55	19.11	23.44	1.01	1.75	1.99	0.88	15.23	9.57	nm	nm	0.20
1-JWB-1-BS-43-c	62555	4.54	0.74	1.88	14.00	23.88	0.97	1.80	1.88	0.81	14.44	10.58	nm	nm	0.19
1-JWB-1-BS-43-d- Unconf reject	Cation ratios not determined due to presence of unconformity in cross-sectional analyses.														
1-JWB-1-BS-43-e- Unconf reject	Cation ratios not determined due to presence of unconformity in cross-sectional analyses.														

Sites Used in Calibration

Sample	CR	Ave ± 1 sigma	Na	Mg	Al	Si	P	K	Ca	Ti	Mn	Fe	Cu	Zn	Ba
1-JWB-1-BS34-ICP-a	8.73	9.07	0.32	2.05	14.07	21.34	1.06	3.57	2.20	0.66	7.64	21.70	nm	nm	0.09
1-JWB-1-BS34-ICP-b	8.82	0.20	0.23	2.29	7.75	24.06	0.90	3.91	2.26	0.70	7.89	21.92	nm	nm	0.16
1-JWB-1-BS34-ICP-c	8.99		0.36	2.48	12.45	15.05	0.72	6.64	2.34	1.00	17.46	14.16	nm	nm	0.20
1-JWB-1-BS34-ICP-d	9.06		0.27	2.07	15.23	16.97	1.00	2.89	6.10	0.99	4.62	8.35	nm	nm	0.12
1-JWB-1-BS34-ICP-e	9.08		0.33	2.00	22.20	27.65	0.92	1.82	1.72	0.39	5.75	5.89	nm	nm	0.15
1-JWB-1-BS34-ICP-f	9.19		0.36	1.40	16.97	18.08	0.94	2.75	2.03	0.52	13.89	13.93	nm	nm	0.16
1-JWB-1-BS34-ICP-g	9.23		0.29	2.09	7.14	15.14	0.91	1.50	2.56	0.44	7.99	11.78	nm	nm	0.13
1-JWB-1-BS34-ICP-h	9.24		0.31	1.96	21.81	8.65	0.93	3.30	1.33	0.50	9.83	8.62	nm	nm	0.17
1-JWB-1-BS34-ICP-i	9.31		0.38	1.39	6.08	20.42	0.94	2.97	1.50	0.48	11.80	11.43	nm	nm	0.13
1-JWB-1-BS34-ICP-j-Ca reject	18.95		0.62	1.43	9.42	24.65	1.87	1.94	4.47	0.34	11.04	5.03	nm	nm	0.10
1-JWB-1-BS34-ICP-jk-Ti reject	1.14		0.42	1.58	24.29	30.12	0.67	1.76	0.20	1.72	10.46	7.06	nm	nm	0.14

Sample	Age	CR	Ave ± 1 sigma	Na	Mg	Al	Si	P	K	Ca	Ti	Mn	Fe	Cu	Zn	Ba
1-JWB-1-BS37-ICP-a		5.46	5.50	0.58	1.26	16.73	17.83	1.31	1.10	1.52	0.48	13.70	15.04	nm	nm	0.00
1-JWB-1-BS37-ICP-b		5.64	0.11	2.03	0.98	11.31	26.05	0.34	0.93	5.87	1.20	5.75	6.60	nm	nm	0.20
1-JWB-1-BS37-ICP-c		5.36		1.34	1.85	16.32	39.83	0.89	1.66	1.34	0.56	11.15	13.14	nm	nm	0.12
1-JWB-1-BS37-ICP-d		5.54		0.76	1.65	9.34	25.44	1.03	1.33	2.42	0.68	12.33	8.88	nm	nm	0.14
1-JWB-1-BS37-ICP-e		5.51		1.70	1.04	9.24	33.18	1.64	2.24	1.49	0.68	4.16	6.62	nm	nm	0.00
1-JWB-1-BS37-ICP-f		5.58		0.63	2.02	7.33	36.59	0.86	1.54	1.42	0.53	4.44	9.14	nm	nm	0.10
1-JWB-1-BS37-ICP-g		5.38		0.62	0.89	22.24	23.12	1.50	1.59	1.21	0.52	5.04	6.21	nm	nm	0.11
1-JWB-1-BS37-ICP-h-Ca reject		18.49		0.46	1.90	4.19	14.72	1.01	2.84	6.52	0.51	4.28	12.75	nm	nm	0.15
1-JWB-1-BS37-ICP-i-Ti reject		1.77		0.34	2.77	20.74	32.86	0.60	2.54	0.61	1.78	8.78	7.64	nm	nm	0.00

Sample	CR	Ave ± 1 sigma	Na	Mg	Al	Si	P	K	Ca	Ti	Mn	Fe	Cu	Zn	Ba
1-JWB-1-BS27-ICP-a	5.49	5.42	0.44	1.87	7.46	29.57	1.11	1.65	4.20	1.07	7.37	10.19	nm	nm	0.10
1-JWB-1-BS27-ICP-b	5.53	0.09	0.90	1.03	26.63	31.05	1.14	1.95	0.38	0.42	3.86	5.36	nm	nm	0.13
1-JWB-1-BS27-ICP-c	5.25		0.42	1.04	24.77	25.78	1.56	1.80	1.30	0.59	4.09	4.96	nm	nm	0.10
1-JWB-1-BS27-ICP-d	5.40		0.20	0.95	13.51	41.03	0.93	0.81	2.27	0.57	7.48	9.03	nm	nm	0.12
1-JWB-1-BS27-ICP-e	5.42		0.39	2.11	5.65	8.29	1.25	1.84	3.20	0.93	4.78	29.96	nm	nm	0.11
1-JWB-1-BS27-ICP-f	5.44		0.85	1.99	12.89	17.32	1.11	1.56	0.67	0.41	14.48	8.84	nm	nm	0.19
1-JWB-1-BS27-ICP-g-K reject	10.28		0.09	0.85	6.75	19.58	0.47	7.53	2.92	1.02	11.89	10.01	nm	nm	0.13

Sample	CR	Ave ± 1 sigma	Na	Mg	Al	Si	P	K	Ca	Ti	Mn	Fe	Cu	Zn	Ba
1-JWB-1-CM22-ICP-a	5.45	5.50	1.20	1.10	8.41	27.87	1.30	1.19	2.08	0.60	10.24	11.33	nm	nm	0.14
1-JWB-1-CM22-ICP-b	5.60	0.11	0.35	1.01	4.47	6.67	0.91	2.04	2.61	0.83	9.00	30.03	nm	nm	0.13
1-JWB-1-CM22-ICP-c	5.64		0.87	1.88	15.77	19.31	1.01	1.25	0.92	0.38	14.33	11.11	nm	nm	0.00
1-JWB-1-CM22-ICP-d	5.52		0.32	0.95	34.10	10.64	0.90	1.72	0.99	0.49	2.25	5.90	nm	nm	0.11
1-JWB-1-CM22-ICP-e	5.37		0.15	1.89	17.51	32.53	0.76	1.45	1.50	0.55	11.98	13.27	nm	nm	0.11
1-JWB-1-CM22-ICP-f	5.41		0.32	1.92	19.29	22.77	0.85	1.78	1.03	0.52	6.80	7.16	nm	nm	0.13
1-JWB-1-CM22-ICP-g-Ca-reject	17.26		0.32	1.31	4.68	38.92	2.49	1.77	7.15	0.52	9.55	5.57	nm	nm	0.08

Sample	CR	Ave ± 1 sigma	Na	Mg	Al	Si	P	K	Ca	Ti	Mn	Fe	Cu	Zn	Ba
1-JWB-1-CM18-ICP-a	5.41	5.56	0.26	1.28	20.18	20.39	1.09	2.00	1.35	0.62	6.33	6.03	nm	nm	0.12
1-JWB-1-CM18-ICP-b	5.87	0.23	0.48	1.63	18.63	26.52	1.07	1.20	0.66	0.32	5.87	13.09	nm	nm	0.15
1-JWB-1-CM18-ICP-c	5.52		0.66	0.94	17.30	19.53	0.97	1.30	1.24	0.46	10.01	9.15	nm	nm	0.11
1-JWB-1-CM18-ICP-d	5.78		0.29	1.98	17.80	25.95	1.22	0.91	0.75	0.29	10.25	12.15	nm	nm	0.14
1-JWB-1-CM18-ICP-e	5.37		0.71	1.26	14.22	26.35	0.97	1.70	0.70	0.45	15.72	6.56	nm	nm	0.00
1-JWB-1-CM18-ICP-f	5.24		0.25	0.65	14.48	25.74	1.92	3.68	1.56	1.00	13.67	14.50	nm	nm	0.00
1-JWB-1-CM18-ICP-g	5.71		0.56	0.91	13.62	15.27	2.44	1.86	0.99	0.50	6.90	11.02	nm	nm	0.16

Sample	CR	Ave ± 1 Sigma	Na	Mg	Al	Si	P	K	Ca	Ti	Mn	Fe	Cu	Zn	Ba
1-JWB-1-CM33-ICP-a	6.78	6.59	0.55	1.34	14.68	13.96	2.24	1.13	1.24	0.35	12.19	10.28	nm	nm	0.11
1-JWB-1-CM33-ICP-b	6.55	0.10	0.38	1.81	31.72	29.13	0.97	1.81	0.81	0.40	3.58	5.20	nm	nm	0.15
1-JWB-1-CM33-ICP-c	6.60		0.62	0.83	4.54	16.64	1.41	2.45	1.71	0.63	13.80	12.72	nm	nm	0.12
1-JWB-1-CM33-ICP-d	6.51		0.25	2.15	10.70	23.62	1.02	1.22	1.64	0.44	13.26	7.62	nm	nm	0.15
1-JWB-1-CM33-ICP-e	6.51		0.38	1.13	14.24	27.85	1.60	1.83	3.53	0.82	3.67	13.81	nm	nm	0.08
1-JWB-1-CM33-ICP-f	6.61		0.48	0.14	11.33	22.21	0.10	3.54	2.41	0.90	16.26	12.04	nm	nm	0.14
1-JWB-1-CM33-ICP-g-K-reject	11.01		0.21	0.37	18.77	18.45	0.42	6.64	2.30	0.81	12.35	14.36	nm	nm	0.00

Sample	CR	Ave ± 1 Sigma	Na	Mg	Al	Si	P	K	Ca	Ti	Mn	Fe	Cu	Zn	Ba
1-JWB-1-CM35-ICP-a	7.13	7.03	0.36	1.56	17.35	19.13	1.12	2.02	1.46	0.49	7.41	7.38	nm	nm	0.13
1-JWB-1-CM35-ICP-b	7.18	0.10	0.49	1.13	19.74	22.35	1.23	1.23	1.64	0.40	7.00	19.22	nm	nm	0.15
1-JWB-1-CM35-ICP-c	6.87		0.48	1.24	11.44	31.41	1.41	2.08	2.59	0.68	5.37	9.92	nm	nm	0.11
1-JWB-1-CM35-ICP-d	6.95		0.55	0.97	10.79	30.79	1.26	2.35	3.42	0.83	5.35	11.97	nm	nm	0.13
1-JWB-1-CM35-ICP-e	7.01		0.43	1.57	28.64	25.68	1.27	2.34	1.02	0.48	4.95	5.21	nm	nm	0.11
1-JWB-1-CM35-ICP-f	7.05		0.28	1.53	13.83	16.48	0.65	1.66	1.37	0.43	8.23	9.24	nm	nm	0.10
1-JWB-1-CM35-ICP-g	7.05		0.45	1.84	12.72	17.01	1.14	2.96	1.97	0.70	11.58	16.74	nm	nm	0.15
1-JWB-1-CM35-ICP-h-MCF-reject	3.22		0.43	2.07	23.97	26.08	0.74	0.97	1.32	0.71	4.99	4.85	nm	nm	0.08

Sample	CR	Ave ± 1 Sigma	Na	Mg	Al	Si	P	K	Ca	Ti	Mn	Fe	Cu	Zn	Ba
1-JWB-1-BS8-probe-a1	5.24		0.02	0.93	17.27	23.09	0.73	0.90	1.46	0.45	18.49	10.12	nm	nm	0.09
1-JWB-1-BS8-probe-a2	5.31	5.41	0.00	0.82	17.89	23.23	0.81	0.94	0.97	0.36	18.75	9.25	nm	nm	0.18
1-JWB-1-BS8-probe-a3	5.41	0.12	0.02	0.56	17.31	20.71	0.60	0.72	0.74	0.27	27.69	6.38	nm	nm	0.09
1-JWB-1-BS8-probe-b	5.48		0.24	0.92	16.66	31.46	1.17	1.09	0.72	0.33	17.78	12.72	nm	nm	0.04
1-JWB-1-BS8-probe-c	5.51		0.01	0.61	15.73	20.12	1.00	0.80	1.46	0.41	25.90	8.60	nm	nm	0.09
1-JWB-1-BS8-probe-d	5.53		0.00	0.68	16.05	22.11	1.12	0.72	1.05	0.32	21.20	11.94	nm	nm	0.08
Sample	CR	Ave ± 1 Sigma	Na	Mg	Al	Si	P	K	Ca	Ti	Mn	Fe	Cu	Zn	Ba
1-JWB-1-BS46-probe-a	8.90	8.95	0.04	0.53	11.72	28.07	0.25	0.88	0.90	0.20	4.05	11.29	nm	nm	0.09
1-JWB-1-BS46-probe-b	9.00	0.12	0.00	0.70	16.83	21.46	0.77	1.28	1.51	0.31	2.09	13.48	nm	nm	0.11
1-JWB-1-BS46-probe-c	9.13		0.00	0.59	15.29	20.72	1.39	1.38	1.45	0.31	3.27	11.52	nm	nm	0.14
1-JWB-1-BS46-probe-d	8.90		0.00	0.42	13.76	19.28	1.04	1.22	1.45	0.30	2.61	12.36	nm	nm	0.11
1-JWB-1-BS46-probe-e	8.83		0.00	0.99	18.00	24.14	0.78	1.63	0.93	0.29	1.74	10.12	nm	nm	0.11
Sample	CR	Ave ± 1 Sigma	Na	Mg	Al	Si	P	K	Ca	Ti	Mn	Fe	Cu	Zn	Ba
1-JWB-1-BS10-probe-a	8.71	8.66	0.00	0.76	18.16	22.41	0.72	1.08	1.36	0.28	2.44	9.08	nm	nm	0.09
1-JWB-1-BS10-probe-b	8.83	0.14	0.00	0.58	15.00	19.31	0.61	1.03	1.09	0.24	3.60	11.34	nm	nm	0.06
1-JWB-1-BS10-probe-c	8.45		0.00	0.87	14.35	20.71	0.67	1.24	1.38	0.31	2.23	13.36	nm	nm	0.12
1-JWB-1-BS10-probe-d	8.65		0.00	0.54	15.11	19.31	0.74	0.98	1.27	0.26	3.69	9.47	nm	nm	0.07
1-JWB-1-BS10-probe-e	8.63		0.03	0.78	17.18	23.10	0.64	1.12	1.21	0.27	2.93	8.57	nm	nm	0.10
Sample	CR	Ave ± 1 Sigma	Na	Mg	Al	Si	P	K	Ca	Ti	Mn	Fe	Cu	Zn	Ba
1-JWB-1-BS9-probe-a	8.41	8.66	0.08	0.90	17.18	22.36	0.93	1.25	1.19	0.29	1.33	11.86	nm	nm	0.12
1-JWB-1-BS9-probe-b	8.64	0.19	0.01	0.80	17.44	21.85	0.97	0.96	1.20	0.25	2.24	9.22	nm	nm	0.14
1-JWB-1-BS9-probe-c	8.89		0.00	0.50	13.78	19.62	0.56	1.01	1.39	0.27	2.91	11.21	nm	nm	0.12
1-JWB-1-BS9-probe-d	8.56		0.04	0.64	14.92	20.00	0.57	0.82	1.49	0.27	3.39	10.74	nm	nm	0.03
1-JWB-1-BS9-probe-e	8.79		0.00	0.41	15.15	19.30	1.08	0.91	1.20	0.24	2.96	11.59	nm	nm	0.09
Sample	CR	Ave ± 1 Sigma	Na	Mg	Al	Si	P	K	Ca	Ti	Mn	Fe	Cu	Zn	Ba
11 mile wash-probe-a	8.52	8.63	0.00	0.52	14.61	19.96	1.13	0.89	1.58	0.29	2.08	11.52	nm	nm	0.12
11 mile wash-probe-b	8.65	0.07	0.00	0.73	17.12	22.52	0.95	1.04	1.21	0.26	2.10	9.06	nm	nm	0.13
11 mile wash-probe-c	8.64		0.02	0.91	16.84	24.87	0.72	1.07	1.09	0.25	1.52	10.61	nm	nm	0.08
11 mile wash-probe-d	8.61		0.00	0.66	16.24	21.42	1.12	0.68	1.30	0.23	2.80	10.47	nm	nm	0.12
11 mile wash-probe-e	8.71		0.00	0.96	14.73	20.32	0.40	0.70	1.13	0.21	3.48	11.38	nm	nm	0.04

Sample	CR	Ave ± 1 Sigma	Na	Mg	Al	Si	P	K	Ca	Ti	Mn	Fe	Cu	Zn	Ba
1-JWB-1-BS75-probe-a	7.19	7.31	0.03	1.10	20.48	25.97	0.74	1.09	1.14	0.31	5.42	8.47	nm	nm	0.08
1-JWB-1-BS75-probe-b	7.32	0.21	0.00	0.78	15.55	21.03	0.54	1.03	1.24	0.31	4.53	9.88	nm	nm	0.08
1-JWB-1-BS75-probe-c	7.23		0.00	0.55	15.34	19.74	0.78	1.03	1.50	0.35	4.18	9.32	nm	nm	0.06
1-JWB-1-BS75-probe-d	7.03		0.00	0.02	12.96	14.64	0.97	1.34	1.40	0.39	5.91	10.81	nm	nm	0.08
1-JWB-1-BS75-probe-e	7.47		0.05	0.87	17.49	23.57	0.92	1.22	1.17	0.32	7.64	10.14	nm	nm	0.10
1-JWB-1-BS75-probe-f	7.61		0.00	0.59	16.36	20.47	0.91	0.87	1.26	0.28	5.24	8.43	nm	nm	0.12

Footnotes:

* nm means not measured

+ICP refers to inductively coupled plasma.

& probe refers to analysis by wavelength dispersive electron microprobe

$ ICP and probe analyses from the same site are not on the same material

'MCF reject' means the sample was rejected due to anomalous concentrations of microcolonial fungi that reduced the cation ratio

'K reject' means the sample was rejected due to anomalous concentrations of potassium

'Ca reject' means the sample was rejected due to anomalous concentrations of calcium

'Ti reject' means the sample was rejected due to anomalous concentrations of titanium

'Unconf reject' means an unconformity was present in the sample, hence a period of erosion separated episodes of varnishing.

Figure 2 presents examples of varnish cross-sections from different sites. This figure illustrates the type of analysis necessary before varnish dating should be conducted. Figures 2A-G are all imaged with a backscatter detector, where brightness is a function of chemistry. The brighter zones in the varnish typically have higher concentrations of manganese. The darker zones typically have less manganese. The underlying rock is typically darker, because of the high concentration of Si (as opposed to higher Mn and Fe in the varnish). The brighter crystals in the underlying rock in Fig. 2C and 2F are magnetite grains rich in Fe.

2A: BS-42: Note the simple stratigraphy of a uniform brightness, where the varnish is mostly Mn-poor. Note also the fracture running from top to bottom that has been refilled with reprecipitated Mn.

2B: BS-75: The varnish stratigraphy is quite similar to other Holocene sections: a surface layer mostly Mn-poor, but with occasional zones of Mn-enrichment such as those found along fractures zones.

2C: BS-8: As is typical of the latest-Pleistocene varnishes, a Mn-rich (brighter) layer can be found underneath the Mn-poor (darker) layer. This stratigraphy can also be seen in color in BS-8 in Figure 3. Note, again, the fracture lines with reprecipitated Mn. The manganese that is dissolved in the pockets of leaching seen throughout the varnish moves through these fractures and reprecipitates, leaving bright lines.

2D: CM-22: The stratigraphy is similar to BS-8, manganese-poor layer (darker) on top of manganese-rich layer (brighter).

2E: BS-35: The stratigraphy is much more complex that the latest-Pleistocene varnishes, lending support to the lower cation-ratio as indicating a much older age. Still, the surface layer is not enriched in manganese, giving it a darker appearance. Note the extensive zones of cation leaching (porous texture) is the very bottom layers. It is common to find these leaching zones close to the rock interface, because water can pond there.

2F: BS-43: The stratigraphy of this radiocarbon 'dead' sample is quite similar to BS-35, as are the cation ratios from these two sites.

2G: BS-43: The stratigraphy of the upper part of the varnish is quite similar to Figure 2E (as well as 2D), but there is a clear angular unconformity that runs through the bottom layer. My interpretation is that varnish developed on the boulder that was partially abraded off during transport. Then, after deposition in the BS-43 unit, newer varnish started to grow on top of this partially eroded varnish.

2H: BS-10: This figure is composed of three parts: map (upper); backscatter image (middle); and secondary image (bottom). The reason for including the secondary image is that organic matter appears black in backscatter (because low atomic number), but is often found charging (bright) in secondary imagery. The locations of the larger pockets of subvarnish organic matter are identified in the corresponding map. I should note the varnish on BS-10 was patchy. The organic matter in the weathering rinds, therefore, was only collected from underneath the varnish patches.

FIGURE 2 (Parts A-G)

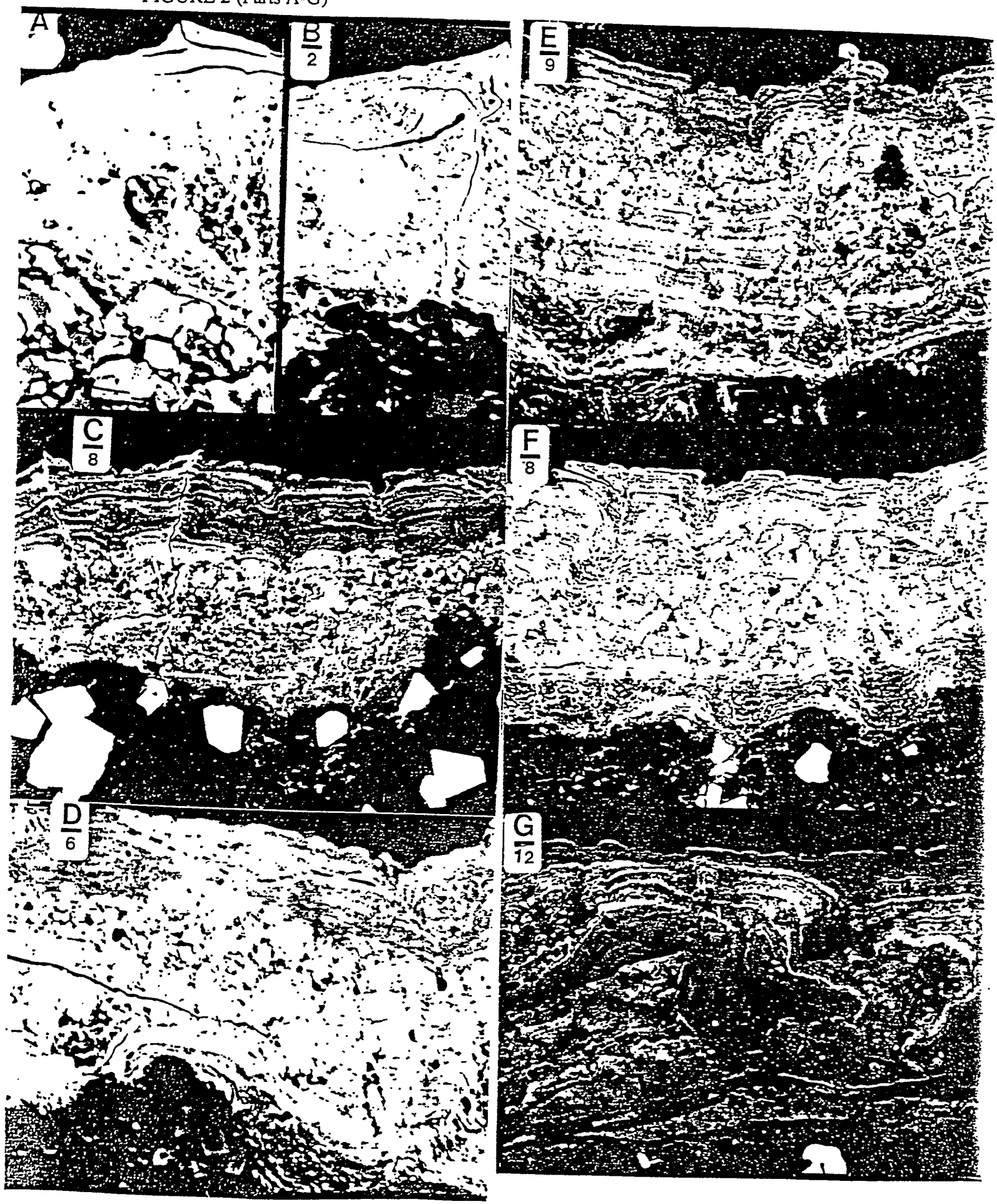

FIGURE 2 (Part H)

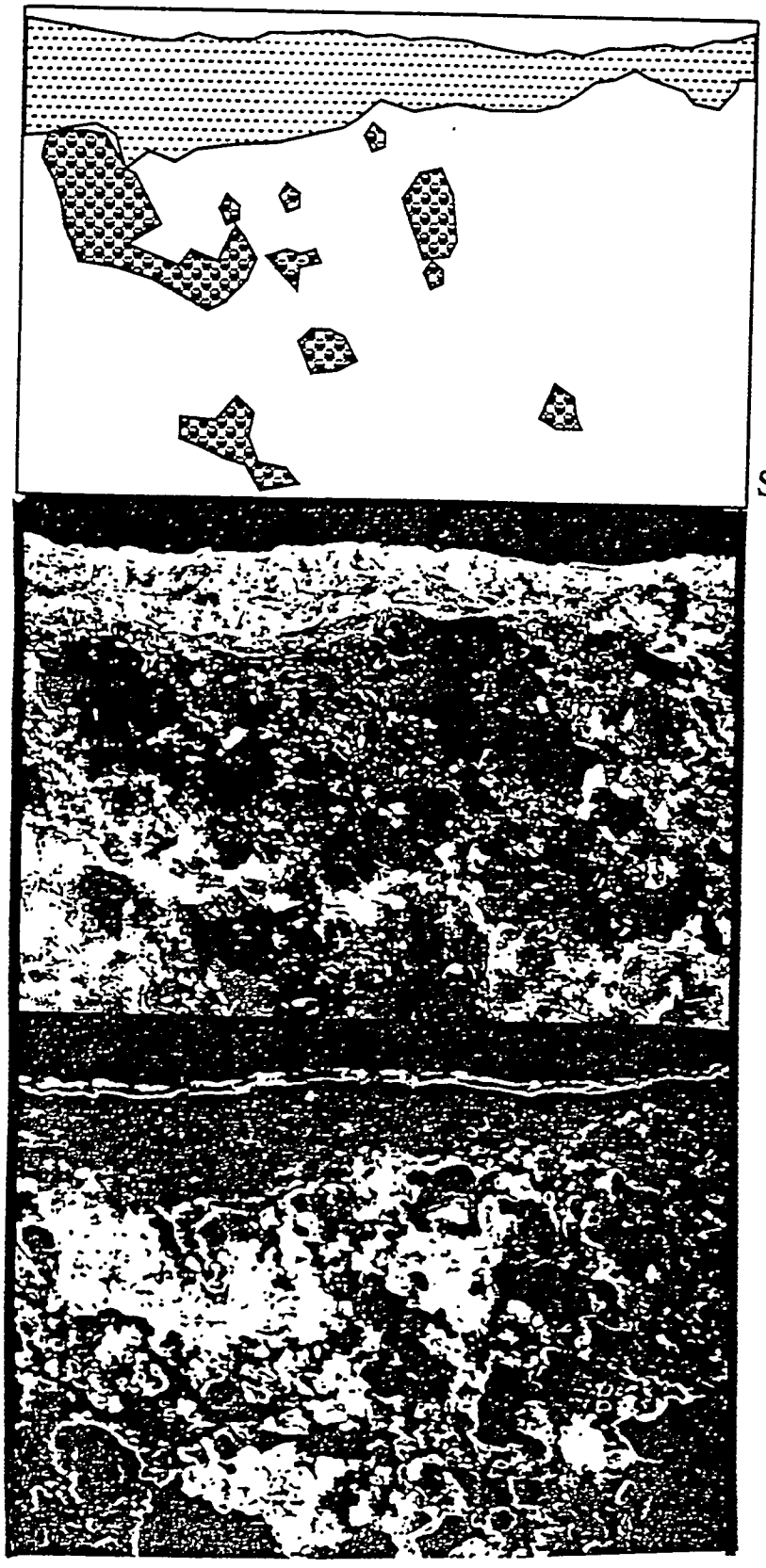

H- Map of BSE/SE Image of Varnish from BS-10

Varnish

Mostly Organic Matter

Rock Material

Scale bar 100 micrometers

Figure 3 presents examples of ultra-thin sections of varnish from the Monte Cristo Valley study area. The dark layers are black because they are enriched in manganese. The orange layers, in contrast, emphasize the iron content because they are not enriched in manganese.

Top Image: This varnish (~20 micrometers thick) is from site CM-35. Although there are some areas of greater concentration of manganese (black zones) that meander through the varnish, the overall low concentration is revealed in the orange color.

Middle Left Image: From site BS-8, the stratigraphy of orange on black indicates a substantial environmental change from less alkaline (more moist) to more alkaline conditions (drier). The varnish is ~70 micrometers at its thickest in the middle.

Middle Right Image: From site BS-35. Note the greater complexity in the microlaminations, as compared to BS-8, reflecting the greater antiquity of the site.

Lower Image: From 11-mile wash, this cross-section shows an eroded, but well developed varnish. This sample was collected in the field as obviously inherited. The abrasion of the varnish layers probably occurred during the flood event that deposited the alluvial unit. The varnish is about 140 micrometers at its thickest. Note the very thin (<1-5 micrometer) layer of orange varnish deposited over the truncated layers. It is the beginning of an unconformity in varnish development. Tens of thousands of years from now, the sequence could look like Figure 2G.

FIGURE 3

DISCUSSION

Field Complications

Several potential complications in sampling in the field were encountered in 1990 that will influence the interpretation.

1-JWB-1-BS-37 and BS39: Samples were collected from small (5-15 cm diameter) cobbles that were close to the soil surface. If this particle size reflects weathering, the dating could reflect the time of weathering.

1-JWB-1-BS-41: The surface of the landform did not look constructional. It looked eroded from an original depositional surface. Therefore, any varnish dates must be considered minimums, reflecting the time since last erosion.

1-JWB-1-BS-35: Very few original, fluvially rounded cobbles were found on the surface at this site. These rounded cobbles, however, were the ones sampled. It is possible that these rounded cobbles were eroded out of the subsurface. If this is the case, the tentative cation-ratio age-estimates are of course minimum dates for the deposit.

1-JWB-1-CM-35: There were lots of unvarnished (or little varnished) finger-sized weathered fragments of metamorphic rocks. These were not sampled, because I felt they represent ongoing weathering of the foliated metamorphic clasts. Only rounded clasts were sampled. However, it is theoretically possible that these unvarnished fragments represent a recent shallow flooding event at the site that left larger, rounded clasts sticking up (tens of cm's) above the weathered fragments.

1-JWB-1-CM-33: All of the collected cobbles are less than 10 cm in diameter and resting on the surface of a desert pavement. Cobbles with rounded edges were sampled, assuming the rounding occurred during fluvial transport. It is conceivable, however, that the small fragment size is a reflection of ongoing weathering. If so, the varnish ages for this site must be considered minimums.

Several potential complications in sampling in the field were encountered in 1992 that will influence the interpretation.

11-Mile Wash: Two different types of samples were collected, ones that clearly had varnish 'inherited' from prior exposure on an older alluvial unit, and material with rounded surfaces of ignimbrite cobbles. Laboratory evaluation of the obviously inherited varnishes revealed multiple layers indicative of a Pleistocene age. This verified the field-based interpretation.

In the field, John Bell and I suspected that a problem may occur with a prior development of varnish. In cross-sections, the varnish development was absolutely minimal -- similar to BS9 and BS10. Laboratory evaluation of the very slight varnish development on the abraded surfaces of ignimbrite cobbles would be consistent with a late Holocene age. The cation-ratios for this varnish indicate a younger age than the radiocarbon age would suggest. It is *possible*, but difficult to assess without further ^{14}C tests, that the prior varnish was abraded off during transport, but some of the organics in the weathering rind remained from the prior exposure.

1-JWB-1-BS-8: Most of the pavement looked like it had already weathered along joint faces, producing cobbles with smooth surfaces and a high degree of angularity. Only four cobbles had rounded surfaces that would indicate fluvial transportation.

1-JWB-1-BS-9 (1992 Collection): Samples from this site in the 1992 collection were taken from what appears to be an old levee (bar). The cobbles that were collected had remnants of carbonate rinds; this indicates that they did not have a prior development of rock varnish, because the cobble surfaces must have been in the soil to develop the carbonate rind. This is significant because the lack of a prior subaerial exposure prevents the accumulation (before exposure in BS-9 unit) of weathering rind organics emplaced by lichens and other organisms that grow into weathering rinds in the subaerial environment.

1-JWB-1-BS-10: Samples collected from this site had pieces of pedogenic carbonate on the surface. See discussion in BS-9.

1-JWB-1-BS-43: The sample was collected from extremely well varnished basaltic cobbles with nicely rounded (fluvial abrasion) surfaces. Unlike the other samples, two of the boulders showed evidence of a prior development of varnish as evidenced by unconformities (e.g., Figure 2G) within the varnish. Boulders with unconformities were not used in the radiocarbon dating.

1-JWB-1-BS-46 Samples collected from this site had pieces of pedogenic carbonate on the surface. See discussion in BS-9.

1-JWB-1-BS-75 The samples were collected from the rounded edges of clasts at least 50 cm in diameter. Several pieces of evidence suggest that prior exposure (to varnishing) was not a significant problem. The development of varnish was minimal on virtually all cobbles (no obviously inherited varnish as at BS9 and BS10). The sampled cobbles had good development of an orange bottom varnish, indicating *in situ* development of the varnish. In addition, none of the cross-sections indicated any evidence of angular unconformities, like those associated with BS-43.

Interpretation of Radiocarbon Ages

The radiocarbon dates in Table 2 must be viewed as minimum ages for the exposure of the underlying rock, but it is *possible* that 11-mile wash could have a problem with 'inheritence' of older weathering rind organics. This is suggested by the field context, discussed above, as well as the off-set between the cation ratio and the radiocarbon age that can be seen in Figure 1 and Tables 2 and 3.

Although it is theoretically possible that older organic matter, blown up out of fossil lake sediments was incorporated into varnish, the most likely sources of subvarnish organic matter are organisms like lichens and cyanobacteria that deposit organics in weathering rinds, as well as adjacent plants. This interpretation is supported by the stable carbon isotope values of the dated organics. $\delta^{13}C$ values ranged from -19.5 to -27.8, typical of the types of rock-surface and vascular organisms found in the macrofossil record during the Holocene and Pleistocene in the Great Basin.

Although organic matter was not found under varnish at BS9 in 1990, a recollection of varnish from a fossil bar revealed abundant organic matter in the weathering rind encapsulated by the varnish. The younger cation-ratio age for the varnish from BS9

collected in 1990 is still quite reasonable. The varnish at that collection site could have easily started to form substantially later than the varnish in the 1992 collection.

The 'dead' radiocarbon date for BS-43 is consistent with the older cation-ratio age for BS-35 and BS-43, as well as the more complex microstratigraphy found at these sites.

Interpretation of Cation-Ratio Age Estimates

Table 3 is broken down into different categories. The first category provides cation-ratio ages samples that were not radiocarbon dated, including the 1990 collection of BS9. The average and error for the age estimates are based on chemical measurements by inductively coupled plasma (ICP) and wavelength dispersive microprobe (probe) on varnishes on individual boulders. Keep in mind that the cation ratios are all calibrated by the radiocarbon timescale.

The cation ratios for Sites BS35 and BS41 are beyond the range of the radiocarbon calibration. The cation-ratio ages for the cation ratios from these sites, based on equation 1 are speculative, since there are no calibration points beyond 25 ka. However, the microstratigraphic analysis in Figures 2 and 3 would suggest that the age range provided by cation ratios is reasonable.

The last set of measurements in table 3 are the data used in the construction of the cation-leaching curve.

REFERENCES

Dorn, R.I. 1989. Cation-ratio dating: a geographic perspective. Progress in Physical Geography, v. 13, p. 559-596.

Dorn, R.I., Clarkson, P.B., Nobbs, M.F., Loendorf, L.L., and Whitley, D.S. 1992. Radiocarbon dating inclusions of organic matter in rock varnish, with examples from drylands. Annals of the Association of American Geographers v. 82, p. 136-151.

Dorn, R.I., Jull, A.J.T., Donahue, D.J., Linick, T.W., and Toolin, L.T. 1989. Accelerator mass spectrometry radiocarbon dating of rock varnish. Bulletin, Geological Society of America, v. 101, p. 1363-1372.

Dorn, R.I.. Cahill, T.A., Eldred, R.A., Gill, T.E., Kusko, B.H., Bach, A.J., and Elliott-Fisk, D.L. 1990. International Journal of PIXE, v. 1, 157-195.

Krinsley, D.H., Dorn, R.I., and Anderson, S.W. 1990. Factors that interfere with the age determination of rock varnish. Physical Geography, v. 11, p. 97-119.

Lowe, D.C., Brenninkmeijer, C.A.M., Manning, M.R., Sparks, R., and Wallace, G. 1988. Radiocarbon determination of atmospheric methane at Baring Head, New Zealand. Nature, v. 332, p. 522-525.

APPENDIX B

THE OHIO STATE UNIVERSITY

Byrd Polar Research Center

108 Scott Hall
1090 Carmack Road
Columbus, OH 43210-1002

Phone 614-292-6531
FAX 614-292-4697
Telex 4945696
OSUPOLAR

July 12, 1993

John Bell
Nevada Bureau of Mines and Geology
University of Nevada-Reno
Reno, Nevada 89557-0088

Dear John,

We have completed most of the analyses associated with the thermoluminescence dating of the sediment from the Monte Cristo Valley Trenches. Potassium analyses are outstanding; the OSU K/Ar lab is rather slow these days. The enclosed ages may change by 10% or perhaps 20% with the exact K content (current estimated value: 2.00%), which should arrive in the next month or so.

The TL ages for these sediments is a mixed bag and its difficult to evaluate the ultimate accuracy of the age estimates. In general, the precision and reproducibility of analysis was good, which is independent of the assumed accuracy. I advise a conservative use of these TL age estimates; regard the ages as possible maximums and finite estimates. Below I discuss each individual analysis and my favored age assessment.

F93-NV1: Trench 6; Age of the Penultimate Faulting Event

This sample of the upper 1 cm of a buried Av horizon yielded the most consistent age estimates. The fine-silt fraction yielded TL age estimates by the total and partial bleach methods, respectively of 12.6 ± 1.1 and 10.6 ± 1.0 ka. The concordancy of the total and partial bleach analyses indicates that this sediment was well light exposed prior to deposition and the resultant ages are probably finite estimates. The best estimate for tectonic burial of this horizon is 11 ± 2 ka.

F93-NV3: Trench 3 North; Age of Penultimate Faulting Event

Sample from the upper 1-2 cms of a gypsized Av horizon. This sampled yielded the erroneous age of 128 ± 9 ka. The identification of an Av horizon at this site is suspect. Age reflects the level of inherited TL from unlight exposed colluvium, providing an absolute maximum on faulting.

F93-NV4: Trench 3 North; Age of Penultimate Faulting Event

Sample from upper most distal-colluvium associated with the penultimate faulting event. The fine-silt fraction yielded TL age estimates by the total and partial bleach methods, respectively of 21. 4 ± 2.0 and 25.3 ± 2.9 ka. The partial bleach analysis showed unusual behavior and should not be used in the final age assessment. This faulting event may be 21 ± 4 ka or younger.

T · H · E
OHIO
STATE
UNIVERSITY

Byrd Polar Research Center

108 Scott Hall
1090 Carmack Road
Columbus, OH 43210-1002

Phone 614-292-6531
FAX 614-292-4697
Telex 4945696
OSUPOLAR

F93-NV6: Trench 6; Age of the Pre-Penultimate Faulting Event

Sample of distal wedge of pre-penultimate faulting event. The fine-silt fraction yielded the total bleach age of 25.1 ± 4.0 ka. This may be a maximum estimate for the timing of faulting.

The analysis from Trench 6 are stratigraphically consistent and I have higher confidence that ages may be finite age estimates. Analyses from Trench 3 are problematic and require more work to determine if F93-NV4 yielded a finite estimate.

John, additional resources and time would be needed to sort out Trench 3 chronology and strengthen the chronology at Trench 6. We will try to analyze more samples, particularly from trench 3, with the limited time and resources available in the lab this summer. Let me know what you think and how these age jive with your radiocarbon results. I determined these analysis blind....without knowing what to expect!

I will be away in the Russian Arctic from July 19 to Sept. 4; the main reason I writing you with the results. I would like to touch base with you in the fall so we can further sort out these ages. There is some sense in them....somewhere!

Have a good summer.

Best Wishes,

Steve

Steve Forman

P.S. Invoice for four TL ages; pay at your will

Table 1: Thermoluminescence data and age estimates for samples collected from Monte Cristo Valley Trenches, Nevada

Field No.	Lab sample No.	Strat. Unit	Equivalent Dose Method[1]	Light Exposure[2]	Temperature (°C)[3]	Equivalent Dose (grays)	TL age est. (ka)[4]
F93-NV1	OTL426	Buried Av	TL-Total Bleach	16h sun	300-400	63.4 ± 3.6	12.6 ± 1.1
			TL-Part. Bleach	1h	300-400	58.2 ± 3.4	10.6 ± 1.0
F93-NV3	OTL427	Buried Av	TL-Total Bleach	16h sun	250-400	570.8 ± 10.1	128 ± 9**
F93-NV4	OTL433	Colluvium	TL-Total Bleach	16h sun	250-400	78.3 ± 4.9	21.4 ± 2.0
			TL-Part. Bleach	1h	280-310	92.5 ± 9.7	25.3 ± 2.9**
F93-NV6	OTL432	Colluvium	TL-Total Bleach	16h sun	270-400	100.9 ± 3.1	25.1 ± 2.0

****Problematic analysis; do not use in final age assessment.**

[1]All TL measurements were made with a 5-58 filter (blue wavelengths) and HA-3 filters in front of the photomultiplier tube. Samples were preheated to 124 °C for 2 days prior to analysis.

[2]Hours or minutes of light exposure to define residual level. "Sun" is natural sunlight in Columbus, Ohio.

[3]Temperature range used to calculate equivalent dose.

[4] All errors are at one sigma and calculated by averaging the errors across the temperature range.

APPENDIX C

SYMPOSIUM 1: LATEST PLEISTOCENE AND HOLOCENE SURFACE FAULTING, BASIN AND RANGE (I)
Reno Hilton, Adelphi, 8:10 A.M.

Craig M. dePolo and Alan Ramelli, Presiding

INTRODUCTION: Craig M. dePolo ..... 8:10 A

1 P. A. Pearthree*, K. A. Demsey, S. Hecker: THE LONGER-TERM CONTEXT OF THE NEVADA SEISMIC BELT: PATTERNS OF HOLOCENE-LATEST PLEISTOCENE FAULTING IN CENTRAL NEVADA [006173] ..... 8:20 A

2 Michael N. Machette*, Kathleen M. Haller, Kelvin R. Berryman: PREHISTORIC MOVEMENT ALONG THE 1915 PLEASANT VALLEY FAULT ZONE AND IMPLICATIONS FOR THE CENTRAL NEVADA SEISMIC BELT [021829] ..... 8:40 A

3 John W. Bell*: BEHAVIOR OF LATE QUATERNARY AND HISTORICAL FAULTS IN THE WESTERN BASIN AND RANGE PROVINCE [006189] ..... 9:00 A

4 Alan R. Ramelli*, Craig M. dePolo: EXAMPLES OF HOLOCENE AND LATEST PLEISTOCENE FAULTING IN NORTHERN AND EASTERN NEVADA [004739] ..... 9:20 A

BREAK ..... 9:40 A

5 William R. Lund*: SUMMARY OF HOLOCENE SURFACE FAULTING AND FAULT SEGMENTATION, WASATCH FAULT ZONE, UTAH [006172] ..... 10:00 A

6 David B. Mason*, Robert B. Smith: PALEOSEISMICITY OF THE INTERMOUNTAIN SEISMIC BELT FROM LATE QUATERNARY FAULTING AND PARAMETER SCALING OF NORMAL FAULTING EARTHQUAKES [006178] ..... 10:20 A

7 James P. McCalpin*: SPATIAL/TEMPORAL PATTERNS OF QUATERNARY FAULTING IN THE SOUTHERN LIMB OF THE YELLOWSTONE-SNAKE RIVER PLAIN SEISMIC PARABOLA, NORTHEASTERN BASIN AND RANGE MARGIN [006171] ..... 10:40 A

8 Peter L.K. Kneupfer*: LATE QUATERNARY BASIN-RANGE FAULTING NORTH OF THE EASTERN SNAKE RIVER PLAIN, IDAHO [006182] ..... 11:00 A

9 M. A. Hemphill-Haley*, G. A. Simpson, D. N. Lindberg, G. F. Craven, G. A. Carver: LATEST PLEISTOCENE AND HOLOCENE TECTONIC DEFORMATION ALONG THE NORTHWESTERN MARGIN OF THE BASIN AND RANGE PROVINCE, SOUTHEASTERN AND SOUTH-CENTRAL OREGON [005571] ..... 11:20 A

10 Silvio K. Pezzopane*, Ray J. Weldon II: PALEOSEISMOLOGY OF LATEST PLEISTOCENE AND HOLOCENE FAULT ACTIVITY IN CENTRAL OREGON [006176] ..... 11:40 A

SYMPOSIUM 1: LATEST PLEISTOCENE AND HOLOCENE SURFACE FAULTING, BASIN AND RANGE (II)
Reno Hilton, Adelphi, 1:20 P.M.

Michael Machette and John Bell, Presiding

1 William A. Bryant*: HOLOCENE FAULTING IN THE WESTERN BASIN AND RANGE, CALIFORNIA [006174] ..... 1:20 P

2 W. D. Page*, T. L. Sawyer, M. K. McLaren, W. U. Savage, J. Wakabayashi: THE QUATERNARY TAHOE-MEDICINE LAKE TROUGH: THE WESTERN MARGIN OF THE BASIN AND RANGE TRANSITION, NE CALIFORNIA [005046] ..... 1:40 P

3 John Wakabayashi*, W. D. Page: QUATERNARY FAULTING OF BASALT FLOWS ON THE MELONES AND ALMANOR FAULT ZONES, NORTH FORK FEATHER RIVER, NORTHEASTERN CALIFORNIA [004296] ..... 2:00 P

4 Malcolm M. Clark*, Alan R. Gillespie: VARIATIONS IN LATE QUATERNARY BEHAVIOR ALONG AND AMONG RANGE-FRONT FAULTS OF THE SIERRA NEVADA, CALIFORNIA [006184] ..... 2:20 P

5 Craig H. Jones*, Steven G. Wesnousky: IMPLICATIONS REGARDING THE TEMPORAL AND SPATIAL VARIATION OF STRESS IN THE SOUTHWESTERN BASIN AND RANGE FROM OBSERVATIONS OF SLIP PARTITIONING [002417] .... 2:40 P

BREAK ..... 3:00 P

6 J. S. Noller*, M. C. Reheis: STYLE OF DEFORMATION ALONG THE DEATH VALLEY-FURNACE CREEK FAULT ZONE AND OTHER FAULTS IN THE SOUTHERN WALKER LANE, NEVADA AND CALIFORNIA [024837] ..... 3:20 P

7 Larry W. Anderson*, Daniel R. O'Connell: LATE QUATERNARY FAULTING AND HISTORIC SEISMICITY IN THE WESTERN LAKE MEAD AREA, NEVADA, ARIZONA, AND CALIFORNIA [006177] ..... 3:40 P

8 Stephen L. Salyards*: SEISMIC HAZARD ANALYSIS OF THE RIO GRANDE RIFT IN NEW MEXICO [006175] ..... 4:00 P

9 K. I. Kelson*, M. A. Hemphill-Haley, I. G. Wong, J. N. Gardner, S. L. Reneau: PALEOSEISMOLOGIC STUDIES OF THE PAJARITO FAULT SYSTEM, WESTERN MARGIN OF THE RIO GRANDE RIFT NEAR LOS ALAMOS, NM [005044] ..... 4:20 P

10 Daning Wu*, Ronald L. Bruhn: GEOMETRY OF ACTIVE NORMAL FAULTS AND ITS IMPLICATION TO FAULT GROWTH [017870] ..... 4:40 P

POSTER SYMPOSIUM 1: LATEST PLEISTOCENE AND HOLOCENE SURFACE FAULTING, BASIN AND RANGE
CONVENERS: CRAIG DEPOLO AND ALAN RAMELLI
Reno Hilton, Goldwyn Ballroom, 9:00 A.M. - 12:00 Noon

Authors will be present from 9:30 to 12:00 noon

Michael N. Machette*, Kathleen M. Haller, Richard L. Dart: THE UNITED STATES MAP OF MAJOR ACTIVE FAULTS [005451] ..... Booth 1

Charles W. Jennings, George J. Saucedo*: NEW FAULT ACTIVITY MAP OF CALIFORNIA [006186] ..... Booth 2

John C. Dohrenwend*, Barry C. Moring: RECONNAISSANCE PHOTOGEOLOGIC MAP OF LATE TERTIARY AND QUATERNARY FAULTS IN NEVADA [002334] ..... Booth 3

Kathleen M. Haller*, Richard L. Dart, Michael C. Stickney: A COMPILATION OF MAJOR ACTIVE FAULTS FOR PARTS OF MONTANA AND IDAHO [005460] ..... Booth 4

Suzanne Hecker*: RATES AND PATTERNS OF HOLOCENE-LATEST PLEISTOCENE FAULTING, EASTERN BASIN AND RANGE, UTAH [025175] ..... Booth 5

C. M. Menges*, P. A. Pearthree: TEMPORAL AND SPATIAL PATTERNS OF LATE PLEISTOCENE-HOLOCENE FAULTING IN ARIZONA [004955] ..... Booth 6

Donald L. Wells*: ANALYSIS OF PRIMARY AND SECONDARY SURFACE FAULTING ASSOCIATED WITH HISTORICAL NORMAL AND STRIKE-SLIP EARTHQUAKES [024913] ..... Booth 7

Eutizio Vittori, A. M. Michetti*, David B. Slemmons, Gary Carver: STYLE OF RECENT SURFACE DEFORMATION AT THE SOUTH END OF THE OWENS VALLEY FAULT ZONE, EASTERN CALIFORNIA [002414] ..... Booth 8

S. J. Caskey*, S. G. Wesnousky, P. Zhang, D. B. Slemmons: REINVESTIGATION OF FAULT TRACE COMPLEXITY AND SLIP DISTRIBUTION FOR THE 16 DECEMBER 1954 FAIR VIEW PEAK (Ms = 7.2) AND DIXIE VALLEY (Ms = 6.8) EARTHQUAKES, CENTRAL NEVADA [002433] ..... Booth 9

Alessandro M. Michetti*, Steven G. Wesnousky: HOLOCENE SURFACE FAULTING ALONG THE WEST FLANK OF THE SANTA ROSA RANGE (NEVADA-OREGON) AND THE POSSIBLE NORTHERN EXTENSION OF THE CENTRAL NEVADA SEISMIC BELT [002402] ..... Booth 10

Thomas L. Sawyer*, W. D. Page, Mark A. Hemphill-Haley: RECURRENT LATE QUATERNARY SURFACE FAULTING ALONG THE SOUTHERN MOHAWK VALLEY FAULT ZONE, NE CALIFORNIA [006183] ..... Booth 11

Sally F. McGill*: LATE QUATERNARY SLIP RATE OF THE OWL LAKE FAULT AND MAXIMUM AGE OF THE LATEST EVENT ON THE EASTERNMOST GARLOCK FAULT, S. CALIFORNIA [003974] ..... Booth 12

M. A. Hemphill-Haley*, T. L. Sawyer, I. G. Wong, P.L.K. Knuepfer, S. L. Forman, R. P. Smith: LATE QUATERNARY FAULTING ALONG THE SOUTHERN LEMHI FAULT, SOUTHEASTERN IDAHO: A COMPLEX SEGMENTATION HISTORY [005572] ..... Booth 13

Dean A. Ostenaa*, Ralph E. Klinger, Daniel R. Levish: HOLOCENE FAULTING ON THE MISSION FAULT, NORTHWEST MONTANA [006060] ..... Booth 14

Susan S. Olig*, William R. Lund, Bill D. Black: EVIDENCE FOR MID-HOLOCENE SURFACE RUPTURE ON THE OQUIRRH FAULT ZONE, UTAH [005587] ..... Booth 15

J. R. Unruh, J. S. Noller*, W. R. Lettis, I. G. Wong, T. L. Sawyer, J.D.J. Bott: QUATERNARY FAULTS OF THE CENTRAL ROCKY MOUNTAINS, COLORADO: A NEW SEISMOTECTONIC EVALUATION [005041] ..... Booth 16

Edward W. Collins*, Jay A. Raney: QUATERNARY FAULTS OF WEST TEXAS [006180] ..... Booth 17

APPENDIX D

BEHAVIOR OF LATE QUATERNARY AND HISTORICAL FAULTS IN THE WESTERN BASIN AND RANGE PROVINCE.

BELL, John W., Nevada Bureau of Mines and Geology, University of Nevada, Reno, NV 89557.

Quaternary stratigraphic relations and exploratory trenching in zones of historical surface faulting in the western Basin and Range Province suggest that faults with historical surface ruptures have similar, and in some cases lower, long-term (late Quaternary) and short-term (Holocene) slip rates than other adjacent and regional non-historical Quaternary faults. In the 1954 Dixie Valley earthquake (M6.8) zone, the range-front and piedmont faults collectively record a late Quaternary (200 ka) slip rate on the order of 0.2 mm/yr and a Holocene (7-12 ka) slip rate of 0.5-0.8 mm/yr. The principal segment of the 1932 Cedar Mountain earthquake (M7.2) zone has an estimated latest Quaternary (25-35 ka) slip rate of 0.2-0.7 mm/yr and a Holocene (6-13 ka) slip rate of 0.3-0.7 mm/yr. The 1954 Rainbow Mountain earthquakes (M6.6 and M6.8) and 1954 Fairview Peak earthquake (M7.1) zones have late Quaternary slip rates that are lower (<0.1 mm/yr), and although there are adjacent Holocene faults, neither zone shows surficial evidence of a previous Holocene event as do the first two zones. The 13 ka Lahontan shoreline at Rainbow Mountain is displaced only by the 1954 faulting, and the main segment of the Fairview Peak zone is overlain by a late Pleistocene (60-120 ka) alluvial fan which is offset by only the 1954 event.

Geologic uncertainties associated with distributive rupture patterns and with vertical to horizontal slip ratios may influence the estimates. Given these uncertainties, however, the slip rates for these five historical zones are not significantly different than those estimated for most other major non-historical faults in the region, especially if all faults are compared on the basis of non-historical slip. An important observation is that the central Nevada seismic belt is not unique based on slip rates. The greatest slip rates in the central and western Nevada region are associated with the Sierra Nevada frontal fault zone and the northern Walker Lane (Pyramid Lake) fault zone where Holocene slip rates are ≥ 1 mm/yr. Based on a comparison of Holocene and late Quaternary rates, many, but not all, historical and non-historical zones show evidence of temporal clustering.

ANALYSIS OF THE SEISMIC HAZARD OF FAULTS IN NEVADA

DEPOLO, Craig M., Nevada Bureau of Mines and Geology,
University of Nevada, Reno, NV, 89557

Major Quaternary faults throughout Nevada were analyzed to estimate characteristic earthquake (CE), maximum credible earthquake (MCE), slip rate, and the average recurrence of the CE. Earthquake sizes were estimated using historical seismicity, the fault zone length, maximum surface displacement, seismic-moment estimates, and consideration of earthquakes from the historical record. The CE is the expected or "best guess" event for a fault and is associated with a recurrence interval whereas the MCE is a physical maximum that can reasonably be associated with the fault. Slip rates are estimated from offset Quaternary units, or a relative comparison of tectonic geomorphology with faults with known slip rates. To estimate the average frequency or recurrence of the CE, an assumption is made that all of the deformation along these faults occurs during these events, and that these events have a periodic recurrence. This allows the estimation of earthquake recurrence by focusing on the time interval required to accumulate the strain released during the CE. This assumption is made because there is very little direct data of the recurrence intervals of most faults in Nevada (e.g., trenching studies, etc.). The results of this study suggest that the magnitudes associated with faults in Nevada range from 6.6 to about 8, with most values around 7 to 7.3. Magnitude estimates obtained from this study are considered to have an uncertainty of about 1/4 a magnitude unit. There is much less confidence associated with the earthquake recurrence estimates because there is significant uncertainty associated with the slip rate estimates, including the possibility that these rates are highly variable through time, as suggested by temporal clustering of earthquake events. This study indicates that there is a significant seismic hazard throughout the state, in contrast to the distribution of historical earthquakes which have been concentrated in western Nevada.

APPENDIX E

DISTRIBUTED SURFACE FAULTING FROM THE 1932 CEDAR MOUNTAIN EARTHQUAKE, WEST-CENTRAL NEVADA: SEISMIC HAZARD IMPLICATIONS FOR THE BASIN AND RANGE PROVINCE

Craig M. dePolo, John W. Bell, and Alan R. Ramelli

Nevada Bureau of Mines and Geology
Mackay School of Mines
University of Nevada, Reno

October 1, 1993

Submitted to GEOLOGY

Abstract

The 1932 Cedar Mountain earthquake (M_s 7.2) in west-central Nevada was a complex earthquake with distributed surface ruptures. The extent and breadth of surface rupturing associated with this event would have been difficult to predict using standard fault analysis techniques. Surface ruptures were very discontinuous and occurred along several different faults, in three different valleys. At least thirty-seven surface breaks occurred over an area 60 km long and up to 14 km wide. These breaks ranged from minor surface fissuring to ruptures up to 5.6 km long and with up to 2 m of right-lateral displacement.

Distributive surface rupturing is not unique to the 1932 Cedar Mountain earthquake. Several other earthquakes in the Basin and Range province have similarly caused surface rupture of multiple faults over broad areas. The possibility of distributed rupture events should therefore be considered in seismotectonic analyses in the Basin and Range province. Although complicated, distributed surface ruptures can be modeled both deterministically and probabilistically in assessing earthquake hazard.

Introduction

Complex, distributive earthquakes are common in the Basin and Range province, but are difficult to model given current seismotectonic approaches. The 1932 Cedar Mountain, Nevada earthquake (fig. 1) is a little known, but excellent example of this behavior, and illustrates some problems involved in modeling paleoseismic behavior and assessing earthquake hazard.

Numerous techniques have been developed to scale the estimated size of earthquakes (Slemmons, 1977, 1984; dePolo and Slemmons, 1990; Coppersmith, 1991). Implicit in many of these techniques is the assumption that earthquake ruptures follow singular, discrete faults or segments, forming simple rupture patterns, and allowing straightforward measurement of fault lengths and displacements. Although this simple fault rupture approach has been successfully employed in many paleoseismic analyses, it does not adequately model distributed, multiple-fault ruptures.

Several parameters typically used to estimate earthquake size are directly dependent on rupture pattern: surface-rupture length, rupture area, seismic moment, and maximum surface displacement. Variations in rupture dimensions can lead to significant differences in earthquake size estimates. For example, rupture of multiple faults can affect rupture length and displacement along overlapping faults can affect maximum surface displacement. Additionally, other fault activity parameters (e.g., earthquake recurrence intervals, slip rates, moment rates) can also be affected by distributed rupture patterns.

The 1932 Cedar Mountain earthquake (M_s 7.2) was a dominantly right-lateral event with surface ruptures widely distributed over an area roughly 14 by 60 km (fig. 1 and table 1). The event involved many different faults in three valleys, with the longest zone of faulting only about 16 km long. This paper reviews pertinent aspects of the 1932 earthquake and discusses ways to handle distributed earthquakes in seismic hazard analyses.

Gianella and Callaghan (1934a) visited the 1932 earthquake area shortly after the event and mapped and described most of the known surface breaks. Molinari (1984) studied the regional geology of the rupture area, described additional ruptures, and suggested that significant surficial deformation took place as folding, producing an incomplete surficial slip record. Doser (1988) modeled global body waveforms and concluded that the earthquake was composed of at least two right-lateral subevents, one to the north and one to the south. Our studies include detailed examination of surficial ruptures and deposits, detailed displacement measurements, and exploratory trenching. Low-sun-angle photography (scale 1:12,000) taken over the entire

rupture zone allowed more complete mapping of surface ruptures (fig. 2). From this study, additional ruptures were identified, and several previously mapped fissures were found to be no longer visible.

Seismotectonic Setting

The 1932 Cedar Mountain earthquake occurred in the western part of the extensional Basin and Range province, within the Walker Lane belt, a region of diverse topography and structural domains (Stewart, 1988). This belt extends from the Sierra Nevada eastward to the Walker Lane, a northwest zone across which the general topographic grain distinctly changes and along which discontinuous strike-slip faults of varying ages occur (Gianella and Callaghan, 1934b; Locke and others, 1940; Hardyman and Oldow, 1991). The Walker Lane belt is partly characterized by wrench tectonics and has many strike-slip faults, commonly with conjugate northwest- or northeast-trending orientations. Lateral deformation is evidenced by large historical strike-slip earthquakes (e.g., 1872 Owens Valley earthquake), large strike-slip faults (e.g., Death Valley fault system), and geodetic studies (Savage, 1983; Savage and others, 1990). The 1932 earthquake, which lies along the eastern side of the Walker Lane belt, further attests to the significance of lateral deformation.

Quaternary fault patterns adjacent to the 1932 earthquake area can be divided into two types. On the west is a strong north-northwest-trending grain of right-lateral faults with secondary faults crossing between them (fig. 3); many of these were formed during the Miocene and have since been reactivated to varying degrees along different reaches (Ekren and Byers, 1984). To

the east is a north-northeast-trending pattern of normal faults, more typical of the central Great Basin (fig. 3).

The state of contemporary tectonic stress in the Cedar Mountains area is not well constrained, but has been inferred from seismicity and geodetic measurements. Earthquake focal mechanism studies by Vetter (1984, 1988, 1990) found that although there is some directional variability between events in this region, there is a persistent northwest-southeast-trending tension direction. In general aggreement with this, a trilateration network in the region (the Fairview network) was first surveyed in 1972, and during a six year period of observation, an extension direction of N78°W $\pm$11° measured (Savage, 1983).

Surface Rupture Pattern

Surface ruptures associated with the 1932 earthquake can be generally divided geographically into three areas: Gabbs Valley, Stewart Valley, and Monte Cristo Valley. Faulting in each valley had distinctive characteristics. Gabbs Valley had mostly normal surface faulting. Surface ruptures in Stewart Valley were very discontinuous, with both lateral and normal displacements. Faulting in Monte Cristo Valley was relatively continuous and was clearly dominated by right-lateral displacement.

Gabbs Valley

The northern part of the 1932 earthquake rupture area occurred in Gabbs Valley, a broad, 20 to 30 km wide valley with several fault-bounded, northeast-trending low hills in its southern

part. At least six principal surface breaks occurred in Gabbs Valley, ranging in length from 0.3 to 5.6 km, and in displacement from minor cracking to 30 cm of vertical offset (Table 1). These surface ruptures are generally northeast-striking and northwest-dipping, and are subparallel, with 2 to 7 km between breaks and an overall cross-strike width of 17 km. All the breaks in Gabbs Valley had essentially normal slip with minor lateral components along a few faults locally.

Most of the Gabbs Valley ruptures occurred along faults displaying evidence of prior Quaternary activity. At least two of the surface ruptures were small breaks (10 to 15 cm) at the base of significantly larger scarps, suggesting that some of these faults at times rupture with larger displacements than occurred in 1932.

In and adjacent to the small hills between Gabbs and Stewart Valleys, small, scattered normal breaks and fractures and one small right-lateral break had short lengths (generally <0.5 km in length) and fairly minor offsets ($<$ 10 cm). A gap in known surface faulting of about 9 km separates these minor breaks from those to the south in Stewart Valley.

Stewart Valley

Surface faulting in Stewart Valley was the most discontinuous and generally involved small offsets. Seven identified breaks in Stewart Valley were all fairly short ($<$ 1.5 km), had small displacements, and only parts are still visible today. In several cases, strike-slip displacement was noted or can be inferred from descriptions of echelon-stepping fracture patterns or

"molehills" (pushed up areas) described by Gianella and Callaghan (1934a). Vertical offsets were generally less than ~15 cm, although one rupture near Stewart Springs had between 30 and 46 cm of vertical offset over a short distance.

Stewart Valley is largely floored by folded and faulted Tertiary lacustrine sediments and some displacements were probably "absorbed" into further deforming these sediments (Molinari, 1984). This may accouont for the relative lack of surface ruptures in this area.

Monte Cristo Valley

The largest and most distinct surface ruptures occurred in Monte Cristo Valley. Most of these lie in a north-northwest-trending zone about 16 km long and 2 km wide. Within this belt, most breaks are northerly-trending and show clear evidence of strike-slip displacement. Minor faulting occurred outside this zone, mostly at the northern end. The northern end is located in the western piedmont of the Cedar Mountains, whereas most of the zone is in the eastern piedmont of the Pilot Mountains (fig. 1). The most pronounced surface rupturing occurred along a fault zone with well-developed geomorphic expression, including fault scarps, fault-line scarps, grabens, linear ridges, and a general change in drainage pattern from transport or deposition in stream channels to incision of stream channels due to relative uplift of the eastern side of the fault. Secondary faulting and folding around the main rupture zone also occurred.

At least fifteen ruptures are scattered along the western flank of the Cedar Mountains. Gianella and Callaghan (1934a) noted eleven generally north-trending breaks along an east-west road over

a distance of nearly 3 km; the most pronounced of these (over 850 m long) is near the easternmost part of this zone and had right-lateral displacement. Taken with other surface ruptures to the west, the breaks in northern Monte Cristo Valley have a cross-strike width of 8 km. South of these breaks, at least six N to N35°E surface ruptures with lengths of 0.5 to 1.5 km cut the Cedar Mountains piedmont. These ruptures had mostly normal displacement (offsets up to 65 cm), but a right-lateral component is evidenced by small topographic swells along some of the more northerly-trending parts of at least two breaks. Surface rupturing was probably continuous from the southern part of these breaks to faulting southward in Monte Cristo Valley, but evidence of this has been removed by fluvial erosion.

Surface rupturing of the Pilot Mountains piedmont consisted principally of two pronounced fault zones with consistent evidence of 1 to 2 m right-lateral offset. These fault zones exhibit nicely-developed microtectono-geomorphic features including right-laterally offset stream channels and bar and swale topography, swells and depressions due to minor steps in the fault trace, and echelon-ramped scarps. These are clearly the most continuous, robust surface ruptures from the 1932 earthquake, and appear to represent primary rupture. These northerly-striking fault zones are 2.5 and 4.5 km long, and are connected by a contractional pressure ridge at a left step of about 1 km. Several secondary breaks occur adjacent to the main ruptures. One pronounced secondary break is a graben zone about 2 km long, subparallel to the main ruptures. These secondary ruptures also have significant strike-slip components.

Near the north end of the central part of the Monte Cristo Valley ruptures, folds in Tertiary sediments, and possibly in mantling Quaternary alluvial deposits, appear to have been directly involved in rupturing during the 1932 earthquake. These folds have axes that end near the ends of distinct surface ruptures, suggesting some of the displacement was transferred into growth of the folds.

Discussion

Further insight into the mechanics of the 1932 earthquake can be gained by comparing the surface ruptures to seismological observations of the epicenter, waveform modeling, and background seismicity. The epicenter was in southern Gabbs Valley, within the northern part of the surface rupture zone (Byerly, 1985). Doser (1988) used this epicenter for waveform modeling, and defined at least two subevents. The first subevent, which would have nucleated at the hypocenter, was a north-striking right-lateral event with a slight easterly dip, if the nodal plane most parallel to the surface ruptures is chosen. The surface ruptures trend generally more northeasterly than this nodal plane by 10° to 20°, and had dominantly normal slip with only minor lateral slip. However, these ruptures, including those between Gabbs and Stewart Valley, have an overall north-south orientation. The second subevent located by Doser was 14 to 18 km south of the epicenter. Although located west of the surface ruptures, this event is poorly constrained in an east-west direction, and was more likely proximal to the surface ruptures in Stewart Valley (Doser, 1988). The 1932 earthquake appears to have begun in the northern part of the surface ruptures and propagated to the south with at least two successive subevents.

Many factors operating singularly or in combination are potentially responsible for the distributed nature of the 1932 surface ruptures. These include distribution and splaying of the rupture upwards into discontinuous multiple breaks, absorption of some ruptures into soft sediments and/or deforming these sediments, multiple ruptures along different faults, sympathetic slip on adjacent faults, and detachment within or between the bedrock or Tertiary sediments and volcanics. Evidence exists for secondary faulting, folding, and multiple subevents. Sympathetic displacement may have been induced by the static or dynamic deformational field of the 1932 earthquake. Detachment faults have been noted at the base of Tertiary sediments in the northern part of the rupture area, and within weaker airfall members of ashflow tuff units to the west of Gabbs Valley (Ekren and Byers, 1984; Hardyman, 1984). Although the subsurface Tertiary geology is poorly known, it is likely that ashflow tuffs underlie much of the rupture area.

It seems unlikely so many faults would rupture together characteristically. More likely, an earthquake in Gabbs Valley triggered one or more events in Stewart and Monte Cristo Valleys, and induced secondary and sympathetic movement on adjacent faults. Trenching studies in Monte Cristo Valley suggest that the style and size of the largest 1932 ruptures were typical of paleoevents. In Gabbs Valley, however, 10 to 15 cm surface breaks occurred in places at the base of paleoearthquake scarps up to one meter high.

The 1932 earthquake was not confined to a single fault zone, but rather involved several zones and had a distributed, discontinuous pattern at the surface. This is not unique in the Basin and Range province; the 1915 Pleasant Valley earthquake (M_s 7.6), the 1954 Fairview Peak-Dixie Valley earthquake sequence (M_s 7.2 and $\sim$6.8), and the 1959 Hebgen Lake earthquake (M_s 7.5)

ruptured multiple faults, and the 1954 Fairview Peak and 1986 Chalfant Valley (M_s 6.2) earthquakes had distributed surface rupture patterns (dePolo and others, 1989, 1991; see fig. 1). More recently, the 1992 Landers earthquake (M_s 7.5) in the Mojave Desert (adjacent to or transitional with the Basin and Range province) also involved as many as five faults.

Implications for Seismic Hazards

The 1932 Cedar Mountain earthquake is one of several historical earthquakes illustrating that distributed surface faulting must be considered in seismic hazard studies conducted within the Basin and Range province. The possibility of distributed earthquakes can be inferred from adjacent faults having very similar ages of displacement, either during a single event or for the overall paleoearthquake history, and from structural continuity and/or similarity with adjacent faults. Distributed earthquakes may not typically occur as characteristic events (i.e., events with highly similar rupture distributions and displacements during earthquakes). Alternatively, distributed earthquakes may be more random events, only occurring when conditions are right for extending a rupture in an unusual manner, or through triggering of adjacent subevents.

Precise timing constraints are needed to confidently determine the areal extent of surface rupture associated with paleoseismic events. Unfortunately, this is often not possible due to limitations of dating techniques, lack of suitable materials and opportunities for dating, and limited resources normally available, prohibiting the study of many faults in detail.

Difficulties in evaluating contemporanity of adjacent ruptures make it important to consider structural continuity and similarity. Structural continuity and similarity are especially useful in consideration of parallel structures being part of a distributed package. When faults respond to the same slip vector and show structural connections, it is more likely that they move at the same time.

The extent of surface rupturing (about 60 km) and maximum surface displacement (about 2m) associated with the 1932 event suggest that distributed events can be modeled. Considering magnitude versus rupture parameter relationships (e.g., dePolo and others, 1990), these values are reasonably consistent with the surface-wave magnitude of 7.2 (Abe, 1981), suggesting that the size of distributed earthquakes can be characterized if the overall dimensions of rupturing and maximum surface displacement can be determined.

Distributed surface rupture events can be modeled deterministically or probabilistically. If paleoseismic data suggest distributed rupture behavior, a deterministic framework can simply assume that all the faults involved are part of the same event; the estimated length could be adjusted appropriately and the largest surface displacement adopted for the group of faults. In a probabilistic framework, distributed events could be cast into the overall paleoseismic record for the faults, and these data used to calculate the probability of a distributed event occurring. If no paleoseismic data are available, structural relationships of a group of faults might be evaluated, using one or more historical distributed earthquakes as a guide to a reasonable model for a design earthquake. A deterministic approach would apply this model event directly,

whereas a probabilistic approach again could consider the likelihood of the event, perhaps using regional data. A probabilistic approach may be used on individual faults as well to judge the likelihood of a fault participating in a distributed event using paleoseismic and structural information as input data.

Conclusions

The 1932 Cedar Mountains earthquake had a widely-distributed, discontinuous surface-rupture pattern that involved several different faults in three different valleys. Surface ruptures from this event were scattered over 60 km. At least six surface breaks occurred in Gabbs Valley; these had inter-fault distances of 2 to 7 km, and an overall cross-strike width of 17 km. A 9 km gap in surface faulting occurs between the surface ruptures in Gabbs and Stewart Valleys. Surface breaks were discontinuous in Stewart Valley, and slip at the surface was potentially absorbed by deformation of relatively soft sediments. The most pronounced surface ruptures occurred in Monte Cristo Valley over a zone about 16 km in length, and maximum surface displacements were up to 2 m right lateral.

Distributed ruptures can be identified by examining the timing of paleoevents and examining the overall paleohistory of adjacent faults, and by judging their structural continuity and/or structural similarity with one another. If this activity is not characteristic of an area, a more random consideration may be necessary, considering the rupture of multiple structural or geometric segments. In more critical or high risk situations, a design event with a distributed nature may simply be assumed. The maximum length of surface rupturing and the maximum surface

displacement may be reasonable guides for estimating sizes of distributed earthquakes, although this would not always be the case, especially for more random events. If surface rupture zone length and maximum surface displacement do not jibe for distributed events, the larger of the two should probably be used, as the other may be incompletely expressed.

Distributed rupture earthquakes are common in the Basin and Range province and should be considered in seismotectonic analyses. Single-fault and/or fault segment magnitude estimates may underestimate the potential size of the event and can involve a wider swath of surface faulting hazard than would be anticipated. Although distributed ruptures are a severe complication in seismotectonic analyses, they must be considered, and can be modeled several ways.

References

Abe, K. 1981, Magnitudes of large shallow earthquakes from 1904 to 1980: Physics of the Earth and Planetary Sciences, v. 27, p. 72-80.

Byerly, P., 1935, The first preliminary waves of the Nevada earthquake of December 20, 1932: Bulletin of Seismological Society of America, v. 25, p. 62-80.

Coppersmith, K. J., 1991, Seismic source characterization for engineering analyses, in proceedings of the Fourth international conference on seismic zonation: Earthquake Engineering Research Institute, v. 1, p. 3-60.

dePolo, C. M., Clark, D. G., Slemmons, D. B., and Aymard, B. A., 1989, Historical Basin and Range province surface faulting and fault segmentation, in Schwartz, D. P. and Sibson , R. H. (Editors), Fault segmentation and controls of rupture initiation and termination: U. S. Geological Survey, Open-File Report. 89-315, p. 131-162.

dePolo, C. M., 1990, Estimating earthquake sizes in the Basin and Range province, western North America: perspectives gained from historical earthquakes, in High Level Waste Management 1, Proceedings: American Nuclear Society, p. 117-123.

dePolo, C. M., Clark, D. G., Slemmons, D. B., and Ramelli, A. R., 1991, Historical surface faulting in the Basin and Range province, western North America: implications for fault segmentation: Journal Structural Geology, v 13, p. 123-136.

dePolo, C. M., and Slemmons, D.B., 1990, Estimation of earthquake size for seismic hazards, in Krinitzsky, E.L. and Slemmons, D.B., edts., Neotectonics in earthquake evaluation: Geological Society of America, Reviews in Engineering Geology, V. III, p. 1-28.

Dohrenwend, J. C., 1982, Map showing late Cenozoic faults in the Walker Lake 1° x 2° quadrangle, Nevada-California: U.S. Geological Survey, Miscellaneous Field Studies Map, MF-1382-D, 1:250,000.

Doser, D. I., 1988, Source parameters of earthquakes in the Nevada seismic zone, 1915-1943: Journal Geophysical Research, v. 93, p. 15,001-15,015.

Ekren, E. B. and Byers, F. M., 1984, The Gabbs Valley Range - a well-exposed segment of the Walker Lane in west-central Nevada, in Lintz, J., edt., Western Geological Excursions: Geological Society of America Guidebook, v.4., p. 203-215.

Gianella, V. P. and Callaghan, E., 1934a, The Cedar Mountain, Nevada, earthquake of December 20, 1932: Bulletin Seismological Society America, v. 24, p. 345-377.

Gianella, V. P. and Callaghan, E., 1934b, The earthquake of December 20, 1932, at Cedar Mountain, Nevada, and its bearing on the genesis of Basin and Range structure: Journal of Geology, v. 42, p. 1-22.

Hardyman, R. F., 1984, Strike-slip, normal, and detachment faults in the Gillis Range, Walker Lane of west-central Nevada, in Lintz, J., edt., Western Geological Excursions: Geological Society of America Guidebook, v.4., p. 184-199.

Hardyman, R. F., and Oldow, J. S., 1991, Tertiary tectonic framework and Cenozoic history of the central Walker Lane, Nevada, in Raines, G. L., Lisle, R. E., Schafer, R. W., and Wilkinson, W. H., 1991, Geology and ore deposits of the Great Basin, symposium proceedings: Geological Society Nevada, v. 1, p. 279-301.

Locke, A., Billingsley, P. R., and Mayo, E. B., 1940, Sierra Nevada tectonic pattern: Bulletin Geological Society America, v. 51, p. 513-540.

Molinari, M. P., 1984, Late Cenozoic geology and tectonics of Stewart and Monte Cristo Valleys, west-central Nevada: University of Nevada - Reno, Masters thesis, 122 p.

Savage, J. C., 1983, Strain accumulation in western United States: Annual Review of Earth and Planetary Sciences, v. 11, p. 11-43.

Savage, J. C., Lisowski, M. and Prescott, W. H., 1990, An apparent shear zone trending north-northwest across the Mojave Desert into Owens Valley, eastern California: Geophysical Research Letters, v. 17, p. 2113-2116.

Slemmons, D. B., 1977, Faults and earthquake magnitude, in State of the art for assessing earthquake hazards in the United States: U. S. Army Engineers Waterways Experiment Station Miscellaneous Paper S-73-1, 129 p.

Slemmons, D. B., 1984, Evaluation of seismic hazards in earthquake-resistant design; identification and characterization of active faults, in Evaluation of seismic hazards in earthquake-resistant design: Earthquake Engineering Research Institute, Specialty Seminars on Earthquake Engineering, Publication No. 84-06, p. 1-17.

Stewart, J. H., 1988, Tectonics of the Walker Lane belt, western Great Basin: Mesozoic and Cenozoic deformation in a zone of shear, in Ernst, W.G., edt., Metamorphism and crustal evolution of the western United States: Rubey Volume VII, Prentice-Hall, publisher, p. 683-713.

Vetter, U. R., 1984, Focal mechanisms and crustal stress patterns in western Nevada and eastern California: Annales Geophysicae, v. 2, p. 699-710.

Vetter, U. R., 1988, Characterization of regional stress patterns in the western Great Basin using grouped earthquake focal mechanisms: Tectonophysics, v. 152, p. 239-251.

Vetter, U. R., 1990, Variation of the regional stress tensor at the western Great Basin boundary region from the inversion of earthquake focal mechanisms: Tectonics, v. 9, p. 63-79.

TABLE

Table 1 Surface ruptures from the 1932 Cedar Mountain, Nevada earthquake. Reported values are from Gianella and Callaghan (1934a) and dePolo (unpublished mapping). Numbers correspond to Figure 2. RL=right lateral, RN=right normal, N=normal, Ext.=extension.

FIGURES

Figure 1 Earthquakes discussed in this paper. The Walker Lane is shown as a dashed line and the Walker Lane belt from Stewart (1988) is shown with a diagonal-line pattern.

Figure 2 Surface ruptures from the 1932 Cedar Mountain earthquake. Numbers correspond to those in Table 1. Surface ruptures taken from Gianella and Callaghan (1934a), Molinari (1984), and dePolo (unpublished mapping).

Figure 3 Late Cenozoic fault pattern of the Cedar Mountain region. The surface rupture area of the 1932 earthquake is shaded. Faults taken from Dohrenwend (1982) and Dohrenwend (1991, written communication).

TABLE 1

RUPTURE #	STRIKE	LENGTH	SENSE OF DISPL.	MAXIMUM SURFACE DISPL.
1	N5-15°E	0.5 km	Ext.	$\leq$ 2 cm
2	~N54°E	0.7 km	N	1.3 cm
3	N12°E	5.6 km	N	10 cm
3A	N16°E	2.2-3.3 km	N	30 cm
4	N12°E	3.7 km	N	15 cm
5	N0-20°E	>335 m	RN?	cracks
6	N11°E	152 m	N	7.6 cm
6A	N2°E-N18°W	366 m	N	5 cm
7	N57°E	0.4 km	N	cracks
8	N15°E	~120 m	?	<1 cm?
9	N16°E	~1.4 km	N	7.6 cm
10	N17°E	488 m	Ext.	2.5 cm
11	N0°E	244 m	Ext./RL?	cracks
12	N15°E	549 m	N	10 cm
13	N20°W	?	RL	10's cm??
13A	N18°E	~1 km	N	30-46 cm
14	N15°W	?	N	20 cm
15	non-tectonic			
16	N10°E	?	?	1.9 cm
17	N9-18°W	640 m	RL	<<2 cm
18	N19°W-N8°E	1.4 km	RL/N?	?/15 cm?
18A	N7°E	567 m	RL/N?	?/2.5 cm?
19	N4°W	719 m	RL	?
20	N1°W-N40°E	853 m	RN/RL	?
21	N12°W	700 m	N	15 cm
22	N5°W?	?	RL/N?	0.5-1 m? RL
23	N10°W-N9°E	~9 km	RL/RN	1-2 m RL
24	N15°W	?	N	5 cm
25	N30°W	165 m	RN	~2.5 cm

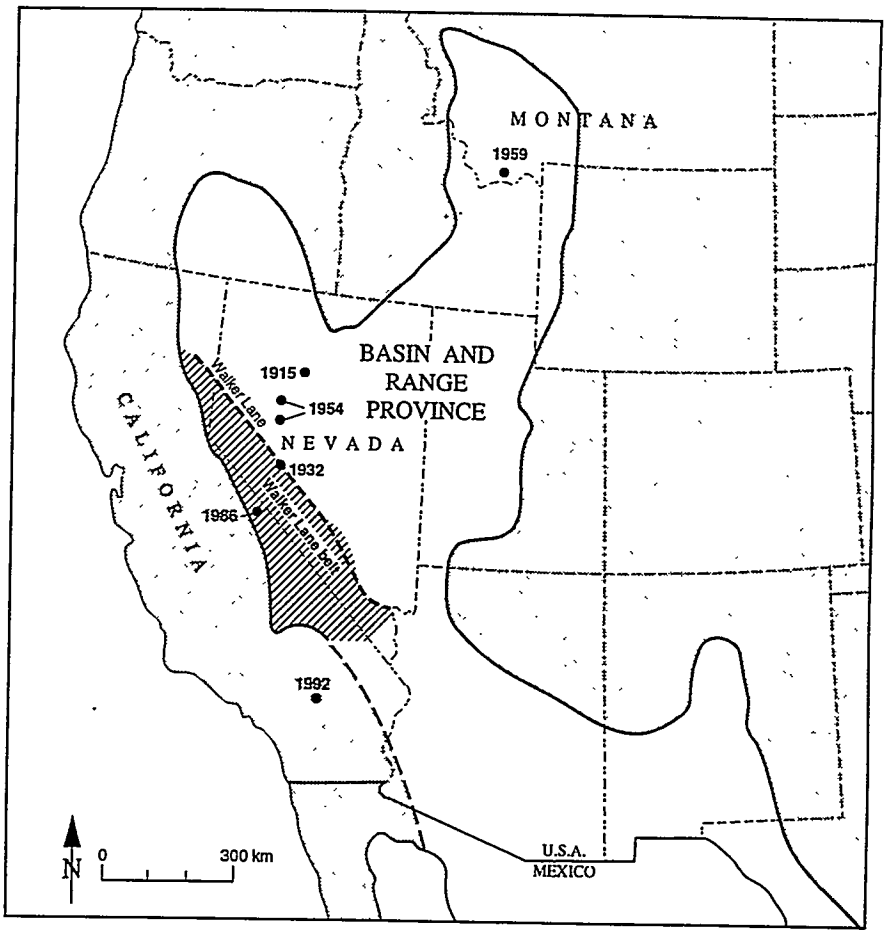
MONTANA
1959
BASIN AND
RANGE
PROVINCE
1915
1954
NEVADA
1932
Walker Lane
Walker Lane Belt
1986
CALIFORNIA
1992
N
0
300 km
U.S.A.
MEXICO

FIGURE 1

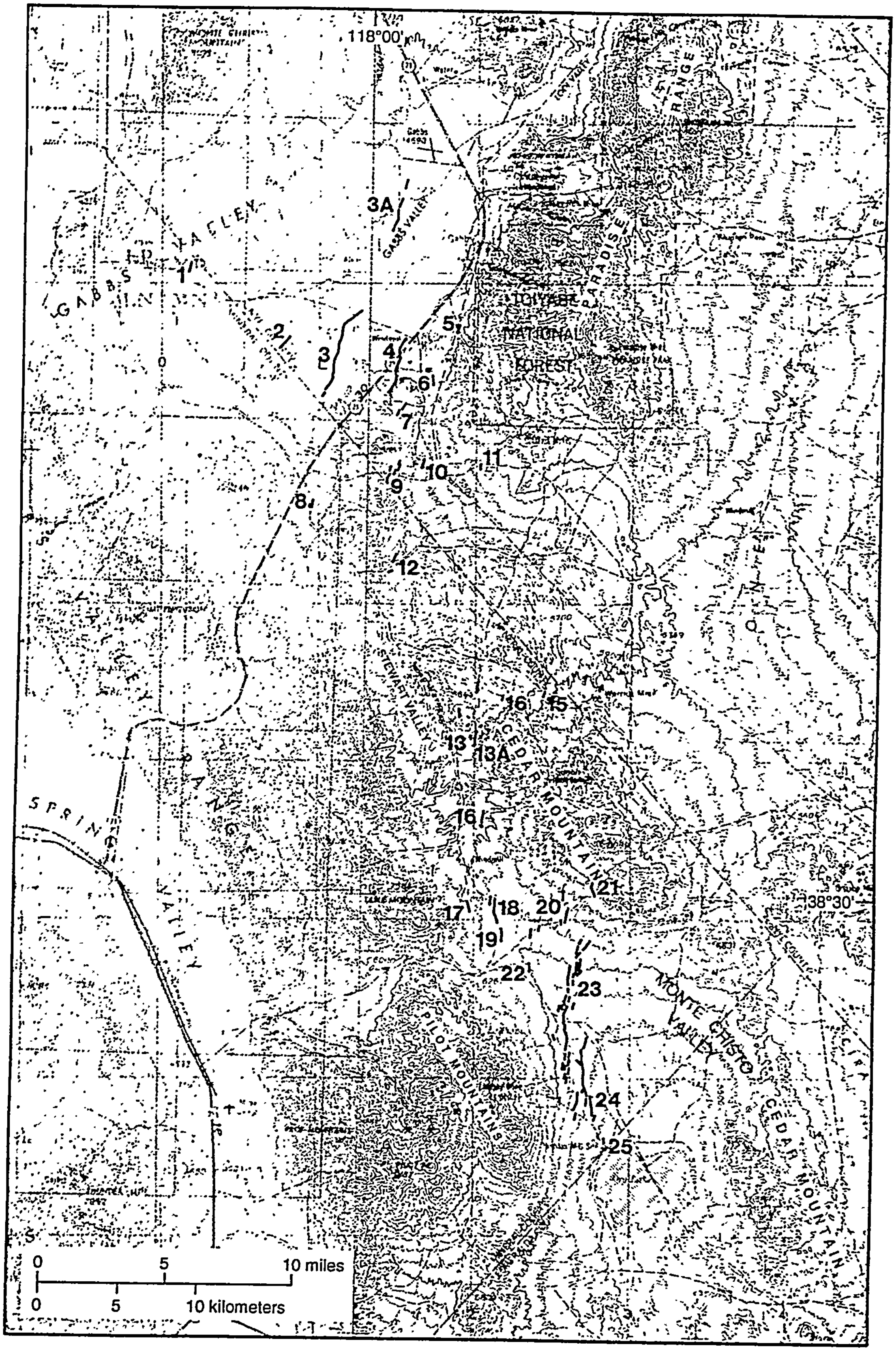
118°00'
3A
GABBS VALLEY
1
2
3
4
5
6
7
8
9
10
11
12
TOIYABE
NATIONAL
FOREST
PARADISE
RANGE
STEWART VALLEY
16
15
13
13A
CEDAR MOUNTAIN
16
SPRING
RANGE
VALLEY
21
38°30'
17
18
20
19
22
23
MONTE CRISTO VALLEY
PILOT MOUNTAINS
24
25
CEDAR MOUNTAIN
0
5
10 miles
0
5
10 kilometers

FIGURE 2

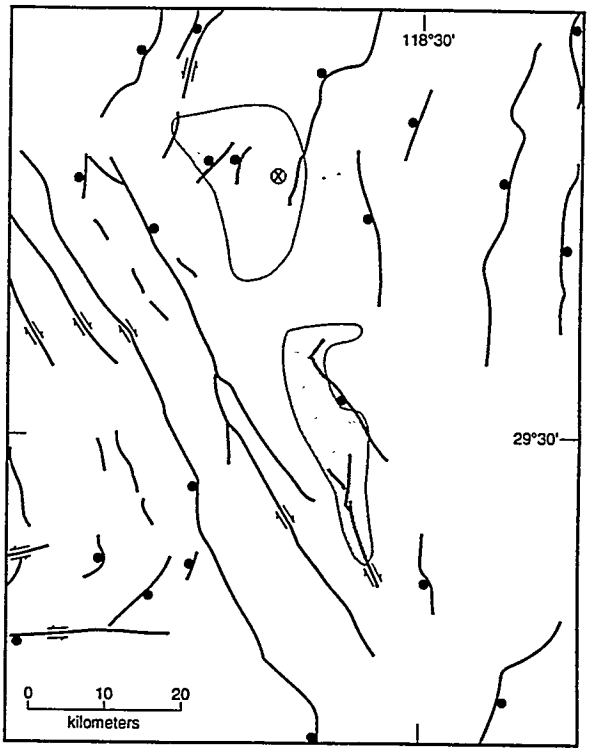

Late Cenozoic faults

1932 earthquake surface rupture area

⊗ Byerly's (1935) epicenter

FIGURE 3

APPENDIX F

3 May 1993

ASEISMIC SLIP ON AN EXTENSIONAL BASIN AND RANGE FAULT: EVIDENCE FOR TECTONIC CREEP

Manuscript submitted to the Journal of Geophysical Research

John W. Bell, Donald C. Helm, Alan R. Ramelli,
Craig M. dePolo, and Joanne L. Hoffard

Nevada Bureau of Mines and Geology
University of Nevada, Reno

ABSTRACT

Dilational ground cracks formed along a late Quaternary fault within the Pine Nut Mountains fault zone of western Nevada in the summer of 1988. Crack widths ranged from 1 to 2 cm and 21 individual fractures comprised a zone with an end-to-end length of 1 km. Detailed mapping and exploratory trenching indicated that the cracks propagated directly upwards along a major recently active fault plane. No seismic events were associated with the fracturing, and examination of catalogued seismicity indicated that the cracking occurred within a 10-km-long portion of the fault zone characterized by an unusually low level of seismicity compared to the entire fault zone. Based on several lines of direct and circumstantial evidence, the ground cracking is most likely the product of a short-lived aseismic tectonic creep event. Calculations show that seismic moment and stress drop were insufficient to attribute the cracking to coseismic slip or afterslip. A lack of any regional seismic event of $M > 3.5$ indicates that the cracking was not the result of dynamically triggered slip. Modeling of hydraulic conditions induced by nearby water-well pumping indicates that the fracturing was unlikely to be caused by vertical or horizontal hydraulic stresses. Ground-water levels had remained essentially unchanged for the seven years preceding the cracking. Theoretical radial horizontal displacements of 0.03 cm per pumping event and cyclic horizontal strains of $< 5.5 \times 10^{-5}$ are regarded as too small to have induced the ground fracturing. The creep fits no seismic or hydraulic model known for normal extensional faults. Based on seismic and hydraulic calculations, we believe that tectonic stress is the only plausible mechanism for the fracturing. We speculate that the fracturing was related to shallow aseismic creep along an easy- or free-slip portion of the fault zone situated between

fault segments which are seismically releasing strain. Simplistic comparisons indicate that the creep is somewhat similar to that observed along the central San Andreas fault system where creep and seismicity are related to frictional asperities along the fault.

INTRODUCTION

In July 1988, dilational ground cracks were discovered by local residents in the western foothills of the Pine Nut Mountains in western Nevada (Figures 1, 2). The cracks remained extremely fresh through November 1988 when this study was initiated (Figures 3, 4). The crack walls contained clast-and-impression sets which allowed precise measurement of amount and sense of displacement. Displacements were extensional in nature, with mean separations of about 1½ cm and maximum separations of about 2 cm. One location later showed 1-2 cm of right-lateral movement (Figure 5). No vertical displacements were observed.

Detailed surveying indicated that the cracks consisted of a series of predominantly left-stepping fractures collectively forming a curvilinear, north-trending zone with a total end-to-end length of about 1 km. The cracks were located along one of the numerous late Quaternary extensional faults in the Pine Nut Mountains fault zone [*Dohrenwend*, 1981], with this particular fault bounding the western margin of Fish Spring Flat, a small basin east of Carson Valley (Figure 2). The fractures cut both unconsolidated Quaternary alluvium and well-consolidated Tertiary

sedimentary rocks.

No local seismic events could be associated with the ground fracturing. Residents reported a felt earthquake in the spring of 1988, but a review of the catalogued seismicity at the University of Nevada Seismological Laboratory indicated that there was no significant local seismicity that could account for the fracturing. The area around the ground fracturing had in fact been aseismic for the historical and instrumental record periods.

We present here an analysis of surficial geologic and seismic data, together with a test for a possible hydraulic origin, which suggest that the fracturing was the result of an aseismic tectonic event. We evaluate first the possibility that the cracking could have been the result of seismic slip processes by calculating conventional seismic parameters (magnitude, moment, and stress drop) and then comparing these data with analogues. We find that the required parameters for seismically induced slip are insufficient to account for the cracking. We then model the theoretical horizontal strains induced by nearby water-well pumping, and we note that it is unlikely that the cracking was due to hydraulic strains which appear to be very low. Lastly, we speculate on possible tectonic origins based on our conclusion that the observed fault slip was most probably caused by fault slip related to a shallow aseismic creep event.

Types of Minor Fault Slip and Creep

Sylvester [1986] provided a useful nomenclature for different types of minor fault slip events that allows the genetic differentiation of small-scale movements which might otherwise be collectively classified as creep. In this classification, tectonic stresses may induce several types of minor fault movements: tectonic creep, preseismic slip, dynamically triggered slip, and afterslip. Nontectonic creep originates most commonly from hydraulically induced stresses such as ground-water pumping.

Well-documented cases of tectonic creep are uncommon, and are in general restricted to strike-slip faults, most notably the central and southern California (San Andreas) and Anatolian, Turkey fault systems. The reader is referred to *Wesson* [1988] for an extensive overview of creep phenomena and dynamics. The central San Andreas fault zone region has historically provided the most convincing evidence for tectonic creep. Creep along the fault was first noted by *Steinbrugge et al.* [1960] near Hollister, California where right-lateral movements on the order of 12 mm/year were recorded by creepmeters. Installation of additional instruments in this region since the 1960's has provided a substantial data set documenting the behavior of creep along the San Andreas, Hayward, and Calaveras faults [*King et al.*, 1973; *Nason*, 1973; *Wesson et al.*, 1973; *Johnston et al.*, 1977; *Evans et al.*, 1981]. Creep along the central portion of the San Andreas fault near Parkfield has also been instrumentally monitored [cf., *Savage and Burford*, 1973; *Bufe and Tocher*, 1974; *Schulz et al.*, 1982], and in southern California creep has been observed on the Imperial fault since the 1970's [cf., *Goulty et al.*, 1978; *Cohn et al.*,

1982]. Tectonic cracking near the left-lateral, strike-slip Garlock fault system has been described by *Zellmer et al.* [1985].

Tectonic creep on normal faults has not been well demonstrated, although several cases have been reported on the basis of geodesy. *Ruegg et al.* [1984] attributed geodetic movement across the Asal-Ghoubbet rift in East Africa to creep, and recent elevation changes across the Teton fault in western Wyoming are inferred to be the result of creep [*Sylvester et al.*, 1990]. In the Basin and Range province, cases of possible tectonic creep are inferred from historical benchmark changes coincident with mapped faults [*Gilmore*, 1989]. Some ground cracks and fissures in southern Nevada have been attributed to creep on the basis of spatial associations with known active faults [*Carr*, 1974; *Keaton and Miller*, 1992].

Preseismic slip, afterslip, and dynamically triggered slip, on the other hand, are common types of minor fault movements observed on both strike-slip and normal-slip faults. Instrumentally recorded creep has been observed precursory to moderate- to large-magnitude earthquakes [cf., *Nason*, 1973], and zones of preseismic creep are believed to interact with locked patches, or asperities, in defining locations and magnitudes of earthquakes along the San Andreas fault [*Wesson et al.*, 1973; *Bakun et al.*, 1980; *Tse et al.*, 1985]. Afterslip has frequently been detected along portions of the San Andreas system following moderate- to large-magnitude earthquakes [cf., *Burford*, 1972; *Harsh*, 1982], and extensional afterslip in the form of ground cracking occurred after the 1975 Oroville M5.9 earthquake [*Clark et al.*, 1976]. In the Basin and Range province, *Savage and Church* [1974] found that the 1954 Dixie Valley (M6.9)-Fairview

Peak (M7.1)-Rainbow Mountain (M6.6, 6.8) earthquakes were followed by regional geodetic deformation that amounted to about 5% of the coseismic slip. Ground cracking attributed to dynamically triggered slip has followed moderate- to large-magnitude earthquakes on the San Andreas system [*Allen et al.*, 1972; *Burford*, 1972; *Fuis*, 1982; *Sieh*, 1982]. Triggered slip is a poorly understood tectonic process, but it is believed to be related to transitory dynamic strains which exceed static strains on faults tens of kilometers from the epicenter [*Allen et al.*, 1972; *Sieh*, 1982]. The 1992 Landers earthquake (M7.5) triggered 1- to 2-cm-wide ground cracks on several Imperial Valley faults [*Sharp*, 1992], and it is believed to have triggered small- to moderate-magnitude seismicity on faults as far as 1250 km from the epicenter [*Reasenberg et al.*, 1992].

GEOLOGIC SETTING OF THE GROUND CRACKING

Regional Structural Setting

The Pine Nut Mountains are one of several major north-trending ranges east of the Sierra Nevada in the western Basin and Range province (Figure 1). Although wrench tectonics of the right-lateral Walker Lane belt influence the tectonic style throughout much of the western Basin and Range province [*Stewart*, 1988], geologic mapping indicates that Quaternary displacements on major faults in this region are predominantly normal, with most faults exhibiting down-to-the-

east throw [*Moore*, 1969].

In the eastern Carson Valley area (Figure 2), late Quaternary geologic structure is characterized by swarms of distributive-normal faults occurring in a 10-km-wide zone along the western flank of the Pine Nut Mountains [*Dohrenwend*, 1981, 1982; *Bell*, 1984]. This complex system of nested faults, here called the Pine Nut Mountains fault zone (PNMFZ), contains predominantly east-dipping faults. Carson Valley is a large structural graben bounded on the west by the Sierra Nevada (Genoa) fault zone (Figure 6). Gravity data [*Maurer*, 1984] indicate that a major west-dipping fault lies beneath Gardnerville about 8 km west of the study area; this is most likely the principal fault bounding the eastern side of the Carson Valley graben. The Pine Nut Mountain block is a horst bounded by east-dipping, listric-normal faults along which movement has resulted in back-rotation of individual blocks, an antithetic relation first suggested by *Moore* [1969].

Structural Setting of the Cracking

The cracking occurred directly along one of the largest (>30 m high) scarps among a set of late Quaternary step-faults within the PNMFZ (Figure 7). In Buckeye Wash (Figure 2), several of these faults offset mid- to late Holocene age wash terrace deposits. Structural-stratigraphic relations identified through detailed surficial mapping and exploratory trenching as part of this

study indicate that the most recent coseismic surface faulting event occurred less than 5,000 years ago. The Holocene scarps in Buckeye Wash have heights of about 1 m, displacements consistent with the scale of coseismic surface rupture typically accompanying earthquakes of $M > 6.5$ [cf., *Doser and Smith*, 1989]. The 1988 fractures followed a recent 30-cm-high scarp, or inflection on the larger compound scarp, which we have verified as a vertical fault displacement in the exploratory trench.

The set of easterly down-stepping faults displays a curvilinear trend to the northeast that is suggestive of sigmoidal bending. South of the unnamed wash at the southern end of the zone of cracking (Figures 2, 7), the fault along which the fracturing has propagated has a west-facing scarp, suggesting that it is a scissors fault. Fault scissoring and sigmoidal bending are commonly indicative of some measure of oblique- or strike-slip movement.

THE GROUND CRACKS

Distribution and Displacement

When we mapped the cracks in November 1988, the zone consisted of 21 individually separable and continuous cracks (Figure 8). The cracks had little end-to-end overlap and were predominantly left-stepping, particularly along the northern half of the zone; cross-step distances

ranged from 15 to 50 cm. The northern and southern terminations of the zone were abrupt with no significant diminishment in the size of crack dilation. Extensive ground surveys beyond the northern and southern terminations confirmed that the visible cracking was confined to the 1-km-long zone. The southern projection of the zone crossed several roads which showed no visible signs of offset. All other principal fault scarps within the Fish Spring Flat area were searched, but no evidence of movement was found.

Each of the 21 individual cracks showed consistent horizontal separations of between 1 and 2 cm irrespective of distance along the zone (Figure 8). One separation of 4.5 cm was observed, but we attributed its size to erosion. No vertical displacements were observed. The fresh preservation of the crack walls allowed precise measurements of horizontal slip directions to be made by matching offset clasts with corresponding impressions. Ten displacement vectors were measured along the principal fractures of the zone, and only purely dilational movements were noted during the initial survey. The azimuths of the slip vectors ranged from 90° to 101° with a mean of 95.6°, indicating that the dominant displacement direction was approximately east-west. These slip directions were independent of the strike orientation of the cracking, which ranged from nearly north-south along the middle and northern portions of the zone to northwest-trending in the southern portion of the zone. Thus, although we noted no lateral component across individual cracks during the initial survey, the slip geometry requires that the southern portion of the zone-- which strikes approximately N65°W-- must contain at least a small component of right-oblique slip in order to account for the east-west-oriented slip vector.

The cracking occurred during July 1988, based on conversations with local residents who

regularly traversed the area. One resident reported that the cracks continued to grow throughout late summer, but we were unable to verify this. The cracks were mapped in detail by us in November 1988 at which time we installed several simple extensometer and slip-direction control sites. We found no significant evidence of continued dilation following this initial investigation.

Three extensometer stations were constructed across the northern, central, and southern portions of the zone and monitored using a Soiltest mechanical extensometer calibrated to 0.0025 mm. The sites were measured three times until November 1989 when they were disturbed. No displacements greater than 1 mm (average operator error) were recorded during these resurveys. Paint stripes were sprayed across the cracks at several locations in November 1988. These sites were inspected several times through November 1989 when they were eroded. In March 1989 one paint stripe showed about 1-2 cm of right slip (Figure 5).

The zone of cracking was visually reexamined several times during 1990-92 to determine if any additional cracking had occurred, but none was found. In March 1989, the cracks were substantially weathered and subdued compared to their appearance in November, and by May 1989, the cracks were only locally visible as a discontinuous series of small holes beneath protective brush cover. Field observations in July 1991 and May 1992 confirmed that no additional cracking had occurred.

Exploratory Trenching

Exploratory backhoe trenching across one of the principal cracks in the central portion of the zone revealed that the surface crack, as well as several concealed cracks, propagated directly upward from a major late Quaternary fault (Figures 9, 10). The trench exposed a moderately dipping (~60°), 1-m-wide fault zone juxtaposing a sequence of late Quaternary colluvial deposits down against highly sheared and tilted late Tertiary sandstones and siltstones. The colluvial deposits consisted of reddish-brown, muddy, cobbly sands and gravels containing several paleosols, with the sequence capped by a strongly developed argillic soil. The base of the uppermost soil was offset about 30 cm by the most recent faulting event. The buried soils may represent earlier faulting events with each event having a displacement on the order of ½-1 m, if we interpret each colluvial unit to be a tectonically derived colluvial wedge.

Dilational openings were traceable from the ground surface to the bottom of the trench at about 3 m depth. Discontinuous dilational openings 4-5 cm in width were present along the dipping fault contact near the base of the trench and about 1½ m up from the base. At a depth of about 1.2 m below the surface a continuous, open crack 2-3 cm in width splayed from the dipping fault plane and extended vertically to the surface. About 20 cm east of this crack, a second 2-cm-wide vertical crack was found at a 1-m depth but did not extend to the surface. Older carbonate-filled fractures in the sediments near this second crack may be related to previous dilational events, although they could also be by-products of coseismic slip along the fault. As observed on the surface, no vertical offset was detected across cracks exposed in the trench

although the evidence was not conclusive due to the occurrence of the crack directly along the fault plane.

SEISMICITY

Plots of catalogued seismicity from the University of Nevada Seismological Laboratory for 1988 and for 1983-92 (Figures 11, 12) indicate that the cracking occurred along a portion of the PNMFZ having an unusually low level of seismicity in contrast to the fault zone as a whole. This is a persistent pattern for the entire catalogue period (1852-1992). During the 1983-92 period more than 800 events of $M>1$ were recorded within about a 30-km radius of the cracks, but virtually no activity was recorded along or near the 10-km-long PNMFZ segment containing the cracking (Figure 12). Regional seismograph station density is sufficient to ensure confident detection of $M>1$ events; the Buffalo Canyon station (BFC) is located 8 km southeast of the cracks. No events of $M>3.5$ occurred during 1988 within a 50-km radius of the cracks (Figure 11).

A portable microseismic array was deployed near the cracks by the University of Nevada Seismological Laboratory in January 1989 in an effort to detect small magnitude ($M<1$) earthquakes that may be associated with the cracking and be undetected by the regional network. Two portable recorders capable of detecting earthquakes of $M<0$ were installed; one was

located directly over the cracks and the other was located 1 km east of the cracks. The recorders were continuously operated for a four-day period, and the data obtained from this brief deployment showed no evidence of microearthquake activity in the vicinity of the cracks. However, since the arrays were deployed several months after the formation of the cracks, the results are regarded as inconclusive (Martha K. Savage, unpublished data, 1989).

Small-magnitude swarms in part characterize seismic activity along the PNMFZ, a pattern which has persisted for the entire instrumental record period [*VanWormer and Ryall*, 1980]. In April 1988, a M3.5 event located a few kilometers east of Carson City (Figure 12) was accompanied by two M2.7 earthquakes and a number of smaller magnitude events. This swarm is the closest temporal event that could be associated with the cracking, and it is most likely the event reported felt by Fish Spring Flat residents. However, as we show in a later discussion, this M3.5 event was of insufficient magnitude and moment to account for the cracking. A swarm in January 1991 was located 5 km northwest of the 1988 swarm, and it had dozens of $M<3$ earthquakes accompanying a main M4.6 event. Swarms occurred in 1976 and 1989 at Virginia City (VC on Figure 11), which lies along the northern portion of the PNMFZ. The 1989 sequence consisted of 20 events in the M1- M3 range and hundreds of microseismic events [*dePolo et al.*, 1992]. A 1978 swarm in Diamond Valley [DV on Figure 12; *Somerville et al.*, 1980] was located at the southern end of the PNMFZ where it structurally joins with the Sierra Nevada fault zone, an area that still exhibits clustered activity. Several other unstudied clusters are also evident in the southern portion of the PNMFZ.

A north-trending cross section which projects all recorded seismicity within a 14-km-wide zone along the PNMFZ (Figure 13) shows that an approximately 10-km-long fault section containing the ground cracks was aseismic during the period 1983-1992. In contrast, the 30-km-long sections of the zone to the north and south of the ground cracking show significant levels of seismicity, including several earthquakes of $M > 4$. The cross section indicates that event depths range from 0-15 km with numerous small-magnitude events occurring in the upper few kilometers. Shallow depths may be artifacts of the velocity model used to calculate depth (Diane M. dePolo, unpublished data, 1992), but many of these events have been verified as shallow. Microseismic arrays deployed over the 1989 Virginia City swarm, for example, confirmed depths in the range of 1-4 km [*dePolo et al.*, 1992].

DISCUSSION

An aseismic tectonic creep origin for the 1988 ground cracking is postulated on the basis of several lines of evidence: regional structural-tectonic relations, lack of local seismicity, calculated seismic moments and stress drops, and nontectonic (hydraulic) strain modeling. We present here a series of arguments demonstrating that the cracking was most probably the product of a short-lived creep event. We do not discuss alternative origins that we consider improbable, such as mass wasting.

Large-scale desiccation cracking [cf., *Neal et al.*, 1968] is ruled out on the basis of laboratory shrink-swell and clay content analyses performed on colluvium collected from the exploratory trench, and on the basis that the cracking also occurred in bedrock. The cracks are within Tertiary sandstone where exposed in the unnamed wash at the southern end of the zone (Figure 8). Although we have observed minor polygonal desiccation cracking in the shallow sediments of the basin floor, the extension of the cracking through bedrock precludes a desiccation origin.

Structural-tectonic relations

Given a normal faulting stress regime suggested by surficial geologic relations, the east-west dilation measured along the cracks (Figure 8) is consistent with the estimated tectonic stress orientation for this region. The north-south orientations of the distributive-normal fault swarms along the PNMFZ suggest that the regional extension direction (σ_3) is roughly east-west. This agrees with the stress orientation estimated by *Zoback* [1989] from dip-slip slickensides measured on the Genoa fault on the west side of the Carson Valley (Figure 6). However, as noted, an oblique-slip component of movement along the PNMFZ is also suggested by localized fault patterns, slip orientations of the cracks, and the offset paint stripe. There are also other indicators suggesting some measure of right-lateral slip in the region. Eight kilometers southeast of the study area, slickensides on bedrock surfaces along the PNMFZ locally have plunges of 60-70° to the north indicative of right-oblique slip. The focal mechanism for the April 1988

M3.5 Carson City earthquake (Figure 12) indicates that a preferred nodal plane would be a fault trending due north and having purely right-lateral displacement. This mechanism agrees with known mapped fault orientations, and the right-lateral, strike-slip character of the event is consistent with some other regional focal mechanisms, in particular, the 1978 Diamond Valley sequence [*Somerville et al.*, 1980].

Seismically induced slip

Earthquake magnitude and seismic moment (M_o) can be used to model the boundary conditions necessary for establishing a creep origin, and for determining if there was sufficient tectonic strain to attribute the cracking to coseismic slip, afterslip, or dynamically triggered slip. Fault dimensions and measured displacement can be used to calculate M_o [cf., *Aki*, 1966; *Brune*, 1968; *Hanks and Kanamori*, 1979] from the equation

$$M_o = \mu AD \qquad (1)$$

where μ is the shear modulus, A is the area of the fault rupture plane, and D is the average displacement. Calculated moments are dependent upon assumed depth of the rupture surface, and in this instance the total depth is poorly constrained. However, we can assume a shallow (1-3 km) depth for the fault slip based on several lines of evidence; this allows us to conservatively

estimate the minimum required seismic moment and stress drop.

We infer a shallow slip depth for several reasons. First, the depths depicted on the seismic cross section (Figure 13) indicate that many small-magnitude events were occurring within the upper few kilometers along the length of the PNMFZ, suggesting that a significant amount of seismic energy was being released at shallow crustal depths. The 1988 M3.5 earthquake at Carson City, which occurred shortly before the cracking, and the 1989 Virginia City earthquake swarm, which occurred shortly after the cracking, both had shallow depths (½ and 1-4 km, respectively). We believe that this activity is suggestive of a sequence of shallow crustal strain events along the PNMFZ.

Using a nominal value of 2×10^{11} dyne/cm^2 for the shear modulus of sedimentary rocks, a 2 cm nominal displacement for the cracking, and a fault rupture area determined by the 1 km mapped length of the cracking and the assumed 1-3 km depth for the fault slip surface, seismic moments of 6-18 x 10^{21} dyne-cm are derived from equation (1).

Seismic moment can be related to radiated seismic energy by a moment magnitude (M_w) scale [*Hanks and Kanamori*, 1979] where

$$M_w = 2/3 \log M_o - 10.7 \qquad (2)$$

Using the calculated range in M_o of 6-18 x 10^{21} dyne-cm from equation (1), corresponding

moment magnitudes on the order of M_w 3 3/4 to 4 are derived from equation (2). These are the minimum magnitude earthquakes theoretically necessary to produce coseismic ruptures having the dimensions of these cracks. If larger rupture planes are assumed, i.e., the depth of slip was assumed to be greater than 3 km, slightly larger moments and magnitudes would be calculated. For example, using a 10 km depth for the fault plane in (1) would yield a moment of 6×10^{22} dyne-cm and correspond to a M_w 4.3 earthquake.

Based on the lack of $M>2$ earthquakes within a 20-km radius of the zone of cracking and the absence of any recorded seismicity along the cracks, we find that there was insufficient seismic moment attributable to seismic faulting along the PNMFZ to have produced coseismic cracking. This conclusion is supported by historical seismicity in other portions of the Basin and Range province where magnitude-rupture relations indicate that moderate-magnitude earthquakes are required to produce coseismic surface rupture as either measurable fault slip or as ground cracking. Comparisons of geologic and body-wave moments for historical earthquakes indicate that a minimum magnitude for coseismic fault slip (displacements measured in centimeters to tens of centimeters) is about M6.3-6.5 [*Doser and Smith*, 1989; *dePolo*, in press]. Ground cracking has been associated with smaller magnitude events. Cracks a few centimeters wide occurred along the White Mountains fault zone following the 1986 Chalfant earthquakes [*dePolo and Ramelli*, 1987] which had moment magnitudes (M_w) of 5.5, 5.8, and 6.2 and seismic moments of 0.2-2.5 x 10^{25} dyne-cm [*Doser and Smith*, 1989]. Similar-size fractures were also associated with the 1934 Excelsior Mountain earthquake (M6.1) in central Nevada [*Callaghan and Gianella*, 1935]. One exception to the minimum-magnitude relation is a M3.6 earthquake

that occurred in 1966 on the Imperial fault, which lies outside of the Basin and Range province. This earthquake produced horizontal surface displacements on the order of 1-2 cm, and the rupturing was attributed to a shallow (1.1 km), low-stress drop event having a geologically and instrumentally determined seismic moment of about 2 x 10^{22} dyne-cm (*Brune and Allen*, 1967).

A comparison of stress drops typically accompanying ground rupturing events also supports the conclusion that the cracking was not coseismic. Using the relationship for calculating stress drop (σ) on an infinitely long strike-slip fault [*Knopoff*, 1958; *Brune and Allen*, 1967]:

$$\sigma = \tfrac{1}{2}\, U\mu/w \qquad (3)$$

where U is the displacement, μ is the rigidity, and w is the fault width or depth. Assuming a nominal displacement of 2 cm for fault slip (which is a conservative value since net slip on the fault must necessarily have been greater), a rigidity of 2 x 10^{11} dynes/cm^2, and assumed fault widths or depths (w) ranging between 1 and 3 km, stress drops on the order of 0.6-2 bars are derived. Such stress drops are extremely low when compared to other ground rupturing events, which typically have stress drops on the order of tens of bars. An exception is the M3.6 Imperial Valley earthquake mentioned above [*Brune and Allen*, 1967]. We believe the low stress drops that we have calculated here argue against the possibility that the fracturing is related to seismic strain on the fault. This interpretation is also supported by the stress drop-magnitude relations of *King and Knopoff* [1968] who concluded that the M3.6 Imperial Valley earthquake was an anomalous event, having an unusually low stress drop inconsistent with other stress drops

typically associated with lower magnitude earthquakes.

The possibility that the cracking is related to afterslip is precluded on the same basis as coseismic slip, i.e., the lack of a local earthquake of sufficient magnitude or moment to generate the observed strain. Afterslip has been documented surficially and geodetically following moderate- to large magnitude earthquakes, with slip occurring up to months after the event and in some cases occurring on faults not exhibiting evidence of coseismic slip. *Wesson* [1988] included afterslip in the definition of tectonic creep and presents multiple examples, most notably from the San Andreas system. The 1975 Oroville earthquake (M_b 5.9) is useful here for illustrative purposes. Surface fracturing associated with this earthquake was on the order of 1-3.5 cm, which continued for several months following the earthquake [*Clark et al.*, 1976]. Based on the use of a power law creep model, *Wesson* [1988] showed that the modeled static stress drop of about 13 bars was in good agreement with the assumed stress drop associated with the earthquake. The stress drop associated with the Oroville fracturing is within the range of stress-drops typically associated with moderate-magnitude earthquakes, and it is about an order of magnitude greater than the stress drop calculated for the fractures in this study.

Dynamically triggered slip may occur on faults remote from moderate- to large-magnitude earthquakes where dynamic strains (shaking) can be demonstrated to be larger than static strains resulting from the faulting event [cf., *Allen et al.*, 1972; *Mavko et al.*, 1985; *Anderson et al.*, 1992; *Reasenberg et al.*, 1992]. Well-documented cases of dynamically triggered surface slip, however, are restricted to the well-studied fault systems in California where far-field dynamic

strains resulting from earthquakes of M>6 are large enough to trigger sympathetic surface displacement on other regional faults. *Mavko et al.* [1985] showed that small (mm-scale) displacements were recorded at numerous creepmeter locations along the San Andreas fault following each of multiple moderate earthquakes occurring at distances of >35 km. They instrumentally recorded coseismic steps as large as 8 mm on the San Andreas fault induced by the thrust faulting associated with the 1983 Coalinga earthquake (M6.7). Accelerated rates of creep on the San Andreas also appear to be associated with nearby local earthquakes. *Burford et al.* [1972] and *King et al.* [1977] described coseismic steps detected on multiple creepmeters along the San Andreas system, and they related these events to nearby earthquakes. Displacements on the order of <1 mm were systematically recorded at creepmeter sites 5-30 km distant from the epicenters following a sequence of magnitude 3.9-5.0 earthquakes in 1971-73. These small (<1 mm) surface slips are the largest displacements known to us to be associated with earthquakes of M≤4.

Fuis [1982] and *Sieh* [1982] attributed displacement on the Superstition Hills and San Andreas faults to effects of the 1979 Imperial Valley earthquake (M_L6.6). Although these faults were located 50 and 100 km from the epicenter, respectively, the triggered association is based on the synchroneity of the ground cracking with the event. Small-scale fracturing along the Superstition Hills fault was observed 4 days after the earthquake, and similar movement was found along the San Andreas fault beginning within several hours of the earthquake. The fracture traces on these faults followed the traces of previous triggered slip fractures associated with the 1968 Borrego Mountain earthquake (M6.5) [*Allen et al.*, 1972]. In the 1979 event, the triggered slip model

was the preferred interpretation, although the possibility that migrating creep or regional slip may have affected multiple faults could not be completely dismissed [*Fuis*, 1982]. Most recently, the 1992 Landers earthquake (M7.5) triggered surface slip on some of these same faults [*Sharp*, 1992]; it also triggered seismicity (with no associated surface slip) as far as 1250 km from the epicenter, including events as large as M5.6 in southern Nevada [*Anderson et al.*, 1992; *Reasenberg et al.*, 1992].

Based on examination of seismicity within a 50-km radius of the Fish Spring Flat fracturing (Figure 11), we find no evidence that the ground fracturing was related to dynamic triggering from a regional event. As noted, the largest event was a M3.5 earthquake in April 1988, located about 22 km from the fractures. A catalogue search of the Preliminary Determination of Epicenters (*U.S. Geological Survey*, 1988) indicates that there were no seismic events of $M>6$ in the Nevada-California region (within an approximately 500-km radius of the study area) for the April through July 1988 period. This would rule out the likelihood that a large event comparable to the 1992 Landers earthquake could have dynamically triggered the cracking. Although we cannot rule out the possibility that the fracturing was associated with some unusual form of triggering from the M3.5 Carson City event, documented cases of triggered slip indicate that significantly larger magnitudes are necessary. To our knowledge, no triggered displacements on the scale of 1 cm or larger have occurred in association with earthquakes of magnitude less than 6 (Table 1). The best documented examples of small-scale slip triggered by low-magnitude earthquakes are related to seismic events along the San Andreas system where multiple creepmeters have detected small (<1 mm) displacements temporally associated with nearby

earthquakes of $M \leq 5$. Yet even in these well-instrumented situations, it is not certain whether the movements are clearly the result of triggered secondary faulting or are related to other poorly known coseismic parameters, such as low fault zone rigidity [*King et al.*, 1977].

Hydraulically induced slip

Ground fracturing resulting from hydraulically induced strain sometimes occurs where fluid withdrawals generate vertical effective stress changes in shallow sediments [cf., *Helm*, 1984a; *Holzer*, 1984a], and where they generate horizontal effective stress changes [cf., *Helm*, 1984b, 1992]. The most frequent source of such hydraulic strain is ground-water withdrawal where excessive pumping results in dewatering or depressurizing of saturated sediments and causes vertical subsidence and/or horizontal tension cracking [cf., *Holzer*, 1984b; *Helm*, 1984b, 1992]. In the arid western U.S., ground-water withdrawal induced land subsidence has frequently been accompanied by ground fracturing and, locally, by aseismic surface faulting. Numerous examples are available from central and northern California [*Lofgren and Klausing*, 1969; *Poland et al.*, 1975; *Holzer*, 1980], central Arizona [*Schumann and Poland*, 1969; *Holzer et al.*, 1979] and southern Nevada [*Bell*, 1981]. Because hydraulically induced strains are common, this study includes an examination of the water level and pumping history in Fish Spring Flat and the calculation of theoretical horizontal strains produced by pumping and aquifer conditions proximal to the surface cracking.

Fish Spring Flat is a small subbasin hydraulically connected to the larger Carson Valley ground-water basin to the west. The subbasin contains perched, unconfined ground water with the water table lying at depths of 4.5-15 m [*Maurer*, 1986]. The largest pumping well is an irrigation well calculated to yield 60 acre-feet (0.07 hm^3) of water annually based on consumptive use estimates by the U.S. Geological Survey, (D. Maurer, unpublished data, 1988). This well is located 450 m from the cracking at the closest approach and 750 m at the farthest (Figure 8). Water levels have been annually measured in Fish Spring Flat since the early 1980's [*Maurer*, 1986; *Berger*, 1987].

Vertical effective stresses sufficient to induce vertical strain and subsidence require a decline in the water table under unconfined aquifer conditions. This is based on the relation

$$p = \bar{p} + p_w \tag{4}$$

where p is the total stress affecting buried, saturated sediments, $\bar{p}$ is the effective stress on the sediments, and p_w is the pore-water pressure.

No net water-level declines were observed prior to the cracking, precluding the possibility that the ground fracturing was the result of long-term vertical subsidence. After the appearance of the cracking in November 1988, water levels in selected wells were remeasured by the U. S. Geological Survey, and it was found that water levels had not effectively changed since 1983 (D. Maurer, unpublished data, 1993). A stock well located about 1 km east of the cracking

maintained a consistent water level until 1989 when the level began to decline (Figure 14A). A domestic well 1 km south of the cracking had a similar trend (domestic well 2 on Figure 14B). The water level measured in a domestic well located 100 m east of the cracking (no. 1 on Figure 8) was at the same elevation as the stock well, indicating that water levels were not locally depressed along the fault. The U. S. Geological Survey data indicate that the Fish Spring Flat water table maintained a uniform, unchanged altitude for at least 7 years prior to the occurrence of the cracking. We attribute the water-level declines in 1989-92 to the effects of the 1987-93 drought in western Nevada.

Repeated ground surveys of the zone of cracking through fall 1992 indicate that the cracking has not recurred; the cracks are, in fact, no longer visible. The absence of continued or renewed cracking, given the decline in water levels after 1989, further supports the conclusion that the cracks were not related to either ground-water decline or to drought.

Ground fracturing may also be produced by horizontal strains induced by pumping [*Helm*, 1984b, 1992]. The land surface moves in response to pumping ground water from both unconfined aquifers [*Wolff*, 1970] and confined aquifers [*Poland and Davis*, 1969]. This movement is the surface expression of the three-dimensional change in porosity at depth. *Wolff* [1970] measured in the field the radial strain at land surface that is characteristic of unconfined aquifer horizontal deformation. Figure 15A shows that a zone of radial compression occurs near a pumping well. This inner zone of compression is surrounded by an outer zone of radial extension. Figure 15B illustrates the general relation between radial strain ϵ_{rr} and the radial

component of displacement u_r for axisymmetric deformation. For clastic material, grains constitute the aquifer framework. Within the inner zone of radial compression, a grain that lies farther from the well travels a greater distance towards the well during a unit period of time than does a neighboring grain that lies closer to the well. The reverse is true within the outlying zone of radial aquifer extension. In this outer zone, a grain (which represents a point fixed within the aquifer) that lies farther from the well travels a smaller distance towards the well than does a neighboring grain that lies closer to the well.

Note in Figure 15 the following important fact. The perimeter of no radial strain ϵ_{rr} (namely, where radial strain equals zero) coincides with the perimeter of greatest radial displacement u_r. If an aquifer can be shown to move a maximum cumulative radial distance of, say, 2.5 cm towards a well one would expect the local radial strain to be correspondingly small.

One further point should be made. For axially symmetric deformation, it can be shown that the tangential normal strain $\epsilon_{\theta\theta}$ (sometimes called "hoop" strain) always equals u_r/r where u_r is the radial component of the displacement field of solids $\mathbf{u}$ [$= (u_r, 0, u_z)$] at a distance r from the discharging well. In any region, one can write in terms of skeletal strain that

$$\epsilon_{rr} + \epsilon_{\theta\theta} + \epsilon_{zz} = 0 \qquad (5)$$

which translates to

$$\frac{\partial u_r}{\partial r}+\frac{u_r}{r}+\frac{\partial u_z}{\partial z}=0 \qquad (6)$$

for axisymmetric deformation.

Decrease in aquifer porosity is one possible source of water to a well, and it represents the source that causes aquifer deformation. It is worth discussing the other sources of water that can be derived from an unconfined aquifer before directly calculating the possible horizontal displacement and strain that can occur due to pumping at Fish Spring Flat.

Ground-water discharge from a well can be derived from two basic sources: from recharge and/or from aquifer storage. Because water levels of the unconfined aquifer in Fish Spring Flat remained essentially unchanged prior to 1988, one can reasonably surmise that recharge due to precipitation was sufficient to supply the average annual discharge until 1988. Lowering of the water table (actually dewatering the upper part of the aquifer) represents one possible source from storage. Other sources of water from aquifer storage in response to depressurizing the saturated part of the aquifer are: 1) decrease of porosity; 2) expansion of interstitial water, and 3) expansion of individual solid grains. These latter three sources, however, do not represent dewatering of the aquifer. Within 1000 m of land surface a decrease in the porosity of sedimentary material usually contributes much more water to a well than the expansion of water or individual solids [*Helm*, 1984a]. The question that we address here is whether a cumulative decrease in porosity within the sediments lying between the zone of cracking and the irrigation well would have been sufficient to account for the 2+ cm relative horizontal displacement

necessary for the cracking to occur.

An early-time decrease in porosity can theoretically occur without the water table itself being noticeably affected. If the bottom of an unperforated or unscreened casing or, alternatively, the top of the uppermost screened interval, is sufficiently deep beneath the water table (the top of the unconfined aquifer) and the vertical hydraulic conductivity is sufficiently small, it may take hours or days before the drawdown (induced by continued pumping) migrates upward to the water table surface itself. Until the water table is reached, the aquifer will behave essentially like a confined aquifer. In other words, during an early period of pumping, drawdown near the screened interval can theoretically manifest itself as a depressurization, and time-dependent porosity change becomes the primary source of water from storage. Only this early-time response is analyzed below.

For a transversely isotropic unconfined aquifer where the horizontal hydraulic conductivity K_h is much greater than the vertical hydraulic conductivity K_v, the drawdown cone will migrate from the discharge well outward radially much faster than it will migrate vertically upward (or downward). As mentioned above, the initial drawdown due to depressurization at the bottom of an unperforated casing must migrate upward to the water table before the water table itself can start to decline. Due to the permeability ellipse, the drawdown will have reached outward to a radius R at the same time it reaches upward to the water table. This relation can be expressed by

$$b/R = (K_v/K_h)^{1/2} \qquad (7)$$

where b is the depth beneath the water table to the top of a screened interval, or to the open bottom of an unperforated casing, K_v is the average vertical hydraulic conductivity, and K_h is the average horizontal hydraulic conductivity.

At Fish Spring Flat, the cracking lies between 450 m west and 750 m southwest of the irrigation well. This irrigation well is 46 m deep, extends 30 m beneath the water table, and annually pumps an estimated 60 acre-feet ($0.07 hm^3$) of water (D. Maurer, unpublished data, 1988). Based on the local ground-water model [*Maurer*, 1986], the ratio of average horizontal hydraulic conductivity K_h to average vertical conductivity K_v has been estimated to be roughly 1:1,000 in Fish Spring Flat. Using this ratio, the effective depth of the perforated interval b beneath the water table, determined by

$$b/R \approx (1/1{,}000)^{1/2} = 0.32 \qquad (8)$$

must be between 14 m (for R=450 m) and 24 m (for R=750 m) in order for cumulative early-time decrease in porosity near the well to have any impact on the fault. Because these values are smaller than the 30 m depth beneath the water table, an impact is theoretically feasible. The question remains, how large can one expect this impact to be?

Helm [1984b] introduced a method for calculating this early-time decrease in porosity, using the equation

$$u_{max} \leq (0.15)\ (Q/\pi)(R/b)(S_s/K_h) \quad (9)$$

where u_{max} is the maximum cumulative radial displacement towards a pumping well that occurs before the dewatering process (namely the lowering of the water table of an unconfined aquifer) becomes the dominant source of water. Dewatering dramatically slows any further decrease in porosity and the resulting radial displacement at R.

For Fish Spring Flat (using values given), one finds

$$u_{max} \leq (1.5)Q\ S_s/K_h \quad (10)$$

where Q is the volume rate of pumping and S_s is the specific storage. For representative values of K_h (say, 10^{-3} cm/sec, based on estimates by *Maurer*, 1986) and S_s (say, 10^{-7} cm^{-1}),

$$u_{max} \leq 1.5 \times 10^{-5}\ Q\ cm \quad (11)$$

where Q is expressed in cm^3/sec. Using the average Q of 60 acre-feet (0.07 hm^3) per year estimated for the irrigation well ($\sim 2 \times 10^3$ cm^3/sec), u_{max} equals roughly 0.03 cm, significantly less than the observed 2-4 cm displacement. Upper bounds can be estimated by assuming maximum values. If the cumulative discharge (0.07 hm^3) is concentrated over a four or five week period, the maximum seasonal rate would actually be an order of magnitude larger than the annual average. A corresponding horizontal displacement of about 0.5 cm could theoretically

occur near the fault in response to pumping. If in addition the effective hydraulic conductivity K_h is assumed to be significantly smaller than the one estimated above, say by a factor of five, u_{max} would correspondingly be five times larger. Although speculative, these values, if real, could yield the required 2.5 cm movement during a one-month, maximum-rate, pumping event.

Repeated pumping events can also be modeled. When the pump is shut off, one would expect a near-complete rebound to occur. Hence, the change in porosity and the resulting displacements would tend to be cyclic. One can calculate the theoretical cyclic strain at R. Beyond the perimeter R no decrease in pore volume occurs. This is because of the conversion of confined aquifer behavior to unconfined aquifer behavior when the drawdown reaches b (and correspondingly R). Hence the volume strain of the porous structure ϵ ($\equiv \epsilon_{zz} + \epsilon_{rr} + \epsilon_{\theta\theta}$) equals zero for all $r \geq R$. The vertical normal strain ϵ_{zz} can be assumed to equal zero in the region beyond the perimeter R where no net porosity change has occurred. Hence,

$$\epsilon_{rr} = -\epsilon_{\theta\theta} \tag{12}$$

where ϵ_{rr} is the radial normal strain and $\epsilon_{\theta\theta}$ is the tangential strain on a horizontal plane. For transversely isotropic material, the radial displacements u_r would be axially symmetric and hence

$$\epsilon_{\theta\theta} = u_r / r \tag{13}$$

which means that at R

$$\epsilon_{rr} = -u_r / R \leq -2.5 \text{ cm} / 450 \text{ m to } 750 \text{ m} = -3.3 \times 10^{-5} \text{ to } -5.5 \times 10^{-5}. \quad (14)$$

The local extensional radial strain at R thus might cyclically be as large as -5.5×10^{-5}. For the same volume element the local tangential strain is compressional and might cyclically be as large as $+5.5 \times 10^{-5}$. For the previously assumed specific storage S_s value of 10^{-7} cm^{-1}, the local extensional radial stress is calculated to be no more than 33 to 56 kPa at 450 to 750 m distances. For a larger specific storage, the stresses at R would be proportionately smaller. The authors doubt that such small strains and small extensional stresses would have caused the observed rupture.

We conclude that the calculated theoretical horizontal pumping strain is not sufficient to produce the observed ground cracking. Using conservative assumptions, it is very unlikely that the 0.5 cm displacement induced by a single pumping event of 0.07 hm^3 over one month's duration or longer is sufficient to have caused the observed fracturing. Furthermore, near-complete rebound is likely to occur between seasonal pumping events. In order to obtain a calculated maximum displacement of 2.5 cm, it is necessary to assume both large values for Q and much smaller values for K_h, assumptions that are not strongly supported by the known hydraulic conditions and thus are regarded as speculative upper bound conditions.

The conclusion that the cracking was not related to hydraulically induced displacements is supported by the crack displacement and vector data (Figure 8B) which indicate that the stress direction had no preferential orientation relative to the well. The slip vectors measured along the

length of the zone of cracking show relatively uniform east-west orientations; these orientations are inconsistent with the radial and attenuated strains predicted from modeling axisymmetric pumping strain. If the cracking were controlled by pumping induced strain, one would expect to see slip vectors oriented radially towards the well (Figure 15). The lack of continued ground cracking since 1988, although pumping and drought conditions have continued at the same level through 1992, also tend to argue against a pumping origin.

SPECULATION ON POSSIBLE TECTONIC ORIGINS

Based on our seismic and hydraulic calculations, we believe that tectonic stress is the only plausible mechanism for the cracking. The fault-controlled ground cracking along the PNMFZ, however, fits no known model for seismically or hydraulically induced creep on extensional faults, and we speculate that the observed creep may have originated from one or more possible tectonic origins. We stress that these possibilities are based on simplistic comparisons, and that more explicit models would require additional detailed assessments, including analyses of regional strain patterns and the frictional and rheological properties of the faults, topics which are beyond the scope of this study.

The seismic slip and creep pattern of the PNMFZ is somewhat similar to that observed along some portions of the San Andreas fault system that are characterized by frictional asperities.

Although there are significant differences in tectonic style and strain rate between the two fault zones, the spatial distribution of seismicity along the PNMFZ in cross section (Figure 13) is analogous to that noted along the central San Andreas system by *Wesson et al.* [1973]. There, rapidly creeping segments exhibited lower levels of seismicity in comparison to adjacent seismically active segments. Although the PNMFZ faults and seismicity are more diffuse than along the San Andreas system, there is a comparable pattern of seismically active fault segments separated by a low seismicity, creeping section. Figure 12 shows a northern grouping of epicenters along the fault zone beginning about 10 km north of the cracking (Zone A). A second grouping occurs along the southern portion of the fault zone beginning near the BFC seismograph station and continuing down the length of the Pine Nut Mountains (Zone B). The approximately 20-km segment between these two clusters contains only a few scattered earthquakes of M 1-2, and the 10-km segment along which the cracking occurs is, as noted, aseismic.

These similarities suggest that the asperities, or locked patches, concept for seismically active faults [cf., *Bakun et al.*, 1980; *Tse et al.*, 1985] may be applicable. These models propose that active faults have inhomogeneous strength characteristics that result in parts of the fault zone having difficult, or retarded, slip and other portions having free slip or creep. In the study by *Wesson et al.* [1973], they hypothesized that the segments exhibiting higher levels of seismic slip reflect zones where fault slip is relatively difficult; elastic strain is stored along these difficult-slip patches until sporadically released as earthquakes. The coincidence between the site of ground cracking along the PNMFZ section and a very low level of seismicity (Figure 13)

suggests a genetic connection. Although the PNMFZ is a highly complex, distributive shear zone, the observed aseismic slip is likely related to some unique rheological property of that part of the zone.

Recorded seismicity (Figures 11 and 12) indicates that the PNMFZ was tectonically active during the period that ground cracking occurred, and that much of the activity was shallow (<5 km). Both seismicity groupings A and B are punctuated by shallow activity, including swarms, which suggests that shallow crustal deformation in part characterized tectonic activity along the PNMFZ during the time of cracking. We used this observation to infer a shallow depth (1-3 km) for the creep. Shallow depths are also inferred for creep along portions of the San Andreas fault [cf., *Johnston et al.*, 1977]. *Evans et al.* [1981] used near-field strain measurements to determine that aseismic creep along the Calaveras fault was confined to the upper 1 km of the crust, possibly representing the response of the surface layers to a longer-term form of aseismic slip at greater depths.

The creep was more likely associated with a singular strain event than with a secular displacement. Although we have no definitive record of the timing of the cracking, the recognition and description of the cracking by local residents indicates that the cracks appeared during a time window that likely did not exceed a few weeks, suggesting that the fault slip occurred as a discrete event. The short-lived dilation and the lack of any other evidence of creep along the fault appears to rule out more regular secular creep, but we cannot prove this. These observations are somewhat similar to known behavior of the San Andreas fault system which

exhibits both secular and episodic creep. Creepmeters along the San Andreas fault show that creep commonly occurs as discrete strain events superimposed on a secular rate [*Steinbrugge et al.*, 1960; *Bufe and Tocher*, 1974; *King et al.*, 1973; *Johnston et al.*, 1977]. *Goulty et al.* [1978] also described large discrete creep events on the Imperial fault where creepmeters recorded 1.5-2.4 cm of rapid creep without any significant prior secular slip.

We speculate that the observed fault dilation is likely related to large-scale, but poorly known, vertical-slip kinematics of the PNMFZ which may involve shallow listric fault relations. The occurrence of surface dilation on the fault without any observable vertical slip is not unique. Vertical displacements were not detected on the ground surface or in the trench, but we cannot preclude a deeper-seated vertical displacement. The observed extensional relations observed in the trench fit well with the known mechanical behavior of shallow consolidated sediments when vertical slip is translated into near-surface extension due to lower confining overburden stress [cf., *Cloos*, 1968]. Similar centimeter-scale dilational fractures have been associated with some seismic slip events. As previously mentioned, *Clark et al.* [1976] mapped some purely dilational fractures related to the 1975 Oroville earthquake (M 5.9) which was a normal faulting event, and *dePolo and Ramelli* [1987] mapped dilational fractures associated with the 1986 Chalfant earthquake (M6.2) which was predominantly a strike-slip event. Triggered-slip fractures on the Imperial, Superstition Hills, and San Andreas faults have also been predominantly dilational in nature [*Allen et al.*, 1972].

Some evidence indicates that there is a measure of strike-slip behavior on the PNMFZ and

adjacent regional faults. Thus, we speculate that an additional possible origin of the PNMFZ cracking is stress induced by a component of lateral deformation. Focal mechanisms for the Sierra Nevada (Genoa) fault show a component of strike-slip displacement [*VanWormer and Ryall*, 1980]. A well-constrained focal mechanism from the 1988 Carson City M3.5 earthquake similarly indicates dominantly right-lateral displacement on the preferred north-trending nodal plane (Figure 12). As previously noted, the southern end of the cracking terminates along a scissors fault, a feature commonly observed along strike- or oblique-slip faults, and the sigmoidal pattern of fault scarps in and around the zone of cracking (Figure 7) are suggestive of a torque relation. The slip vectors measured along the fractures also require that a small component of right slip be present in order to account for the east-west vector orientations on northwest-trending faults. Given an east-west-oriented least principal stress (extension) direction, a kinematic model incorporating a component of northwest-oriented, right-lateral wrench faulting could also produce some extension on north-trending faults [cf., *Wilcox et al.*, 1973]. Tension joints and/or normal faults would parallel the short axis of the strain ellipse produced by wrenching.

SUMMARY

In summary, we conclude that the cause of dilational cracking along an active late Quaternary extensional fault in western Nevada was most likely due to aseismic fault creep, a phenomenon

not well documented in the Basin and Range province. We reach this conclusion on several bases: 1) direct and circumstantial geologic and seismologic evidence, 2) hydraulic modeling of vertical and horizontal strains induced by ground-water pumping, and 3) on the basis of simplistic comparisons with other known and better-documented analogues. The cracking occurred as a discrete event which has not recurred in the four years following its detection, and it cannot be associated with any known seismic or hydraulic process. We list here the principal lines of evidence developed from this study supporting this conclusion.

1. Estimates of the seismic moment, earthquake magnitude, and stress drop that would normally accompany 1 to 2 cm of fault slip indicate that the cracking was neither coseismic slip, afterslip, nor triggered slip. Assuming a 1-3 km depth for the slip surface, the seismic moment corresponding to a 2 cm surface slip is calculated to be 6-18 x 10^{21} dyne-cm, comparable to an earthquake of M_w 3 3/4-4. Recorded seismicity indicates that the only significant event within a 50 km radius of the cracks in 1988 was a M3.5 earthquake located about 22 km north of the zone of cracking. This event predates the occurrence of the cracks by several months and was too distant to provide the necessary seismic moment and stress drop. Minimum magnitudes and stress drops typically associated with ground rupture in the Basin and Range province appear to preclude a coseismic origin. Historical surface faulting has typically been associated with earthquakes of $M \geq 6.3$, and ground cracking is typically produced by earthquakes of $M \geq 5.5$. All known cases of coseismic surface rupture are associated with seismic moments that are larger than that calculated here by three to four orders of magnitude. Only one example of coseismic surface rupture associated with a low-magnitude, low stress-drop earthquake is known, the 1966

M3.6 event on the Imperial fault.

Similarly, documented examples of dynamically triggered ground rupture indicate that centimeter-scale displacements are generally all associated with earthquakes having magnitudes greater than 6. No earthquakes of $M>6$ occurred within a 500 km radius of the cracks during the April through July 1988 period. The smallest magnitude earthquakes known to have triggered displacements at remote distances are about $M\geq4$, and the triggered slip was less than 1 mm, substantially smaller than that observed here.

2. A hydraulic origin for the cracking is not likely on the basis of the lack of vertical effective stress changes required for subsidence or on the basis of calculated horizontal displacements and radial strains that may be induced by a nearby irrigation well. Water levels monitored for the seven-year period preceding the appearance of the cracks showed no evidence of basin-wide decline, a requisite for inducing vertical effective stress changes, land subsidence, and ground fracturing. Radial horizontal displacements generated by the irrigation well are estimated to be on the order of 0.03 cm per pumping event, which is not sufficient to account for the observed cracking. Near-complete rebound is expected to occur between pumping events, and the cyclic strain is calculated to be no larger than -5.5×10^{-5}. Calculated extensional stresses related to pumping range between 33 and 56 kPa and are regarded as insufficient to account for the observed ruptures. Slip vectors measured along the zone of cracking indicate that the fracturing had a relatively uniform east-west movement along the entire length of the zone, in contrast to the radial pattern oriented toward the well which is predicted by the model. Likewise, calculated

radial strains attenuate with distance from the pumping center; hence consistent displacements measured along the strike of the cracks further indicates that the strain is not linked to the pumping. Lastly, the cracking was a discrete event that has not recurred in the following four years, even though pumping has continued at the same rate.

3. The observed ground cracking fits no known model for seismically or hydraulically induced creep on extensional faults. Based on simple comparisons, we speculate that the creep may have originated from one or a combination of several possible tectonic origins. Unknown frictional and rheological properties of the fault zone likely play a major role in the origin.

The seismic slip and creep pattern of the PNMFZ is somewhat analogous to that observed along the San Andreas fault system where seismically active fault segments are separated by low seismicity, rapidly creeping segments. Tectonic strain release along the central San Andreas fault is in part characterized by zones of difficult slip, or asperities, and zones of easy slip, or creep. The PNMFZ cracks propagated along a fault segment characterized by an unusually low level of seismic activity in contrast to portions of the zone to the north and south which display moderate levels of seismicity punctuated by swarm activity. This spatial pattern may be explained by the models proposed for the San Andreas fault where locked patches along the fault are separated by actively creeping, lower seismicity segments of the fault.

The areal and depth distribution of seismicity recorded along the PNMFZ indicates that the fault zone was tectonically active during the period of ground cracking, and that much of the activity

was shallow. We therefore infer that the fracturing was the result of shallow crustal deformation.

4. Although only surficial fault dilation was observed, it is likely that the creep was related to deeper-seated vertical fault slip. The PNMFZ is characterized by dominantly normal slip on north-trending listric faults, and the east-west-oriented extension (σ_3) direction for this region could accommodate vertical slip on this fault. Focal mechanisms and surficial geologic data suggest that there is a component of right-lateral strain in this region, which could also account for the extensional character of the cracks by producing a torquing relation.

ACKNOWLEDGMENTS

Diane M. dePolo of the University of Nevada Seismological Laboratory provided very valuable assistance in compiling and cataloguing the seismicity data used in this study. Douglas Maurer provided the initial description of the cracks as well as numerous preliminary observations. Fish Spring Flat resident Linda Monahan gave us detailed descriptions of the cracks and allowed us access through her property. James Yount and James Brune provided valuable review comments. This study was in part supported by the U.S. Geological Survey COGEOMAP program.

REFERENCES

Aki, K. Generation and propagation of G waves from the Nigata earthquake of June 16, 1964. Part 2. Estimation of earthquake moment, released energy, and stress-strain drop from the G wave spectrum, *Bull. Earthquake Res. Inst. Tokyo Univ., 72*, 1217-1231, 1966.

Allen, C.R., Wyss, M., Brune, J.N., Grantz, A., and Wallace, R.E., Displacements on the Imperial, Superstition Hills, and San Andreas faults triggered by the Borrego Mountain earthquake, the Borrego Mountain Earthquake of April 9, 1968, *U.S. Geol. Surv. Prof. Pap., 787*, 87-104, 1972.

Anderson, J.G., Louie, J., Brune, J.N., dePolo, D., Savage, M., and Yu, G., Seismicity in Nevada triggered by the Landers, California earthquake, June 28, 1992, *EOS Trans. AGU, 73*, 393, 1992.

Bell, J.W., Subsidence in Las Vegas Valley, *Nevada Bur. Mines and Geol. Bull. 95*, 84 pp., 1981.

Bell, J.W., Quaternary fault map of the Reno 2° sheet, *Nevada Bur. Mines and Geol. Map 79*, 1984.

Berger, D.L., Ground-water levels in water years 1984-86 and estimated ground-water pumpage in water years 1984-85, Carson Valley, Douglas County, Nevada, *U.S. Geol. Surv. Open-file Rpt., 86-539*, 16 pp., 1987.

Brune, J.N., Seismic moment, seismicity, and rate of slip along major fault zones, *J. Geophys. Res., 73*, 777-784, 1968.

Brune, J.N., and Allen, C.R., A low stress-drop, low-magnitude earthquake with surface faulting: the Imperial, California, earthquake of March 4, 1966, *Bull. Seismol. Soc. Am., 57*, 501-514, 1967.

Bakun, W.H., Stewart, R.M., Bufe, C.G., and Marks, S.M., Implication of seismicity for failure of a section of the San Andreas fault, *Bull. Seismol. Soc. Am., 70*, 185-201, 1980.

Bufe, C.G., and Tocher, D., Central San Andreas fault: strain episodes, fault creep, and earthquakes, *Geology, 2*, 205-207, 1974.

Burford, R.O., Continued slip on the Coyote Creek fault after the Borrego Mountain earthquake, the Borrego Mountain Earthquake of April 9, 1968, *U.S. Geol. Surv. Prof. Pap., 787*, 105-111, 1972.

Burford, R.O., Allen, S.A., Lamson, R.J., and Goodreau, D.D., Accelerated creep along the central San Andreas fault after moderate earthquakes during 1971-1973, in *Proceedings of the Conference on Tectonic Problems of the San Andreas Fault System*, edited by R.L. Kovach and A. Nur, pp. 268-274, Stanford University Publications, Geological Sciences, v. XIII, Stanford, California, 1973.

Callaghan, E. and Gianella, V.P., The earthquake of January 30, 1934, at Excelsior Mountains, Nevada, *Bull. Seismol. Soc. Am., 46*, 1-40, 1935.

Carr, W.J., Summary of tectonic and structural evidence for stress orientations at the Nevada Test Site, *U.S. Geol. Surv. Open-file Rpt., 74-176*, 53 pp., 1974

Clark, M.M., Sharp, R.V., Castle, R.O., and Harsh, P.W., Surface faulting near Lake Oroville, California in August, 1975, *Bull. Seismol. Soc. Am., 66*, 1101-1110, 1976.

Cloos, E., Experimental analysis of Gulf Coast fracture patterns, *Am. Assoc. Pet. Geol. Bull., 52*, 420-444, 1968.

Cohn, S.N., Allen, C.R., Gilman, R., and Goulty, N.R., Preearthquake and post earthquake creep on the Imperial fault and the Brawley fault zone, the Imperial Valley, California, earthquake of October 15, 1979, *U.S. Geol. Surv. Prof. Pap., 1254*, 161-167, 1982.

dePolo, C.M., The maximum background earthquake for the Basin and Range province, western North America, *Bull. Seismol. Soc. Am.*, in press.

dePolo, C.M., and Ramelli, A.R., Preliminary report on surface fractures along the White Mountains fault zone associated with the July 1986 Chalfant earthquake sequence, *Bull. Seismol. Soc. Am., 77*, 290-296, 1987.

dePolo, D.M., Peppin, W.A., Aburto, A.A., and Savage, M.K., Seismicity in the western Great Basin May 10, 1984-December 31, 1989, *Bull. Seismol. Lab.*, University of Nevada, Reno, Seismological Laboratory, Reno, Nevada, 57 pp. 1992.

Dohrenwend, J.C., Reconnaissance surficial geologic map of the Mt. Siegel quadrangle, Nevada-California, *U.S. Geol. Surv. Open-file Rpt., 81-1156*, 1981.

Dohrenwend, J.C., Map showing late Cenozoic faults in the Walker Lake 1° by 2° quadrangle, Nevada-California, *U.S. Geol. Surv. Misc. Field Studies Map, MF-1382-D*, 1982.

Doser, D.I., and Smith, R.B., An assessment of source parameters of earthquakes in the Cordillera of the western United States, *Bull. Seismol. Soc. Am., 79*, 1383-1409, 1989.

Evans, K.F., Burford, R.O., and King, G.C.P., Propagating episodic creep and the aseismic slip behavior of the Calaveras fault north of Hollister, California, *J. Geophys. Res., 86*, 3721-3735, 1981.

Fuis, G.S., Displacement on the Superstition Hills fault triggered by the earthquake, the Imperial Valley, California, earthquake of October 15, 1979, *U.S. Geol. Surv. Prof. Pap., 1254*, 145-154, 1982.

Gilmore, T.D., Selected examples of historical height changes in the southern Great Basin, in *Proceedings Nuclear Waste Isolation in the Unsaturated Zone Focus '89*, p. 335, American Nuclear Society, La Grange Park, Illinois, 1989.

Goulty, N.R., Burford, R.O., Allen, C.R., Gilman, R., Johnson, C.E., and Keller, R.P., Large creep events on the Imperial fault, California, *Bull. Seismol. Soc. Am., 68*, 517-521, 1978.

Hanks, T.C., and Kanamori, H., A moment magnitude scale, *J. Geophys. Res., 84*, 2348-2350, 1979.

Harsh, P.W., Distribution of afterslip along the Imperial fault, the Imperial Valley, California, earthquake of October 15, 1979, *U.S. Geol. Surv. Prof. Pap., 1254*, 193-203, 1982.

Helm, D.C., Field-based computational techniques for predicting subsidence due to fluid withdrawal, in *Man-induced Land Subsidence*, edited by T.L. Holzer, pp. 1-22, Geological Society of America Reviews in Engineering Geology, v. VI, Boulder, CO, 1984a.

Helm, D.C., Analysis of sedimentary skeletal deformation in a confined aquifer and the resulting drawdown, in *Ground Water Hydraulics*, edited by J. Rosenshein and G.D. Bennett, pp. 29-82, Water Resources Monograph no. 9, Am. Geophys. Union, Washington, D.C., 1984b.

Helm, D.C., Hydraulic forces that play a role in generating fissures at depth, in *Proceedings of the 35th Annual Meeting of the Assoc. of Engr. Geol.*, pp., Los Angeles, CA, pp. 7-16, 1992.

Holzer, T.L. (Ed.), Man-induced Land Subsidence, 221 pp., Geological Society of America, Reviews in Engineering Geology, v. VI, Boulder, CO, 1984a.

Holzer, T.L., Ground failure by ground-water withdrawal from unconsolidated sediment, in *Man-induced Land Subsidence*, edited by T.L. Holzer, pp. 67-105, Geological Society of America Reviews in Engineering Geology, v. VI, Boulder, CO, 1984b.

Holzer, T.L., Faulting caused by ground-water level declines, San Joaquin Valley, California, *Water Resources Res., 16*, 1065-1070, 1980.

Holzer, T.L., Davis, S.N., and Lofgren, B.E., Faulting caused by ground-water extraction in south-central Arizona, *J. Geophys. Res., 84*, 603-612, 1979.

Johnston, M.J.S., Jones, A.C., and Daul, W., Continuous strain measurements during and preceding episodic creep on the San Andreas fault, *J. Geophys. Res., 82*, 5683-5691, 1977.

Keaton, J.R., and Miller, J.J., Dry Lake earth fissure system, Clark County, Nevada, in *Proceedings of the 35th Annual Meeting of the Assoc. of Engr. Geol.*, Los Angeles, CA, pp. 129-133, 1992.

King, C.Y., and Knopoff, L., Stress drop in earthquakes, *Bull. Seismol. Soc. Am., 58*, 249-257, 1968.

King, C.Y., Nason, R.D., and Tocher, D., Kinematics of fault creep, *Phil. Trans. R. Soc. Lond. Ser A, 274*, 365-360, 1973.

King, C.Y., Nason, R.D., and Burford, R.O., Coseismic steps recorded on creep meters along the San Andreas fault, *J. Geophys. Res., 82*, 1655-1662, 1977.

Knopoff, L., Energy release in earthquakes, *Geophys. J., 1*, 44-52, 1958.

Lofgren, B.E., and Klausing, R.L., Land subsidence due to ground-water withdrawal, Tulare-Wasco area, California, *U.S. Geol. Surv. Prof. Pap., 437-B*, B1-B103, 1969.

Marone, C., and Scholz, C.H., The depth of seismic faulting and the upper transition from stable to unstable slip regimes, *Geophys. Res. Letters, 15*, 621-624, 1988.

Maurer, D.K., Gravity survey and depth to bedrock in Carson Valley, Nevada-California, *U.S. Geol. Surv. Water-Res. Inv. Rpt., 84-4202*, 20 pp., 1984.

Maurer, D.K., Geohydrology and simulated response to ground-water pumpage in Carson Valley, a river-dominated basin in Douglas Count, Nevada, and Alpine County, California, *U.S. Geol. Surv. Water-Res. Inv. Rpt., 86-4328*, 109 pp., 1986.

Mavko, G.M., Schulz, S., and Brown, B.D., Effects of the 1983 Coalinga, California, earthquake on creep along the San Andreas fault, *Bull. Seismol. Soc. Am., 75*, 475-489, 1985.

Moore, J.G., Geology and mineral resources of Lyon, Douglas, and Ormsby Counties, Nevada, *Nevada Bur. Mines and Geol. Bull., 75*, 42 pp., 1969.

Nason, R.D., Fault creep and earthquakes on the San Andreas fault, in *Proceedings of the Conference on Tectonic Problems of the San Andreas Fault System*, edited by R.L. Kovach and A. Nur, pp. 275-285, Stanford University Publications, Geological Sciences, v. XIII, Stanford, California, 1973.

Neal, J.T., Langer, A.M., and Kerr, P.F., Giant desiccation polygons of Great Basin playas, *Geol. Soc. Amer. Bull., 79*, 69-90, 1968.

Poland, J.F., Lofgren, B.E., Ireland, R.L., and Pugh, R.G., Land subsidence in the San Joaquin Valley, California, as of 1972, *U.S. Geol. Surv. Prof. Pap., 437-H*, 78 pp., 1975.

Poland, J.F., and Davis, G.H., Land subsidence due to withdrawal of fluids, in *Reviews in Engineering Geology v. II*, edited by D.J. Varnes and G. Kiersch, pp. 1887-268, Geological Society of America, Boulder, CO, 1969.

Reasenberg, P.A., and fifteen others, Remote seismicity triggered by the M7.5 Landers, California, earthquake of June 28, 1992, *EOS Trans. AGU, 73*, 392, 1992.

Ruegg, J.C., Kasser, M., and Lepine, J.C., Strain accumulation across the Asal-Ghoubbet rift, Djibouti, East Africa, *J. Geophys. Res., 89*, 6237-6246, 1984.

Schumann, H.H., and Poland, J.F., Land subsidence, earth fissures and ground-water withdrawal in south-central Arizona, U.S.A., in *Proceedings, First International Land Subsidence Symposium, Tokyo*, Internat. Assoc. Hydrol. Sci. Pub., 88, pp. 295-302, 1969.

Savage, J.C., and Burford, R.O., Strain accumulation in California, *Bull. Seismol. Soc. Am., 60*, 6469-6479, 1973.

Savage, J.C., and Church, J.P., Evidence for postearthquake slip in the Fairview Peak, Dixie Valley, and Rainbow Mountain fault areas of Nevada, *Bull. Seismol. Soc. Am., 64*, 687-698, 1974.

Schulz, S.S., Mavko, G.M., Burford, and Stuart, D., Long-term creep observations in central California, *J. Geophys. Res., 87, 6977-6982*, 1982.

Sharp, R., Surface faulting in the Imperial Valley triggered by the 1992 Landers, California, earthquake (abstract), *EOS Trans. AGU*, 73, 380, 1992.

Sieh, K.E., Slip along the San Andreas fault associated with the earthquake, the Imperial Valley, California, earthquake of October 15, 1979, *U.S. Geol. Surv. Prof. Pap., 1254*, 155-159, 1982.

Somerville, M.R., Peppin, W.A., and VanWormer, J.D., An earthquake sequence in the Sierra Nevada-Great Basin boundary zone: Diamond Valley, *Bull. Seismol. Soc. Am., 70*, 1547-1555, 1980.

Steinbrugge, K.V., Zacher, E.G., Tocher, D., Whitten, C.A., and Claire, C.N., Creep on the San Andreas fault, *Bull. Seismol. Soc. Am., 50*, 389-415, 1960.

Stewart, J.H., Tectonics of the Walker Lane belt, western Great Basin: Mesozoic and Cenozoic deformation in a zone of shear, in *Metamorphism and Crustal Evolution of the Western United States, Rubey Volume VIII*, edited by W.G. Ernst, pp. 684-713, Prentice-Hall, Englewood Cliffs, New Jersey, 1988.

Stewart, J.H., and Noble, D.C., Preliminary geologic map of the Mount Siegel quadrangle, Nevada, *U.S. Geol. Surv. Open-file Rpt., 79-225*, 1979.

Sylvester, A.G., Near-field tectonic geodesy, in *Active Tectonics*, pp. 164-180, National Academy Press, Washington, D.C., 1986.

Sylvester, A.G., Byrd, J.O.D., and Smith, R.B., Aseismic (?) reverse creep along the Teton fault, Wyoming with

implications for interseismic strain (abstract), *Geol. Soc. Am. Abs. with Prog.*, *22*, 88, 1990.

Tse, S.T., Dmowska, R., and Rice, J., Stressing of locked patches along a creeping fault, *Bull. Seismol. Soc. Am.*, *75*, 709-736, 1985.

VanWormer, J.D., and Ryall, A.S., Sierra Nevada-Great Basin boundary zone: earthquake hazard related to structure, active tectonic processes, and anomalous patterns of earthquake occurrence, *Bull. Seismol. Soc. Am.*, *70*, 1557-1572, 1980.

U.S. Geological Survey, *Preliminary determination of epicenters, monthly listings, April-July, 1988*, 110 pp., Natl. Earthquake Inf. Ctr., U.S. Govt. Print. Off., Washington, D.C., 1988.

Wesson, R.L., Dynamics of fault creep, *J. Geophys. Res.*, *93*, 8929-8951, 1988.

Wesson, R.L., Burford, R.O., and Ellsworth, W.L., Relationship between seismicity, fault creep and crustal loading along the central San Andreas fault, in *Proceedings of the Conference on Tectonic Problems of the San Andreas Fault System*, edited by R.L. Kovach and A. Nur, pp. 302-321, Stanford University Publications, Geological Sciences, v. XIII, Stanford, California, 1973.

Wilcox, R.E., Harding, T.P., and Seely, D.R., Basic wrench tectonics, *Am. Assoc. Petrol. Geol. Bull.*, *57*, 74-96, 1973.

Wolff, R.G., Relationship between horizontal strain near a well and reverse water level fluctuation, *Water Resources Res.*, *6*, 1721-1728, 1970.

Zellmer, J.T., Roquemore, G.R., and Blackerby, B.A., Modern tectonic cracking near the Garlock fault, California, *Geol. Soc. Am. Bull.*, *96*, 1037-1042, 1985.

Zoback, M.L., State of stress and modern deformation in the northern Basin and Range province, *J. Geophys. Res.*, *94*, 7105-7128, 1989.

Table 1. Documented cases of dynamically triggered surface slip.

Triggered fault	Amount of triggered slip	Causative earthquake	Distance to triggered slip	Reference
Imperial	1-2 cm along 22 km	1968 Borrego Mt. (M6.4)	70 km	*Allen et al.* [1972]
Superstition Hills	1½-2½ cm along 23 km	1968 Borrego Mt. (M6.4)	45 km	*Allen et al.* [1972]
Superstition Hills	1-22 mm along 22.5 km	1979 Imperial Valley (M6.6)	50-70 km	*Fuis* [1982]
San Andreas	½-1 cm along 30 km	1968 Borrego Mt. (M6.4)	50 km	*Allen et al.* [1972]
San Andreas	4-10 mm along 39 km	1979 Imperial Valley (M6.6)	90-130 km	*Sieh* [1982]
San Andreas	.04-.48 mm along 130 km	1982 Coalinga (M5.4)	35 km	*Mavko et al.* [1985]
San Andreas	.16-8.2 mm along 200 km	1983 Coalinga (M6.7)	35 km	*Mavko et al.* [1985]
San Andreas	<1 mm*	1972 Melendy Ranch (M5.0)	10-30 km	*King et al.* [1977]
San Andreas	.4 mm*	1972 San Juan Bautista (M4.8)	5 km	*Burford et al.* [1972]
Coyote Creek	1.3 cm along 2.5 km	1992 Landers (M7.5)	Not given	*Sharp* [1992]
Elmore Ranch	0.7 cm along 6.5 km	1992 Landers (M7.5)	Not given	*Sharp* [1992]

* Denotes accelerated creep which was either dynamically or coseismically triggered.

List of Figures

11. Seismicity recorded January through December 1988 within a 50-km radius of the zone of cracking. The largest event was a M3.5 earthquake occurring in April about 10 km east of Carson City. CC: Carson City; GV: Gardnerville; VC Virginia City; DV:Diamond Valley. (Seismicity plot provided by Diane M. dePolo, University of Nevada Seismological Laboratory).

12. Seismicity $M \geq 2$ recorded during the period 1983-1992 within a 30-km radius of the cracking; map base shows Quaternary fault traces and physiography corresponding to Figure 1. Clusters of earthquakes are related to swarms discussed in the text; location of the April, 1988 M3.5 earthquake indicated by the focal mechanism. The zone of cracking is located within a region characterized by a very low level of earthquake activity. A seismograph station (BFC) is located about 8 km south of the cracking. The 14-km-wide zone of north-south seismicity used to construct the seismic cross section (Figure 13) is outlined. CC: Carson City; GV: Gardnerville; VC: Virginia City; DV: Diamond Valley. (Seismicity plot provided by Diane M. dePolo, University of Nevada Seismological Laboratory).

13. Seismic cross section showing recorded seismicity $M \geq 2$ and focal depths for the period 1983-1992. All seismicity recorded within a 14-km-wide, 75-km-long band extending north-south along the Pine Nut Mountains fault zone is projected onto the cross section. The zone of cracking occurs within a 10-km-long segment of the cross section noticeably lacking seismicity (Seismicity plot provided by Diane M. dePolo, University of Nevada Seismological Laboratory).

14. Hydrographs showing recorded water levels in wells in Fish Spring Flat for the period 1982-1992. Top hydrograph (A) is for a stock well located 1.5 km east of the cracking; lower hydrograph (B) is for a domestic well (2) located 1 km south of the cracking (see Figure 8) (D. Maurer, unpublished data, 1993).

15. **A.** Contour map of radial strains measured at the surface as a result of pumping an unconfined aquifer; "-" indicates points moving together; "+" indicates points moving apart; contours are strain x 10^{-6} [*Wolff*, 1970]. **B.** Diagrammatic representation of a zone of skeletal compression developed near a discharging well in response to fluid withdrawal. An outer zone of skeletal extension develops beyond a radius R of no horizontal strain. Arrows schematically represent radial displacement (u_r) of aquifer solids during unit time. $\epsilon_{rr} \equiv \partial u_r / \partial r$ [*Helm*, 1984b].

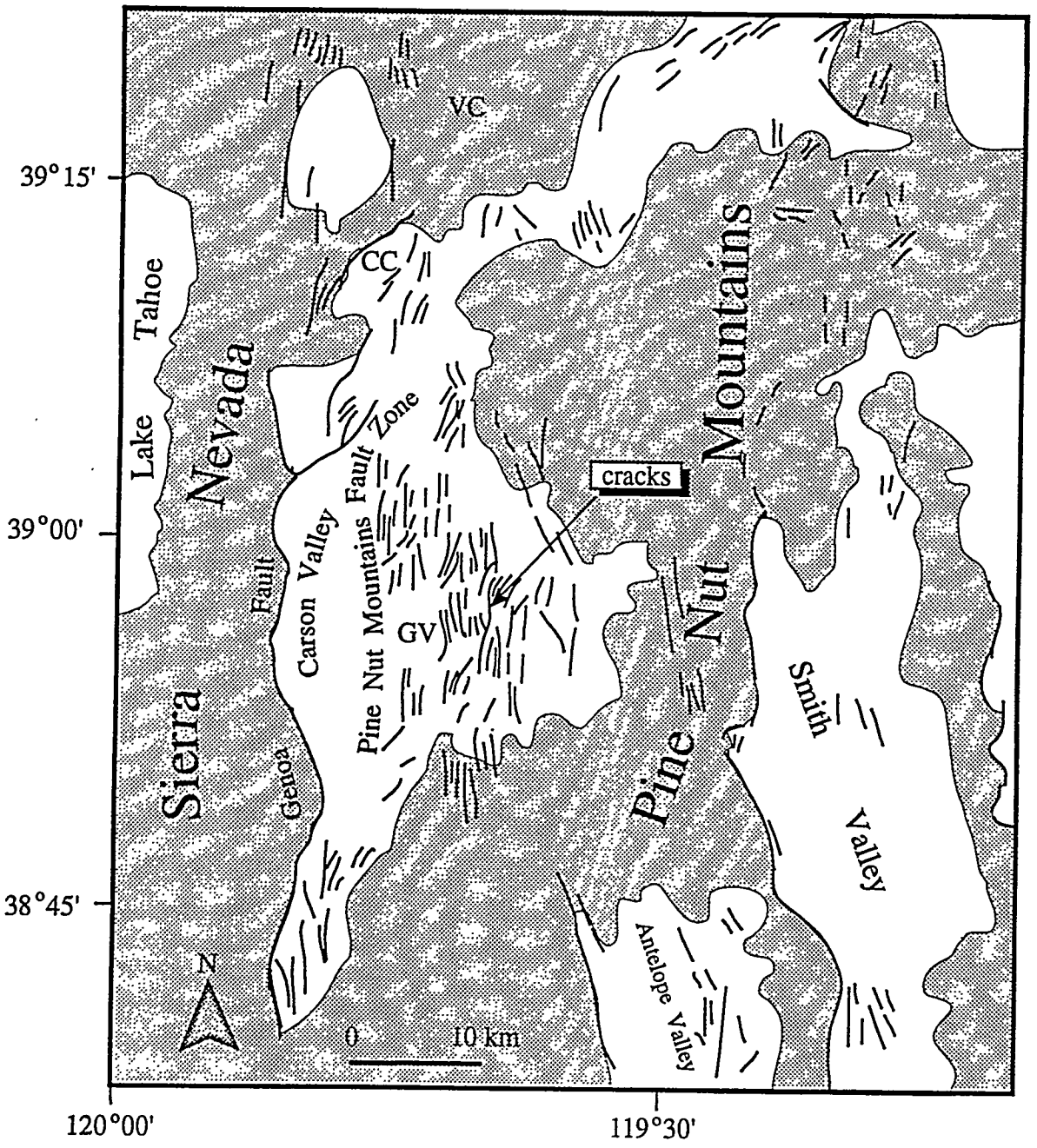
39°15'
39°00'
38°45'
120°00'
119°30'
Lake Tahoe
Sierra Nevada
Fault
Genoa
Carson Valley
Pine Nut Mountains Fault Zone
VC
CC
GV
cracks
Pine Nut Mountains
Smith Valley
Antelope Valley
N
0
10 km

Fig. 1

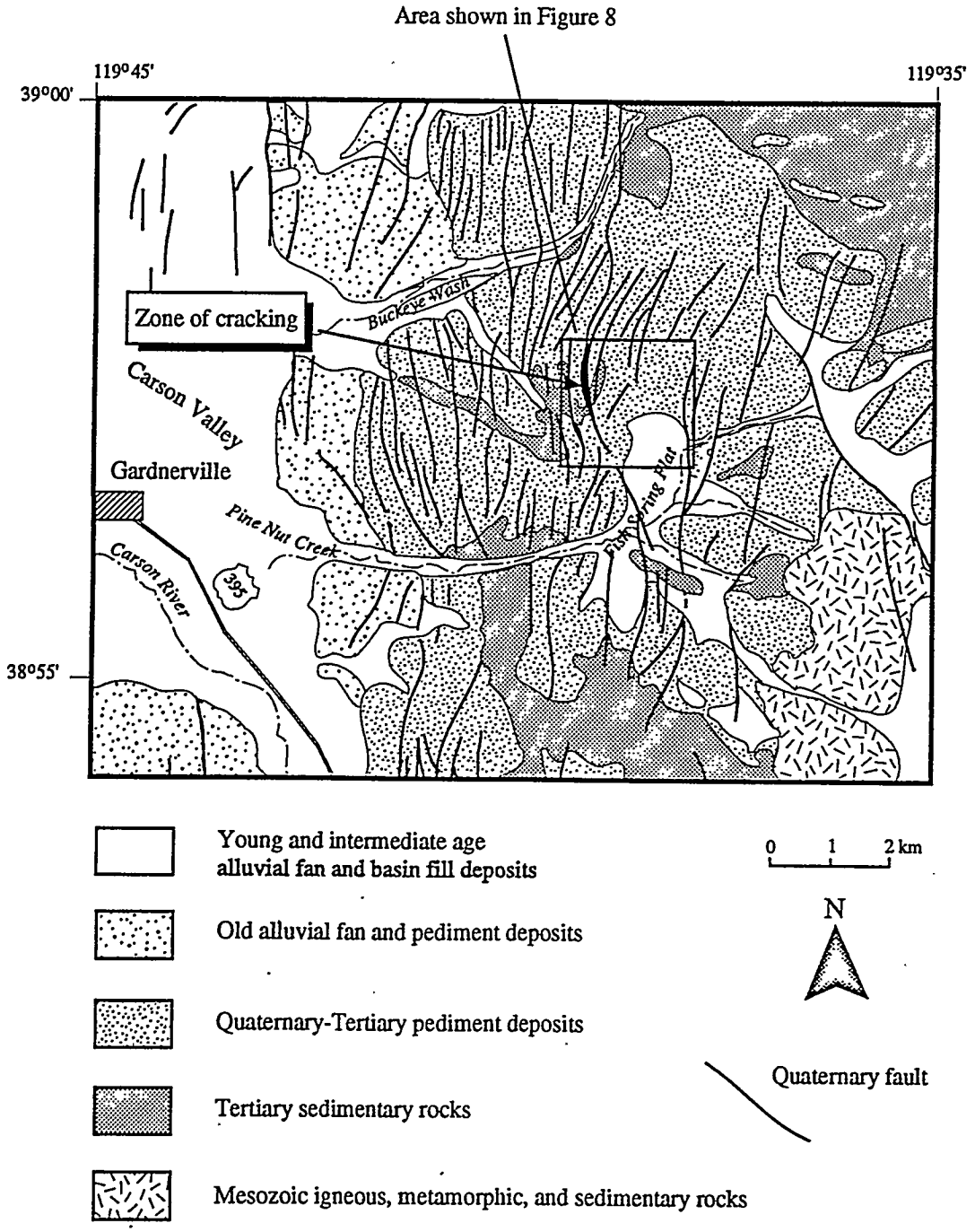
Area shown in Figure 8
119°45'
119°35'
39°00'
38°55'
Zone of cracking
Buckeye Wash
Carson Valley
Gardnerville
Pine Nut Creek
Carson River
395
Young and intermediate age alluvial fan and basin fill deposits
Old alluvial fan and pediment deposits
Quaternary-Tertiary pediment deposits
Tertiary sedimentary rocks
Mesozoic igneous, metamorphic, and sedimentary rocks
0 1 2 km
N
Quaternary fault

Fig. 2

Fig. 3

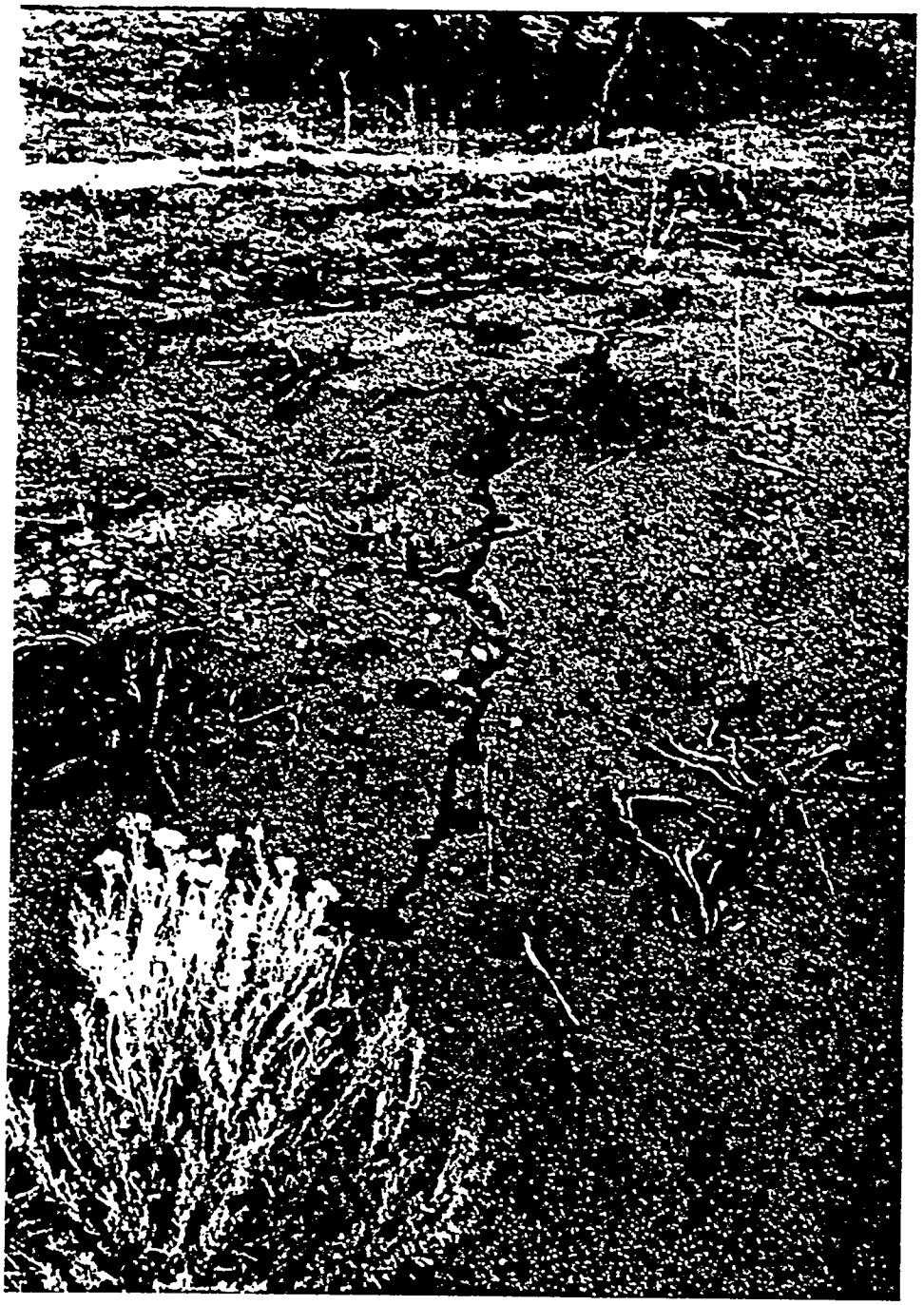

Fig. 4

Fig. 5

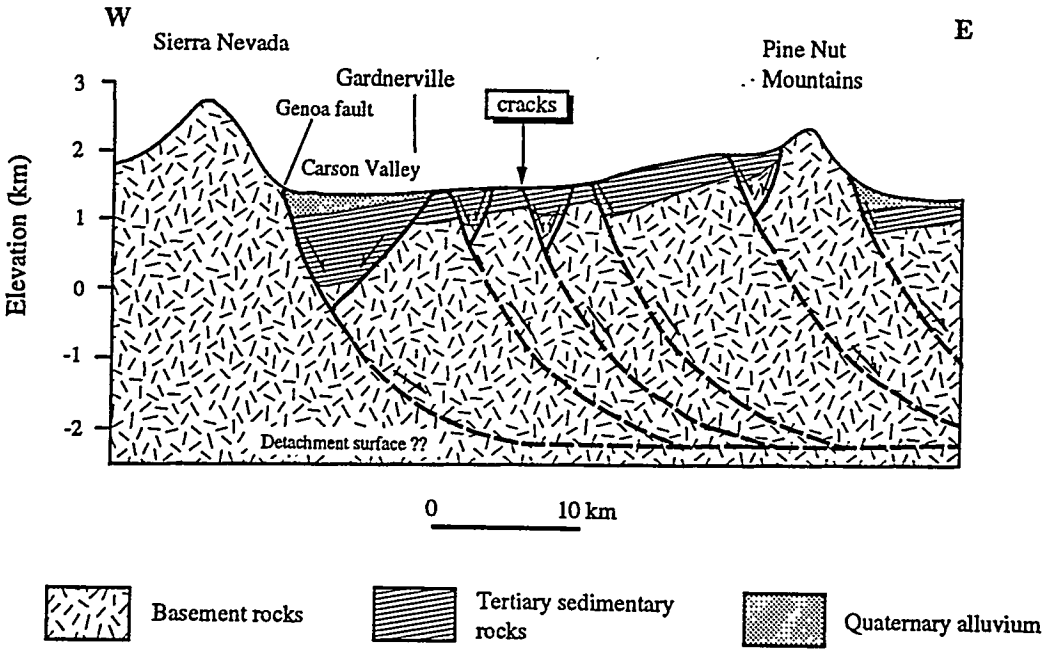
W
E
Sierra Nevada
Gardnerville
Genoa fault
Carson Valley
cracks
Pine Nut
Mountains
Elevation (km)
3
2
1
0
-1
-2
Detachment surface ??
0
10 km
Basement rocks
Tertiary sedimentary rocks
Quaternary alluvium

Fig. 6


Buckeye Wash
Down-to-east step faults
Fish Spring Flat
area of cracking
N
0
500 m
0
1000
2000 ft

Fig. 7

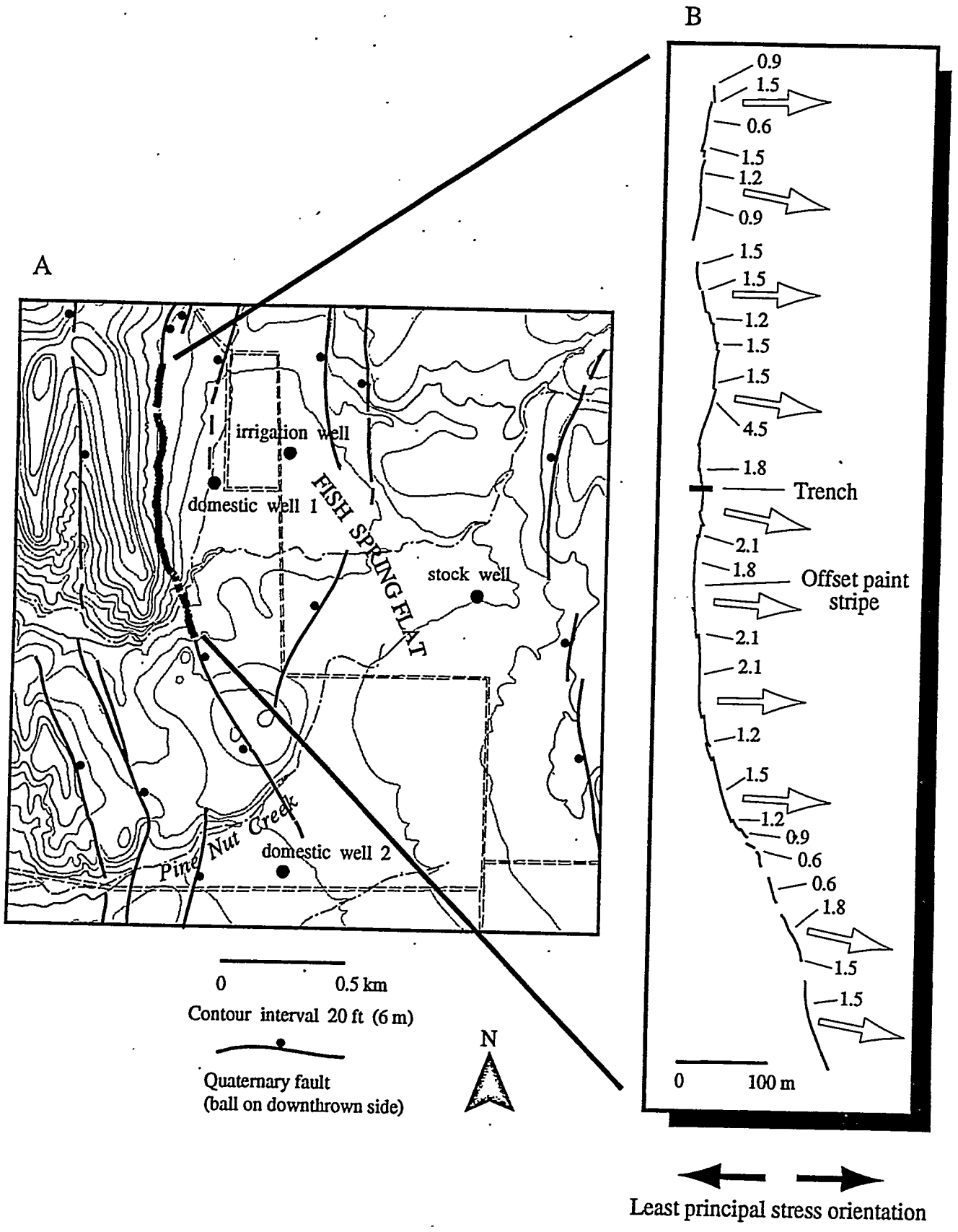
A
B
irrigation well
domestic well 1
FISH SPRING FLAT
stock well
Pine Nut Creek
domestic well 2
0
0.5 km
Contour interval 20 ft (6 m)
Quaternary fault
(ball on downthrown side)
N
0.9
1.5
0.6
1.5
1.2
0.9
1.5
1.5
1.2
1.5
1.5
4.5
1.8
Trench
2.1
1.8
Offset paint stripe
2.1
2.1
1.2
1.5
1.2
0.9
0.6
0.6
1.8
1.5
1.5
0
100 m
Least principal stress orientation

Fig. 8

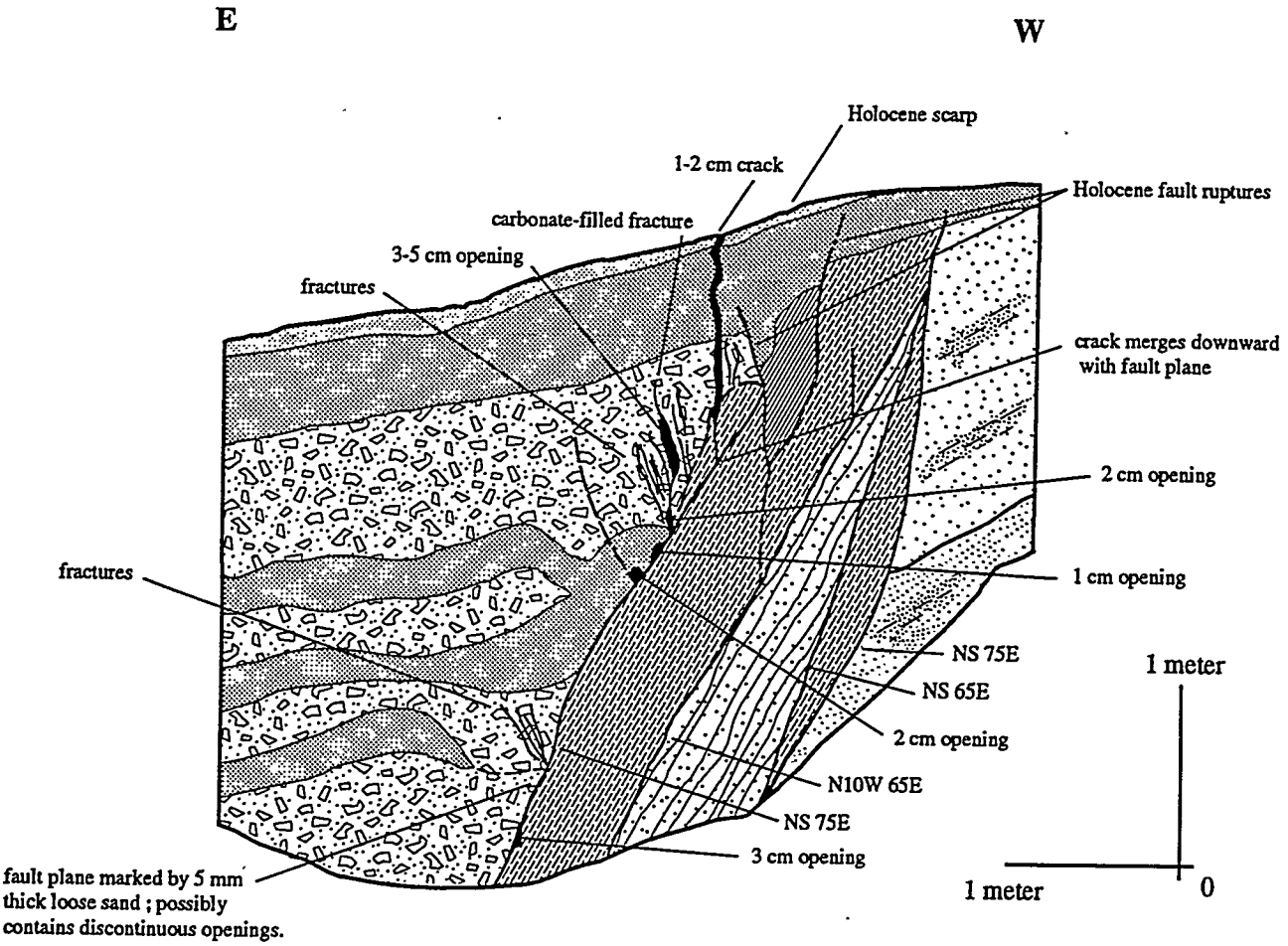

Soil A-horizon. Brown sandy loam; 10YR 5/3 D; 10YR 4/3 M; fine, platy structure; stripped at west end of trench.

Soil Bt-horizon. Dark brown to yellowish red clay loam; 10YR 4/3 to 5YR 6/6 D; 10YR 3/3 to 5YR 5/6 M; weak, medium prismatic structure.

Late Quaternary colluvium. Dark brown gravelly, sandy loam; poorly stratified, poorly sorted; angular to sub-rounded cobbles .

Fissure or graben filling. Grayish brown, silty, small pebble sand; slightly organic, A-horizon material.

Tertiary rocks. Light brown, silty, fine sandstone with lenses of sandy, small pebble gravel; thin bedding laminations and cross bedding; fractured, tilted.

Tertiary rocks. Medium brown sandstone; lenses of sandy, pebble gravel, interbeds of light brown, silty sandstone; fine bedding laminations; highly sheared and fractured.

Tertiary rocks. Light brown clayey siltstone; highly brecciated and tilted; clasts coated with dark gray manganese stain.

Shear zone. Light gray silty, sandy, small pebble gravel; highly granulated and crushed Tertiary rocks and locally colluvial deposits.

Fig. 9

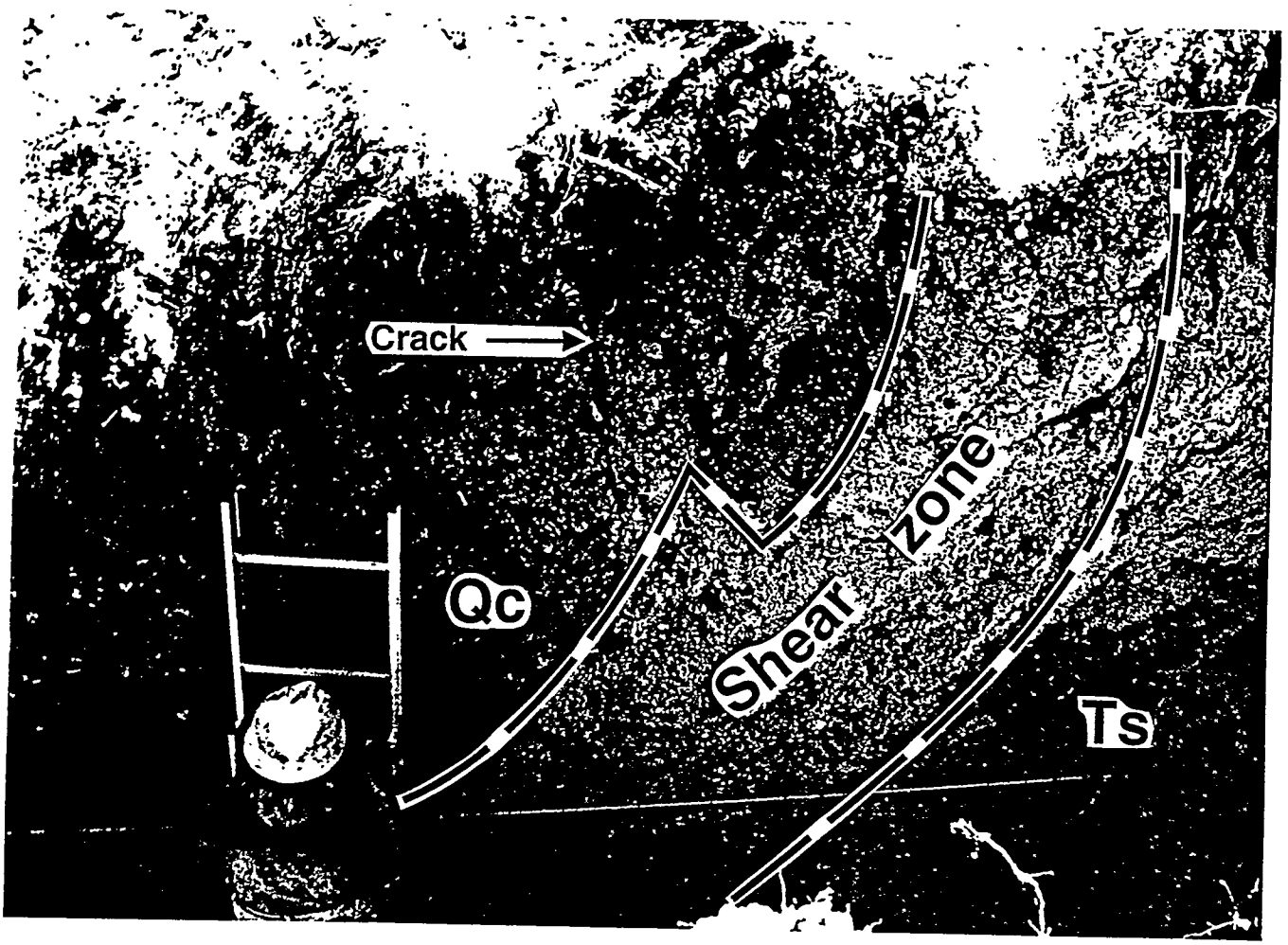

Fig. 10

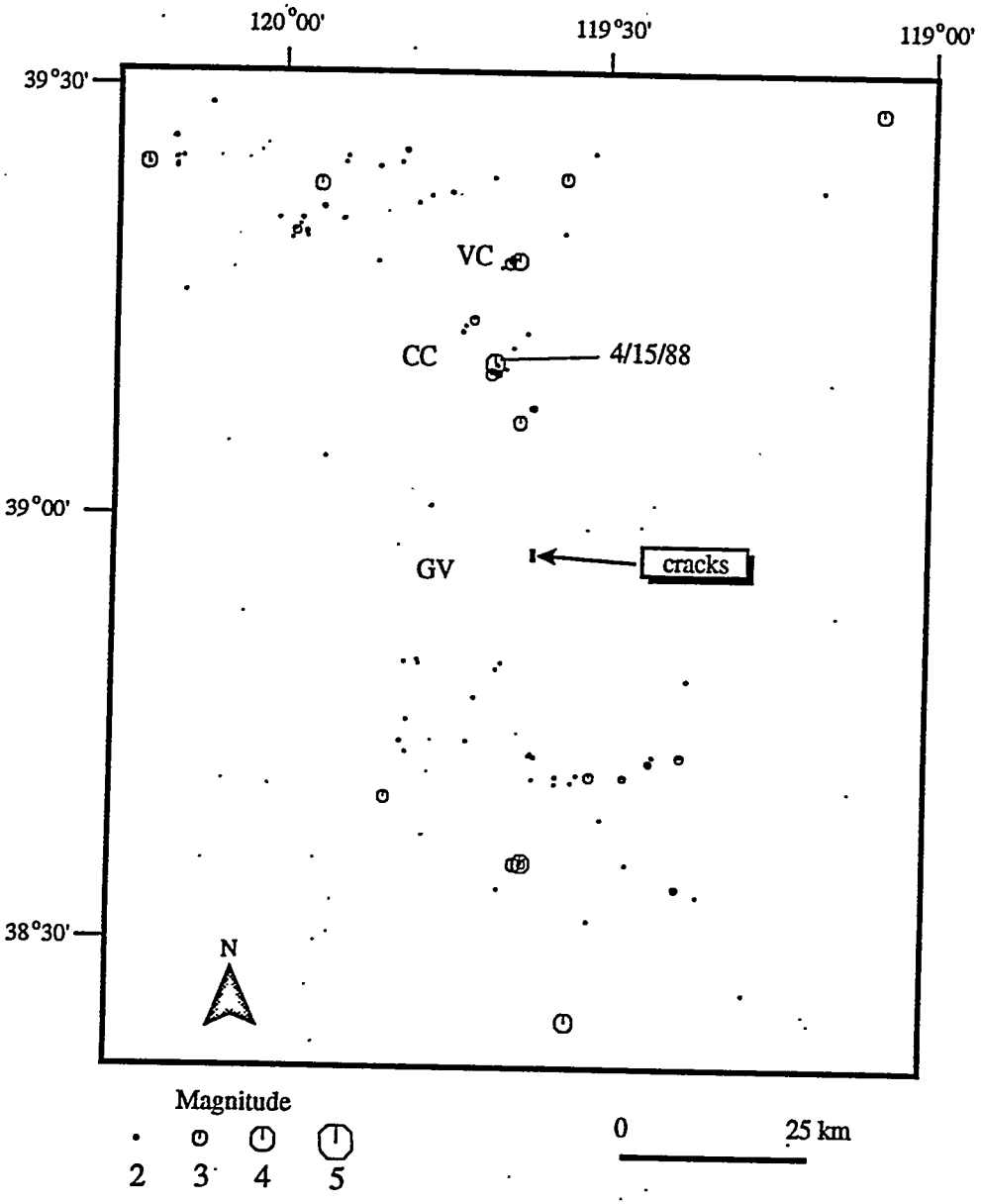
120°00'
119°30'
119°00'
39°30'
39°00'
38°30'
VC
CC
4/15/88
GV
cracks
N
Magnitude
2
3
4
5
0
25 km

Fig. 11

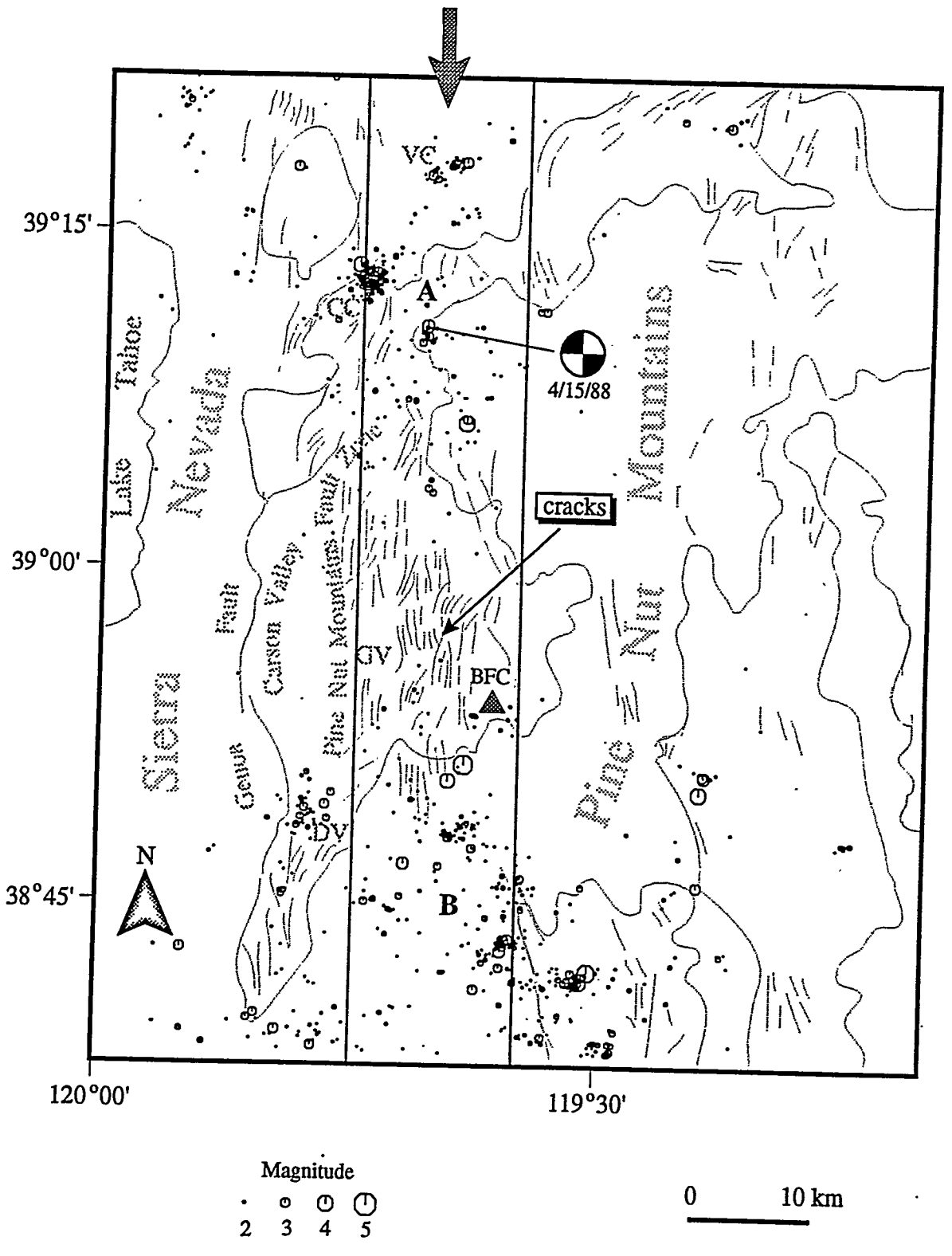
Area projected onto seismic cross section (Figure 13)
39°15'
39°00'
38°45'
120°00'
119°30'
VC
A
4/15/88
cracks
CV
BFC
B
N
Lake Tahoe
Sierra Nevada
Fault Zone
Genoa
Carson Valley
Pine Nut Mountains
Pine Nut
Magnitude
2 3 4 5
0 10 km

Fig. 12

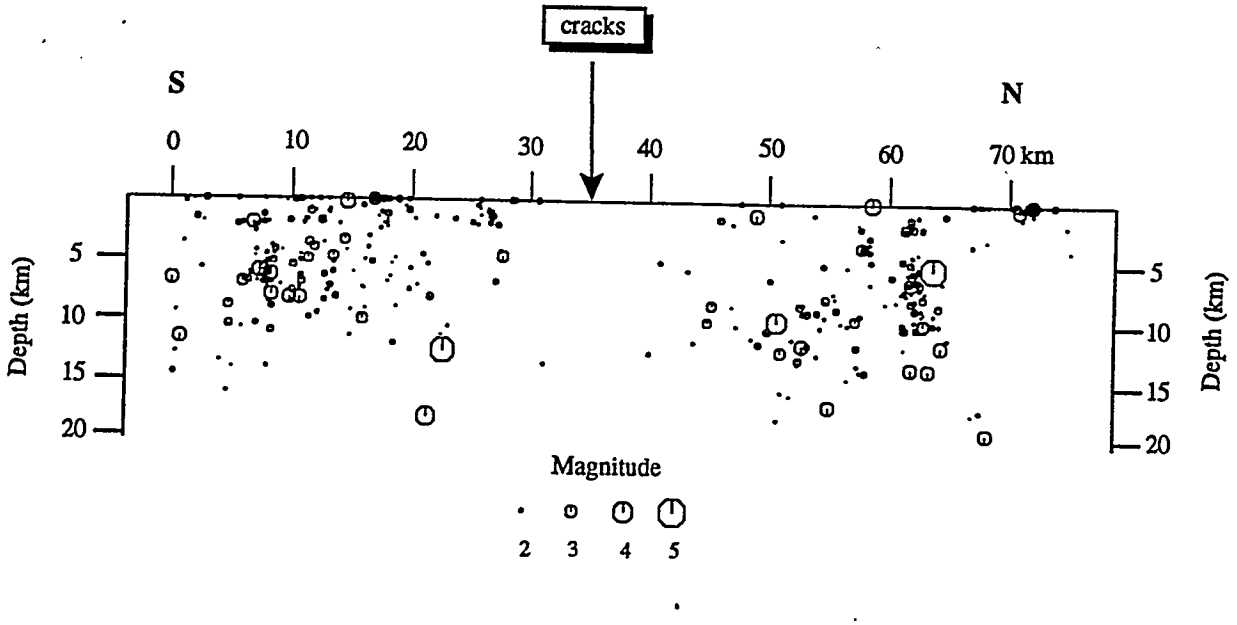
cracks
S
N
0
10
20
30
40
50
60
70 km
5
10
15
20
Depth (km)
Magnitude
2
3
4
5

Fig. 13

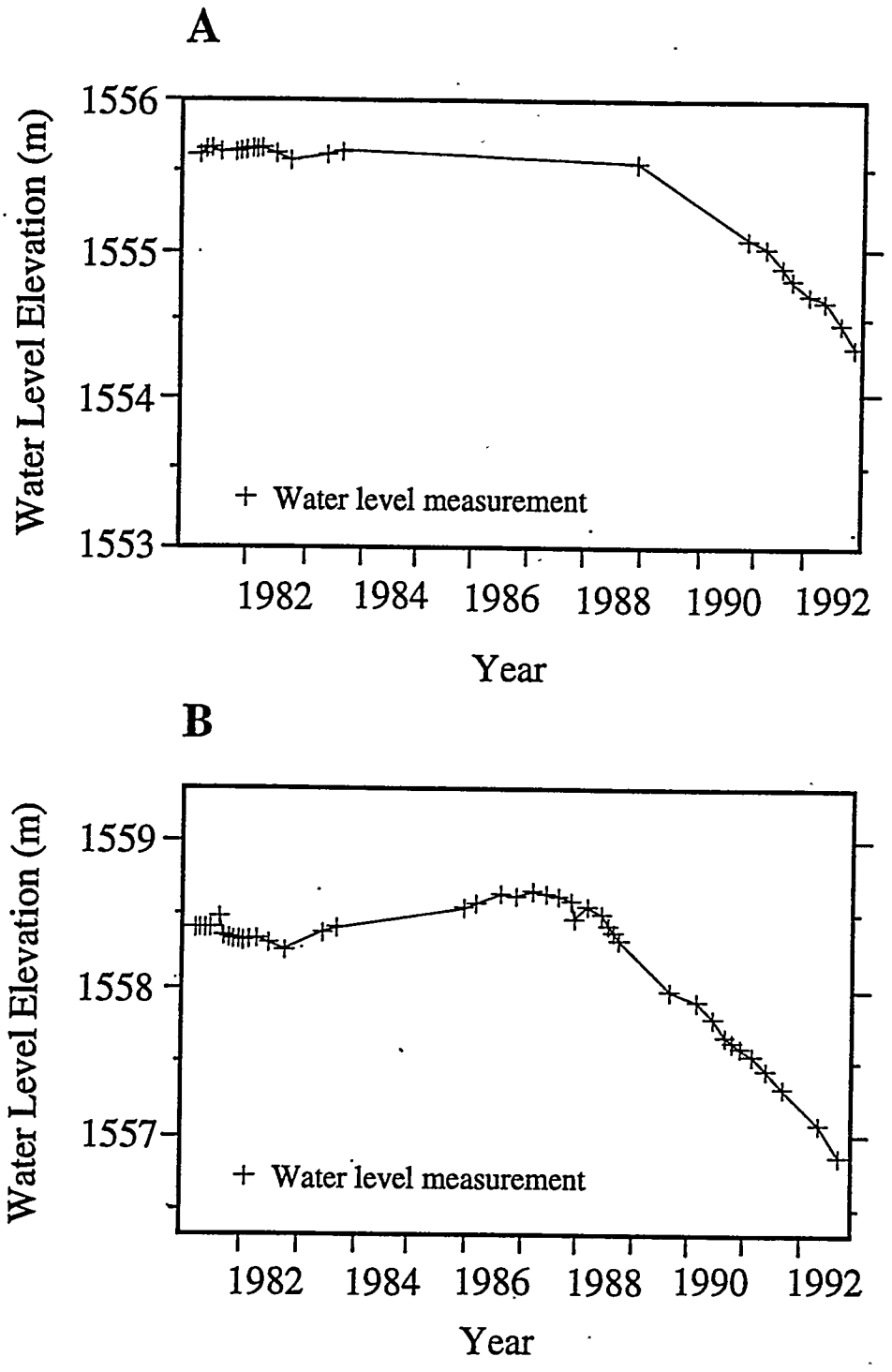
A
Water Level Elevation (m)
1556
1555
1554
1553
+ Water level measurement
1982
1984
1986
1988
1990
1992
Year
B
Water Level Elevation (m)
1559
1558
1557
+ Water level measurement
1982
1984
1986
1988
1990
1992
Year

Fig. 14

A

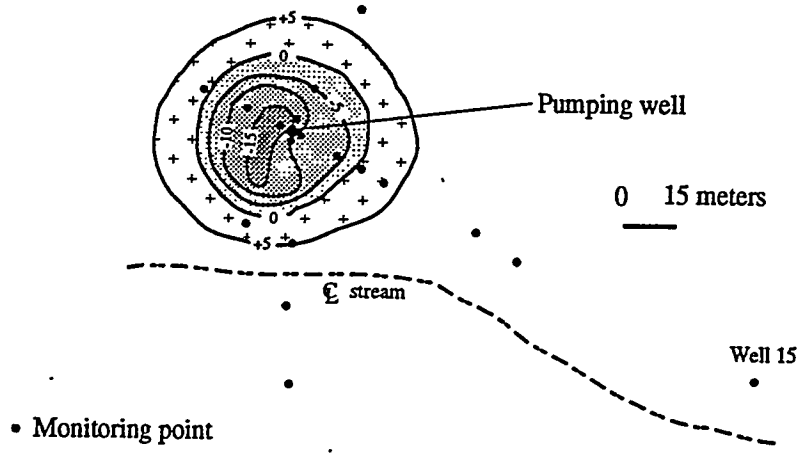
+5
0
-15
0
+5
Pumping well
0 15 meters
℄ stream
Well 15
• Monitoring point

B

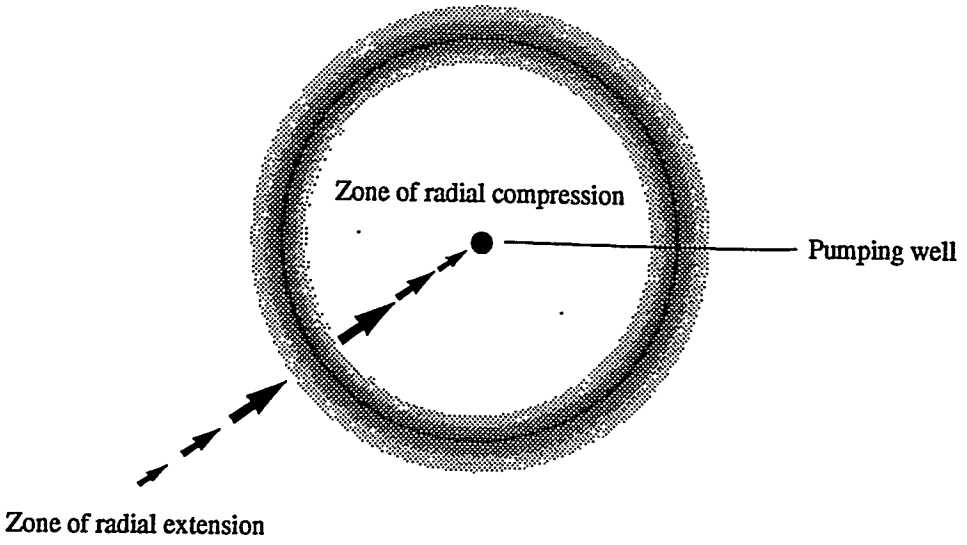
Zone of radial compression
Pumping well
Zone of radial extension

Fig. 15

TASK 3: EVALUATION OF MINERAL RESOURCE POTENTIAL, CALDERA GEOLOGY, AND VOLCANO-TECTONIC FRAMEWORK AT AND NEAR YUCCA MOUNTAIN

REPORT FOR OCTOBER, 1992 - SEPTEMBER, 1993

Steven I. Weiss,[1] Donald C. Noble,[2] and Lawrence T. Larson[2]

Department of Geological Sciences, Mackay School of Mines, University of Nevada, Reno

[1] Research Associate
[2] Co-principal Investigators and Professors of Geology and Economic Geology

INTRODUCTION

This report summarizes the results of Task 3 work that was initially discussed in our monthly reports for the period October 1, 1992 through September 30, 1993, and contained in our various papers and abstracts, both published and currently in press or in review (see appendices). Our work during this period has involved a) the continuation of studies begun prior to October, 1992, focussed mainly on aspects of the caldera geology, volcanic stratigraphy, magmatic activity, hydrothermal mineralization and extensional tectonics of the western and northwestern parts of the southwestern Nevada volcanic field (SWNVF), studies of the subsurface rocks of Yucca Mountain utilizing drill hole samples obtained in 1991 and 1992, and b) new studies of veins and siliceous rocks cropping out in northwestern Yucca Mountain that provide evidence for previously unrecognized hydrothermal activity during the Crater Flat Tuff period of volcanism.

VEINS AND SILICEOUS DEPOSITS IN NW YUCCA MOUNTAIN: EVIDENCE FOR HYDROTHERMAL ACTIVITY PRIOR TO 13.1 Ma

To date there has been little direct evidence for hydrothermal activity within or directly adjacent to Yucca Mountain prior to deposition of the *ca.* 12.8 Ma Paintbrush Tuff. Most currently recognized episodes of hydrothermal activity in the southwestern Nevada volcanic field were contemporaneous with, or shortly post-dated, culminations in magmatic and volcanic activity of the main and Timber Mountain magmatic stages at about 12.8 and 11.4 Ma, respectively (Noble et al., 1991; Weiss et al., in prep.). Although hydrothermal activity took place in the Sleeping Butte area early in the evolution of the SWNVF and Au-Ag mineralization formed in the Wahmonie-Salyer center at about 13 to 12.5 Ma (Jackson, 1988; Noble et al., 1991; Weiss et al., in prep.), only indirect evidence, such as the possible alteration of wallrock in the vent areas of the Lithic Ridge and Crater Flat Tuffs (Castor et al., 1992; in press; Weiss et al., in prep.), has been recognized for hydrothermal activity predating the Paintbrush Tuff in or near Yucca Mountain. Such activity and possible associated mineralization prior to 12.9 Ma at Yucca Mountain can not be recognized by surficial sampling programs (e.g. Castor et al., 1989; 1990) and would likely remain undetected with the present widely spaced drill holes that penetrate the Crater Flat Tuff or older volcanic rocks.

Recent geologic mapping of the East of Beatty Mountain 7.5' quadrangle (Fridrich et al., in review), has identified siliceous veins and layered opaline silica deposits in an area of northwestern Yucca Mountain (Figure 1) that provide evidence strongly suggestive of pre-13.1 Ma, near-surface hydrothermal activity. The veins are hosted by the Tram Member of the Crater Flat Tuff. Two thin siliceous horizons, in part composed of layered opal provisionally interpreted as silica sinter, are interbedded with nearby thin, unwelded units of ash-flow tuff and surge deposits between the Tram Member and overlying, unaltered tuffs of the Bullfrog Member of the Crater Flat Tuff (C. J. Fridrich, personal commun., 1993). The area of most abundant veins is located approximately 300 m southwest of hilltop 4900T, in the NW 1/4 of unsurveyed section 36, T11S, R48E, East of Beatty Mountain 7.5' quadrangle (Figure 2). The veins are hosted by densely to moderately welded, devitrified and vapor-phase crystallized ash-flow tuff of the Tram Member and consist of variable proportions of grey to white, angular to subrounded, cm to sub-mm sized fragments of bleached tuff and phenocrysts cemented by a dark reddish brown mixture of very fine grained silica and iron oxide (Figure 3). Many of the veins contain bands of grey to white chalcedony and opal, and in some cases can be traced laterally into segments composed entirely of banded silica. The veins range from about 1 mm to about 5 cm in thickness and occupy shallow- to steeply-dipping fractures with generally sharp margins. Commonly the veins branch into thin, irregular, discontinuous and often anastamosing veinlets in the wallrocks adjacent to the fractures. The most continuous veins, traceable in outcrop for as much as about 15 m, tend to follow fractures that strike N30-45E, with steep northwest dips, and N50-60W with steep northeast

dips. In the upper, less densely welded portion of the Tram Member the veins are less continuous and commonly grade into breccia composed of reddish brown iron oxide and bleached fragments of vapor phase crystallized tuff.

Two lines of evidence are consistent with a shallow hydrothermal origin for the veins. These are: 1) multi-element trace metal contents, and 2) textural characteristics of the veins.

Multi-element analyses by sensitive inductively-coupled plasma emission spectrographic (ICP-ES) and hydride-generator atomic absorption (AA) methods show that the veins contain concentrations of As, Hg, Sb, and Mo, ±Tl, ±Bi inconsistent with an origin by descending surface water (Table 1). Although Au and Ag concentrations are not significant, the analyses show that a suite of metals commonly observed in the upper parts of active and fossil geothermal systems was carried by the fluids that formed the veins. The iron oxide-silica cemented breccia composing many of the veins commonly pinches, swells, penetrates the wall rocks at high angles along jagged, irregular fractures, splays into thin, anastomosing veinlets and dies out into undisturbed welded tuff. These features, along with the epithermal trace-element signature, are most consistent with an origin by hydrothermal brecciation and injection, rather than by passive filling of open spaces by descending surface water. In addition, feldspar phenocrysts in wallrocks of the vein zone south of hilltop 4900T are partially pseudomorphed by adularia and small amounts of euhedral adularia are present with fine grained quartz in the groundmass. This alteration is more typical of distal hydrothermal activity than of pedogenic processes or the effects of rock interaction with cold groundwater. Veins and brecciation of this type could not be traced up into the overlying pre-Bullfrog Member ash-flow and surge deposits, implying that vein formation occurred at shallow depths prior to the eruption of the Bullfrog Member at about 13.1 Ma.

At the scale of individual hand-specimens, the veins and breccia within the Tram Member are strikingly similar to, if not indistinguishable from, veins and breccia in welded tuffs of the Crater Flat Tuff of drill holes UE25-C1, -C2 and -C3, assigned by Geldon (in press) to the Tram Member. Vein-bearing specimens from these drill holes have lower concentrations of Tl, higher concentrations of Mo and Bi, similar amounts of As, Sb, and Hg, and in some cases contain fluorite, which has not been identified in the veins in northwestern Yucca Mountain (Weiss et al., 1992).

In the area of Figure 2 the Tram Member is overlain by an approximately 60 m sequence of southwest dipping unwelded, thin rhyolitic ash-flow tuffs and interbedded pyroclastic surge deposits. Relict glass shards and pumice textures indicate a lack of primary crystallization, although the sequence is partially zeolitized. This sequence has been interpreted to reflect local pyroclastic volcanism precursor to the eruptions of the Bullfrog Member of the Crater Flat Tuff (Carr et al., 1986; Fridrich et al., in review). Within this sequence are exposed two siliceous horizons which comprise ledges separated by approximately 5 - 6 m of less resistant interbedded pyroclastic surge and thin ash-flow deposits dipping to the southwest, approximately conformable with the underlying and overlying ash-flow sheets (Figure 2). The lower ledge consists of 1 - 2 m of slightly opalized ash-flow tuff and surge that directly overlies a poorly exposed, tabular body of laminated, red, brown, clear, white and dark grey opal. The opal laminae do not have discernable internal clastic texture and appear to represent submillimeter- to cm-thick layers of chemical precipitate. Individual laminae are discontinuous and show evidence for both soft-sediment deformation and brittle fracturing (Figure 4a), features not uncommon in silica-sinter deposits. A major- and minor-element whole-rock analysis of the laminated opal (specimen 3SW693, Table 2) shows very little TiO_2 and only about 2 weight % Al_2O_3 are present in this material, arguing against an origin by replacement of rhyolitic tuff or tuffaceous sediment. Trace-metal concentrations are low, except for Hg and Mo (Table 1).

Float from this silica body is scattered downslope along much of the lower ledge, indicating a lateral extent approaching 600 to 700 m (Figure 2). The best exposure is in an old

prospect pit where the thickness is about 0.5 m, but the base is not exposed. Two lines of evidence support an origin by deposition at the paleosurface: 1) float blocks with polygonal dessication cracks and trace fossils of probable worm burrows (Figure 4b) argue strongly for deposition at the paleosurface, and 2), rip-up clasts of the laminated opal as much as a few cm in maximum dimension are incorporated in the lower parts of the overlying surge and ash-flow deposits, indicating exposure at the paleosurface during emplacement of the overlying units. Based on the lithology, texture and chemical composition of the opal layers, we believe the opal body of the lower ledge is best interpreted as a thin, laterally extensive silica sinter. The lack of elevated trace metals is not unusual as many hot-spring silica sinters contain little more than modest amounts of Hg.

Most of the lower ledge consists of unwelded tuff made resistant to weathering by weak opalization. In addition, at several localities tuff is hardened adjacent to WNW-trending, steeply dipping veins of opal, chalcedony and smaller amounts of granular quartz as much as 10 cm in thickness. Analyses of the opalized tuff and silica veins of the lower ledge (specimens 11, 12 and 14) do not show the As, Sb, Hg ±Tl signature found in the veins in the Tram Member. However, examination of thin sections shows that the tuffs adjacent to these veins contain euhedral adularia intergrown with chalcedony, illite/smectite and quartz in the groundmass, and adularia as partial to complete pseudomorphs of plagioclase and sanidine phenocrysts. This alteration assemblage is suggestive, but not unequivocal, evidence for elevated temperatures near the veins. Unfortunately, fluid inclusions suitable for microthermometry have not been found if they are present. Nevertheless, adularia is now widely recognized in wallrock alteration assemblages associated with epithermal base- and precious-metals deposits and is considered by many explorationists to be an important and favorable sign of potential for mineralization.

The upper ledge consists of light brown, silicified ash-flow and surge deposits overlain by distinctive, hard and dense, dark grey, thinly bedded fine siltstone and sandy siltstone 10 to 30 cm in thickness (Figure 5). Silicification of the siltstone is demonstrated by its high SiO_2 content (specimen 3SW685, Table 2) and hard, resistant character. The grey siltstone locally shows evidence of soft-sediment slumping and is directly overlain by thin, slightly silicified surge and ash-flow deposits containing rip-up clasts of the grey siltstone. The siltstone crops out for about 500 m along strike and at sample locality 687 contains an interbed nearly 0.5 m in thickness of laminated opal lithologically and chemically similar to that of the lower ledge (field # 3SW687, Tables 1 and 2). Elevated concentrations of Hg, Sb, Mo, Tl, Pb and Zn, and possibly Bi, are present in the siltstone, reflecting the presence of metal-bearing solutions during deposition and/or silicification. Although the siltstone is most reasonably interpreted as a local sedimentary unit within the tuff sequence, the presence of solutions with this suite of trace elements at or near the paleosurface argues for an input of shallow hydrothermal fluids.

ANALOGUE STUDY OF THE BALD MOUNTAIN GOLD DEPOSITS

A collaborative study of the Bald Mountain gold deposits, located in White Pine County, eastern Nevada, was initiated during 1993. The Bald Mountain mine is one of the larger and more important gold producers in Nevada, with reserves that are conservatively calculated to exceed ten years of production. Individuals involved include D. C. Noble and Jared Beebe of the Mackay School of Mines, Alan Hitchborn and other geologists of Placer Dome, and Dr. Steven Peters of the U.S. Geological Survey. Our collegue Dr. Edwin H. McKee of the U.S. Geological Survey, Menlo Park, is involved with the radiometric dating program. The principal purpose of the study is to better quantify and understand the nature and formation of disseminated gold mineralization at the Bald Mountain mine. D. C. Noble was the driving force behind the setting up of this project. Although funding is almost entirely from sources other than NNWPO, it appears desirable to include a short discussion

of this work because of its potential significance with regard to the Yucca Mountain project.

One of the principal reasons that the Bald Mountain deposits are of interest is the close spatial association between major economic gold mineralization of both sedimentary rock-hosted and porphyry-hosted type to igneous activity. In initiating this study we had in mind the very similar association that we have recognized and have been studying at the Bare Mountain district directly west of Yucca Mountain. More closely defining the similarities between the prospects and mines at Bare Mountain and economically important deposits of the Bald Mountain system increases the attractiveness and potential economic significance of the Bare Mountain district.

To date Mr. Beebe has spent several months carrying out detailed mapping and sampling in several of the mineralized areas at Bald Mountain, working closely with the mine geologists. Dr. Peters has spent several weeks mapping various of the open pits in which sedimentary rock-hosted ores are exposed and/or have been mined. D. C. Noble has spent at total of about a week making reconnaissance observations, discussing geologic information with company geologists, and handling other on-site logistic and administrative matters.

At present we have only initial results. Four radiometric ages by McKee on biotite from the large main stock and from a porphyry dike all give latest Jurassic ages, showing the magmatic activity is clearly of pre-Cenozoic age. (Previously the magmatic system had been variously considered to be of Cenozoic (Eocene?) or Mesozoic age.) We are presently in the process of obtaining additional radiometric ages on hydrothermal alteration minerals to determine how closely mineralization followed the dated pulse of igneous activity. An areally extensive and, in detail, complex system of dikes and irregular bodies of intrusive breccia have been recognized by Noble and Peters. Peters has made some significant revisions in the structural patterns from those recognized by the mine geologists. Noble has recognized the existence of hypersaline (high-salinity) fluid inclusions in one of the porphyry dikes and work is in process to determine if the inclusion-bearing rocks are in place or were vertically transported to their present position by high-energy magmatic vapors as blocks of intrusive breccia, relations that are critical to determine the level of emplacement of the gold mineralization and the depth to which the deposit has been eroded since formation.

Preliminary evaluation has been made of a large body of geochemical data obtained over a period of almost 10 years by Placer Dome geologists. In addition to the usual elevated contents of As, Sb, Hg, etc., some of the deposits have high concentrations of Te, Bi, Mo and Cu, elements which suggest direct magmatic inputs of gold and other components of the hydrothermal fluids.

In summary, although work is still in its initial stages, a number of new relations have been recognized and data obtained. We hope that in a year we will have a much better understanding of the genetic similarities (or lack thereof) between the Bare Mtn. and Bald Mtn. mineral systems and the implications of these relations for the potential economic importance of the Bare Mountain mineral systems.

PROGRESS IN RADIOMETRIC DATING STUDIES

Timing of Au-Ag mineralization at the Mother Lode mine, northern Bare Mountain

The timing of disseminated gold mineralization at the Mother Lode mine has been inferred to be about 12.9 to 12.5 Ma, based on age determinations on adularia and alunite from nearby areas and on similarities to alteration and mineralization elsewhere in northern and eastern Bare Mountain (Noble et. al., 1991; Castor et al., 1992). Direct radiometric dating of the Mother Lode mineralization is desirable because of the close proximity of the deposit to Yucca Mountain, but has been hampered by a lack of material unequivocally suitable for dating (see below), as has been the case with many sedimentary-rock hosted, disseminated gold deposits in the Great Basin. Examination of surface samples and drill-hole cuttings from the deposit shows that a birefringent phyllosilicate phase often referred to as "sericite" is abundant as an alteration phase in the mineralized rocks, replacing phenocrysts and in the groundmass. Reconnaissance X-ray diffraction analyses show that this mineral consists of mixed layer illite-smectite, that is, illite having discernable amounts of interstratified montmorillonite. During 1992 samples of mineralized dike rock and limestone were forwarded to Dr. Giday Woldegabriel of Los Alamos National Laboratory for evaluation of the possibility of obtaining K-Ar ages from the illite/smectite. Dr. Woldegabriel carried out detailed X-ray diffraction studies of the samples and was successful in separating sufficient clay-sized (0.1-0.35 μm) illite/smectite grains for K-Ar age determinations from three specimens (two altered dike specimens and one altered limestone specimen). Illite/smectite concentrates from the two dike specimens were found to contain acceptable amounts of K_2O (7.76 and 7.73 wt.%, respectively). Argon extractions were carried out and K-Ar ages of 13.1 ± 0.3 Ma and 12.2 ± 0.4 Ma were calculated (G. Woldegabriel, written commun., 1993). The calculated ages, although significantly different, are considered by Dr. Woldegabriel to be reasonably concordant for clay-sized illite/smectite concentrates. Moreover, both age determinations are consistent with the timing of hydrothermal activity and fluorite ±disseminated gold mineralization in northern and eastern Bare Mountain inferred from previously obtained K-Ar and $^{40}Ar/^{39}Ar$ ages.

The mineralized limestone was almost completely decarbonatized and argillized and prior to partial oxidation contained pyrite and marcasite. Illite/smectite separated from the limestone gave a K_2O content of 6.13 wt.% and a K-Ar age of 26.85 ± 0.62 Ma (G. Woldegabriel, written commun., 1993). There is no clear geologic or petrographic evidence to explain the apparent age discordance with the illite/smectite ages of the adjacent altered dike rock. One possibilty may be the incorporation of excess radigenic argon, perhaps released by hydrothermal fluids from deeper Paleozoic strata, within the illite/smectite of the altered limestone.

The apparent discordance in alteration ages led us to further investigate the feasibilty of separating adularia from the altered dike rocks. The problem has been that sanidine phenocrysts in the altered dike rocks at the Mother Lode deposit show little, if any, petrographic evidence for recrystallization or replacement by adularia, although adularia and quartz replace the groundmass and the plagioclase phenocrysts are thoroughly altered to illite-, calcite-, albite-, and adularia-bearing assemblages. This sanidine would be difficult to separate from groundmass adularia and, if primary, would result in an incorrect, older apparent age of alteration and mineralization. To evaluate this possibility, semiquantitative

energy-dispersive scanning-electron microscopic analyses of sanidine phenocrysts in polished specimens of altered dike rocks were obtained at the U.S. Bureau of Mines in Reno, under the supervision of Dr. James Sjoberg. Primary sanidine commonly contains appreciable amounts of sodium, whereas adularia in altered silicic volcanic rocks generally contains very little sodium, as indicated by both bulk chemical and microprobe analyses (e.g., Sander, 1988). For comparison, thoroughly adularized sanidine phenocrysts (adularization inferred from mottled extinction and common turbid appearance reflecting innumerable small solid and fluid inclusions) in ore from the Lac Gold Bullfrog mine were analyzed consecutively with the Mother Lode rocks. Sodium concentrations of the adularized sanidine phenocrysts in the Lac Gold Bullfrog sample were barely detectable at about 0.01 wt. % Na_2O. In contrast, measured Na_2O contents of sanidine in the altered dike rocks from the Mother Lode mine ranged from 0.96 wt. % to 2.28 wt. %, providing evidence that the sanidine is primary and remained stable during hydrothermal activity. This suggests that the possibilty of obtaining meaningful alteration ages with standard K-Ar methods or multi-grain fusion-type $^{40}Ar/^{39}Ar$ methods is unlikely. During the next year we plan to evaluate the possibility of obtaining meaningful alteration ages by step-heating $^{40}Ar/^{39}Ar$ methods.

STUDIES OF DRILL CORE AND CUTTINGS FROM THE SUBSURFACE OF YUCCA MOUNTAIN

Update on the Distribution and Nature of Subsurface Alteration

Studies of core and cuttings from drill holes USW G1, USW G2, USW G3, UE25 P1, UE25 B1H, UE25 C1, UE25 C2, UE25 C2, UE25 A1 and UE25 A4 continued with specimens obtained in 1991 and 1992. The purpose of these studies is to investigate the nature, spatial distribution and origin(s) of alteration within the subsurface of Yucca Mountain in order to evaluate the potential for undiscovered mineral resources.

No evidence was found in thin sections for the silicification reported by Spengler et al. (1979) within the Prow Pass Member of the Crater Flat Tuff in drill hole UE25 A1. However, definite silicification of gropundmass and partial replacement of feldspar phenocrysts by adularia were recognized in the Bullfrog Member at a depth of 2478-2479' in UE25 A1. Examination of a thin section from this interval shows that glass shards and small pumice fragments have been replaced largely by a mosaic of interlocking quartz grains. Approximately 50 percent of the feldspar phenocrysts have been replaced by somewhat turbid adularia with mottled extinction and small amounts of albite. This alteration occurs at a higher stratigraphic level and shallower depth than has been acknowledged by previous workers, and suggests that the depth to hydrothermal alteration does *not* increase southwards from USW G2 as reported by Bish (1987). An updated summary of alteration features and other data of the drill holes is given in Figure 6.

Although systematic chemical studies of altered silicic tuffs near volcanic-hosted precious metal deposits have not yet been carried out for comparison to data from Yucca Mountain and to investigate the aerial dispersion of trace metals in tuffs in mineralized areas, we have obtained some preliminary data that bears on this topic. Blind duplicate analyses of altered Timber Mountain Tuff from within 30 m of ore at the Lac Gold Bullfrog mine (Table 1) demonstrate that As, Sb, Hg and other elements that provide chemical evidence for mineralization may not be widely dispersed and may remain unrecognized when only data from widely spaced drill holes are available.

Critical Observations on the Origin and Significance of Pyrite in Tuffs of Yucca Mountain

Contactors for the Department of Energy and Science Applications International (Castor et al., 1992; in press) have argued that pyrite disseminated in tuffs in the subsurface of Yucca Mountain is of lithic or xenocrystic origin and provides no evidence for sulphidic

hydrothermal activity *in situ*. In contrast, textural information and doubts about the stability of small pyrite grains incorporated in large pyroclastic flows have led us to argue that the groundmass pyrite formed by sulphidation (introduction of reduced sulphur) *after* deposition of the ash-flow units and provides clear evidence for hydrothermal activity *within* Yucca Mountain (Weiss et al., 1992). Several observations bearing on this controversy merit emphasis here.

First, pyrite is present as disseminated anhedral to subhedral grains in altered tuff fragments at various depths between 3890' and 4215' in drill hole UE25 P1, approximately 400' below the base of the Lithic Ridge Tuff. Although this pyritic alteration and that of the pre-Lithic Ridge silicic lavas in USW G2 (various USGS and LANL reports; Weiss et al., 1992) could have taken place prior to deposition of the Lithic Ridge Tuff, the pyritic alteration of the lavas *overlying* the Lithic Ridge Tuff in USW G2 (Caporuscio et al., 1982) must *post-date* deposition of the Lithic Ridge and requires *in situ* introduction of aqueous reduced sulphur!

The next problem is that lithic fragments with radii of 1 mm or less can be expected to heat up to the bulk temperature of pyroclastic flows within 1 second or less (Marti et al., 1991). In most large pyroclastic eruptions this bulk temperature approaches magmatic temperatures. Although published temperature data are not available for the Lithic Ridge Tuff and units of the Crater Flat Tuff, large-volume ash-flow units of the Timber Mountain and Paintbrush tuffs were erupted from magamas with estimated temperatures mainly between 700° and 900°C (Warren et al., 1989). Heating to such temperatures would result in the decomposition of small pyrite fragments unless the fugacity of S_2 gas is close to unity (Figure 7). At lower fS_2 destabilization of pyrite would be expected at temperatures below 743°C with conversion of pyrite to pyrrhotite and/or iron oxide phases, depending on the fO_2 (Kullerude and Yoder, 1959; Barton and Skinner, 1979). Calculations by Marti et al. (1991) suggest that even with large volumes of lithic fragments derived from cold wallrocks in the vent area, bulk pyroclastic flow temperatures are not reduced below about 500°C until after times on the order of 40 seconds to minutes. Thus, it seems likely that small pyrite lithic fragments would be heated to near magmatic temperatures and would probably begin to lose sulphur even in lithic-rich units. We have not observed pyrrhotite rims on any of the pyrite in the groundmass or in pyritic lithic clasts in Yucca Mountain rocks. Moreover, we estimate that less than one third of the pyrite grains in the groundmass of the Lithic Ridge Tuff and the Tram Member have rims of hematite or other iron oxides. Indeed, we have observed fresh pyrite in the groundmass adjacent to lithic clasts containing thoroughly oxidized pyrite (pseudomorphed by hematite/goethite). Such oxidized clasts, with fresh, subhedral pyrite adjacent to the edges of the clasts and disseminated in the surrounding tuff matrix, are particularly common in specimens of the Lithic Ridge Tuff from drill hole USW G3.

Finally, Castor et al. (in press) report the presence of rounded grains of groundmass pyrite and attribute this to the effects of abrasion during ash flow eruption and deposition. We find it surprising that the delicate cuspate glass shards (now generally pseudomorphed by alteration phases) and angular phenocryst fragments of the pyritic units would persist in an environment of inter-particle abrasion sufficient to round off the harder pyrite. Our observations indicate that although some groundmass pyrite of anhedral, round form is present, much, if not most, groundmass pyrite is of anhedral to subhedral, angular to filmy forms inconsistent with strong abrasion.

Fluid Inclusion Studies

All of the drill core samples from Yucca Mountain currently in our possession and in the possession of the Nevada Bureau of Mines and Geology were reviewed in efforts to locate veins and other open-space fillings of quartz, fluorite and barite that might contain fluid inclusions useful in constraining the temperature(s) of past water-rock interaction in

Yucca Mountain. Eight core specimens were identified containing potentially useful vein materials. Preparation of polished chips from each specimen has been nearly completed and study of the chips will commence shortly. Chips are also being prepared from drusy quartz crystals lining lithophysal cavities in the Tiva Canyon Member of the Paintbrush Tuff at Exile Hill, to investigate the nature of quartz deposition near the Bow Ridge fault.

UPDATE ON MINING AND MINERAL EXPLORATION

Precious metals prices have been relatively weak during the past year, but exploration and mining efforts continued in the Beatty area of the SWNVF. A new program of exploratory drilling in northern Bare Mountain, about 1.5 to 2 km southwest of the Mother Lode mine, was carried out by Cordex Exploration to explore for blind Au mineralization beneath thin alluvial deposits north of the Fluorspar Canyon - Tate's Wash fault system. At the Mother Lode mine production from heap leaching operations ceased. Total mine recovery is estimated at about 35,000 oz Au from approximately 840,000 tons of ore. A drill-indicated resource of approximately 9.4 million tons of refractory gold mineralization with an average grade of 0.046 oz Au/ton remains at the Mother Lode mine, but is subeconomic at current gold prices.

Gold production at the Lac Gold Bullfrog mine surpassed 1,000,000 ounces in July, 1993. In general, average grades and ore zone widths have exceeded drilling-based projections. Ores now include zones of stockwork veins in altered silicic lavas in the footwall of the main fault-bounded vein system. Underground production continues beneath and to the north of the open pit operations. Lac Minerals Ltd. continued exploratory drilling near the mine and carried out new exploratory drilling at locations north of Sawtooth Peak in the Bullfrog Hills. In the face of sharply increased federal fees for maintaining lode mining claims, Sunshine Mining and Lac Minerals continue to hold extensive land positions in the northern Bullfrog Hills.

HG Mining Inc. of Beatty, NV. continues production of cut stone products from ash-flow tuffs quarried in northern Crater Flat, the Transvaal Hills and upper Oasis Valley area. A new quarry was opened about 1.5 miles northwest of the Mother Lode mine.

Efforts to re-enter and deepen the Coffer #1 wildcat oil well in Oasis Valley, beginning in June, 1992, were abandoned prior to new drilling due to the operator's financial problems.

REVIEWS, PUBLICATIONS AND PRESENTATIONS

Reviews

D. C. Noble provided a technical review of DOE study plan 8.3.1.9.2.1, Rev. 0, *Natural Resource Assessment of Yucca Mountain*, to the Nuclear Waste Project Office via a memorandum to Carl Johnson dated April 26, 1993. S. I. Weiss provided E. H. McKee of the U. S. Geological Survey with a technical review of a paper by McKee and J. R. Bergquist entitled *New radiometric ages related to alteration and mineralization in the vicinity of Yucca Mountain, Nye County, Nevada*. This paper is in review as a U.S. Geological Survey Open-file Report to provide detailed locations and sample descriptions (provided by S. I. Weiss) and radiometric age data for age determinations of hydrothermal adularia and alunite previously reported by Jackson (1988), Noble et al. (1991) and in various abstracts by Task 3 personnel. The descriptive sample information was originally obtained and summarized by Task 3 and will be included in abbreviated form in the Weiss et al. manuscript entitled *Multiple episodes of hydrothermal activity and precious-metal mineralization in the southwestern Nevada volcanic field and their relation to magmatic activity, volcanism and regional extension* (see below).

Publications

The following abstracts and articles resulting from Task 3 studies were produced and(or) published during the period covered by this report, and are contained in the appendices as follows:

Appendix A:

Connors, K., A., Noble, D. C., Bussey, S., D., and Weiss, S. I., 1993, The initial gold contents of silicic volcanic rocks: bearing on the behavior of gold in magmatic systems, *Geology*, v. 21, p. 937-940.

Appendix B:

Weiss, S. I., Noble, D. C., Worthington, J. E., IV., and McKee, E. H., 1993, Neogene tectonism from the southwestern Nevada volcanic field to the White Mountains, California Part I. Miocene volcanic stratigraphy, paleotopography, extensional faulting and uplift between northern Death Valley and Pahute Mesa, p. 353-369, *in* Lahren, M. M., Trexler, J. H., Jr., and Spinosa, C., eds., 1993, Crustal Evolution of the Great Basin and Sierra Nevada: Cordilleran/Rocky Mountain Section, Geological Society of America Guidebook, Department of Geological Sciences, University of Nevada, Reno, 496 p.

Appendix C:

Weiss, S. I., Ristorcelli, S. J., and Noble, D. C., 1993, Mother Lode gold deposit, southwestern Nevada: another example of Carlin-type mineralization associated with porphyry magmatism: Geological Society of America Abstracts with Programs, v. 25, p. 161.

Appendix D:

Noble, D. C., Weiss, S. I., Worthington, J. E. IV., and McKee, E. H., 1993, Neogene structural evolution of Gold Mountain, Slate Ridge and adjacent areas, Esmeralda and Nye Counties, SW Nevada: Geological Society of America Abstracts with Programs, v. 25, p. 127.

Appendix E:

Farmer, G. L., Scott, R. B., Weiss, S. I., and Noble, D. C., 1993, Geochemical expression of a major E-W trending lithospheric boundary at 37° N latitude, southern Nevada: Geological Society of America Abstracts with Programs, v. 25, p. 36

Three additional manuscripts were produced during the period of this report but are not included in the appendices. A considerable amount of time was devoted by S. I. Weiss to preparation of an entirely new manuscript entitled *Multiple episodes of hydrothermal activity and precious-metal mineralization in the southwestern Nevada volcanic field and their relation to magmatic activity, volcanism and regional extension.* This paper, complete now except for figures, integrates the results of various Task 3 studies carried out between 1987 and 1993 concerning hydrothermal activity and mineralization within the Yucca Mountain region of the southwestern Nevada volcanic field. Pending completion of the figures the paper will be submitted for publication in *Economic Geology*. An initial draft of a manuscript entitled *Mount Jackson dome field: a long-lived late Neogene silicic magmatic system in Esmeralda County, Nevada* was prepared by D. C. Noble. This paper will be readied for submission to Journal of Volcanology and Geothermal Research following submission of the *Economic Geology* paper. Finally, Ted Worthington's masters thesis entitled *Neogene structural and volcanic geology of the Gold Mountain - Slate Ridge area, Esmeralda County, Nevada*, partially supported by funds from Task 3, was completed and accepted by the

Graduate School (Worthington, 1992).

Presentations

D. C. Noble presented the paper entitled *Neogene structural evolution of Gold Mountain, Slate Ridge and adjacent areas, Esmeralda and Nye Counties, SW Nevada* at the joint Cordilleran-Rocky Mountain Section meeting of the Geological Society of America in Reno, Nevada. S. I. Weiss presented the paper entitled *Mother Lode gold deposit, southwestern Nevada: another example of Carlin-type mineralization associated with porphyry magmatism* at the joint Cordilleran-Rocky Mountain Section meeting of the Geological Society of America in Reno, Nevada.

D. C. Noble and S. I. Weiss, together with E. H. McKee and M. Reheis of the U. S. Geological Survey, led a Geological Society of America field trip entitled *Neogene tectonism from the southwestern Nevada volcanic field to the White Mountains, California.*

S. I. Weiss gave an invited presentation entitled *Mid-Miocene precious metals deposits of the Bullfrog Hills and Bare Mountain, Nye County, NV: variable relations to magmatic and tectonic activity in the SW Nevada volcanic field* to the May, 1993 meeting of the southern Nevada chapter of the Geological Society of Nevada.

SUMMARY OF CONCLUSIONS AND RECOMMENDATIONS

Veins and siliceous deposits hosted by the Tram Member of the Crater Flat Tuff and units underlying the Bullfrog Member in northwestern Yucca Mountain locally contain elevated concentrations of Hg, As, Sb, Mo, Tl, Pb, and Zn, ±Bi. These elements are commonly elevated in the upper and distal parts of active and fossil hydrothermal systems and commonly are associated with epithermal precious-metal mineralization. The elevated concentrations of these elements, together with breccia textures and the style of branching, irregular veinlets that widen into brecciated wallrocks, provide additional evidence for the involvement of hydrothermal fluids (hot, slightly to moderately saline fluids derived from appreciable depth) in the formation of the veins and siliceous ledges in northwestern Yucca Mountain. Unaltered rocks of the Bullfrog Member overlie the siliceous ledges and underlying veins, demonstrating that the siliceous deposits formed after deposition of the Tram Member, but prior to the eruption of the Bullfrog Member at about 13.1 Ma.

By definition, siliceous sinter forms from the surface discharge of heated waters. Evidence from active and fossil geothermal/hydrothermal systems has led to the widely, if not universally, accepted view that these heated waters are supersaturated with respect to amorphous silica. If, as we suspect, the laminated opal deposits in the area of Figure 2 comprise siliceous sinter they provide evidence for hot-spring activity in the Yucca Mountain area during the Crater Flat Tuff cycle of volcanism. Although adularia is locally present adjacent to the veins and can be deposited at or near the surface by the interaction of rocks with hot water, we have no direct evidence that the waters were heated and it is conceivable that large amounts of silica could perhaps be leached from the glassy tuff and redeposited at the paleosurface by cold groundwater. This explanation for the origin of the sinter (or sinter-like) deposits seems unlikely considering the abundance and wide distribution of glassy tuffs in the SWNVF and the scarcity of similar deposits within them. This explanation also does not account for the elevated concentrations of a number of trace elements indicative of hydrothermal activity in the silicified siltstone, or for the similar chemical signature and style of brecciation within the nearby veins in the Tram Member. Our preferred interpretation is that the siliceous veins and ledges in the area of Figure 2 provide important evidence for at least one, and perhaps multiple, hydrothermal events in northwestern Yucca Mountain prior to the deposition of the Bullfrog Member of the Crater Flat Tuff. In most areas of Yucca Mountain surface sampling can not possibly detect potential mineralization associ-

ated with this early hydrothermal activity due to the cover of the Bullfrog and Prow Pass members and the overlying units of the Paintbrush Tuff.

The absolute age of gold mineralization at the Mother Lode gold mine in northern Bare Mountain remains under investigation. Two of three K-Ar age determinations on illite/smectite are consistent with cross-cutting relations and an inferred age of about 12.9 to 12.5 Ma based on previously obtained adularia and alunite ages in the district. We consider the *ca.* 27 Ma illite/smectite age to be too old and intend to pursue the possibility of obtaining step-heating $^{40}Ar/^{39}Ar$ ages from mineralized, adularia-bearing, altered dike rocks that may contain primary sanidine and/or high-temperature, disordered hydrothermal feldspar.

Consideration of textural, thermal and stratigraphic information leads us to re-emphasize our previous interpretation that pyrite disseminated in the groundmass of the Lithic Ridge Tuff, units of the Crater Flat Tuff, and other units of lava and tuff in the subsurface of Yucca Mountain is *not* of xenocrystic origin as has been proposed by contractors to the Department of Energy. Although pyritic hydrothermal alteration may have taken place in the vent area(s) of the Lithic Ridge and Crater Flat Tuffs prior to their eruption, the groundmass pyrite is most simply explained as the result of *in situ* sulphidation by aqueous solutions containing reduced sulphur. This sulphidation, in addition to alteration features summarized in Figure 6, provides evidence for one or more episodes of hydrothermal activity within Yucca Mountain and reflects the passage of fluids potentially capable of forming precious metal mineralization.

An area of research planned for the coming year will be to investigate the precious metals and trace-element contents of hydrothermally altered (but unmineralized) rocks from within and peripheral to several silicic volcanic-rock hosted epithermal mineral deposits. This would involve the same types of low-level, multi-element analyses reported in Table 1. If possible, we will obtain specimens from a number of deposits, including Round Mountain, Secret Pass, Rawhide, Paradise Peak and Wonder, Nevada, and perhaps Castle Mountain, California. The resulting data will provide important information on the dispersion of trace elements around mineralization in volcanic rocks.

REFERENCES CITED AND OTHER PERTINENT LITERATURE

The following references were selected because of their direct bearing on the Cenozoic volcanic stratigraphy and caldera geology, hydrothermal activity, and mineral potential of Yucca Mountain and the surrounding region of the southwestern Nevada volcanic field. Additional pertinent references on mineral potential, and particularly unpublished data in files of the Nevada Bureau of Mines and Geology, are given by Bell and Larson (1982b). A compendium of information from the U.S. Geological Survey's Mineral Resource Data System is given by Bergquist and McKee (1991).

Ahern, R., and Corn, R.M., 1981, Mineralization related to the volcanic center at Beatty, Nevada: Arizona Geological Society Digest, v. XIV, p. 283-286.

Albers, J. P., and Stewart, J. H., 1972, Geology and mineral deposits of Esmeralda County, Nevada, Nevada Bur. Mines and Geol. Bull. 78, 80 p.

Ander, H.D., and Byers, F.M., 1984, Nevada Test Site field trip guidebook; Reno, Nevada, University of Nevada-Reno, Department of Geological Sciences, v. 2, 1984, 35 p.

Anderson, R.E., Ekren, E.B., and Healey, D.L., 1965, Possible buried mineralized areas in Nye and Esmeraldo Counties, Nevada: U.S. Geological Survey Professional Paper 525-D, p. D144-D150.

Anonymous, 1928, One strike of real importance made at Nevada's new camp: Engineering and Mining Journal, v. 125, no. 1, p. 457.

Aronson, J.L., and Bish, D.L., 1987, Distribution, K/Ar dates, and origin of illite/smectite in tuffs from cores USW G-1 and G-2, Yucca Mountain, Nevada, a potential high-level radioactive waste repository: Abstract of presentation at Clay Minerals Society Meeting, Socorro, NM, 1987.

Armstrong, R. L., Ekren, E. B., McKee, E. H., and Noble, D. C., 1969, Space-time relations of Cenozoic silicic volcanism in the Great Basin of the western United States: Am. Jour. Sci., v. 267, p. 478-490.

Bailey, E.H., and Phoenix, D.A., 1944, Quicksilver deposits in Nevada: Nevada Bureau of Mines and Geology Bulletin 41.

Barton, C.C., 1984, Tectonic significance of fractures in welded tuff, Yucca Mountain, Southwest Nevada: Geological Society of America, Abstracts with Programs, v. 16, p. 437.

Barton, P. B., and Skinner, B. J., 1979, Sulfide mineral stabilities: *in* Barnes, H. L., ed., Geochemistry of Hydrothermal Ore Deposits, Wiley and Sons, New York, 798 p.

Bath, G.D., and Jahren, C.E., 1984, Interpretations of magnetic anomalies at repository site proposed for Yucca Mountain area, Nevada Test Site: U.S. Geological Survey Open-File Report 84-120, 40 p.

Bath, G.D., and Jahren, C.E., 1985, Investigation of an aeromagnetic anomaly on west side of Yucca Mountain, Nye County, Nevada: U.S. Geological Survey Open-File Report 85-459, 24 p.

Beck, B. A., 1984, Geologic and gravity studies of the structures of the northern Bullfrog Hills, Nye County, Nevada: California State University at Long Beach, unpublished MSc Thesis, 86 p.

Bedinger, M.S., Sargent, K.A., and Langer, W.H., 1984, Studies of geology and hydrology in the Basin and Range Province, Southwestern United States, for isolation of high-level radioactive waste; characterization of the Death Valley region, Nevada and California: U.S. Geological Survey Open-File Report 84-743, 173 p.

Bedinger, M.S., Sargent, K.A., and Langer, W.H., 1984, Studies of geology and hydrology in the Basin and Range Province, Southwestern United States, for isolation of high- level radioactive waste; evaluation of the regions: U.S. Geological Survey Open-File Report 84-745, 195 p.

Bell, E.J., and Larson, L.T., 1982a, Overview of energy and mineral resources of the Nevada Nuclear Waste Storage Investigations, Nevada Test Site, Nye County, Nevada: U.S. Department of Energy Report NVO-250 (DE83001418), 64 p. plus maps.

Bell, E.J., and Larson, L.T., 1982b, Annotated bibliography, Overview of energy and mineral resources for the Nevada Nuclear Waste Storage Investigations, Nevada Test Site, Nye County, Nevada: U.S. Department of Energy Report NVO-251 (DE83001263), 30 p.

Benson, L.V. and McKinley, P.W., 1985, Chemical composition of the ground water in the Yucca Mountain area, Nevada: U.S. Geological Survey Open-File Report 85-484, 10 p.

Bentley, C.B., 1984, Geohydrologic data for test well USW G-4, Yucca Mountain area, Nye County, Nevada: U.S. Geological Survey Open-File Report 84-63, 67 p.

Bergquist, J. R., and McKee, E. H., 1991, Mines, prospects and mineral occurrences in Esmeralda and Nye Counties, Nevada, nera Yucca Mountain: U.S. Geological Survey Administrative Report to the Department of Energy, Yucca Mountain Project, 385 p.

Bish, D.L., 1987, Evaluation of past and future alteration in tuff at Yucca Mountain, Nevada based on clay mineralogy of drill cores USW G-1, G-2, and G-3: Los Alamos, New Mexico, Los Alamos National Laboratory Report LA-10667-MS, 42 p.

Bonham, H. F., Jr., and Garside, L. J., 1979, Geology of the Tonopah, Lone Mountain, Klondike and northern Mud Lake Quadrangles, Nevada: Nevada Bureau of Mines and Geology Bulletin 92, 142 p., 1:48,000.

Booth, M., 1988, Dallhold finalizes plans for huge Nevada mine: The Denver Business Journal, April 4, 1988, p. 10.

Boyle, R. W., 1979, The geochemistry of gold and its deposits: Geological Survey of Canada Bulletin 280, 584 p.

Boyle, R.W., and Jonasson, I.R., 1973, The geochemistry of arsenic and its use as an indicator element in geochemical prospecting: Journal of Geochemical Exploration, v. 2, p. 251-296.

Broxton, D. E., Vaniman, D., Caporuscio, F., Arney, B., and Heiken, G., 1982, Detailed petrographic descriptions and microprobe data fro drill holes USW-G2 and UE25b-1H, Yucca Mountain, Nevada: Los Alamos, New Mexico, Los Alamos National Laboratory Report LA-10802-MS, 168 p.

Broxton, D.E., Byers, F.M., Warren, R.G. and Scott, R.B., 1985, Trends in phenocryst chemistry in the Timber Mountain-Oasis Valley volcanic field, SW Nevada; evidence for isotopic injection of primitive magma into an evolving magma system: Geological Society of America, Abstracts with Programs, v. 17, p. 345.

Broxton, D. E., Warren, R. G., and Byers, F. M., Jr., 1989, Chemical and mineralogic trends within the Timber Mountain-Oasis Valley caldera complex, Nevada: Evidence for multiple cycles of chemical evolution in a long-lived silicic magma system: Journal of Geophysical Research, v. 94, p. 5961-5985.

Broxton, D.E., Warren, R.G., Byers, F.M., Jr., Scott, R.B., and Farner, G.L., 1986, Petrochemical trends in the Timber Mountain-Oasis Valley caldera complex, SW Nevada: EOS (American Geophysical Union Transactions), v. 67, p. 1260.

Broxton, D.E., Warren, R.G., Hagan, R.C. and Luedemann, G.,1986, Chemistry of diagenetically altered tuffs at a potential nuclear waste repository, Yucca Mountain, Nye County, Nevada: Los Alamos, New Mexico, Los Alamos National Laboratory Report LA-10802-MS, 160 p.

Byers, F. M., Jr., Carr, W. J., and Orkild, P. P., 1989, Volcanic centers of southwestern Nevada: evolution of understanding, 1960-1988: Journal of Geophysical Research, v.94, p. 5908-5924.

Byers, F.M., Jr., Carr, W.J., and Orkild, P.P., 1986, Calderas of southwestern Nevada-Evolution of understanding, 1960-1986: EOS (American Geophysical Union Transactions), v. 67, p. 1260.

Byers, F.M., Jr., Carr, W.J., Orkild, P.P., Quinlivan, W.D. and Sargent, K.A., 1976a, Volcanic Suites and related cauldrons of Timber Mountain-Oasis Valley caldera complex: U.S. Geological Survey Professional Paper 919, 70 p.

Byers, F.M., Jr., Carr, W.J., Christiansen, R.L., Lipman, P.W., Orkild, P.P., and Quinlivan, W.D., 1976b, Geologic map of the Timber Mountain Caldera area, Nye County, Nevada: U.S. Geological Survey Miscellaneous Investigations Series, I-891, sections, 1:48,000 scale.

Byers, F.M., Jr., Orkild, P.P, Carr, W. J., and Quinlivan, W.D., 1968, Timber Mountain Tuff, southern Nevada, and its relation to cauldron subsidence: Geological Society of America Memoir 110, p. 87-97.

Caporuscio, F., Vaniman, D.T., Bish, D.L., Broxton, D.E., Arney, D., Heiken, G., Byers, F.M., and Gooley, R., 1982, Petrologic studies of drill cores USW-G2 and UE25b-1H,Yucca Mountain, Nevada: Los Alamos, New Mexico, Los Alamos National Laboratory Report LA-9255-MS, 114 p.

Carr, M.D., and Monsen, S.E., 1988, A field trip guide to the geology of Bare Mountain: Geological Society of America Field Trip Guidebook, Cordilleran Section Meeting, Las Vegas, Nevada, p. 50-57.

Carr, M.D., Waddell, S.J., Vick, G.S., Stock, J.M., and Monsen, S.A., Harris, A.G., Cork, B.W., and Byers, F.M., Jr., 1986, Geology of drill hole UE25p-1: A test hole into pre-Tertiary rocks near Yucca Mountain, southern Nevada: U.S. Geological Survey Open File Report 86-175.

Carr, W.J., 1964, Structure of part of the Timber Mountain dome and caldera, Nye County, Nevada: U.S. Geological Survey Professional Paper 501-B, p. B16-B20.

Carr, W.J., 1974, Summary of tectonic and structural evidence for stress orientation at the NTS: U.S. Geological Survey Open-File Report 74-176, 53 p.

Carr, W.J., 1982, Volcano-tectonic history of Crater Flat, southwestern Nevada, as suggested by new evidence from drill hole USW-VH-1 and vicinity: U.S. Geological Survey Open-File Report 82-457, 23 p.

Carr, W.J., 1984a, Regional structural setting of Yucca Mountain, southwestern Nevada, and late Cenozoic rates of tectonic activity in part of the southwestern Great Basin, Nevada and California: U.S. Geological Survey Open-File Report 84-0854, 114 p.

Carr, W.J., 1984b, Timing and style of tectonism and localization of volcanism in the Walker Lane belt of southwestern Nevada: Geological Society of America, Abstracts with Programs, v. 16, p. 464.

Carr, W.J., 1988a, Styles of extension in the Nevada Test Site region, southern Walker Lane Belt: an integration of volcano-tectonic and detachment fault models: Geological Society of America, Abstracts with Programs, v. 20, p. 148.

Carr, W. J., 1988b, Volcano-tectonic setting of Yucca Mountain and Crater Flat, *in* Carr, M. D., and Yount, J. C., eds., Geologic and hydrologic investigations of a potential nuclear waste disposal site at Yucca Mountain, southern Nevada: U.S. Geol. Survey Bull. 1790, p. 35-49.

Carr, W.J., and Quinlivan, W.D., 1966, Geologic map of the Timber Mountain quadrangle, Nye County, Nevada: U.S. Geological Survey Geologic Quadrangle Map GQ-503, 1:24,000 scale, sections.

Carr, W.J., and Quinlivan, W.D., 1968, Structure of Timber Mountain resurgent dome, Nevada Test Site: Geological Society of America Memoir 110, p. 99-108.

Carr, W.J. and Parrish, L.D., 1985, Geology of drill hole USW VH-2, and structure of Crater Flat, southwestern Nevada: U.S. Geological Survey Open-File Report 85-475, 41 p.

Carr, W.J., Byers, F.M., and Orkild, P.P., 1984, Stratigraphic and volcano-tectonic relations of Crater Flat Tuff and some older volcanic units, Nye County, Nevada: U.S. Geological Survey Open-File Report 84-114, 97 p.

Carr, W.J., Byers, F.M., and Orkild, P.P., 1986, Stratigraphic and volcano-tectonic relations of Crater Flat Tuff and some older volcanic units, Nye County, Nevada: U.S. Geological Survey Professional Paper 1323, 28p.

Castor, S. B., and Weiss, S. I., 1992, Contrasting styles of epithermal precious-metal mineralization in the southwestern Nevada volcanic field, USA: Ore Geology Reviews, v. 7, p. 193-223.

Castor, Feldman and Tingley, 1989, Mineral evaluation of the Yucca Mountain Addition, Nye County, Nevada: Nevada Bureau of Mines and Geology, Open-file Report 90-4, 80 pp.

Castor, Feldman and Tingley, 1990, Mineral potential report for the U.S. Department of Energy, Serial No. N-50250: Nevada Bureau of Mines and Geology, University of Nevada, Reno, 24 pp.

Castor, S. B., Tingley, J. V., and Bonham, H. F., Jr., 1991, Yucca Mountain Addition subsurface mineral resource analysis: unpub. proposal to Science Applications International Corp., 10 p.

Castor, S. B., Tingley, J. V., and Bonham, H. F., Jr., (*in review*), Pyritic ash-flow tuff in Yucca Mountain: manuscript submitted in 1992 to Geology.

Christiansen, R.L., and Lipman, P.W., 1965, Geologic map of the Topopah Spring NW quadrangle, Nye County, Nevada: U.S. Geological Survey Geologic Quadrangle Map GQ-444, 1:24,000 scale, sections.

Christiansen, R.L., Lipman, P.W., Carr, W.J., Byers, F.M., Jr., Orkild, P.P., and Sargent, K.A., 1977: Timber Mountain-Oasis Valley caldera complex of southern Nevada: Geological Society of America Bulletin, v. 88, p. 943-959.

Christiansen, R.L., Lipman, P.W., Orkild, P.P., and Byers, F.M., Jr., 1965, Structure of the Timber Mountain caldera, southern Nevada, and its relation to basin-range structure: U.S. Geological Survey Professional Paper 525-B, p. B43-B48.

Connors, K. A., (*in preparation*), Studies in silicic volcanic geology: Part I: Compositional controls on the initial gold contents of silicic volcanic rocks; Part II: Geology of the western margin of the Timber Mountain caldera complex and post-Timber Mountain volcanism in the Bullfrog Hills: unpublished PhD dissertation, University of Nevada, Reno.

Connors, K.A., Weiss, S.I., Noble, D.C., and Bussey, S.D., 1990, Primary gold contents of some silicic and intermediate tuffs and lavas: evaluation of possible igneous sources of gold: Geological Society of America Abst. with Programs, v. 22, p. A135.

Connors, K.A., Noble, D.C., Weiss, S.I., and Bussey, S.D., 1991a, Compositional controls on the gold contents of silicic volcanic rocks: 15th International Geochemical Exploration Symposium Program with Abstracts, p. 43.

Connors, K. A., McKee, E. H., Noble, D. C., and Weiss, S. I., 1991, Ash-flow volcanism of Ammonia Tanks age in the Oasis Valley area, SW Nevada: Bearing on the evolution of the Timber Mountain calderas and the timing of formation of the Timber Mountain II resurgent dome: EOS, Trans. Am. Geophys. Union., v. 72, p. 570.

Connors, K., A., Noble, D. C., Bussey, S., D., and Weiss, S. I., 1993, Initial gold contents of silicic volcanic rocks: bearing on the behavior of gold in magmatic systems: Geology, v. 21, p. 937-940.

Cornwall, H.R., 1962, Calderas and associated volcanic rocks near Beatty, Nye County, Nevada: Geological Society of America, Petrologic Studies, A.F. Buddington Volume, p. 357-371.

Cornwall, H.R., 1972, Geology and mineral deposits of southern Nye County, Nevada: Nevada Bureau of Mines and Geology Bulletin 77, p. 49.

Cornwall, H.R., and Kleinhampl, F.J., 1961, Geology of the Bare Mountain quadrangle, Nevada: U.S. Geological Survey Geologic Quadrangle Map GQ-157, 1:62,500 scale.

Cornwall, H.R., and Kleinhampl, F.J., 1964, Geology of the Bullfrog quadrangle and ore deposits related to the Bullfrog Hills caldera, Nye County, Nevada, and Inyo County, California: U.S. Geological Survey Professional Paper 454-J, 25 p.

Cornwall, H.R., and Norberg, J.R., 1978, Mineral Resources of the Nellis Air Force Base and the Nellis Bombing and Gunnery Range, Clark, Lincoln, and Nye Counties, Nevada: U.S. Bureau of Mines Unpublished Administrative Report, 118 p.

Craig, R.W. and Robinson, J.H., 1984, Geohydrology of rocks penetrated by test well UE-25p#1, Yucca Mountain area, Nye County, Nevada, U.S. Geological Survey Water-Resources Investigations 84-4248, 57 p.

Craig, R.W., Reed, R.L., and Spengler, R.W., 1983, Geohydrologic data for test well USW H-6, Yucca Mountain area, Nye County, Nevada: U.S. Geological Survey Open-File Report 83-856, 52 p.

Crowe, B.M., 1980, Disruptive event analysis: Volcanism and igneous intrusion: Batelle Pacific Northwest Laboratory Report PNL-2822, 28 p.

Crowe, B.M., and Carr, W.J., 1980, Preliminary assessment of the risk of volcanism at a proposed nuclear waste repository in the southern Great Basin: U.S. Geological Survey Open-File Report 80-357, 15 p.

Crowe, B.M., Johnson, M.E., and Beckman, R.J., 1982, Calculation of probability of volcanic disruption of a high-level radioactive waste repository within southern Nevada, USA: Radioactive Waste Management and the Nuclear Fuel Cycle, v. 3, p. 167-190.

Crowe, B.M., Vaniman, D.J., and Carr, W.J., 1983b, status of volcanic hazard studies for the Nevada nuclear waste storage investigations: Los Alamos, New Mexico, Los Alamos National Laboratory Report LA-9325-MS.

Deino, A.L., Hausback, B.P., Turrin, B.T., and McKee, E.H., 1989, New $^{40}Ar/^{39}Ar$ ages for the Spearhead and Civet Cat Canyon Members of the of Stonewall Flat Tuff, Nye County, Nevada: EOS, Trans. American Geopphysical Union, v. 70, p. 1409.

Drexler, J. W., 1982, Mineralogy and geochemistry of Miocene volcanic rocks related to the Julcani Ag-Au-Cu-Bi deposit, Peru: Physiochemical conditions of a productive magma body: unpublished PhD dissertation, Houghton, Michigan Technical University, 250 p.

Eckel, E.B., ed., 1968, Nevada Test Site: Geological Society of America Memoir 110, 290 p.

Ekren, E.B., and Sargent, K.A., 1965, Geologic map of Skull Mountain quadrangle at the Nevada Test Site, Nye County, Nevada: U.S. Geological Survey Geologic Quadrangle Map GQ-387.

Ekren, E.B., Anderson, R.E., Rodgers, C.L., and Noble, D.C., 1971, Geology of northern Nellis Air Force Base Bombing and Gunnery Range, Nye County, Nevada: U.S. Geological Survey Professional Paper 651, 91 p.

Feitler, S., 1940, Welded tuff resembling vitrophyre and pitchstone at Bare Mountain, Nevada: Geological Society of America Bulletin, v. 51, p. 1957.

Flood, T.P., and Schuraytz, B.C., 1986, Evolution of a magmatic system. Part II: Geochemistry and mineralogy of glassy pumices from the Pah Canyon, Yucca Mountain, and Tiva Canyon Members of the Paintbrush Tuff, southern Nevada: EOS Trans. American Geophysical Union, v. 67, p. 1261.

Foley, D., 1978, The geology of the Stonewall Mountain volcanic center, Nye County, Nevada: Ohio State University, Columbus Ohio, unpublished PhD Dissertation, 139 p.

Fouty, S.C., 1984, Index to published geologic maps in the region around the potential Yucca Mountain Nuclear Waste Repository site, southern Nye County, Nevada: U.S. Geological Survey Open-File Report 84-524, 31 p.

Fridrich, C. J., Orkild, P. P., Murray, M., Price, J. R., Christiansen, R. L., Lipman, P. W., Carr, W. J., Quinlivan, W. D., and Scott, R. B., (in review), Geologic map of the East of Beatty Mountain Quadrangle, Nye County, Nevada: U.S. Geological Survey Open-file Report, 4 sheets, 1:12,000.

Frischknecht, F.C. and Raab, P.V., 1984, Time-domain electromagnetic soundings at the Nevada Test Site, Nevada, Geophysics, v. 49, p. 981-992.

Frizzell, Virgil, and Shulters, Jacqueline, 1986, Geologic map of the Nevada Test Site: EOS Trans. American Geophysical Union, v. 67, p. 1260.

Frizzell, Virgil, and Shulters, Jacqueline, 1990, Geologic map of the Nevada Test Site: U.S. Geological Survey Misc. Invest. Map I-2046, 1:100,000.

Gans, P. B., Mahood, G. A., and Schermer, E., 1989, Synextensional magmatism in the Basin and Range province; A case study from the eastern Great Basin: Geological Society of America Spec. Paper 233, 53 p.

Garside L.J. and Schilling, J.H., 1979, Thermal waters of Nevada: Nevada Bureau of Mines and Geology, Bulletin 91, 163 p.

Geehan, R.W., 1946, Exploration of the Crowell fluorspar mine, Nye County, Nevada: U.S. Bureau of Mines Report of Investigations 3954, 9 p.

Geldon, A. L., (in press) Preliminary hydrogeologic assessment of boreholes UE-25c #1, UE-25c #2 and UE-25c #3, Yucca Mountain, Nye County, Nevada: U.S. Geological Survey Water-Resources Investigations Report 91-XXX.

Greybeck, J. D., and Wallace, A. B., 1991, Gold mineralization at Fluorspar Canyon near Beatty, Nye County, Nevada: *in* Raines, G. L., Lisle,R. E., Shafer, R. W., and Wilkinson, W. W., eds., Geology and ore deposits of the Great Basin: Symposium Proceedings, Geol. Soc. of Nevada, sp. 935-946.

Hagstrum, J.T., Daniels, J.J., and Scott, J.H., 1980, Interpretation of geophysical well-log measurements in drill hole UE 25a-1, NTS, Radioactive Waste Program: U.S. Geological Survey Open-File Report 80-941, 32 p.

Hall, R.B., 1978, World nonbauxite aluminum resources--Alunite: U.S. Geological Survey Professional Paper 1076-A, 35 p.

Hamilton, W. B., 1988, Detachment faulting in the Death Valley region, California and Nevada, *in* Carr, M. D., and Yount, J. C., eds., Geologic and hydrologic investigations of a potential nuclear waste disposal site at Yucca Mountain, southern Nevada: U.S. Geol. Survey Bull. 1790, p. 51-86.

Hausback, B. P., and Frizzell, V. A. Jr., 1987, Late Miocene syntectonic volcanism of the Stonewall Flat Tuff, Nye County, Nevada [abs.]: Geological Society of America Abst. with Programs, v. 19, p. 696.

Hausback, B.P., Deino, A.L., Turrin, B.T., McKee, E.H., Frizzell, V.A., Noble, D.C., and Weiss, S.I., 1990, New $^{40}Ar/^{39}Ar$ ages for the Spearhead and Civet Cat Canyon Members of the Stonewall Flat Tuff, Nye County, Nevada: Evidence for systematic errors in standard K-Ar age determinations on sanidine: Isochron/West, No. 56, p. 3-7.

Harris, R.N., and Oliver, H.W., 1986, Structural implications of an isostatic residual gravity map of the Nevada Test Site, Nevada: EOS (American Geophysical Union Transactions), v. 67, p. 1262.

Heald, P., Foley, N.K., and Hayba, D.O., 1987, Comparative anatomy of volcanic-hosted epithermal deposits: acid-sulfate and adularia-sericite types: Economic Geology, v. 82, no. 1, p. 1-26.

Heikes, V.C., 1931, Gold, silver, copper, lead and zinc in Nevada--Mine report, in Mineral Resources of the U.S., 1928: U.S. Department of commerce, Bureau of Mines, pt. 1, p. 441-478.

Hildreth, E. W., 1977, The magma chamber of the Bishop Tuff: Gradients in temperature, pressure and composition: unpublished PhD dissertation, Univ. California-Berkely, 328 p.

Hill, J.M., 1912, The mining districts of the western U.S.: U.S. Geological Survey Bulletin 507, 309 p.

Holmes, G.H., Jr., 1965, Mercury in Nevada, in Mercury potential of the United States: U.S. Bureau of Mines I.C., 8252, p. 215-300.

Hoover, D.L., Eckel, E.B., and Ohl, J.P., 1978, Potential sites for a spent unreprocessed fuel facility (SUREF), southwest part of the NTS: U.S. Geological Survey Open-File Report 78-269, 18 p.

Hoover, D. B., Chornack, M. P., Nervick, K. H., and Broker, M. M., 1982, Electrical studies at the proposed Wahmonie and Calico Hills Nuclear Waste Sites, Nye County, Nevada: U.S. Geol. Survey Open-File Rept. 82-466, 45 p.

Hudson, M. R., 1992, Paleomagnetic data bearing on the origin of arcuate structures in the Frenchman Peak - Massachusetts Mountain area of southern Nevada: Bull. Geol. Soc. Am., v. 104, p. 581-594.

Jackson, M. J., 1988, The Timber Mountain magmato-thermal event: an intense widespread culmination of magmatic and hydrothermal activity at the southwestern Nevada volcanic field: University of Nevada, Reno - Mackay School of Mines, Reno, Nevada, unpublished MSc Thesis.

Jackson, M.R., Noble, D.C., Weiss, S.I., Larson, L.T., and McKee, E.H., 1988, Timber Mountain magmato-thermal event: an intense widespread culmination of magmatic and hydrothermal activity at the SW Nevada volcanic field, Geol. Soc. Am. Abstr. Programs, v. 20, p. 171.

Jorgensen, D. K., Rankin, J. W., and Wilkins, J., Jr., 1989, The geology, alteration and mineralogy of the Bullfrog gold deposit, Nye County, Nevada: Soc. Mining Eng. Preprint 89-135, 13 p.

Kane, M.F., and Bracken, R.E., 1983, Aeromagnetic map of Yucca Mountain and surrounding regions, southwest Nevada: U.S. Geological Survey Open-File Report 83-616, 19 p.

Kane, M.F., Webring, M.W., and Bhattacharyya, B.K., 1981, A preliminary analysis of gravity and aeromagnetic surveys of the Timber Mountain areas, southern Nevada: U.S. Geological Survey Open-File Report 81-189, 40 p.

Keith, J. D., Dallmeyer, R. D., Kim, Choon-Sik, and Kowallis, B. J., 1991, The volcanic history and magmatic sulfide mineralogy of latites of the central East Tintic Mountains, Utah: *in* Raines, G. L., Lisle,R. E., Shafer, R. W., and Wilkinson, W. W., eds., Geology and ore deposits of the Great Basin: Symposium Proceedings, Geol. Soc. of Nevada, p. 461-483.

Kistler, R.W., 1968, Potassium-argon ages of volcanic rocks on Nye and Esmeralda Counties, Nevada: Geological Society of America Memoir 110, P. 251-263.

Knopf, A., 1915, Some cinnabar deposits in western Nevada: U.S. Geological Survey Bulletin 620-D, p. 59-68.

Kral, V.E., 1951, Mineral resources of Nye County, Nevada: University of Nevada Bulletin, v. 45, no. 3, Geological and Mining Series 50, 223 p..

Kullerude, G., and Yoder, H.S., 1959, Pyrite stability relations in the Fe-S sytem: Economic Geology, v. 54, p. 533-572.

Lahoud, R.G., Lobmeyer, D.H. and Whitfield, M.S., 1984, Geohydrology of volcanic tuff penetrated by test well UE-25b#1, Yucca Mountain, Nye County, Nevada: U.S. Geological Survey Water-Resources Investigations 84-4253, 49 p.

Larson, L. T., Noble, D. C., and Weiss, S. I., 1988, Task 3 report for January, 1987 - June, 1988: Volcanic geology and evaluation of potential mineral and hydrocarbon resources of the Yucca Mountain area: unpublished report to the Nevada Nuclear Waste Project Office, Carson City, Nevada.

Le Bas, M. J., Le Maitre, R. W., Streckheisen, A., and Zenettin, B., 1986, A chemical classification of volcanic rocks based on the total alkali-silica diagram: Journal of Petrology, v. 27, p. 745-750.

Lincoln, F.C., 1923, Mining districts and mineral resources of Nevada: Reno, Nevada, Nevada Newsletter Publishing Co., Reno, 295 p.

Lipman, P.W., Christiansen, R.L., and O'Connor, J.T., 1966, A compositionally zoned ash-flow sheet in southern Nevada: U.S. Geological Survey Professional Paper 524-F, p. F1-F47.

Lipman, P.W., and McKay, E.J., 1965, Geologic map of the Topopah Spring SW quadrangle, Nevada: U.S. Geological Survey Geologic Quadrangle Map GQ-439, 1:24,000 scale.

Lipman, P.W., Quinlivan, W.D., Carr, W.J., and Anderson, R.E., 1966, Geologic map of the Thirsty Canyon SE quadrangle, Nye County, Nevada: U.S. Geological Survey Geologic Quadrangle Map GQ-489, 1:24,000 scale.

Lobmeyer, D.H., Whitfield, M.S., Lahoud, R.G., and Bruckheimer, L., 1983, Geohydrologic data for test well UE-25bH, Nevada Test Site, Nye County, Nevada: U.S. Geological Survey Open-File Report 83-855, 54 p.

Luedke, R.G., and Smith, R.L., 1981, Map showing distribution, composition, and age of late Cenozoic volcanic centers in California and Nevada: U.S. Geological Survey Miscellaneous Investigation Series, I-1091-C, 2 sheets.

Maldonado, F., 1985, Late Tertiary detachment faults in the Bullfrog Hills, southwestern Nevada: Geol. Soc. Am. Abstr. Programs, 17, p. 651.

Maldonado, F., 1988, Geometry of normal faults in the upper plate of a detachment fault zone, Bullfrog Hills, southern Nevada: Geological Society of America, Abstracts with Programs, v. 20, P. 178.

Maldonado, F, 1990, Structural geology of the upper plate of the Bullfrog Hills detachment fault system, southern Nevada: Geological Society of America Bulletin, v. 102, p. 992-1006.

Maldonado, F, and Hausback, B.P., 1990, Geologic map of the northeastern quarter of the Bullfrog 15-minute quadrangle, Nye County, Nevada: U.S. Geological Survey Misc. Investigations Series Map I-2049, 1:24,000.

Maldonado, F, and Koether, S.L., 1983, Stratigraphy, structure, and some petrographic features of Tertiary volcanic rocks at the USW G-2 drill hole, Yucca Mountain, Nye County, Nevada: U.S. Geological Survey Open-File Report 83-732, 83 p.

Maldonado, F, Muller, D.C., and Morrison, J.N., 1979, Preliminary geologic and geophysical data of the UE25a-3 exploratory drill hole, Nevada Test Site, Nevada: U.S. Geological Survey Report, USGS-1543-6, 47 p.; available only from U.S. Department of Commerce, National Technical Information Service, Springfield, VA 22161.

Maldonado, Florian, Muller, D.C., and Morrison, J.N., 1979, Preliminary geologic and geophysical data of the UE25a-3 exploratory drill hole, Nevada Test Site, Nevada: U.S. Geological Survey Open-File Report 81-522.

Mapa, M.R., 1990 Geology and mineralization of the Mother Lode mine, Nye County, Nevada, *in* Hillmeyer, F., Wolverson, N., and Drobeck, P., 1990 spring fieldtrip guidebook, Volcanic-hosted gold deposits and structural setting of the Mohave region: Reno, Geol. Soc. Nevada, 4 p.

Marti, J., Diez-Gil, J. L., and Ortiz, R., 1991, Conduction model for the thermal influence of lithic clasts in mixtures of hot gases and ejecta: Journal of Geophysical Research, v. 96, p. 21,879-21,885.

Marvin, R.F., Byers, F.M., Mehnert, H.H., Orkild, P.P, and Stern, T.W., 1970, Radiometric ages and stratigraphic sequence of volcanic and plutonic rocks, southern Nye and western Lincoln Counties, Nevada: Geological Society of America Bulletin, v. 81, p. 2657-2676.

Marvin, R. F., and Cole, J. C., 1978, Radiometric ages: Compilation A, U.S. Geological Survey: Isochron/West, no. 22, p. 3-14.

Marvin, R. F., Mehnert, H. H., and Naeser, C. W., 1989, U.S. Geologic Survey radiometric ages - compilation "C", part 3: California and Nevada: Isochron/West, no. 52, p. 3-11.

McKague, H.L. and Orkild, P.P., 1984, Geologic Framework of the Nevada Test Site: Geological Society of America, Abstracts with Programs, v. 16, p. 589.

McKay, E.J., 1963, Hydrothermal alteration in the Calico Hills, Jackass Flats quadrangle, Nevada Test Site: U.S. Geological Survey Technical Letter NTS-43, 6 p.

McKay, E.J., and Sargent, K.A., 1970, Geologic map of the Lathrop Wells quadrangle, Nye County, Nevada: U.S. Geological Survey Geologic Quadrangle Map GQ-883, 1:24,000 scale.

McKay, E.J., and Williams, W.P., 1964, Geology of Jackass Flats quadrangle, Nevada Test Site, Nevada: U.S. Geological Survey Geologic Quadrangle Map GQ-368, 1:24,000 scale.

McKee, E.H., 1983, Reset K-Ar ages: evidence for three metamorphic core complexes, western Nevada: Isocron/West, no.38, p 17-20.

McKee, E. H., Noble, D. C., and Weiss, S. I., 1989, Very young silicic volcanism in the southwestern Great Basin: The late Pliocene Mount Jackson dome field, SE Esmeralda County, Nevada: EOS, Trans. Am. Geophys. Union., v. 70, p. 1420.

McKee, E. H., Noble, D. C., and Weiss, S. I., 1990, Late Neogene volcanism and tectonism in the Goldfield segment of the Walker Lane belt: Geological Society of America Abstracts with Programs, v. 22, p. 66.

Miller, D.C. and Kibler, J.E., 1984, Preliminary analysis of geological logs from drill hole UE-25p#1, Yucca Mountain, Nye County, Nevada: U.S. Geological Survey Open-File Report 84-649, 17 p.

Mills, J.G., Jr., and Rose, T.P., 1986, Geochemistry of glassy pumices from the Timber Mountain Tuff, southwestern Nevada: EOS (American Geophysical Union Transactions), v. 67, p. 1262.

Monsen, S.A., Carr, M.D., Reheis, M.C., and Orkild, P.P., 1990, Geologic map of Bare Mountain, Nye County Nevada: U.S. Geological Survey Open-file Report 90-25, 1:24,000.

Monsen, S.A., Carr, M.D., Reheis, M.C., and Orkild, P.P., 1992, Geologic map of Bare Mountain, Nye County Nevada: U.S. Geological Survey Miscellaneous Investigations Map I-2201, 1:24,000.

Morton, J. L., Silberman, M. L., Bonham, H. F., Garside, L. J., and Noble, D. C., 1977, K-Ar ages of volcanic rocks, plutonic rocks, and ore deposits in Nevada and eastern California - Determinations run under the USGS-NBMG cooperative program: Isochron/West, n. 20, p. 19-29.

Noble, D. C., and Christiansen, R. L., 1974, Black Mountain volcanic center, in Guidebook to the geology of four Tertiary volcanic centers in central Nevada: Nevada Bur. Mines Geol. Rept. 19, p. 22-26.

Noble, D. C., McKee, E. H., and Weiss, S. I., 1988, Nature and timing of pyroclastic and hydrothermal activity and mineralization at the Stonewall Mountain volcanic center, southwestern Nevada: Isochron/West, No. 51, p. 25-28.

Noble, D. C., Weiss, S. I., and Green, S. M., 1989, High-salinity fluid inclusions suggest that Miocene gold deposits of the Bare Mtn. district, NV, are related to a large buried rare-metal rich magmatic system: Geological Society of America Abs. with Programs, v. 21, p. 123.

Noble, D. C., Weiss, S. I., and McKee, E. H., 1990a, Style, timing, distribution, and direction of Neogene extension within and adjacent to the Goldfield section of the Walker Lane structural belt: EOS, Trans. American Geophysical Union, v. 71, p. 618-619.

Noble, D. C., Weiss, S. I., and McKee, E. H., 1990b, Magmatic and hydrothermal activity, caldera geology and regional extension in the western part of the southwestern Nevada volcanic field: Great Basin Symposium, Program with Abstracts, Geology and ore deposits of the Great Basin, Geol. Soc. of Nevada, Reno, p. 77.

Noble, D. C., Weiss, S. I., and McKee, E. H., 1991a, Magmatic and hydrothermal activity, caldera geology, and regional extension in the western part of the southwestern Nevada volcanic field: *in* Raines, G. L., Lisle,R. E., Shafer, R. W., and Wilkinson, W. W., eds., Geology and ore deposits of the Great Basin: Symposium Proceedings, Geol. Soc. of Nevada, p. 913-934.

Noble, D. C., Worthington, J. E., and McKee, E. H., 1991b, Geologic and tectonic setting and Miocene volcanic stratigraphy of the Gold Mountain-Slate Ridge area, southwestern Nevada: Geol. Soc. America Abstr. with Prog., v. 23, p. A247.

Noble, D. C., Sargent, K. A., Ekren, E. B., Mehnert, H. H., and Byers, F. M., Jr., 1968, Silent Canyon volcanic center, Nye County, Nevada: Geological Society of America Spec. Paper 101, p. 412-413.

Noble, D.C., Vogel, T. A., Weiss, S.I., Erwin, J.W., McKee, E.H., and Younker, L.W., 1984, Stratigraphic relations and source areas of ash-flow sheets of the Black Mountain and Stonewall Mountain volcanic centers, Nevada: Journal of Geophysical Research, v. 89, p. 8593-8602.

Norberg, J.R., 1977, Mineral Resources in the vicinity of the Nellis Air Force Base and the Nellis Bombing and Gunnery Range, Clark, Lincoln, and Nye Counties, Nevada: U.S. Bureau of Mines Unpublished Report, 112 p.

Orkild, P.P., 1968, Geologic map of the Mine Mountain quadrangle, Nye County, Nevada: U.S. Geological Survey Geologic Quadrangle Map GQ-746, 1:24,000 scale.

Orkild, P.P., and O'Connor, J.T., 1970, Geologic map of the Topopah Springs quadrangle, Nye County, Nevada: U.S. Geological Geologic Quadrangle Map GQ-849, 1:24,000 scale.

Odt, D. A., 1983, Geology and geochemistry of the Sterling gold deposit, Nye County, Nevada: Unpub. M.S. thesis, Univ. Nevada-Reno, 91 p.

Papike, J. J., Keith, T. E. C., Spilde, M. N., Galbreath, K. C., Shearer, C. K., and Laul, J. C., 1991, Geochemistry and mineralogy of fumarolic deposits, Valley of Ten Thousand Smokes, Alaska: bulk chemical and mineralogical evolution of dacite-rich protolith: American Mineralogist, v. 76, p. 1662-1673.

Papke, K.G., 1979, Fluorspar in Nevada: Nevada Bureau of Mines and Geology, Bulletin 93, 77 p.

Ponce, D.A., 1981, Preliminary gravity investigations of the Wahmonie site, Nevada Test Site, Nye County, Nevada: U.S. Geological Survey Open-File Report 81-522, 64 p.

Ponce, D.A., 1984, Gravity and magnetic evidence for a granitic intrusion near Wahmonie site, Nevada Test Site, Nevada, Journal of Geophysical Research, v. 89, p. 9401-9413.

Ponce, D.A., Wu, S.S. and Speilman, J.B., 1985, Comparison of survey and photogrammetry methods to positive gravity data, Yucca Mountain, Nevada: U.S. Geological Survey Open-File Report 85-36, 11 p.

Poole, F.G., 1965, Geologic map of the Frenchman Flat quadrangle, Nye, Lincoln, and Clark Counties, Nevada: U.S. Geological Survey Geological Quadrangle Map GQ-456, 1:24,000 scale.

Poole, F.G., Carr, W.J., and Elston, D.P., 1965, Salyer and Wahmonie Formations of southeastern Nye County, Nevada: U.S. Geological Survey Bulletin 1224-A, p. A44-A51.

Poole, F.G., Elston, D.P., and Carr, W.J., 1965, Geologic map of the Cane Spring quadrangle, Nye County, Nevada: U.S. Geological Survey Geological Quadrangle Map GQ-455, 1:24,000 scale.

Powers, P.S. and Healey, D.L., 1985, Free-air gradient observations in Yucca Flat, Nye County, Nevada: U.S. Geological Survey Open-File Report 85-530, 18 p.

Quade, J., and Tingley, J.V., 1983, A mineral inventory of the Nevada Test Site and portions of the Nellis Bombing and Gunnery Range, southern Nye County, Nevada: DOE/NV/10295-1, U.S. Department of Energy, Las Vegas.

Quade, J., and Tingley, J.V., 1984, A mineral inventory of the Nevada Test Site, and portions of Nellis Bombing and Gunnery Range southern Nye County, Nevada: Nevada Bureau of Mines and Geology Open File Report 82-2, 40 p. plus sample descriptions and chemical analyses.

Quade, J., and Tingley, J.V., 1986a, Mineral inventory and geochemical survey Groom Mountain Range Lincoln County, Nevada: Nevada Bureau of Mines and Geology Open File Report 86-9, 66 p. plus sample descriptions and chemical analyses.

Quade, J., and Tingley, J.V., 1986b, Mineral inventory and geochemical survey appendices F., G., & H Groom Mountain Range, Lincoln County, Nevada: Nevada Bureau of Mines and Geology Open File Report 86-10.

Quinlivan, W.D., and Byers, F.M., Jr., 1977, Chemical data and variation diagrams of igneous rock from the Timber Mountain-Oasis Valley caldera complex, southern Nevada: U.S. Geological Survey Open-File Report 77-724, 9 p.

Ramelli, A. R., Bell, J. W., and dePolo, C. M., Late Quaternary faulting at Crater Flat and Yucca Mountain, southern Nevada: Nevada Bureau of Mines and Geology (in review).

Raney, R. G., and Wetzel, N., Natural resource assessment methodologies for the proposed high-level nuclear waste repository at Yucca Mountain, Nye County, Nevada: U.S. Bureau of Mines report NRC FIN D1018, prepared for the Office of Nuclear Safety and Safeguards, U.S. Nuclear Regulatory Commission, 353 p.

Ransome, F.L., 1907, Preliminary account of Goldfield, Bullfrog, and other mining districts in southern Nevada: U.S. Geological Survey Bulletin 303, 98 p.

Ransome, F.L., Emmons, W.H., and Garrey, G.H., 1910, Geology and ore deposits of the Bullfrog district, Nevada: U.S. Geological Survey Bulletin 407, 130 p.

Reno Gazette-Journal, June 19, 1988, Gold report is favorable: Business page, Gold, J., Business editor.

Robinson, G.D., 1985, Structure of pre-Cenozoic rocks in the vicinity of Yucca Mountain, Nye County, Nevada; a potential nuclear-waste disposal site: U.S. Geological Survey Bulletin 1647, 22 p.

Rowe, J. J., and Simon, F. O., 1968, The determination of gold in geologic materials by neutron-activation analysis using fire assay for the radiochemical separations: U. S. Geological Survey Circular 559, 4 p.

Rush, F.E., Thordason, William, and Bruckheimer, Laura, 1983, Geohydrologic and drillhole data for test well USW-H1, adjacent to Nevada Test Site, Nye County, Nevada: U.S. Geological Survey Open-File Report 83-141, 38 p.

Sander, M. V., 1988, Epithermal gold-silver mineralization, wall-rock alteration and geochemical evolution of hydrothermal fluids in the ash-flow tuff at Round Mountain, Nevada: Unpublished PhD. dissertation, Stanford University, Stanford, California, 283 p.

Sander, M. V., 1990, The Round Mountain gold-silver deposit, Nye County, Nevada: Geol. Soc. Nevada Symposium, Geology and Ore Deposits of the Great Basin, Field Trip Guidebook # 11, p. 108-121.

Sawyer, D. A., and Sargent, K. A., 1989, Petrologic evolution of divergent peralkaline magmas from the Silent Canyon caldera complex, southwestern Nevada volcanic field: Journal of Geophysical Research, v. 94, p. 6021-6040.

Sawyer, D. A., Fleck, R. J., Lanphere, M. A., Warren, R. G., and Broxton, D. E., 1990, Episodic volcanism in the southwest Nevada volcanic field: new $^{40}Ar/^{39}Ar$ geochronologic results: EOS, Transactions of the American Geophysical Union, v. 71, p. 1296.

Schoen, R., White, D.E., and Hemley, J.J., 1974, Argillization by decending acid at Steamboat Springs, Nevada: Clays and Clay Minerals, v. 22, p. 1-22.

Schneider, R. and Trask, N.J., 1984, U.S. Geological Survey research in radioactive waste disposal; fiscal year 1982: U.S. Geological Survey Water-Resource Investigation 84-4205, 116 p.

Schuraytz, B.C., Vogel, T.A., and Younker, L.W., 1986, Evolution of a magmatic system. Part I: Geochemistry and mineralogy of the Topopah Spring Member of the Paintbrush Tuff, southern Nevada: EOS, Transactions of the American Geophysical Union, v. 67, p. 1261.

Scott, R.B., 1984, Internal deformation of blocks bounded by basin-and-range-style faults: Geological Society of America, Abstracts with Programs, v. 16, p. 649.

Scott, R.B., 1986a, Rare-earth element evidence for changes in chemical evolution of silicic magmas, southwest Nevada: Transactions of the American Geophysical Union, v. 67, p. 1261.

Scott, R. B., 1986b, Extensional tectonics at Yucca Mountain, southern Nevada [abs.]: Geological Society of America Abs. with Programs, v. 18, p. 411.

Scott, R.B., 1988, Tectonic setting of Yucca Mountain, southwest Nevada: Geological Society of America, Abstracts with Programs, v. 20, p. 229.

Scott, R.B. and Bonk, J., 1984, Preliminary geologic map of Yucca Mountain, Nye County, Nevada, with geologic sections: U.S. Geological Survey Open-File Report 84-494, scale 1:12,000, plus 10 p.

Scott, R.B. and Castellanos, Mayra, 1984, Stratigraphic and structural relations of volcanic rocks in drill holes USW GU-3 and USW G3, Yucca Mountain, Nye County, Nevada: U.S. Geological Survey Open-File Report 84-491, 121 p.

Scott, R. B., and Whitney, J. W., 1987, The upper crustal detachment system at Yucca Mountain, SW Nevada [abs.]: Geological Society of America Abs. with Programs, v. 19, p. 332-333.

Scott, R.B., Byers, F.M. and Warren, R.G., 1984, Evolution of magma below clustered calderas, Southwest Nevada volcanic field [abstr.], EOS, Transactions of the American Geophysical Union, v.65, p. 1126-1127.

Scott, R.B., Spengler, R.W., Lappin, A.R., and Chornack, M.P., 1982, Structure and intracooling unit zonation in welded tuffs of the unsaturated zone, Yucca Mountain, Nevada, a potential nuclear waste repository: EOS, Transactions of the American Geophysical Union, v. 63, no. 18, p. 330.

Scott, R.B., Spengler, R.W., Diehl, S., Lappin, A.R., and Chornack, M.P., 1983, Geologic character of tuffs in the unsaturated zone at Yucca Mountain, southern Nevada: in Mercer, J.M., Rao, P.C. and Marine, W., eds., Role of the unsaturated zone in radioactive and hazardous waste disposal: Ann Arbor press, Ann Arbor, Michigan, p. 289-335.

Scott, R.B., Bath, G.D., Flanigan, V.J., Hoover, D.B., Rosenbaum, J.G., and Spengler, R.W., 1984, Geological and geophysical evidence of structures in northwest-trending washes, Yucca Mountain, southern Nevada, and their possible significance to a nuclear waste repository in the unsaturated zone: U.S. Geological Survey Open-File Report 84-567, 25 p.

Selner, G.I. and Taylor, R.B., 1988, GSDRAW and GSMAP version 5.0: prototype programs, level 5, for the IBM PC and compatible microcomputers, to assist compilation and publication of geologic maps and illustrations: U.S. Geological Survey Open File Report #88-295A (documentation), 130 p. and #88-295B (executable program disks).

Selner, G.I., Smith, C.L., and Taylor, R.B., 1988, GSDIG: a program to determine latitude/longitude locations using a microcomputer (IBM PC or compatible) and digitizer: U.S. Geological Survey Open File Report #88-014A (documentation) 16 p. and #88-014B (executable program disk).

Smith, C., Ross, H.P., and Edquist, R., 1981, Interpreted resistivity and IP section line W1 Wahmonie area, Nevada Test Site, Nevada: U.S. Geological Survey Open-File Report 81-1350, 14 p.

Smith, R.C., and Bailey, R.A., 1968, Resurgent Cauldrons: Geological Society of America Memoir 116, p. 613-662.

Smith, R.M., 1977, Map showing mineral exploration potential in the Death Valley quadrangle, California and Nevada: U.S. Geological Survey Miscellaneous Field Investigation Map MF-873, 1:250,000 scale.

Snyder, D.B., and Oliver, H.W., 1981, Preliminary results of gravity investigations of the Calico Hills, Nevada Test Site, Nye County, Nevada: U.S. Geological Survey Open-File Report 81-101, 42 p.

Snyder, D.B., and Carr, W.J., 1982, Preliminary results of gravity investigations at Yucca Mountain and vicinity, southern Nye County, Nevada: U.S. Geological Survey Open-File Report 82-701, 36 p.

Snyder, D.B. and Carr, W.J., 1984, Interpretation of gravity data in a complex volcano-tectonic setting, southwestern Nevada: Journal of Geophysical Research. B, v. 89, p. 10,193-10,206.

Spengler, R.W., Byers, F.M., Jr., and Warner, J.B., 1981, Stratigraphy and structure of volcanic rocks in drill hole USW-G1, Yucca Mountain, Nye County, Nevada: U.S. Geological Survey Open-File Report 82-1338, 264 p.

Spengler, R.W. and Chornack, M.P., 1984, Stratigraphic and structural characteristics of volcanic rocks in core hole USW G-4, Yucca Mountain, Nye County, Nevada: U.S. Geological Survey Open-File Report 84-789, 82 p.

Spengler, R.W., Muller, D.C., and Livermore, R.B., 1979, Preliminary report on the geology of drill hole UE25a-1, Yucca Mountain, Nevada Test Site: U.S. Geological Survey Open-File Report 79-1244, 43 p.

Spengler, R.W., and Rosenbaum, J.G., 1980, Preliminary interpretations of geologic results obtained from boreholes UE25a-4, -5, -6, and -7, Yucca Mountain, Nevada Test Site: U.S. Geological Survey Open-File Report 80-929, 35 p.

Spengler, R.W., and Rosenbaum, J.G., 1991, A low-angle breccia zone of hydrologic significance at Yucca Mountain, Nevada: Geological Society of America, Abstracts with Programs, v. 23, p. A119.

Stewart, J. H., 1988, Tectonics of the Walker Lane belt, western Great Basin-Mesozoic and Cenozoic deformation in a zone of shear, *in* Ernst, W. G., ed., Metamorphism and crustal evolution of the western United States, Rubey Vol. VII: Englewood Cliffs, New Jersey, Prentice Hall, p. 683-713.

Stuckless, J. S., Peterman, Z. E. and Muhs, D. R., 1991, U and Sr isotopes in groundwater and calcite, Yucca Mountain, Nevada: evidence against upwelling water: Science, v. 254, p. 551-554.

Sutton, V.D., 1984, Data report for the 1983 seismic-refraction experiment at Yucca Mountain, Beatty, and vicinity, southwestern Nevada: U.S. Geological Survey Open-File Report 84-661, 62 p.

Swadley, W.C., Hoover, D.L. and Rosholt, J.N., 1984, Preliminary report on late Cenozoic faulting and stratigraphy in the vicinity of Yucca Mountain, Nye County, Nevada: U.S. Geological Survey Open-File Report 84-788, 44 p.

Swolfs, H.S. and Savage, W.Z., 1985, Topography, stresses and stability at Yucca Mountain, Nevada, Proceedings - Symposium on Rock Mechanics: Research and engineering applications in rock masses, 26, p. 1121-1129.

Szabo, B.J. and Kyser, T.K., 1985, Uranium, thorium isotopic analyses and uranium-series ages of calcite and opal, and stable isotopic compositions of calcite from drill cores UE25a 1, USW G-2 and USW G-3/GU-3, Yucca Mountain, Nevada: U.S. Geological Survey Open-File 85-224, 30 p.

Szabo, B. J., and Kyser, T. K., 1990, Ages and stable-isotope compositions of secondary calcite and opal in drill cores from Tertiary volcanic rocks of the Yucca Mountain area, Nevada: Geological Society of America Bulletin, v. 102, p. 1714-1719.

Szabo, B.J. and O'Malley, P.A., 1985, Uranium-series dating of secondary carbonate and silica precipitates relating to fault movements in the Nevada Test Site region and of caliche and travertine samples from the Amargosa Desert: U.S. Geological Survey Open-File Report 85-0047, 17 p.

Taylor, E.M., and Huckins, H.E., 1986, Carbonate and opaline silica fault-filling in the Bow Ridge Fault, Yucca Mountain, Nevada -- deposition from pedogenic processes of upwelling ground water: Geological Society of America, Abstracts with Programs, v. 18, no. 5, p. 418.

Thordarson, William, Rush, F.E. , Spengler, R.W. and Waddell, S.J., 1984, Geohydrologic and drill-hole data for test well USW H-3, Yucca Mountain, Nye County, Nevada: U.S. Geological Survey Open-File Report 84-0149, 54 p.

Tingley, J.V., 1984, Trace element associations in mineral deposits, Bare Mountain (Fluorine) mining district, southern Nye County, Nevada: Nevada Bureau of Mines and Geology Report 39, 28 p.

Turrin, B. D., Champion, D., and Fleck, R. J., 1991, $^{40}Ar/^{39}Ar$ age of the Lathrop Wells volcanic center, Yucca Mountain Nevada: Science, v. 253, p. 654-657.

U.S. Department of Energy, 1986, Environmental Assessment Yucca Mountain Site, Nevada Research and Development Area, Nevada, v. 1: Washington, DC, Office of Civilian Radioactive Waste Management.

U.S. Department of Energy, 1988a, Consultation Draft Site Characterization Plan, Yucca Mountain Site, Nevada Research and Development Area, Nevada: Washington, DC,Office of Civilian Radioactive Waste Management, 347 p.

U.S. Department of Energy, 1988b, Site Characterization Plan, Yucca Mountain Site, Nevada Research and Development Area, Nevada: Washington, DC,Office of Civilian Radioactive Waste Management.

U.S. Geologic Survey, 1984, A summary of geologic studies through January 1, 1983 of a potential high-level radioactive waste repository site at Yucca Mountain, southern Nye County, Nevada: U.S. Geological Survey Open-File Report 84-792, 164 p.

Vaniman, D. T., 1991, Calcite, opal, sepiolite, ooids, pellets, and plant/fungal traces in laminar-fabric fault fillings at Yucca Mountain Nevada: Geological Society of America, Abstracts with Programs, v. 23, p. 117.

Vaniman, D.T., and Crowe, B.M., 1981, Geology and petrology of the basalts of Crater Flat: Applications to volcanic risk assessment for the Nevada nuclear waste storage investigations: Los Alamos, New Mexico, Los Alamos National Laboratory Report, LA-8845-MS, 67 p.

Vaniman, D.T., Crowe, B.M., and Gladney, E.S., 1982, Petrology and geochemistry of Hawaiite lavas from Crater Flat, Nevada: Contributions to Mineralogy and Petrology, v. 80, p. 341-357.

Vaniman, D.T., Bish, D.L., and Chipera, S., 1988, A preliminary comparison of mineral deposits in faults near Yucca Mountain, Nevada, with possible analogs: Los Alamos, New Mexico, Los Alamos National Laboratory Report LA-11298-MS, UC-70, 54 p.

Vaniman, D.T., Bish, D., Broxton, D., Byers, F., Heiken, G., Carlos, B., Semarge, E., Caporuscio, F., and Gooley, R., 1984, Variations in authigenic mineralogy and sorptive zeolite abundance at Yucca Mountain, Nevada, based on studies of drill cores USW GU-3 and G-3.

Vogel, T. A., Noble, D. C., and Younker, L. W., 1989, Evolution of a chemically zoned magma body: Black Mountain volcanic center, southwestern Nevada: Journal of Geophysical Research, v. 94, p. 6041-6058.

Vogel, T.A., Ryerson, R.A., Noble, D.C., and Younker, L.W., 1987, Constrains on magma mixing in a silicic magma body: disequilibrium phenocrysts in pumices from a chemically zoned ash-flow sheet: Journal of Geology, v. 95, in press.

Waddell, R.J., 1984, Geohydrologic and drill-hole data for test wells UE-29a#1 and UE-29a#2, Fortymile Canyon, Nevada Test Site: U.S. Geological Survey Open-File Report 84-0142, 25 p.

Wang, J.S.Y., and Narasimhan, T.N., 1985, Hydrologic mechanisms governing fluid flow in partially saturated, fractured, porous tuff at Yucca Mountain: University of California Lawrence Berkeley Laboratory Report SAND84-7202 (LBL-18473), 46 p.

Warren, R.G., and Broxton, D.E., 1986, Mixing of silcic and basaltic magmas in the Wahmonie Formation, southwestern Nevada volcanic field, Nevada: EOS (American Geophysical Union Transactions), v. 67, p. 1261.

Warren, R.G., Byers, F.M., and Caporuscio, F.A., 1984, Petrography and mineral chemistry of units of the Topopah Springs, Calico Hills and Crater Flat Tuffs, and some older volcanic units, with emphasis on samples from drill hole USW G-1, Yucca Mountain, Nevada Test site: Los Alamos, New Mexico, Los alamos National Laboratory Report LA-10003-MS.

Warren, R.G., Nealey, L.D., Byers, F.M., Jr., and Freeman, S.H., 1986, Magmatic components of the Rainier Mesa Member of the Timber Mountain Tuff, Timber Mountain-Oasis Valley Caldera Complex: EOS (American Geophysical Union Transactions), v. 67, p. 1260.

Warren, R. G., Byers, F. M., Jr., Broxton, D. E., Freeman, S. H., and Hagan, R. C., 1989, Phenocryst abundances and glass and phenocryst compositions as indicators of magmatic environments of large-volume ash flow sheets in southwestern Nevada: Journal of Geophysical Research, v. 94, p. 5987-6020.

Warren, R.G., McDowell, F.W., Byers, F.M., Broxton, D.E., Carr, W.J., and Orkild, P.P., 1988, Eposodic leaks from Timber Mountain caldera: new evidence from rhyolite lavas of Fortymile Canyon, southwestern Nevada Volcanic Field: Geological Society of America, Abstracts with Programs, v. 20, p. 241.

Weiss, S.I., 1987, Geologic and Paleomagnetic studies of the Stonewall and Black Mountain volcanic centers, southern Nevada: University of Nevada, Reno-Mackay School of Mines, Reno, Nevada, unpublished MSc Thesis, 67 p.

Weiss, S.I., and Noble, D.C., 1989, Stonewall Mountain volcanic center, southern Nevada: stratigraphic, structural and facies relations of outflow sheets, near-vent tuffs, and intracaldera units: Journal of Geophysical Research, v. 94, 6059-6074.

Weiss, S.I., Noble, D.C., and Mckee, E.H.,1984, Inclusions of basaltic magma in near-vent facies of the Stonewall Flat Tuff: product of explosive magma mixing: Geological Society of America, Abstracts with Programs, v. 16, p. 689.

Weiss, S. I., Noble, D. C., and McKee, E. H., 1988, Volcanic and tectonic significance of the presence of late Miocene Stonewall Flat Tuff in the vicinity of Beatty, Nevada: Geological Society of America Abs. with Programs, v. 20, p. A399.

Weiss, S. I., Noble, D. C., and McKee, E. H., 1989, Paleomagnetic and cooling constraints on the duration of the Pahute Mesa-Trail Ridge eruptive event and associated magmatic evolution, Black Mountain volcanic center, southwestern Nevada: Journal of Geophysical Research, v. 94, p. 6075-6084.

Weiss, S. I., Noble, D. C., and Larson, L. T., 1989, Task 3: Evaluation of mineral resource potential, caldera geology and volcano-tectonic framework at and near Yucca Mountain; report for July, 1988 - September, 1989: Center for Neotectonic Studies, University of Nevad-Reno, 38 p. plus appendices.

Weiss, S. I., Noble, D. C., and Larson, L. T., 1990, Task 3: Evaluation of mineral resource potential, caldera geology and volcano-tectonic framework at and near Yucca Mountain; report for October, 1989 - September, 1990: Center for Neotectonic Studies, University of Nevad-Reno, 29 p. plus appendices.

Weiss, S. I., Noble, D. C., and Larson, L. T., 1991a, Task 3: Evaluation of mineral resource potential, caldera geology and volcano-tectonic framework at and near Yucca Mountain; report for October, 1990 - September, 1991: Center for Neotectonic Studies, University of Nevad-Reno, 37 p. plus appendices.

Weiss, S. I., Noble, D. C., and Larson, L. T., 1992, Task 3: Evaluation of mineral resource potential, caldera geology and volcano-tectonic framework at and near Yucca Mountain; report for October, 1991 - September, 1992: Center for Neotectonic Studies, University of Nevad-Reno, 44 p. plus appendices.

Weiss, S. I., Ristorcelli, S. J., and Noble, D. C., 1993, Mother Lode gold deposit, southwestern Nevada: another example of Carlin-type mineralization associated with porphyry magmatism: Geological Society of America Abstracts with Programs, v. 25, p. 161.

Weiss, S. I., Connors. K. A., Noble, D. C., and McKee, E. H., 1990, Coeval crustal extension and magmatic activity in the Bullfrog Hills during the latter phases of Timber Mountain volcanism: Geological Society of America Abstracts with Programs, v. 22, p. 92-93.

Weiss, S. I., Noble, D. C., Worthington, J. E., IV., and McKee, E. H., 1993, Neogene tectonism from the southwestern Nevada volcanic field to the White Mountains, California Part I. Miocene volcanic stratigraphy, paleotopography, extensional faulting and uplift between northern Death Valley and Pahute Mesa: *in* Lahren, M. M., Trexler, J. H., Jr., and Spinosa, C., eds., 1993, Crustal Evolution of the Great Basin and Sierra Nevada: Cordilleran/Rocky Mountain Section, Geological Society of America Guidebook, Department of Geological Sciences, University of Nevada, Reno, p. 353-369.

Weiss, S. I., McKee, E. H., Noble, D. C., Connors, K. A., and Jackson, M. R., 1991b, Multiple episodes of Au-Ag mineralization in the Bullfrog Hills, SW Nevada, and their relation to coeval extension and volcanism: Geological Society of America Abstracts with Programs, v. 23, p. A246.

Weiss, S. I., Noble, D. C., Connors, K. A., Jackson, M. R., and McKee, E. H., (in preparation), Multiple episodes of hydrothermal activity and precious-metal mineralization in the southwestern Nevada volcanic field and their relations to magmatic activity, volcanism and regional extension: for submission to Economic Geology.

Wernicke, B. P., Christiansen, R. L., England, P. C., and Sonder, L. J., 1987, Tectonomagmatic evolution of Cenozoic extension of the North America Cordillera, *in* Coward, M. P., Dewey, J. F., and Hancock, P. L., eds., Continental extensional tectonics: Geol. Soc. London Spec. Pub. 28, p. 203-222.

White, A.F., 1979, Geochemistry of ground water associated with tuffaceous rocks, Oasis valley, Nevada: U.S. Geological Survey Professional Paper 712-E.

Whitney, J. A., and Stormer, J. C., Jr., 1983, Igneous sulfides in the Fish Canyon Tuff and the role of sulfur in calc-alkaline magmas: Geology, v. 11., p. 99-102.

Whitfield, M.S., Eshom, E.P., Thordarson, W., and Schaefer, D.H., 1985, Geohydrology of rocks penetrated in test well USW H-4, Yucca Mountain, Nye County, Nevada: U.S. Geological Survey Water-Resources Investigations Reports, 1985, 33 p.

Whitfield, M.S., Thordarson, W. and Eshom, E.P., 1984, Geohydrologic and drill-hole data for test well USW H-4, Yucca Mountain, Nye County, Nevada: U.S. Geological Survey

Worthington, J. E., IV., 1992, Neogene structural and volcanic geology of the Gold Mountain - Slate Ridge area, Esmeralda County, Nevada, unpublished MSc. thesis, Univ. Nevada, Reno, 76 p.

Worthington, J. E., IV., Noble, D. C., and Weiss, S. I., 1991, Structural geology and Neogene extensional tectonics of the Gold Mountain-Slate Ridge area, southwestern Nevada: Geol. Soc. America Abstr. with Prog., v. 23, p. A247.

Wu, S.S., 1985, Topographic Maps of Yucca Mountain area, Nye County, Nevada, 6 oversize sheets, scale 1:5,000: U.S. Geological Survey Open-File Report 85-0620.

Zartman, R. E., and Kwak, L. M., 1991, Lead isotopes in the carbonate-silica veins of Trench 14, Yucca Mountain, Nevada: Geological Society of America, Abstracts with Programs, v. 23, p. 117.

Table 1. Precious Metals and Indicator-Element Concentrations in Rocks from Northwestern Yucca Mountain and the Lac Gold Bullfrog mine
(Ag and Au values given in ppb, all others in ppm)

	Field #	Ag	Au	As	Bi	Cd	Hg	HgAA	Sb	Se	Te	Cu	Mo	Pb	Zn	Tl
1	3SW675	11	0.43	11.2	0.173	0.19	0.712	0.824	2.77	<0.25	0.06	5.9	3.32	9.1	11.0	1.000
2	3SW677	9	<0.20	15.3	0.067	0.04	<0.020	0.023	0.63	<0.25	<0.05	3.4	1.15	10.1	39.0	<0.498
3	3SW679A	63	<0.20	21.0	0.095	0.18	0.026	0.045	3.77	<0.25	<0.05	10.4	3.19	13.9	39.9	<0.496
4	3SW679B	23	0.56	11.7	0.105	0.14	0.039	0.056	1.17	<0.25	<0.05	9.6	3.71	12.5	25.5	0.546
5	3SW681A	5	<0.20	46.1	0.149	0.28	0.070	0.106	2.83	<0.25	<0.05	3.8	1.14	20.9	36.1	<0.487
6	3SW681B	<3	0.36	109.0	0.337	0.59	0.189	0.259	9.44	<0.25	<0.05	9.5	1.86	47.0	31.6	<0.493
7	3SW681C	5	<0.20	31.4	0.230	0.26	0.114	0.151	3.63	<0.25	0.05	4.2	1.73	25.2	18.0	2.040
8	3SW683	8	0.56	34.0	0.056	0.05	<0.020	0.038	2.83	<0.25	<0.05	3.1	1.42	16.1	17.8	<0.492
9	3SW685	4	<0.20	6.0	0.075	0.70	0.246	0.304	1.40	<0.25	0.05	5.5	3.41	5.1	16.1	5.460
10	3SW687	4	<0.20	2.4	0.092	0.07	0.034	0.038	3.07	<0.25	0.05	4.5	9.47	1.3	2.3	<0.497
11	3SW689	7	<0.20	3.6	0.099	0.10	0.040	0.045	0.14	<0.25	<0.05	5.9	2.97	11.8	15.7	<0.495
12	3SW691	4	<0.20	11.9	0.178	0.26	0.063	0.069	0.31	<0.25	<0.05	4.4	2.47	16.1	10.9	<0.486
13	3SW693	11	<0.20	2.3	0.208	0.15	0.124	0.139	0.83	<0.25	<0.05	9.9	5.55	9.2	7.9	<0.491
14	3SW695	10	<0.20	5.4	0.078	0.05	0.035	0.043	0.48	<0.25	0.05	6.6	2.80	4.7	12.7	<0.489
15	3SW697	<3	<0.20	4.9	0.256	0.17	0.227	0.274	1.96	<0.25	0.06	6.3	7.56	53.6	107.0	0.626
	Unaltered devitrified Tiva Canyon Member of the Paintbrush Tuff															
16	3SW589	25	0.59	1.6	<0.049	0.04	<0.02	0.017	<0.05	<0.25	<0.05	5.0	1.33	7.3	53.4	<0.495
	Hydrothermally altered Rainier Mesa Member, Timber Mountain Tuff at the Lac Gold Bullfrog mine															
17	3SW699	282	156.00	2.5	0.275	0.211	<0.019	0.010	0.90	<0.243	<0.05	6.8	0.60	32.1	35.0	<0.486
18	893X	232	71.30	2.5	0.282	0.212	<0.020	nd	0.88	<0.249	<0.05	6.7	0.59	32.0	35.2	<0.497

Field numbers correspond to numbered dots in Figure 2. nd = not determined.

HgAA = Hg analyses carried out by the Nevada Mining Analytical Laboratory using hydride-generator atomic absorption methods with 10 gram digestions, M. O. Desilets, analyst. All other values from analyses by U. S. Mineral Laboratories, Inc., (formerly MB Associates) North Highlands, CA, using 15 gram digestions, organic liquid separation and inductively-coupled plasma emission spectrography, except for Au which was determined by graphite furnace - atomic absorption spectrometry. Values as reported by U.S. Mineral Laboratories except Ag rounded to nearest 1 ppb, Au rounded to nearest 0.01 ppb, As, Cu Pb and Zn rounded to nearest 0.1 ppm, and Cd, Sb, Se, Te and Mo rounded to nearest 0.01 ppm. Number of significant figures does not indicate precision or accuracy of analyses.

Detection limits as quoted by U.S. Mineral Laboratories at 3 sigma confidence level:

Ag = 3 ppb; Au = 0.2 ppb; Tl = 0.5 ppm; As, Se and Zn = 0.25 ppm; Bi, Sb, Te and Pb = 0.050 ppm; Cd, Hg and Mo = 0.020 ppm; Cu = 0.010 ppm.

Table 1, continued.

1 Northeast-trending, banded, 1 - 5 cm wide light grey opal-quartz vein with center filled by a mixture of very fine grained reddish iron-oxide and silica.

2 Densely welded, devitrified ash-flow tuff of the Tram Member of the Crater Flat Tuff; contains no veins.

3 Northeast-trending, clear to white, banded opal and fine grained quartz vein largely <3 cm wide; specimen includes about 50 volume % wallrock tuff.

4 Northeast-trending, 3 cm wide dark grey to white, banded opal vein; specimen includes about 50 volume % wallrock tuff.

5 Welded and devitrified ash-flow tuff of the Tram Member with fracture coatings of limonite and soft, tabular barite(?) crystals; specimen includes about 25 volume % thin veins composed of iron oxide and silica cemented wallrock tuff fragments.

6 Northwest-trending 2 cm wide vein filled with reddish brown mixture of iron oxide, silica and wallrock tuff fragments.

7 East-west to northwest-trending vein as much as 3 cm wide composed of reddish brown mixture of iron oxide, silica and wallrock tuff fragments.

8 Bleached, light grey welded and devitrified ash-flow tuff of the Tram Member with thin veins (<3 cm wide) of opal and granular quartz. Partial to complete adularization of feldspar phenocrysts. Float from vein zone about 250' to the north.

9 Dark brownish grey, silicified thin-bedded siltstone with interbeds and veinlets of white opaline silica; upper ledge.

10 Brecciated, coarsely layered reddish brown, clear and white opal containing fine-grained drusy quartz; upper ledge.

11 Silicified unwelded, previously glassy tuff adjacent to WNW-striking, steeply dipping opal and chalcedony vein about 5 cm wide; lower ledge, stratigraphically above silica sinter or sinter-like strata of specimen 13. Partial adularization of feldspar phenocrysts and pervasive replacement of glass shards and pumice by very fine grained mixture of chalcedony, quartz and adularia.

12 WNW-striking, steeply south-dipping vein about 5 cm wide consisting, from the wallrock inward, of banded opal surrounding a core of silica-cemented breccia of opal vein fragments and silicified wallrock fragments; lower ledge, stratigraphically above silica sinter or sinter-like strata of specimen 13.

13 Finely to coarsely layered reddish brown, clear, white and grey opaline silica; silica sinter or sinter-like strata at old prospect; lower ledge.

14 Silicified, unwelded, previously glassy ash-flow tuff with clear to white chalcedony and fine grained granular quartz veins and veinlets to about 1 cm wide; tuff overlies silica sinter or sinter-like strata, lower ledge.

15 Dark greyish brown to black, fine grained, silicified siltstone with irregular pods and boudin-shaped opal bodies; upper ledge.

16 Unaltered, devitrified rhyolite ash-flow tuff of the Tiva Canyon Member of the Paintbrush Tuff prepared and analysed with the other specimens to monitor analytical precision at low concentrations and to confirm the effectiveness of clean preparation procedures. Previous analyses of other splits from same 10 kg specimen given by Weiss et al. (1992).

17 Hydrothermally altered porous ash-flow tuff, lower part of the Rainier Mesa Member of the Timber Mountain Tuff, from unmineralized horse within fault-bounded vein system exposed in the 916 bench, Phase IV, Lac Gold Bullfrog mine, Rhyolite, NV. Sample location is within 30 m of Au-Ag orebody.

18 893X = blind duplicate analysis of split of specimen 17 (3SW699).

Table 2. Major and Trace-element Analyses of Siliceous Strata, Northwestern Yucca Mountain

Major Elements in Weight %

Field #	SiO_2	TiO_2	Al_2O_3	Fe_2O_3	MnO_2	MgO	CaO	Na_2O	K_2O	P_2O_5	Total
3SW685	92.0	0.04	5.16	1.05	0.53	0.14	0.57	0.10	0.31	0.1	100.30
3SW687	96.1	0.03	2.08	1.60	0.04	0.12	0.05	bd	0.03	bd	100.04
3SW693	96.6	0.04	1.93	0.98	0.11	0.12	0.08	0.09	0.17	bd	100.12

Trace-Elements in ppm

	Zr	Y	Sr	Rb	Th	Ba	Cu	Pb	Zn
3SW685	20	5	49	10	8	458	21	13	23
3SW687	7	1	9	bd	2	45	14	9	bd
3SW693	21	4	11	8	5	17	18	3	5

Analyses carried out in the Nevada Mining Analytical Laboratory by X-ray fluorescence methods on pressed-powder pellets; M. O. Desilets and P. J. Lechler, analysts. bd = below detection.

3SW685 Dark brownish grey, silicified thin-bedded siltstone with interbeds and veinlets of white opaline silica; upper ledge.

3SW687 Brecciated, coarsely layered reddish brown, clear and white opal containing fine-grained drusy quartz; upper ledge.

3SW693 Finely to coarsely layered reddish brown, clear, white and grey opaline silica; lower ledge sinter or sinter-like strata at old prospect.

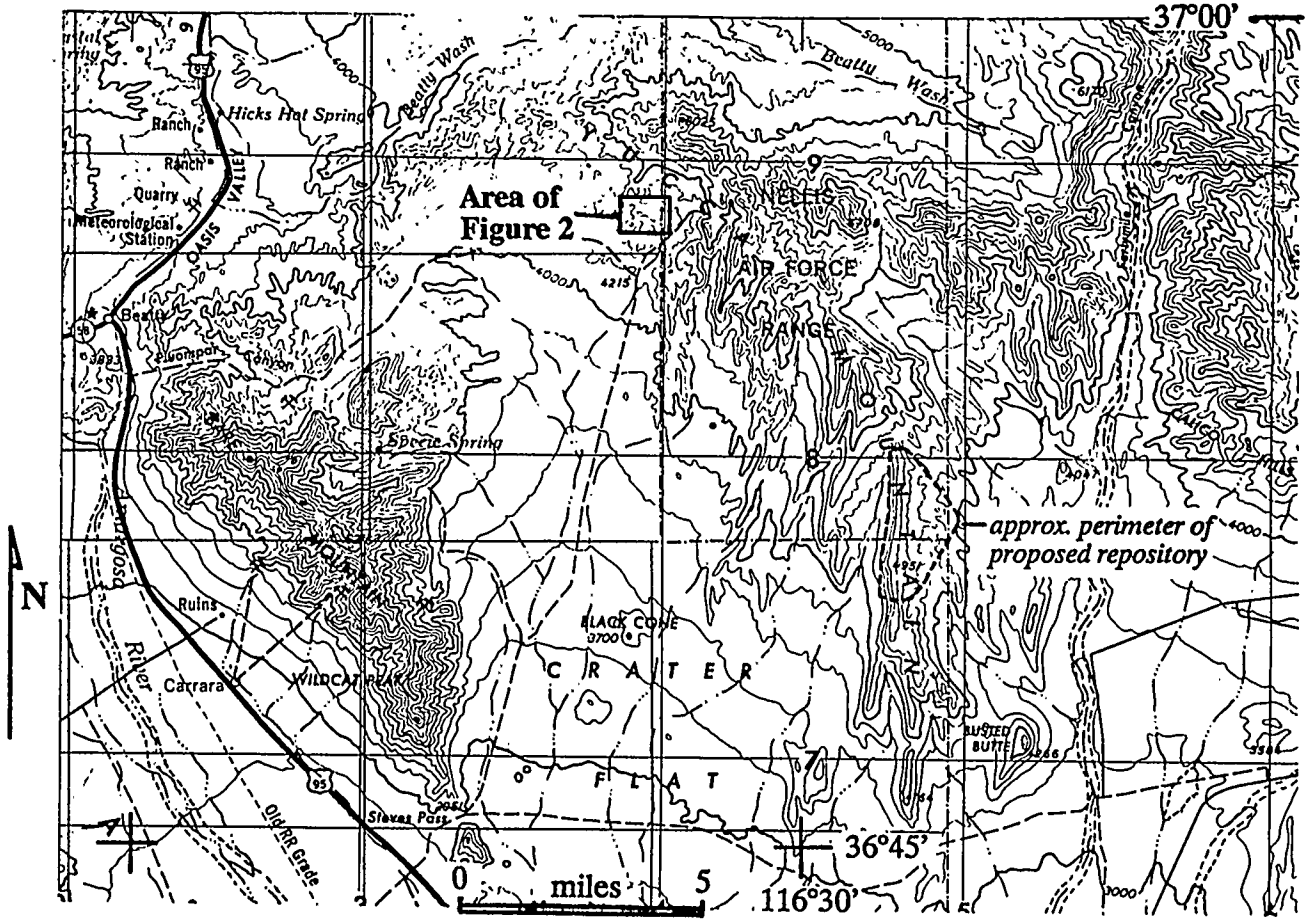

Figure 1. Location map for the area of veins and siliceous ledges in northwestern Yucca Mountain shown in Figure 2.

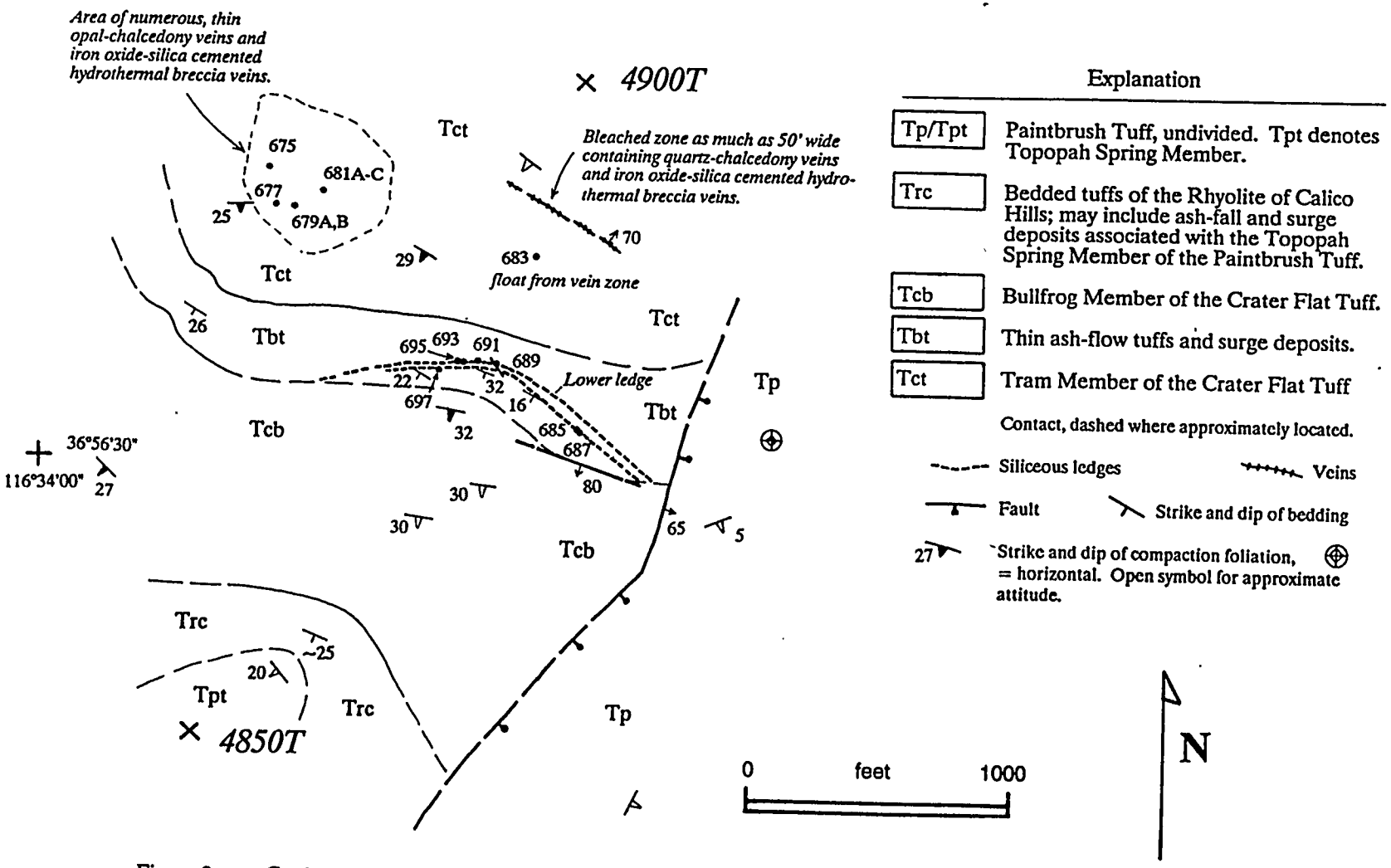

Figure 2. Geologic map of a portion of the East of Beatty Mountain 7.5' quadrangle showing the area of veins and siliceous deposits within units of the Crater Flat Tuff. Numbered dots show locations of samples referred to in Tables 1 and 2 and in the text. Mapping at 1:6000 by S. I. Weiss, August, 1993.

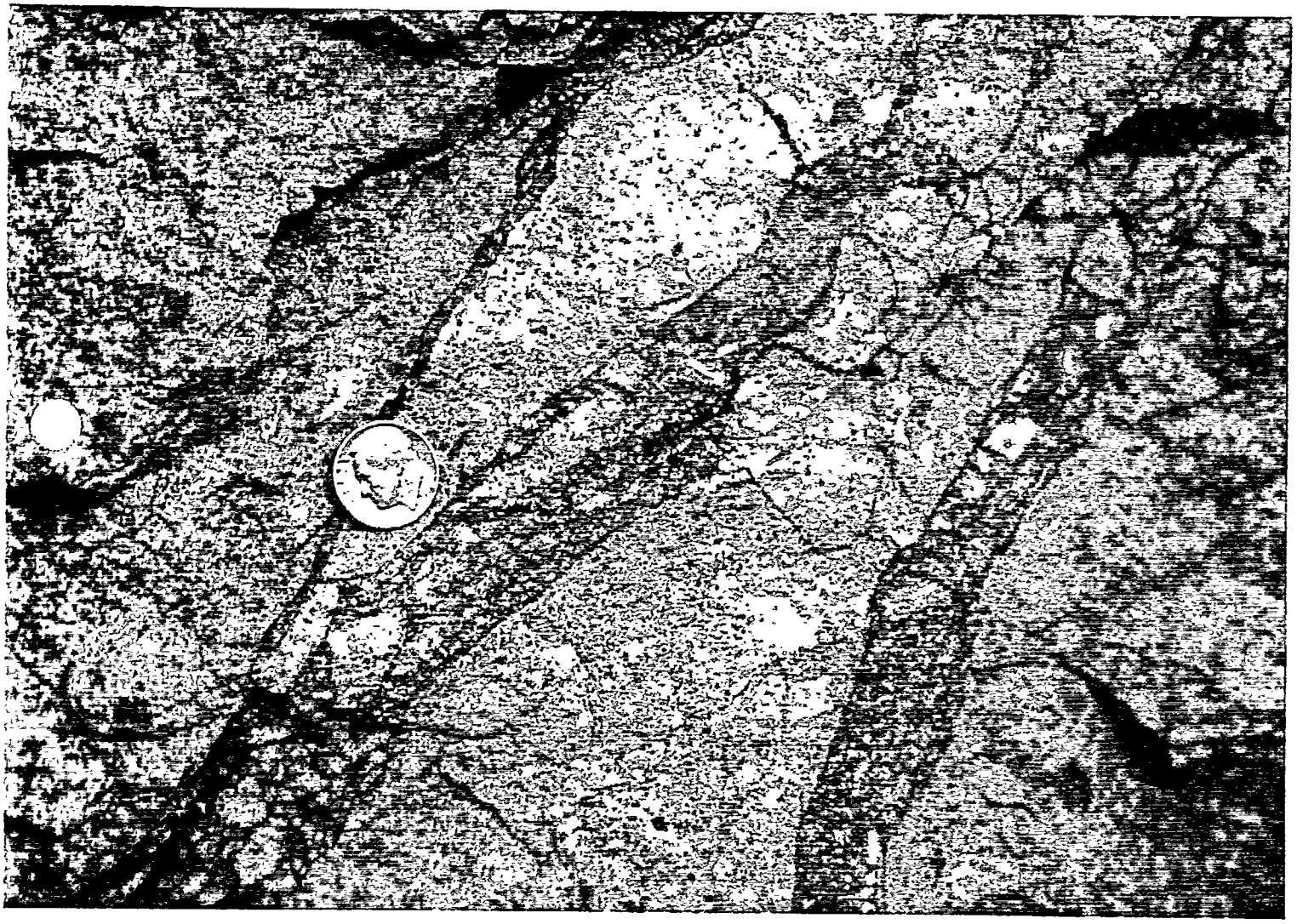

Figure 3. Iron oxide and silica cemented hydrothermal breccia veins cutting the Tram Member of the Crater Flat Tuff in the northwestern part of Yucca Mountain; outcrops located near sample locality 679A,B of Figure 2.

Figure 4a. Laminated opal or siliceous sinter deposits, float block below lower ledge of Figure 2.

Figure 4b. Upper surface of laminated opal or sinter deposits showing mudcracks and probable trace fossils, float block below lower ledge of Figure 2.

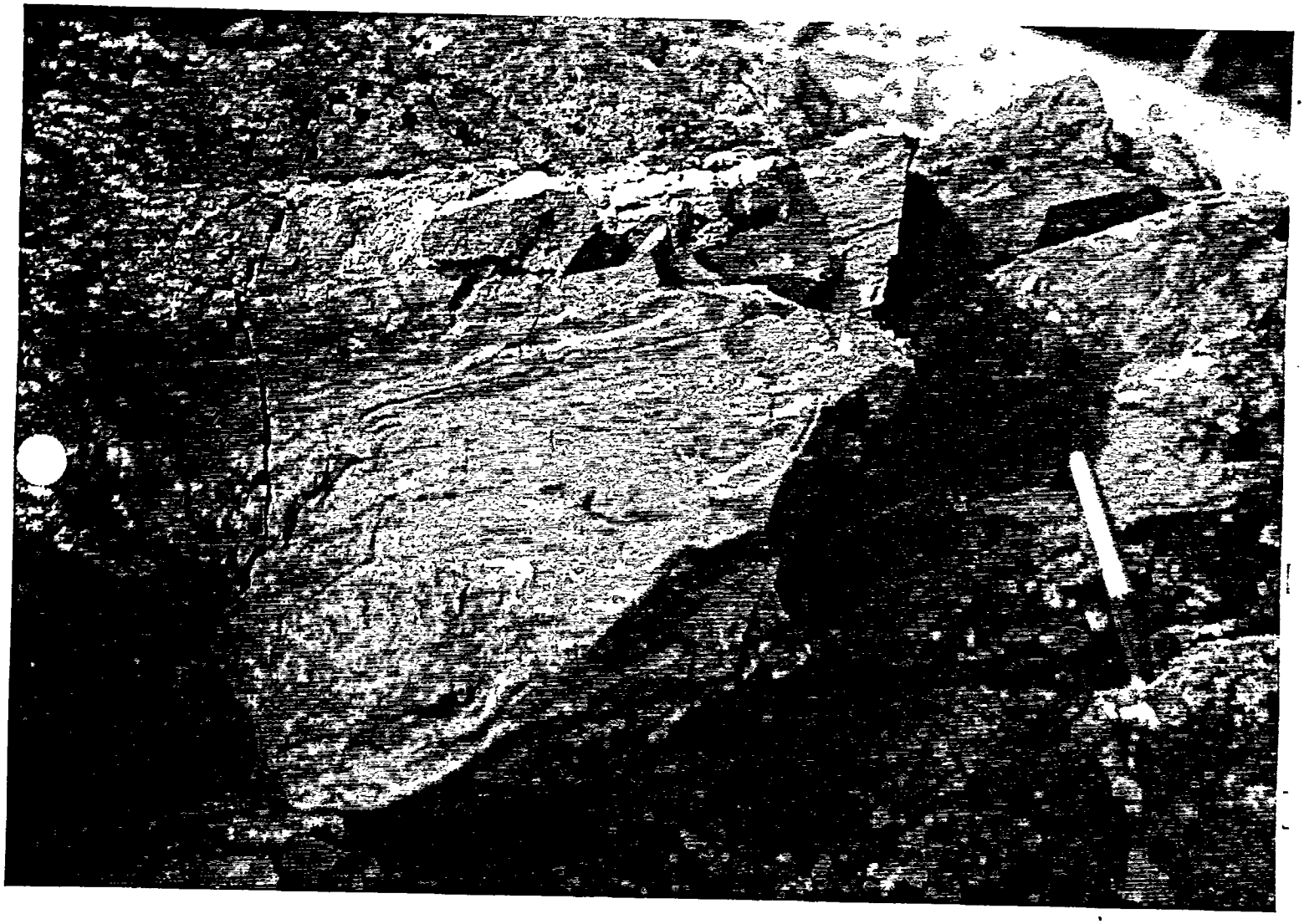

Figure 5. Silicified grey siltstone, upper ledge of Figure 2. Pen straddles irregular contact with underlying ash-flow tuff.

SOUTH

HYDROTHERMAL ALTERATION IN DRILL HOLE

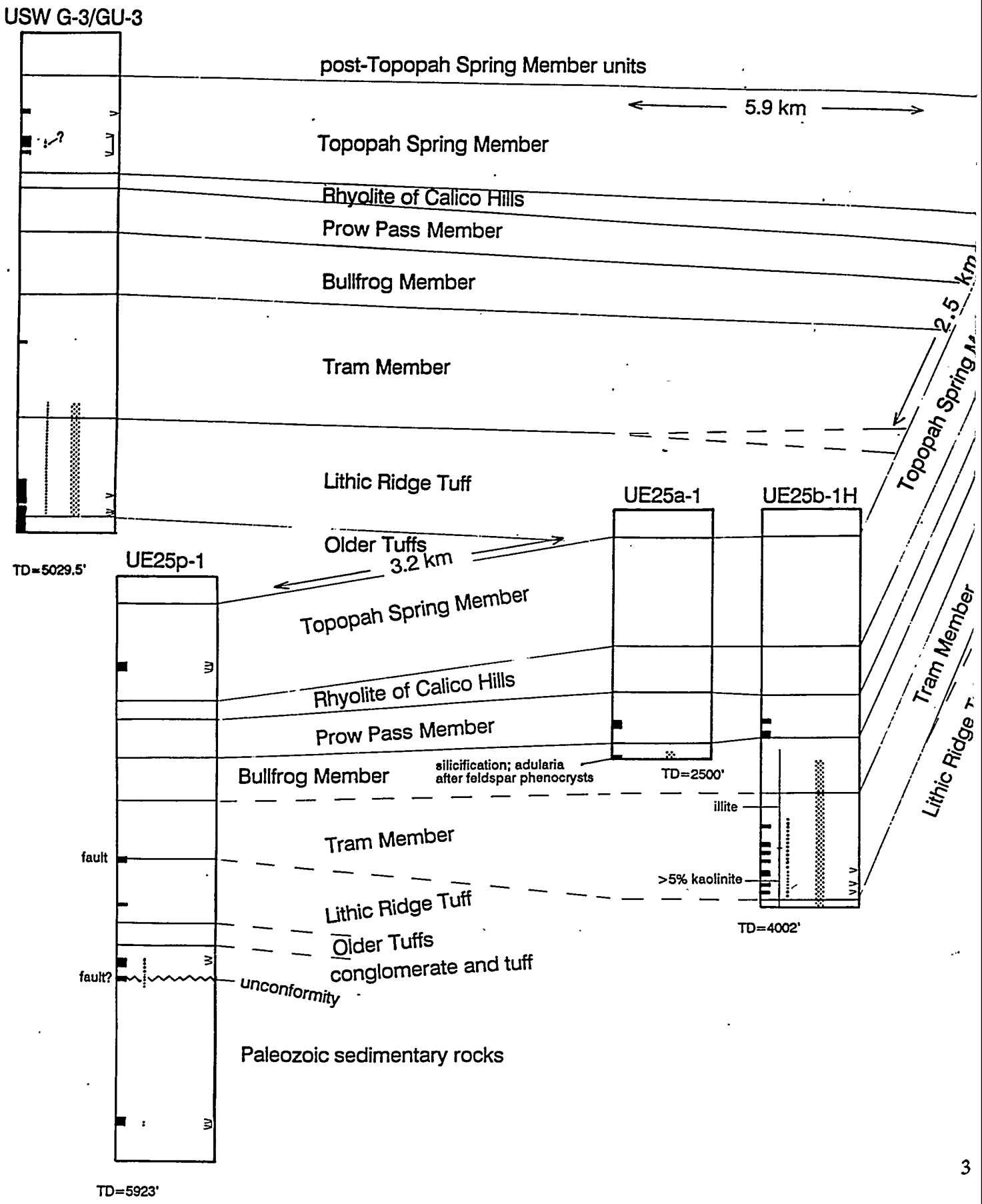

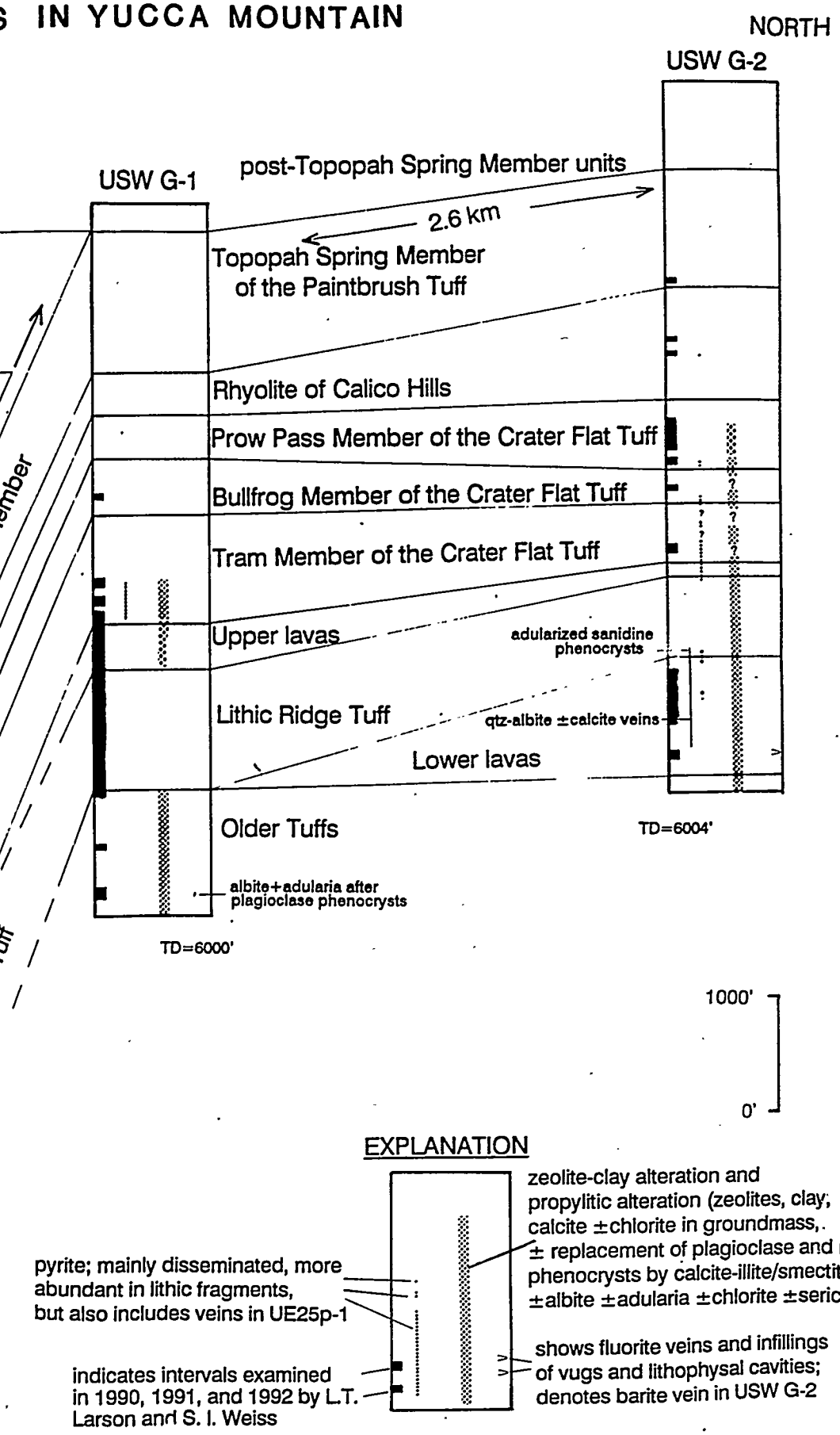

Figure 6. Subsurface stratigraphy and hydrothermal alteration features of deep drill holes in Yucca Mountain. Data from microscopic and macroscopic examination of core and cuttings by Task 3 and numerous published reports of the U.S. Geological Survey and the Los Alamos National Laboratory.

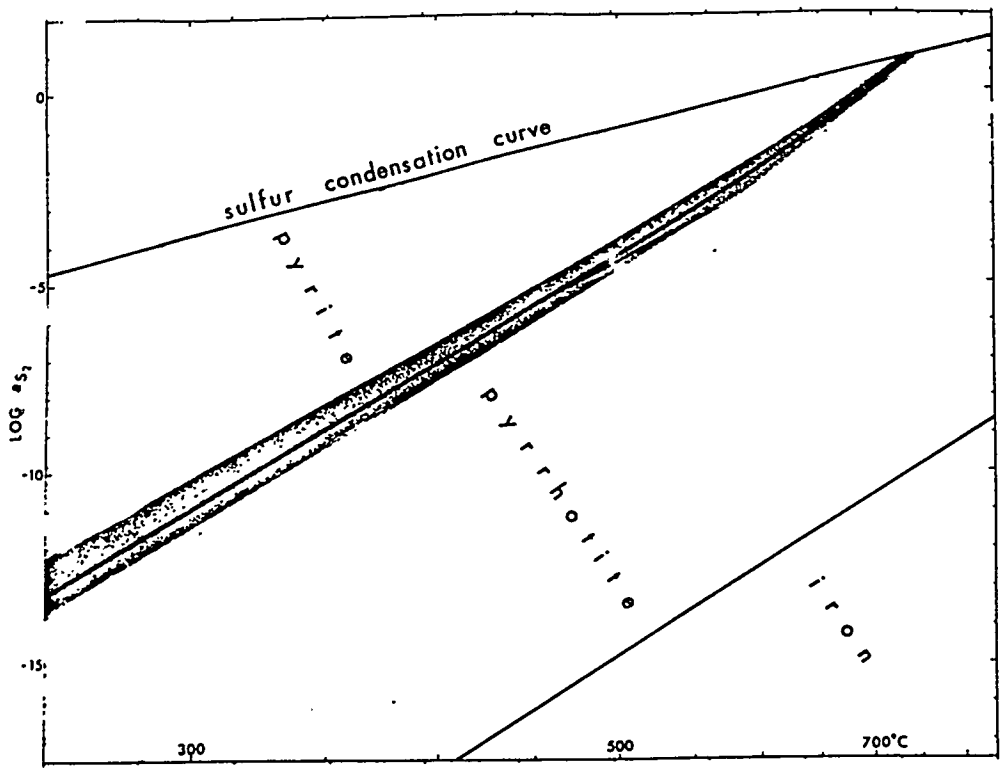

Figure 7. Activity of S_2-temperature diagram for the FeS system; shaded area shows generous estimate of the uncertainty in the location of the pyrite - pyrrhotite curve. Modified from Barton and Skinner (1979).

reprints and abstracts removed. ds

YUCCA MOUNTAIN TASK 4 FINAL REPORT FY 1993
University of Nevada Seismological Laboratory (UNRSL)

James N. Brune

Four major projects at UNRSL have been supported by NWPO-Neotectonics Yucca Mountain Task 4 funds during the last year:

1. Operation and analysis of data from the UNRSL microearthquake network at Yucca Mountain.
2. Continued operation, maintenance, and calibration of three broad-band stations (Troy Canyon, Deep Springs, and Nelson). Limited data analysis was also initiated.
3. Continued review by Dr. Brune of documents and literature related to seismic hazard and tectonics of the Yucca Mountain region.
4. Testing of noise levels in boreholes.

Project 1 The microearthquake network has yielded critical information on the low background microseismicity (down to magnitudes less than 0) at Yucca Mountain. We have been given permission to relocate our sensors into existing drill holes whenever they are not being actively used by other projects. We are currently operating one instrument at a depth of 70 feet in Solitario Canyon and another at a depth of 400 feet on Yucca Crest. We believe this has increased the network sensitivity in magnitude to less than -1. Preliminary noise analysis indicates that we have decreased the noise/signal ratio by a factor of 2 to 4, and greatly reduced wind noise. This project has the potential of enabling us to record very small earthquakes from faults in the immediate vicinity of the repository, and thus provide critical information on the activity and stress level of these faults.

After about one year of operation we should be able to establish a new microearthquake threshold for the Ghost Dance and Solitario Canyon faults, and perhaps for faults on the east side of Yucca Mountain. This will be important information for assessing the tectonic activity and state of stress in the rocks at Yucca Mountain.

We have recorded numerous blasts from the excavation of the first 200 feet of the ESF. We continued to record numerous aftershocks of the Little Skull Mountain Earthquake. We recorded one small earthquake approximately 10 km north of Yucca Wash, but microearthquake activity in the immediate vicinity of the repository remains very low.

Project 2 We have continued to accumulate broad-band information useful for determining the structure of the Yucca Mountain region in future analysis. During FY 1993 there was only one other broad-band seismometer operating in the Yucca Mountain region, the U.S. National Network station at Shoshone Peak. We developed a catalogue of waveforms from the Yucca Mountain region for events of $M > 3.0$. We began analysis to determine the direction of anisotropy in the mantle under these stations.

Project 3 Dr. Brune has continued to keep up to date on seismic hazard and tectonics issues related to Yucca Mountain.

Project 4 We made several tests to determine the causes of noise on the borehole instruments. We piled a mound of dirt around the exposed upper part of the drill hole casing for the 70' hole in Solitario Canyon. We also emplaced foam rubber plugs at several depths in the hole to reduce resonances in the air column. These measures have significantly improved the signal to noise ratio for this station.

The signal to noise ratio for the 400 foot hole at Yucca Crest is not as great as we had hoped, and in next year's effort we hope to determine the cause of this and make appropriate changes.

PROGRESS REPORT--OCTOBER 1, 1992 TO SEPTEMBER 30, 1993

TASK 5 Tectonic and Neotectonic framework of the Yucca Mountain Region

Personnel

Principal Investigator: Richard A. Schweickert

Research Assistant Professor: Mary M. Lahren, February 1, 1993 to March 31, 1993

Visiting Scientist: J. Douglas Walker, University of Kansas, February 1-28, 1993

Graduate Research Assistants:

a. Zhang, Y.--October, 1992-September, 1993

Part I. Highlights of major research accomplishments

a. Structural studies in Grapevine Mountains, Funeral Mountains, Bullfrog Hills, and Bare Mountain

b. Publication of manuscript on Mesozoic thrust belt by S.J. Caskey and R. A. Schweickert in Tectonics

c. Publication of abstract based upon research funded under Task 5: Zhang and others (1993 GSA Reno).

d. Development of structural models for pre-Middle Miocene normal and strike-slip faulting at Bare Mountain (Yang Zhang)

e. Paleomagnetic analysis of Paleozoic and Cenozoic units at Bare Mountain (Yang Zhang, S. Gillette, R. Karlin, and R. Schweickert).

f. Sampling of pegmatites in Bullfrog Hills and Funeral Mountains for U-Pb isotopic analysis (Walker and Schweickert).

g. Review and analysis of Mesozoic structure between eastern Sierra and Nevada Test Site (manuscript in prep.) (Walker and Schweickert)

Part II. *Research projects*

Part II. *Research projects*

This section highlights the research projects conducted by Task 5 personnel.

1. *Regional overview of structure and geometry of Mesozoic thrust faults and folds in the area around Yucca Mountain*; R. A. Schweickert, joined by Doug Walker as Visiting Scientist during February-March, 1993.

The purpose of this study is to provide information about the deep structural geometry of Paleozoic units and their bounding faults, which is necessary both for understanding of Tertiary faults and for the correct formulation of regional tectonic and hydrologic models. It has also provided evidence for a previously unknown strike-slip fault beneath Crater Flat, and for the existence of major pre-Middle Miocene extension in the NTS region. The study has continued with new field work in selected areas and with a synthesis of structural relations in areas both east and west of Yucca Mountain, including the Bare Mountain-Bullfrog Hills-Grapevine Mountains-Funeral Mountains areas. Correlations of Mesozoic fold and thrust fault systems have been reviewed and reevaluated for the entire region from northeast of the Las Vegas Valley shear zone through the NTS and Spring Mountains, from Bare Mountain through the Death Valley region, and from Death Valley to the Eastern Sierra Nevada. New insights are that west-vergent structures, an important element of uniqueness in Snow and Wernicke's recent papers on thrust correlations, are non-unique within the belt; in addition, arguments for a Permian age for the Last Chance thrust system are not compelling and instead a Triassic age is favored by regional evidence.

2. *Kinematic analysis of low and high angle normal faults and strike-slip faults in the Bare Mountain area, study of metamorphic rocks, and comparison of structures with the Grapevine Mountains* Y. Zhang and R. Schweickert

The purpose of this study is to determine the timing and slip directions of high and low-angle normal faults and strike-slip faults exposed at Bare Mountain, which is a direct analogue of the deep structure beneath Yucca Mountain. This will provide better constraints on the

displacement histories of the faults. In addition, metamorphic fabrics have been studied in metamorphic rocks in the northern parts of the mountain and traced to lower grade rocks in the southern part of the mountain. Finally, the development of these structures has been compared with possible analogues in the Grapevine Mountains and the CP Hills to develop firm constraints on the deep structure beneath the Yucca Mountain area.

3. *Evaluation of pre-Middle Miocene structure of Grapevine Mountains and its relation to Bare Mountain.* R. Schweickert and M.M. Lahren

The goal of this project is to establish the Mesozoic and Cenozoic structural geometry and timing of deformation in the Grapevine Mountains, which developed in close proximity to the Bullfrog Hills and Bare Mountain areas, prior to post-10 Ma displacement on the Bullfrog Hills-Boundary Canyon detachment fault. This study has clarified the significance of pre-Middle Miocene and possibly pre-Tertiary extension and detachment faulting on crustal structure in the area between the NTS and Death Valley, and beneath Yucca Mountain. We now have strong evidence for pre-Oligocene low-angle-normal fault displacement on the Titus Canyon fault, and its kinematics seem to have been closely related to the Conejo Canyon fault at Bare Mountain.

4. *Evaluation of paleomagnetic character of Tertiary and pre-Tertiary units in the Yucca Mountain region, as tests of the Crater Flat shear zone hypothesis and the concept of oroclinal bending.* Y. Zhang, S. Gillett, R. Karlin, and R. A. Schweickert.

Paleomagnetic data from various volcanic units at Yucca Mountain show that up to 30° of progressive north-to-south clockwise rotation has occurred since mid-Miocene. These studies are geographically relatively limited; one of the goals of this study has been to expand the data base to various Paleozoic and Mesozoic units to understand the regional variations of magnitude and timing of rotations. Our results on 14 Ma dikes at Bare Mountain show no evidence for vertical axis rotation, indicating that the clockwise rotations to the east must be geographically confined to Yucca Mountain and Crater Flat areas, as predicted by the Crater Flat shear zone

hypothesis. Secondary magnetizations in Cambrian limestones at Bare Mountain and in the Striped Hills suggest the importance of pre-Cenozoic clockwise rotations of the Paleozoic units.

5. *Late Quaternary fault patterns in southern Amargosa Valley, Stewart Valley, and Pahrump Valley.* M.M. Lahren and R.S. Schweickert.

This project has involved the compilation of all available data on the distribution and style of late Quaternary faults in the region, primarily from mapping by Donovan and Hoffard (M.S. Theses completed under Task 5) and USGS mapping. This compilation has revealed evidence for a semicontinuous zone of late Quaternary ffaulting between Pahrump Valley and Yucca Mountain. Field checking of certain key areas is required.

Part III.

Brief summaries of research results during FY 1993

This section presents a summary of progress to date. Because these projects are long-term and field-intensive, the results are still preliminary, and should not be quoted without permission. Many of our interpretations are speculative.

1. *Quaternary fault patterns and basin history of Pahrump and Stewart Valleys, Nevada and California.* (No new work was performed on this project in 1992-93; effort was expended instead on paleomagnetic tests of strike-slip fault hypothesis). See Task 5 1991-92 final report for summary of this project.

2. *Regional overview of structure and geometry of Mesozoic thrust faults and folds in the area around Yucca Mountain.* R. A. Schweickert.

(See reprint by Caskey and Schweickert; Appendix 1). A new manuscript is in preparation by Walker, Schweickert, Lahren, and others.

3. *Evaluation of pre-Middle Miocene structure of Funeral and Grapevine Mountains and its relation to Bare Mountain.* R. Schweickert and M.M. Lahren. (see Figure 3).

New field studies in 1993 were concentrated in the Bullfrog Hills

and the Funeral Mountains at Monarch Canyon. Samples were taken of pegmatite and granitic orthogneiss in the Bullfrog Hills for U-Pb zircon age analysis to determine whether Precambrian rocks exist or whether deformed Cretaceous granitoids exist there as in Monarch Canyon. We are trying to determine whether the metamorphic rocks in the Bullfrog Hills are Precambrian basement or whether they could be metamorphosed Johnnie Formation. The result will have important implications for the extent of denudation by the Bullfrog Hills and possibly older detachments, and this will place constraints on the correlations of normal fault systems.

4. Structural and kinematic analysis of Mesozoic and Cenozoic structures at Bare Mountain. **Yang Zhang**

Upper Precambrian through Mississippian sedimentary strata are well exposed at Bare Mountain, which is a direct analog of the deep structure beneath Yucca Mountain. These rocks are involved in numerous folds, thrust faults, low- and high-angle faults, and strike-slip faults. Thus, Bare Mountain provides an important window into the deep structure of Paleozoic rocks that lie beneath Yucca Mountain. In addition, the development of these structures at Bare Mountain can be compared with possible analogs in the Grapevine Mountain to the west and the CP hill to the east. The purpose of this study is to determine the timing and slip directions of these faults exposed at Bare Mountain

During 1992-93, work continued on geologic mapping and map compilation and synthesis. Compilation of structural maps was done at a scale of 1:24,000, incorporating new mapping and published geologic maps of Bare Mountain. The northern part of Bare Mountain was selected as a key area for larger scale of mapping at 1:12,000. Cross-section constructions interpret the deep structures and reveal the relationships of various faults formed through geologic time. Structural models are approximately half complete. Schematic block diagrams show the interpretation of structural geometry and truncation relationships between Mesozoic thrust faults and pre-Miocene detachment faults.

Both brittle and ductile deformation have been studied and documented along various faults at Bare Mountain, on the basis of field

investigation and micro-structural analysis. Thin-section investigations of structural and metamorphic rocks also have been completed.

Some main conclusions are listed here:

1) Two thrust faults (Mesozoic) existed at Bare Mountain, as shown on the map of Monsen et al. (1992). The Panama thrust is north vergent and the Meiklejohn Peak thrust is south-vergent. North-vergent folds that occur throughout the footwall of the Panama thrust, and south-vergent folds in the footwall of the Meiklejohn Peak thrust are compatible with north-south shortening that resulted from Mesozoic deformation. A south-vergent syncline in the footwall of the Meiklejohn Peak thrust rests on a klippe of the Panama thrust plate. This relationship suggests that the Meiklejohn Peak thrust is younger that the Panama thrust.

2) An older detachment fault (Conejo Canyon Detachment Fault) has been distinguished at Bare Mountain. The detachment fault is exposed in the footwall of the Fluorspar Canyon detachment fault (8-10 Ma) in the northern part of Bare Mountain. The Conejo Canyon detachment fault was responsible for the denudation of amphibolite-facies metamorphic rock at the northwestern end of Bare Mountain. Kinematic and structural data indicate that the Conejo Canyon detachment fault roots to the south. The Wildcat Peak detachment fault exposed in the southern part of Bare Mountain originally was structurally above the Conejo Canyon detachment fault, but kinematic similarities suggest the two top-to-the-south faults may have been related. This higher detachment fault truncated the Panama thrust fault and displaced both hangingwall and footwall blocks of the Panama thrust fault.

3) North-south striking and east-dipping faults fall into different categories, based on structural styles and truncation relationships.

a) Some north-south striking faults exposed in metamorphic rock in the northwest part of Bare Mountain are truncated by the Conejo Canyon detachment fault. They are older faults developed in the footwall of Conejo Canyon detachment fault.

b) Some high angle normal faults exposed in the upper plate of

the Conejo Canyon detachment fault terminate at the detachment fault boundary. They might be syntectonic faults formed during slip along the Conejo Canyon detachment fault.

c) Oblique-slip faults became active with mostly right lateral displacement prior to14 Ma, since most of the faults have not offset 14 Ma dikes. These faults truncated both Mesozoic thrust faults and pre-Miocene detachment faults. They terminate at the Fluorspar Canyon detachment fault at the north end of Bare Mountain. East-side-down oblique displacement implies that rocks in the central part of Bare Mountain have been dropped down from the upper plate of the Conejo Canyon detachment fault. The Conejo Canyon detachment fault roots at depth beneath the southern part of Bare Mountain, thus the Wildcat Peak detachment fault lies structurally above the Conejo Canyon detachment fault.

5. *Evaluation of paleomagnetic character of Tertiary and pre-Tertiary units in the Yucca Mountain region, as tests of the Crater Flat shear zone hypothesis and the concept of oroclinal bending.* S. Gillett, R. Karlin, Y. Zhang, and R. A. Schweickert.

Paleomagnetism is a powerful tool for identifying rotations about both horizontal axes and vertical axes. North-south striking Miocene quartz latite dikes (13.9 Ma) which intruded Paleozoic rocks at Bare Mountain provide an excellent opportunity to constrain the sense of tectonic tilting or rotation of Bare Mountain since middle Miocene times.

Paleomagnetic data (Rosenbaum et al., 1991) from ash flow tuffs at Yucca Mountain demonstrated about 30° of vertical axis rotation (clockwise) over a 25 km north-south extent of Yucca Mountain since emplacement of the Tiva Canyon member (about 13 Ma) of the Paintbrush tuff. Our new paleomagnetic data from the 13.9 Ma dikes at Bare Mountain can provide further insights into interpretation of the rotations at Yucca Mountain.

Oriented samples of quartz latite dikes and wall rocks were collected from Tarantula Canyon (TC) and south of Joshua Hollow (JH) in

the northeast part of Bare Mountain. In the laboratory, specimens from all samples were treated by using progressive thermal demagnetization. Specimens were measured on both a spinner magnetometer and a cryogenic magnetometer in the paleomagnetics laboratory at UNR.

Progressive thermal demagnetization and principal component analysis reveal a stable high temperature component of remanent magnetization that resides in magnetite or hematite in different samples. The stable high temperature components of remanent magnetization are considered to represent the paleomagnetic directions formed during the intrusion and cooling of the dikes. Petrographic investigation indicates that magnetite is a primary phase which crystallized with other igneous minerals. Hematite is a secondary phase in the dike. This is quite common in hydrothermal processes following an igneous intrusion.

The in situ mean magnetization directions from all dikes exhibit negative inclinations that correspond to a Tertiary reversed field. At Tarantula Canyon (Fig. 1), the mean magnetite remanent direction is I=-65.0°, D=189.1° (α_{95}=7.3°, α=69.6); the mean hematite remanent direction is I=-72.0°, D=214.3° (α_{95}=3.9°, α=542.4). Samples from wallrocks 0.5 m away from the dike at TC indicate the remanent magnetization resides in magnetite and yields concordant remanent directions with directions of dikes. The in situ mean paleomagnetic directions from dikes of south of Joshua Hollow (Fig. 2) show steeper inclinations and westerly declinations compared to the dike of TC. The mean magnetite remanent direction is I=-79.1°, D=284.5° (α_{95}=6.0°, α=59.1); the mean hematite remanent direction is I=-69.4°, D=275.4° (α_{95}=11.5°, α α=16.7).

There are two interpretations to explain the differences: The dikes may have formed at different times in same magnetic event and the differences in directions are due to secular variation. Alternatively, the dikes at JH were tilted slightly to the north around a sub-horizontal axis due to post-middle Miocene tectonic activity.

Some conclusions are listed below:

1) A stable high-temperature remanent magnetization resides in both magnetite and hematite in different samples.

2) A Tertiary reversed field is revealed by the mean magnetization direction from dikes and wallrocks.

3) No significant vertical axis rotation of the northeast part of Bare Mountain has occurred since about 14 Ma. Rotations of the Paintbrush tuff at Yucca Mountain along a vertical axis during the Tertiary may thus be limited to Yucca Mountain, and no significant effects were imposed on Bare Mountain. This localized vertical-axis rotation in the Yucca Mountain-Crater Flat area is consistent with the shear zone hypoothesis for Crater Flat.

4) East-west structural trends of Proterozoic and Paleozoic rocks at Bare Mountain are older than the middle Miocene dikes because the dikes have not rotated significantly since intrusion.

Part IV. *Other activities of Task 5 personnel*

1. Technical review of reports for the Center and NWPO

a. Critical review of Department of Energy Yucca Mountain Study Plan 8.3.1.17.4.5, "Detachment faulting at or proximal to Yucca Mountain," submitted in January, 1993.

b. Critical review of Department of Energy Yucca Mountain Study Plan 8.3.1.4.2.2, "Characterization of structural features in the site area," submitted in May, 1993.

2. *Meetings attended in relation to the Yucca Mountain Project and the Center for Neotectonic Studies*

a. Geological Society of America, Joint Meeting of Cordilleran and Rocky Mountain Sections, Reno, Nevada, May 19-21, 1993 (Meeting chaired by R.A. Schweickert, Vice-Chair, Mary Lahren; Co-chair of Field Trip Committee, Mary Lahren; attended by Schweickert, Lahren, and Zhang; see

abstract by Zhang and others)

b. Premeeting fieldtrip planned by Schweickert and Lahren, May 16-18, 1993, to Saddlebag Lake pendant, eastern Sierra Nevada, California; trip cancelled due to heavy winter snows.

3. *Field work*

a. Structural mapping in Bare Mountain, Y. Zhang, November 2-9, 1992

b. Structural analysis in Grapevine Mts., Funeral Mountains, Bullfrog Hills, Bare Mountain--Schweickert, Walker, and Zhang, March 5-7, 1993

4. Professional reports provided to NWPO

none

5. Abstracts published

a. Zhang, Y., Gillett, S. L., Karlin, R.E., and Schweickert, R.A., 1993, Paleomagnetism of the Miocene dikes in Bare Mountain, southwest Nevada (abs.): Geol. Soc. America Abs. with Programs, v. 25, p. 169.

6. Papers published in peer-reviewed literature

a. Caskey, S.J., and Schweickert, R.A., 1992, Mesozoic deformation in the Nevada Test Site region: Implications for the structural framework of the Cordilleran fold and thrust belt and Tertiary extension north of Las Vegas Valley: Tectonics, v. 11, p. 1314-1331.

7. Graduate theses supported by NWPO

a. Zhang, Y., in progress, Structural and kinematic analysis of Mesozoic and Cenozoic structures at Bare Mountain, Nye County, Nevada

Appendix I.

Abstracts and published papers

1. Caskey, S.J., and Schweickert, R.A., 1992, Mesozoic deformation

in the Nevada Test Site region: Implications for the structural framework of the Cordilleran fold and thrust belt and Tertiary extension north of Las Vegas Valley: Tectonics, v. 11, p. 1314-1331. (reprint)

2. Zhang, Y., Gillett, S. L., Karlin, R.E., and Schweickert, R.A., 1993, Paleomagnetism of the Miocene dikes in Bare Mountain, southwest Nevada (abs.): Geol. Soc. America Abs. with Programs, v. 25, p. 169.

FIGURE CAPTIONS

Figure 1. Summary of paleomagnetic data from sites in Tarantula Canyon.

Figure 2. Summary of paleomagnetic data from sites south of Joshua Hollow.

TARANTULA CANYON

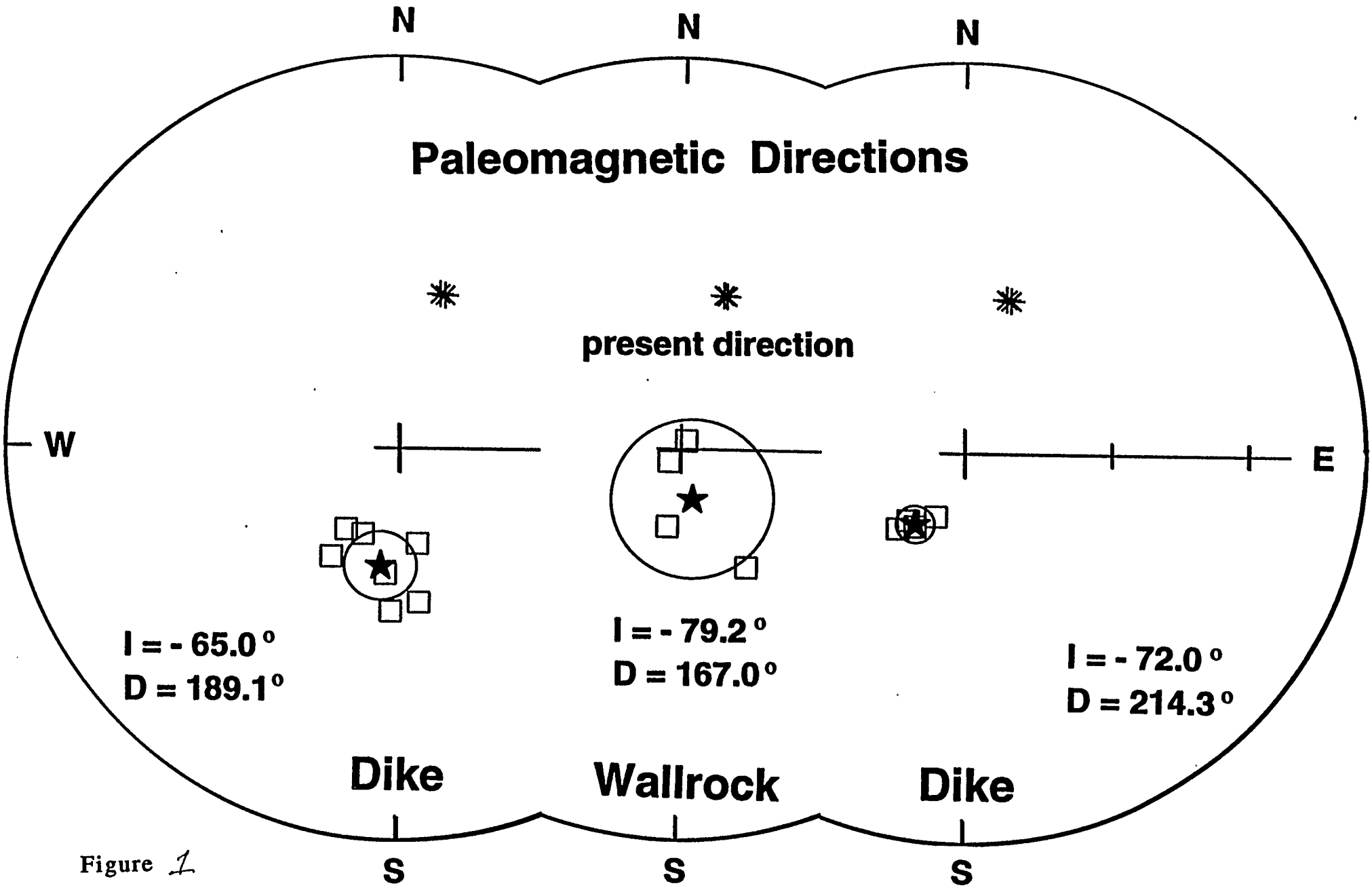

Figure 1

SOUTH OF JOSHUA HOLLOW

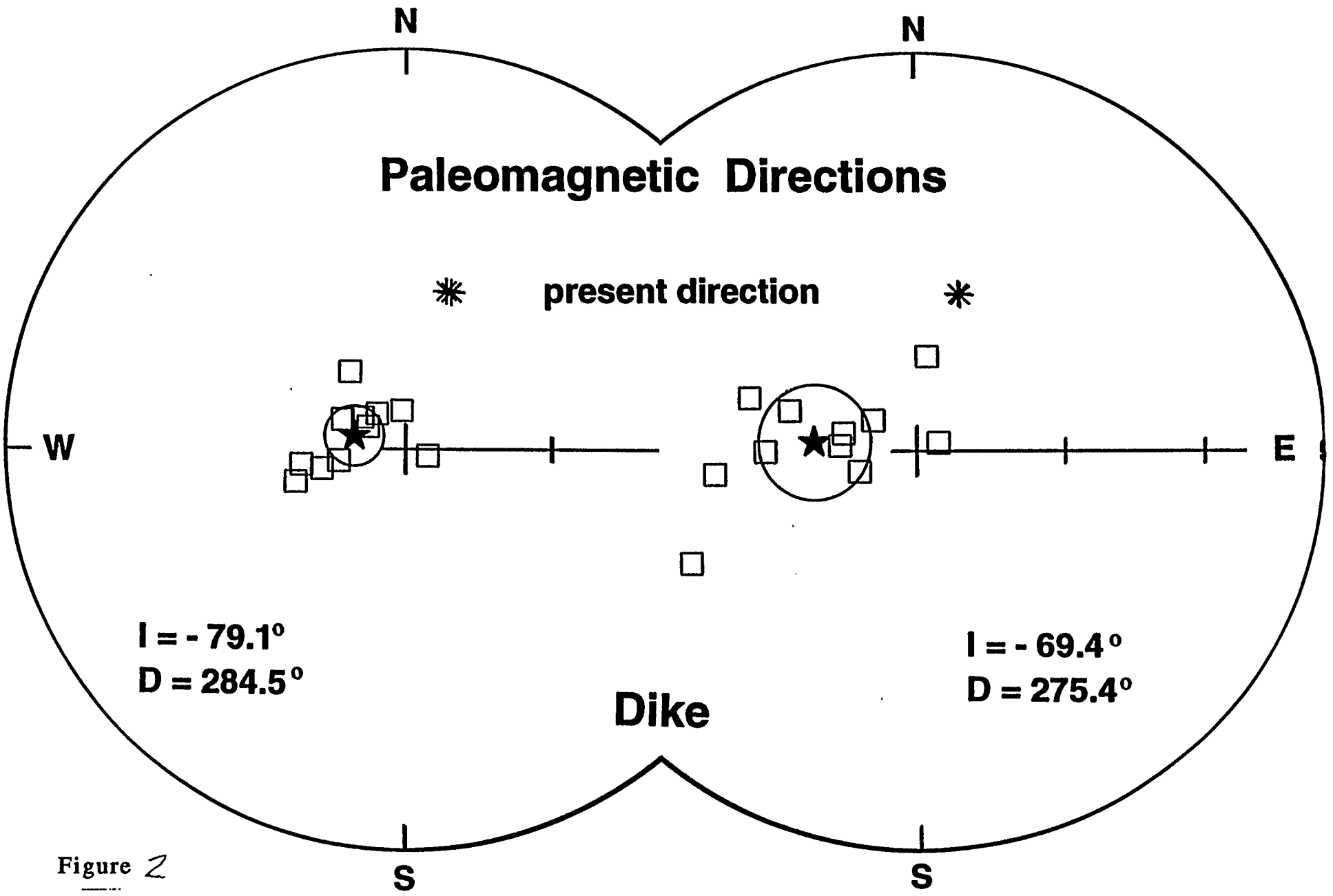

Figure 2

University of Nevada, Reno
Center for Neotectonic Studies

Task 8: Evaluation of Hydrocarbon Potential

Report of Investigations
October, 1992 through September, 1993

Principal Investigators:
Patricia H. Cashman
James H. Trexler, Jr.

EXECUTIVE SUMMARY

Task 8 is responsible for assessing the hydrocarbon potential of the Yucca Mountain vicinity. Our main focus is source rock stratigraphy in the NTS area in southern Nevada. (In addition, Trexler continues to work on a parallel study of source rock stratigraphy in the oil-producing region of east-central Nevada, but this work is not funded by Task 8.) In order to reconstruct the Paleozoic stratigraphy, we are also studying the geometry and kinematics of deformation at NTS. A thorough understanding of the structure will also be essential to predicting the nature of the Late Paleozoic rocks under Yucca Mountain.

Our stratigraphic studies continue to support the interpretation that rocks mapped as the "Eleana Formation" are in fact parts of two different Mississippian units. We are now provisionally limiting the name "Eleana Formation" to the rocks that make up the Eleana Range -- i.e., the rocks that we have been calling "western Eleana". The mudstone section (which we have until now called "eastern Eleana") we are provisionally calling the "Chainman Shale", in keeping with regional lithostratigraphic nomenclature. We continue to work out the internal stratigraphies and basin histories of both units; XRD (x-ray diffraction) determinations of clay mineralogy are an addition to our understanding of the Chainman. The basin histories place important constraints on regional paleogeographic and tectonic reconstructions. This year we have hired a consulting petroleum geologist for two jobs: (1) to review drillhole data from southern Nevada on file at NBMG and make recommendations about more detailed study of any interesting drillholes; and (2) to log the UE17e core (in the Chainman) and evaluate source rock potential. The results of these studies have been incorporated into this report, and the consultant's reports are attached (Appendices 1, 2).

In the last year we have set up a lab to extract conodonts from calcareous rocks, and we continue to extract radiolaria and sponge spicules from siliceous rocks. This has improved our biostratigraphic dating capability, although datable material from the lower (siliciclastic) portion of the Eleana and from the mudstone portion of the Chainman continues to be elusive. More dates tied to measured sections will allow us to refine the basin histories and will aid in regional correlation.

Our structural studies have confirmed the presence of a thrust fault (later reactivated as an extensional fault) in the southern Eleana Range. This fault juxtaposes two laterally equivalent parts of the Eleana Formation. Recognition of the significance of this fault has greatly improved our understanding of the internal stratigraphy of the Eleana Formation -- we now recognize that rocks of the upper plate represent a different (and probably more western) part of the depositional basin than rocks of the lower plate. In contrast to the southern part of the range, the northern Eleana Range appears to be a single, relatively simple, structural block. Continued detailed mapping is necessary to understand both the present surface distribution of Late Paleozoic sedimentary rocks and the geometry, kinematics and relative ages of the various faults that offset them. All of these are necessary in order to predict the subsurface distribution of potential source rocks.

INTRODUCTION

Our studies continue to concentrate on the stratigraphy of Late Devonian through Early Pennsylvanian rocks at NTS, because these have the best potential to be hydrocarbon source rocks. Our work involves structural as well as stratigraphic studies: detailed stratigraphy will identify the extent of potential source rocks, and structural history controls both the maturation and the present structural position of these rocks. This year we have hired a consulting petroleum geologist for two jobs: (1) to review drillhole data from southern Nevada on file at NBMG and make recommendations about more detailed study of any interesting drillholes; and (2) to log the UE17e core (in the Chainman) and evaluate source rock potential. The results of these studies have been incorporated into this report, and the consultant's reports are attached (see Appendices 1 and 2).

This report summarizes new results of our structural, stratigraphic, and hydrocarbon potential studies in southern Nevada. Structure is discussed first, because recognition of structural blocks allows us to understand the details of the stratigraphy. In the stratigraphy section, the Eleana Formation and Chainman Shale are described separately, followed by a depositional history for each, and the implications of these histories for Mississippian paleogeography and tectonics. Directions for future work are included where appropriate in each section. We conclude with a brief summary of implications of these new results for hydrocarbon potential at NTS and vicinity. More detailed discussions of source rock potential of the Chainman Shale in UE17e and of petroleum drillholes in the NTS vicinity (both written by consultant Donna M. Herring) are included as appendices.

STRUCTURAL GEOLOGY

The present distribution of Paleozoic rocks in the Eleana Range and vicinity is governed by (1) Mz(?) thrusting, (2) subvertical, dominantly strike-slip, faulting, and (3) low-angle extensional faulting. The Eleana Range has been mapped as part of a single **thrust** sheet, underlying the Belted Range thrust (of Snow, 1992, and Caskey and Schweickert, 1992) (part of the CP thrust of Barnes and Poole, 1968), by most workers doing regional-scale thrust correlations (e.g., Wernicke and others, 1988; and references cited above), in spite of their differences of opinion regarding other aspects of age, correlation and position of the thrusts. Our mapping has confirmed the presence of a thrust within the Eleana Range (originally mapped by Orkild, 1963) which juxtaposes different parts of the Eleana depositional basin (see below). In addition, we are finding some evidence that the original Eleana/Chainman contact was a low-angle -- presumably thrust -- contact; this would make a second thrust within the Eleana Range. Regional thrusting may have started as early as Permian (Snow, 1992); scattered Cretaceous plutons indicate that most regional-scale thrusting had ended by middle Cretaceous time. A strongly altered dike cuts the Eleana Formation near Captain Jack Spring (see Figure 1); it may be related to the altered 102 Ma

pluton at the bottom of the ER-12-1 drillhole (Cole and others, 1993). Other than this, we have not found any cross-cutting relationships within the Eleana Range to constrain the age of the deformation there. **Low-angle extensional faulting** may have started as early as middle Cretaceous (prior to 102 Ma, Cole and others, 1993); and some extensional faulting was active during Redrock Valley tuff time (ca. 16 Ma, Cole and others, 1991). At least some of the **strike-slip faulting** we have mapped in the southern Eleana Range pre-dates the Redrock Valley Tuff. Nearby, at the north end of Mine Mountain, strike-slip faulting is the most recent deformational event, post-dating the major extensional faulting (Hudson and Cole,1993; and M. Hudson, pers. comm., 1993).

The northern part of the Eleana Range (from Red Canyon north) is a single, generally homoclinal, structural block (Figure 1). The Eleana Formation strikes northeast and dips southeast, exposing lower parts of the section farther north in the (north-trending) range. At the northwestern edge of the range, in the eastern flank of Tongue Wash, the Eleana Formation is folded into chevron-style folds which are locally overturned, apparently due to the emplacement of the Belted Range thrust. Devonian dolomites in a horse of the Belted Range thrust system are exposed in the western flank of Tongue Wash. (Note that the ER-12-1 drillhole spudded in the dolomites of this horse; see reference to this drillhole, below.) In the northern Eleana Range, rocks of the Eleana Formation crop out in the pediment east of the range front; this presents a marked contrast to the southern half of the range, where the range front coincides with the Chainman/Eleana contact. The Chainman Shale is present in drillholes in Yucca Flat, well east of the northern Eleana Range (Jim Cole, pers. comm., and unpublished well logs from Areas 2, 4, and 8), and along the range front as far north as 1 km north of Red Canyon, where the Eleana/Chainman contact jogs east. This geometry is consistent with a low-angle contact, with the Eleana overlying the Chainman, north of the eastward jog.

The homoclinal Eleana section continues into the southern part of the Eleana Range, where it forms the lower of two structural blocks separated by a low-angle fault (Figure 1). The fault was recognized by Orkild (1963), and interpreted to be a thrust fault. Our mapping supports a thrust origin, based on the presence of a hanging-wall anticline , the fault orientation and the stratigraphic contrast across the fault. The offset along this thrust is significant -- it has juxtaposed two different parts of the Eleana depositional basin (see below). The deformation fabric along the thrust (brecciation, iron staining, and polished, striated surfaces) suggests that it has been reactivated as an extensional fault. The extent and age of the extensional faulting are not yet known.

The structure of the southern Eleana Range is further complicated by high-angle faulting; this faulting often represents the Eleana/Chainman contact in this part of the range. The southern Eleana Range is bounded on the east by a poorly exposed, high-angle fault which juxtaposes Eleana Fm with Chainman Shale. The structural contact closely corresponds with the topographic break between the range and the pediment bordering it to the east. In the few places where this contact is exposed, it is vertical and north-striking, but the present distribution of the two units is

too complex to be explained by a single fault surface. Several (at least four) sub-parallel faults of this north-striking system have been mapped in the southern Eleana Range, within a lateral (east-west) distance of 2 km. The orientation of the faults, and small-scale structures on the slip surfaces (mullions and striations), are consistent with primarily strike-slip motion. However, there is also systematic steepening of bedding in the Eleana Formation adjacent to the faults, which is consistent with a relatively small amount (tens of m) of W-over-E motion. This probably represents a later, relatively small, compressional reactivation of the fault surface.

A recent 3500' drillhole (ER-12-1) in Tongue Wash (Figure 1), immediately west of the north end of the Eleana Range, exhibits structure that is dramatically different from that seen at the ground surface in the northern Eleana Range. The following description of the cuttings in this drillhole is from Cole and others (1993), Cole (1993), and personal communication from Jim Cole, of the USGS: The drillhole goes through a complex succession of Paleozoic rocks separated by low-angle faults with substantial stratigraphic offset . The structure has been interpreted as being dominantly extensional in origin, on the basis of similarities in deformational style with surface exposures of extensional faults at NTS. However, earlier thrust faulting is required because the slices of Silurian and Devonian rocks must have been derived from the upper plate of the Belted Range thrust, nearby to the west. All of the rocks have been thermally overprinted following movement on the faults that separate them; the heat source is interpreted to be a 102 Ma intrusion encountered at the base of the hole. If this is the case, the extensional faulting occurred prior to 102.3 $\pm$ 0.5 Ma (middle Cretaceous).

Our future structural studies will continue to unravel the complex structural relationships in the Eleana Range and vicinity, in order to predict the regional subsurface distribution of Mississippian rocks. The structural style seems to change dramatically from range to range in this area -- e.g., there is low-angle extensional faulting in the ER-12-1 drillhole and at Mine Mountain, but thrust faulting and strike-slip faulting seem to dominate in the Eleana Range -- so detailed mapping will continue to be necessary.

STRATIGRAPHY

Eleana Formation

The Eleana Fm has general stratigraphic characteristics that are common to both thrust plates; differences in details between the two plates provide some important insights into the geometry and paleogeography of the Eleana basin (Trexler and Cashman, 1993). The lower part of the Eleana Fm is a siliciclastic submarine fan deposit. Rocks in the lower part are typically chert litharenites, locally interbedded with conglomerates or with finer-grained sediments. Clasts in the conglomerates are primarily chert, quartzite and other clastic sedimentary rocks; limestone clasts and basalt clasts occur locally. The siliciclastic submarine fan is overlain by a carbonate

submarine fan with interbedded spiculite and shale. No datable material has been found in the siliciclastic turbidites, but limestones from carbonate turbidites in both thrust plates are early Chesterian in age.

The lower plate of the thrust has: (1) a poorly exposed lower section of sandy turbidites, (2) a middle section of channel turbidites interbedded with interchannel fines, and (3) an upper section of carbonate turbidites with thin spiculites and shales (Figure 2). The fan channel turbidites are characterized by amalgamated turbidites and conglomerates in broad lenses and lack of pelagic interbeds; this is typical of mid-fan axis. Paleocurrents are strongly bimodal -- from the northeast and the west-northwest -- with very little spread (Figure 2). Paleocurrent indicators from the northeast include flutes, grooves, etc., and are typical of higher energy currents than those from the west-northwest. Heterolithic conglomerates (those containing basalt clasts) occur exclusively in sediments derived from the west-northwest. This suggests that the fan was a "trough" that filled both axially (from a siliclastic source to the northeast) and laterally (from a heterolithic source to the west-northwest). The overlying carbonate turbidite section documents a shift in provenance from siliciclastic to carbonate; this shift is a time marker throughout the Eleana, and occurred in lower Chesterian time (zone 16). The carbonate turbidite section is characterized by coarsening-and-thickening-upward architecture typical of mid to outer fan lobes. Overall, the lower plate section represents a waning fan sequence, with mid-fan channels giving way upward to mid-outer fan lobes with the sediment derived from an organically productive shelf. This shelf may have been to the north and east, based on the better-developed and thicker lobe sequences in the lower plate (which we interpret to have been deposited east of the deposits in the upper plate).

The upper plate of the thrust has: (1) a thick, fan-channel sequence with very coarse turbidites and little fine material, fining upward to (2) spiculitic cherts and a few thin carbonate turbidites (Figure 3) (Trexler and Cashman, 1993). The fan-channel conglomerates are coarse, heterolithic and sandy, with intercalated pebbly mudstone beds. Paleocurrent indicators are bimodal (northeast and west-northwest) (Figure 3). Heterolithic conglomerates are derived from the west-northwest, and appear in the section lower than they do in the lower plate (Figure 4); this supports our interpretation that the lower plate was deposited west of the upper plate. The upper cherty section is usually deformed, and there is evidence that at least some of the deformation is pre-lithification. Individual beds in this interval are often graded; the grains are crinoid fragments and other organic debris. The fine portions of the graded beds are dominated by spiculites (made of sponge spicules and radiolaria) rather than clastic mud. The spicules are characteristic of sponges from two different depths, but even the "deeper" sponges probably were not from more than 150-200m depth (B. Murchey, written comm., 1993). We interpret this section as representing an axial submarine fan sequence, which was gradually abandoned upward. The upper section represents distal submarine fan sediments, dominated by organic debris from a productive shelf. As in the lower thrust plate, the shift in provenance is very apparent, and the timing of the shift (early Chesterian) is identical in both plates.

The two thrust sheets represent different parts of the Eleana basin and submarine fan system, now structurally stacked. Important features from the stratigraphy of the two thrust sheets which bear on the geometry and paleogeography of the Eleana depositional basin follow (Trexler and Cashman, 1993):

(1) the first arrival of carbonates is a time marker (early Chesterian -- zone 16) in both sections;

(2) the upper plate represents a more central position on the fan;

(3) volcanic detritus (derived from the west) arrived much earlier in the upper plate;

(4) the lower plate contains thicker, better developed lobe sequences in the carbonate turbidite section, and hence seems to have been closer to the carbonate production area.

We interpret the upper plate strata to be foreland "keel" deposits, transported eastward on the thrust. Lower plate strata are lateral, off-axis deposits, deposited closer to the carbonate production area.

Chainman Shale

The Chainman Shale is characteristically poorly exposed; the following description is therefore based on a 3000' core from drillhole UE17e at the north end of Syncline Ridge. This core was logged for Task 8 by a consulting petroleum geologist; her complete report is included as an appendix. It is possible to combine the core with surface exposures near the drill pad to see the top of the Chainman and its contact with the overlying Tippipah Limestone, but we do not see the base of the Chainman in the core -- there is an undetermined additional thickness below the sampled interval. The core can be divided into two units – a lower mudstone section (3000' - 241') and an upper section of siltstone, fossiliferous carbonate and interbedded mudstone (241' - 0'). Age data from the mudstone section in the Chainman at NTS are limited to palynology, and suggest a middle Mississippian (Osage - Meramec) age. Age data from the upper section are both macrofossils and forams, and indicate a latest Mississippian - earliest Pennsylvanian age. (See previous Task 8 reports for sample locations and specific paleontology results.)

Most of the core is gray to black mudstone, characterized by lack of bioturbation, preservation of organic detritus and evaporitic mineral assemblages. Even within the monotonous mudstone, there are changes in: color (black may be indicative of higher organic content); pyrite content (indicative of euxinic conditions); swelling clays (probably indicative of a volcanic sediment source); and development of parting (indicative of rate of deposition). Bedding-parallel lamination or parting is the only primary structure in most of the core; rare silty horizons may exhibit starved ripples and/or soft-sediment deformation. There are two thick zones of apparent anoxic deposition, at 900' - 1600' and at 1900' - 3000'. These zones contain unfossiliferous grayish black mudstone with a high percentage of pyrite nodules, interbedded with black mudstone. Shale samples have been sent out for organic carbon content (TOC) and thermal maxima (T_{max}) analyses, but we have not received the results. Multiple diagenetic events are evident in thin section, including episodic veining, stylolitization

and replacement/recrysallization. Vein-carbonate samples have been collected for fluid inclusion analysis -- to determine temperature of crystallization and hydrocarbon association.

X-ray diffraction (XRD) analysis of four samples from the mudstone section shows that clay mineral composition changes with depth (Herring and others, 1993; also, see Appendix 1). Minerals present include fine-grained quartz, smectite, kaolinite, illite and illite/smectite, pyrophyllite, and chlorite. The clay mineral fraction is dominated by interlayered illite/smectite, and in addition shows two compositional trends with depth: (1) interlayered kaolinite/chlorite, present in the upper samples, is replaced by chlorite with depth; and (2) pyrophyllite is present at and below depths of 677'. Both of these are probably provenance-controlled. These compositional changes may be useful for correlation of surface exposures to the cored interval, but more closely spaced samples will be necessary to confirm the trends and to recognize or rule out structural complications.

The presence of smectite provides some interesting paleogeographic information: Smectite is formed from the alteration of volcanic rocks and glass, or from soil processes in temperate climates. Preservation of smectite is dependent on (1) original abundance, (2) pore fluid conservation, and (3) shallow to moderate burial (less than 2000m). The amount of smectite preserved in the Chainman in the UE17e core seems to require a volcanic source, and suggests that the continental margin setting in which the Chainman was deposited was leeward of the continent and within a distal ejecta plume (Herring and others, 1993).

The upper unit is a coarsening-upward, shallow-water sequence of siltstone, sandstone and fossiliferous limestone interbedded with black mudstone. It contains clean, cross-bedded sands, laminated and cross-bedded siltstones, minor silty/sandy limestone, and shales with swelling clays. Fossiliferous horizons and local strong bioturbation indicate that the water column was well oxygenated and well mixed at the time of deposition. Surface exposures of three laterally continuous sandstone beds (along the Pahute Mesa Rd.) have primary structures that document increasing energy (and possibly shallowing) upward in the section. Paleocurrents determined from cross-lamination are variable, ranging from SE to WNW, but generally indicate sediment transport toward the south or west. Sandstones from the Chainman are quartz arenites. These sandstone compositions support the paleocurrent evidence that the sediments were derived from the craton; there is no petrographic evidence of sand derived from the Antler allochthon.

Although many details about the depositional environment of the Chainman Shale are still unclear, the general basin history represented is one of relatively quiet deposition in a shallowing-upward basin, and of sand derivation from a continental source. There is no indication in the Chainman stratigraphic record of the tectonic event (signalled by the abrupt provenance change at early Chesterian time) that is recorded in the Eleana Formation.

HYDROCARBON POTENTIAL

Our studies that pertain most specifically to hydrocarbon potential have focussed primarily on the presence of potential source rocks, and second, on the thermal history of these rocks. Of the two Mississippian units present, the Eleana can probably be ruled out as a source rock, but the Chainman continues to show potential.

Petroleum geologist Donna M. Herring is now logging the UE17e core in detail (see Appendix 1). Preliminary analyses from this core, based on fairly random sampling, showed poor to adequate organic carbon content (TOC), and slightly high maturity (see previous Task 8 reports). Shale samples taken systematically from this core by Herring have been sent out for organic carbon content (TOC) and thermal maxima (T_{max}) analyses. When we receive the results and combine them with the lithologic log, we will have a better estimate of the percentage of the Chainman that is potential source rock. At least one other core of the Chainman, and cuttings from several additional drillholes, are also available; these will constrain estimates of the volume and extent of the potential source rock.

Maturation data obtained to date are mostly TAI values, and they are anomalously high compared to conodont CAI values from nearby surface samples from the Tippipah Limestone at Syncline Ridge. TAI values are reorted to be unreliable in lean source rocks (D. Herring, pers. comm., 1993), so we are attempting to get an independent temperature from the UE17e core. Herring sampled a coarse calcite vein for fluid inclusion analysis to determine the temperature of crystallization. She also sampled the adjacent mudstone for TAI analysis. The results will be instructive, both for the temperature history of a particular part of the UE17e core, and for an idea of the validity of TAI values from these rocks.

FIGURE CAPTIONS

Figure 1: Simplified map of the western side of Yucca Flat, showing the locations mentioned in the text. Paleozoic rocks are shaded; within the Eleana Range, rocks from the upper plate of the thrust are shown in a darker color. Circles show approximate locations of drill holes mentioned in the text.

Figure 2: Composite stratigrahic section of the Eleana Formation in the lower thrust plate, based on measured sections at Red Canyon and Captain Jack Spring. The tie line is the first arrival of carbonate detritus; this contact is mappable between the two measured sections.

Figure 3: Composite statigraphic section of the Eleana Formation in the upper thrust plate, based on measured sections in the southern Eleana Range and at East Ridge. The tie line is the first arrival of carbonate detritus; this contact is readily identifiable in both measured sections.

Figure 4: Comparison of composite sections from the upper and lower thrust plates; first arrival of carbonate detritus is synchronous in the two sections. Note the contrast in first arrival of heterolithic conglomerates between the two sections.

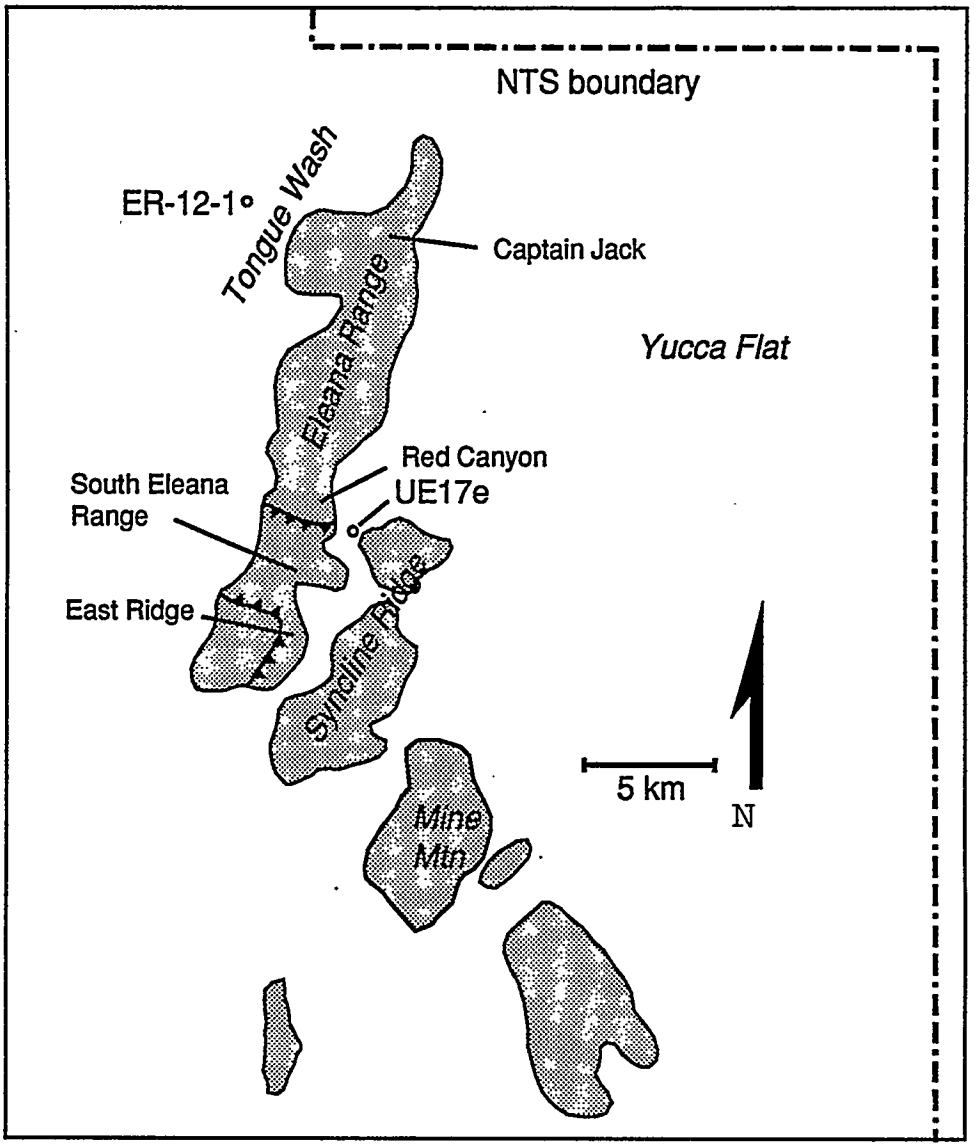
NTS boundary
ER-12-1
Tongue Wash
Captain Jack
Eleana Range
Yucca Flat
Red Canyon
UE17e
South Eleana Range
East Ridge
Syncline Ridge
5 km
N
Mine Mtn

Figure 1

Figure 2: LOWER PLATE STRATA

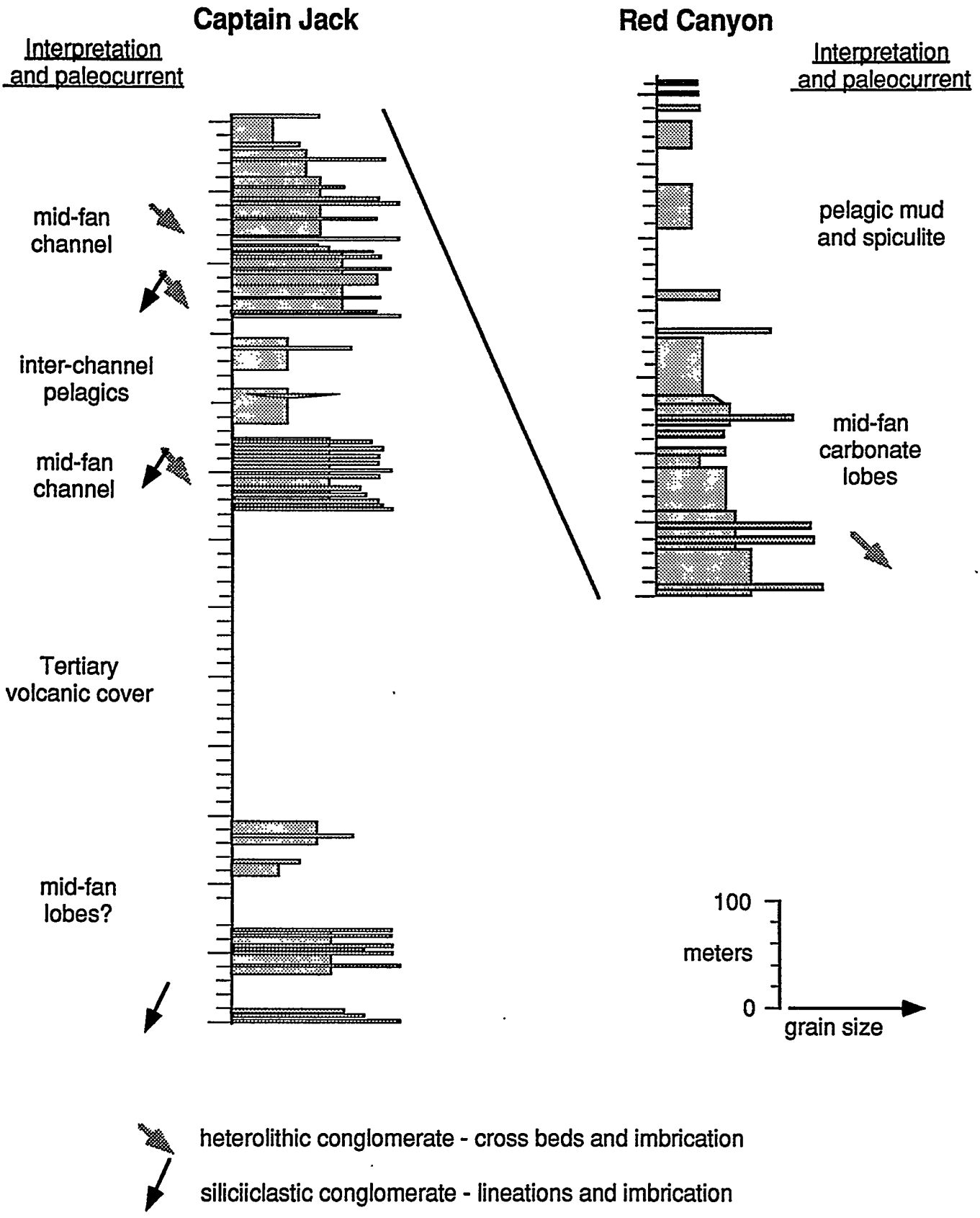

Figure 3: UPPER PLATE STRATA

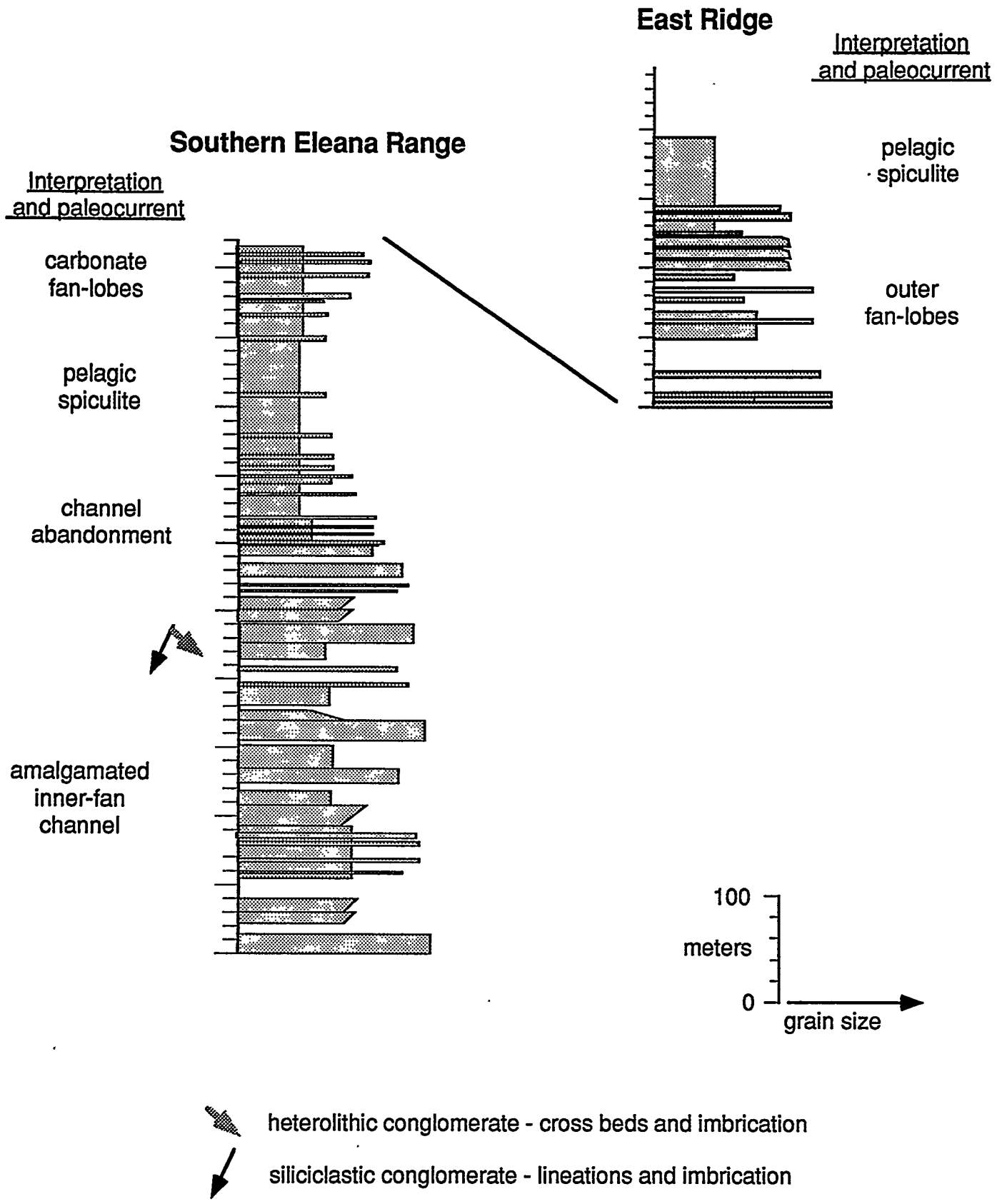

LOWER PLATE
UPPER PLATE
* first arrival of carbonate detritus
+ first arrival of volcanic detritus
*
+
*
+

Figure 4

REFERENCES CITED

Caskey, S.J. and Schweickert, R.A., 1992, Mesozoic deformation in the Nevada Test Site and vicinity: implications for the structural framework of the Cordilleran fold and thrust belt and Tertiary extension north of Las Vegas Valley: Tectonics, v. 11, no. 6, p. 1314 - 1331.

Cole, J.C., Harris, A.G., Lanphere, M.A., Barker, C.E., and Warren, R.G., 1993, The case for pre-middle Cretaceous extensional faulting in northern Yucca Flat, southwestern Nevada (abs.): Geol. Soc. America Abs. with Prog., v. 25, no. 5, p. 22.

Cole, J.C., 1993, Stratigraphy, structure and thermal history of rocks penetrated by well ER-12-1: unpublished ER-12-1 completion report, USGS studies, 12 p.

Herring, D.M., Trexler, J.H., Jr., and Cashman, P.H., 1993, Evidence for local volcanism in Mississippian continental margin strata in southwestern Nevada, Nevada Test Site (abs.): Geol. Soc. America Abs. with Prog., v. 25, no. 5., p. 51.

Hudson, M.R., and Cole, J.C., 1993, Kinematics of faulting in the Mine Mountain area of southern Nevada: evidence for pre-middle Eocene extension (abs.): Geol. Soc. America Abs. with Prog., v. 25, no. 5., p.55.

Orkild, P.P., 1963, Tippipah Spring quadrangle: U.S.G.S. map GQ-213, 1:24,000.

Snow, J.K., 1992, Large-magnitude Permian shortening and continental-margin tectonics in the southern Cordillera: Geol. Soc. America Bull., v. 104, no. 1, p. 80 - 105.

Trexler, J.H., Jr. and Cashman, P.H., 1993, Geometry and depositional history of the southern Antler foreland basin, Eleana Formation, Nevada Test Site (abs.): Geol. Soc. America Abs. with Prog., v. 25, no. 5., p. 156.

Wernicke, B.P, Snow, J.K. and Walker, J.D.,1988, Correlation of early Mesozoic thrusts in the southern Great Basin, and their possible indication of 250-300 km of Neogene crustal extension: *in* Weide, D.L. and M.L. Faber (eds.) This Extended Land: Geological Journeys in the southern Basin and Range: Geol. Soc. America, Cordilleran Section, Field Trip Guidebook, p. 255 - 267.

HYDROCARBON POTENTIAL OF THE UE17e CORE HOLE, NEVADA TEST SITE:

Interim Report

TABLE OF CONTENTS

• Donna M. Herring • P.O. Box 13652, Reno NV 89507-3652 • (702) 786-5620 •

HYDROCARBON POTENTIAL OF THE UE17e CORE HOLE, NEVADA TEST SITE: Interim Report

EXECUTIVE SUMMARY

Core of the Chainman Formation from NTS drill hole UE17e was examined for hydrocarbon source rock potential; secondarily, the sedimentology and stratigraphy of the core was considered, relative to predictability of source facies laterally from the borehole.

The Chainman in UE17e appears to be an adequate hydrocarbon source rock, based on apparent marginal organic carbon content and high maturity. Chainman in nearby outcrop exposures is lower in thermal maturity than in UE17e, suggesting that locally within the NTS area the Chainman may be an excellent to good source rock.

Two thick, apparently anoxic zones in the Chainman of UE17e might be correlatable to outcrop, and appear to be sedimentologically-typical of hydrocarbon source rock facies. Estimation of the volume and extent of these zones is significant to predicting the hydrocarbon source rock potential of the Chainman in and near the NTS area.

Further study might include detailed mineralogy of the anoxic and other mudstone zones, detailed organic carbon content, and detailed diagenetic study. Compilation of a graphic log showing descriptive lithologic variation compared to all other analyses is recommended.

INTRODUCTION AND METHODS

Nearly three thousand feet of core from Nevada Test Site (NTS) drill hole UE17e was examined in the U.S.G.S. Mercury Core Library, under subcontract to Principal Investigator Dr.

• Donna M. Herring • P.O. Box 13652, Reno NV 89507-3652 • (702) 786-5620 •

Patricia H. Cashman; focus of this investigation was hydrocarbon source rock potential. The cored interval (10-3000') was initially described as Mississippian Eleana Formation, Unit "J", and is presently considered to be Mississippian Chainman Formation (Trexler and Cashman, 1993).

Methods of investigation included: A) visual description of water-wet whole core and core chips; B) selected interval reflected-light microscopy (to 30x) of coarsely-crushed chips including reaction with cold and hot hydrochloric acid, plus ultraviolet fluorescence both dry-crushed and reacted with naphtha; C) collection of 50 whole-core samples and 120 core-chip samples for later examination and analysis; D) cursory transmitted-light thin-section petrographic examination of 25 of the sampled whole-core intervals; E) X-ray diffraction analysis, including bulk mineral and glycolated clay mineral analyses, of six of the collected samples; F) review of the drill hole wellfile, including drilling records, engineering tests and wireline logs; and, G) review of reports of biostratigraphic analyses of UE17e samples and biostratigraphic and geochemical analyses of nearby outcrop samples.

Note that one foot of every ten-foot core interval was unavailable for description because of wax coatings, and that many core intervals have had one to three additional feet of core previously removed for various engineering and other destructive testing. The following description and analysis is therefore necessarily incomplete relative to the entire core interval.

Thirty-six core or core-chip samples were recommended for organic carbon and Rock-Eval pyrolysis, including 25 collected for this study and 11 previously collected for conodont analysis by the Principal Investigator. Three samples were recommended for fluid-inclusion analysis, which has not yet been contracted. The organic carbon and Rock-Eval test results are not available as of this writing.

Two facets of the Chainman in UE17e were considered relative to its hydrocarbon source rock potential. The primary, critical components are the specific hydrocarbon indicators of the core itself. Secondarily, the sedimentologic and stratigraphic characteristics of the core can be used to extrapolate results of this study laterally into the NTS area.

DISCUSSION: HYDROCARBON INDICATORS

Specific hydrocarbon source rock potential of the cored interval was the focus of the investigation. Evaluation of source rock potential included consideration of: A) amount of organic carbon in the unit, B) type of organic carbon present, and C) maturity of the organic matter (Barker, 1979). Amount, type, and maturity of contained organic matter were then considered together to determine whether the unit is an economically-significant source rock (Figure 1). Of additional interest is whether any generated hydrocarbons have migrated or are presently migrating, and whether migrated hydrocarbons have nearby traps in which to accumulate.

As noted above, none of the 36 samples sent for organic carbon and Rock-Eval pyrolysis from UE17e have yet returned results. Nearby analyses from outcrop (Micro-Strat Project No.MSI 89-52, p.8; samples 3-89-SN-842, 3-89-SN-874, and 3-89-SN-881; Micro-Strat Project No.MSI 90-15, p.11, sample 4-89-SN-1113) indicate the Chainman ranges from 0.42% total organic carbon (TOC) to 1.16% TOC, with an average for the four samples of 0.8% TOC. Most workers conclude that a rock containing 0.5% TOC is capable of oil or gas production, given correct temperature, time and pressure conditions (Tissot and Welte, 1978).

Black and dark gray color in fine-grained rocks is also directly associated with high organic carbon content (Figure 2),

and the predominance of dark gray and black rocks in the cored interval suggests TOC greater than 0.5% for much of the section and greater than 1.5% for some of the section. However, anomalously-high molal ratios of Fe2+ to Fe3+ also cause dark color in fine-grained rocks (Potter et al, 1980), and several bulk chemical analyses in the wellfile suggest this is a contributing factor for color in at least part of the Chainman of UE17e.

Amount of organic carbon in the total Chainman interval of UE17e can be inferred from statistical treatment of the TOC/Rock-Eval results from the 36 samples when they are received. This estimate of organic content could then be combined with outcrop TOC sample results and with stratigraphic indicators (discussed below) to infer the volume of organic carbon in the Chainman of the greater NTS area.

Type of organic carbon in the Chainman cored in UE17e varies with depth. Five samples previously analyzed for palynological age dates (Micro-Strat Project No.MSI 91-06, pp.8-11, samples UE17e-192, UE17e-602, UE17e-991, UE17e-1889, and UE17e-2993) also characterized kerogen, with equivalent gas-prone Type II and Type III kerogen more common in the sample from 192', and equivalent oil-prone Type II and Type I kerogen more abundant in all the deeper samples. From these analyses, it appears the majority of the sampled Chainman section has oil-prone kerogen.

Maturity of the organic carbon in the Chainman of UE17e was estimated by Micro-Strat (MSI 91-06 samples noted above) based on the Thermal Alteration Index (TAI) of amorphous kerogen. The shallowest sample, from 192', was within the oil generation window (TAI 3+), and the deeper samples were generally beyond generation but within preservation limits (TAI 3+ to 4-), with the exception of the sample from 602' which was within the zone of oil conversion to gas (TAI 4- to 3+). Vein-carbonate samples have been collected from UE17e for fluid-inclusion analysis of

temperature and hydrocarbon association. Nearby outcrop samples (MSI 89-52 samples noted above) had Rock-Eval maximum pyrolysis temperatures (Tmax) of 439°C, which is just within onset of oil generation, and 336°C, which is immature and precludes any previous episode of hydrocarbon generation.

Together, the indices of apparent adequate amount of organic carbon and appropriate kerogen for oil generation are favorable for the Chainman in the core hole UE17e to be an adequate source rock, active in part and spent in part. Further analytical results would be required to estimate volumes of organic carbon in the total core and to extrapolate this estimate accurately, based on stratigraphic work, into the NTS area.

Maturity data from the core and nearby outcrop show that local anomalies in temperature gradient exist. Investigation of these anomalies is significant to estimating the volume of potential oil generation in the Chainman: immature, organic-rich Chainman is capable of generating much more oil than is near-overmature, partially-depleted Chainman.

DISCUSSION: SEDIMENTOLOGY & STRATIGRAPHY

Salient sedimentologic and stratigraphic features were noted during examination of the core (Appendix B), and a pre-existing sample log was available from the wellfile for comparison. Previous workers described three units of the Eleana Unit J: a quartzite subunit, an argillite subunit, and a lower subunit (see Hodson and Hoover, 1979). The UE17e core cuts most of the quartzite subunit (depths 10-241') and most of the argillite subunit (depths 242-3000'). The quartzite subunit is a coarsening-upward shallow-water sequence of siltstones, sandstones and fossiliferous carbonates with interbedded dark swelling clays, which as a whole has little to no source rock potential.

The argillite subunit generally consists of unfossiliferous dark gray and black mudstones and occasional shales, with common zones of veining and of crushed, slickensided, and/or fractured rubble. Thin-bedded laminated siltstones occur sparsely, with the thickest zone of siltstones occurring at 1657.4-1663.5'. Most of the siltstones include convolute slumped bedding and microfaulting, indicating deformation while soft or partially-lithified. Rare starved-ripple silts occur in the lower part of the hole, and a few apparent veins may be completely re-crystallized starved ripples. Cursory examination of 25 thin sections confirmed multiple diagenetic events including episodic veining, stylolitization and replacement/recrystallization.

The mudstones and shales of the argillite subunit contain relatively high percentages of fine quartz and swelling clays, varying with depth (Figure 3; see also Hodson and Hoover, 1979). X-ray diffraction (XRD) was used to determine clay mineralogy of six samples; results (Appendix C) suggest that illite/smectite and pyrophyllite, and possibly chlorite, may be useful tools for the correlation of outcrop intervals to the cored interval. The uneven distribution and specific mineralogy of the swelling clays (Figure 3) suggests an airborne volcanic-debris source is possible (Herring et al, 1993). Matrix mineralogy, identified with crushed-sample reflected-light microscopy and acid and naphtha tests, includes anhydrite, dolomite, other evaporaites and occasionally calcite.

Two thick zones of apparent dominantly-anoxic deposition occur in the argillite subunit, as evidenced by laminated grayish-black mudstone with a high percentage of pyrite nodules and interbedded black mudstone. These anoxic zones occur over the approximate depths of 900-1600' and 1900-3000' in the core, and appear to represent a typical depositional environment of hydrocarbon source rocks: fine-grained sedimentation,

relatively deep water and probable restricted circulation (Tissot and Welte, 1978). Restricted circulation is further evidenced by the matrix mineralogy noted above. The thickness of the anoxic zones (even when corrected for steeply-dipping bedding in the core) suggests these facies may be widespread in the NTS area.

Wireline log character of the argillite subunit rocks includes essentially no distinctive easily-correlatable changes in curve amplitude through the cored interval, though some subtle patterns in curve shape are discernable. These curve shape patterns might be useful for correlation of the anoxic zones to other NTS area holes.

CONCLUSIONS

The Chainman in UE17e appears to be an adequate hydrocarbon source rock, based on apparent marginal organic carbon content and high maturity. However, specific reports of organic carbon and thermal maximums on core and chip samples sent for analysis earlier this year have not yet been received. Chainman in nearby outcrop exposures is lower in thermal maturity than the Chainman in drillhole UE17e, suggesting that locally within the NTS area the Chainman may be an excellent to good source rock.

Two thick, apparently anoxic zones in the Chainman of UE17e might be correlatable to outcrop, and appear to be sedimentologically-typical of hydrocarbon source rock facies. Estimation of the volume and extent of these zones is significant to predicting the hydrocarbon source rock potential of the Chainman in and near the NTS area.

Further study of the hydrocarbon potential of the NTS-area Chainman would benefit from correlation and prediction of the anoxic zones of UE17e laterally into the surrounding area. Characteristics of the UE17e core which would aid in correlation

include detailed mineralogy of the anoxic and other mudstone zones, detailed organic carbon content, and detailed diagenetic study. Specific work on UE17e core to accomplish the correlation and prediction would include reflected-light microscopic examination of crushed chip samples already collected, transmitted-light microscopic examination and description of existing thin sections, correlation of existing XRD (and expected XRD, TOC and fluid inclusion) analyses to wireline logs if possible, and compilation of a graphic log showing descriptive lithologic variation compared to all other analyses.

Donna M. Herring
Petroleum Geologist
Certified Professional Earth Scientist
(D.M.H. Flanigan)

REFERENCES

Barker, Colin, 1979, Organic geochemistry in petroleum exploration: Education Course Notes Series #10, American Association of Petroleum Geologists, Tulsa, Oklahoma, 159pp.

Herring, D.M., J.H. Trexler Jr. and P.H. Cashman, 1993, Evidence for local volcanism in Mississippian continental-margin strata in southwestern Nevada, Nevada Test Site (abs.): G.S.A Abstracts with Programs, v.25 n.5, April 1993, p.51-52.

Hodson, J.N. and D.L. Hoover, 1979, Geology of the UE17e drill hole, Area 17, Nevada Test Site: Nevada Terminal Waste Storage-2 paper, U.S.G.S.-1543-2, 35pp.

Potter, P.E., J.B. Maynard and W.A. Pryor, 1980, Sedimentology of Shale: Springer-Verlag, New York, 310pp.

Tissot, B.P. and D.H. Welte, 1978, Petroleum Formation and Occurrence: Springer-Verlag, New York, 538pp.

Trexler, J.H. Jr. and P.H. Cashman, 1993, Geometry and depositional history of the southern Antler foreland basin, Eleana Fm., Nevada Test Site (abs.): G.S.A Abstracts with Programs, v.25 n.5, April 1993, p.156.

Figure 1. Definition chart for hydrocarbon source rocks (Barker, 1979:108).

Table 7.1: Definitions pertinent to source rocks. (Modified after Dow, 1977).

SOURCE ROCK - A unit of rock that has generated and expelled oil or gas in sufficient quantity to form commercial accumulations. The term "commercial accumulations" is by definition, variable.

LATENT SOURCE ROCK - A source bed that exists but is as yet concealed or undiscovered. Usually refers to unexplored areas or deep portions of developed basins.

POTENTIAL SOURCE ROCK - A unit of rock that has the capacity to generate oil or gas in sufficient quantities to form commercial accumulations but has not yet done so because of insufficient thermal maturation.

ACTIVE SOURCE ROCK - A source bed that is in the process of generating oil or gas.

SPENT SOURCE ROCK - A source bed that has completed the process of oil or gas generation and expulsion. A source bed may be spent for oil and active for gas.

INACTIVE SOURCE ROCK - A source bed that was once active but has temporarily stopped generating prior to becoming spent. Usually associated with thermal cooling due to uplift and erosion. Still has some potential left.

LIMITED SOURCE ROCK - A unit of rock that contains all the prerequisites of a source bed except volume. Commonly refers to thin shale laminations in carbonates or thin coals in continental deposits.

Figure 2. Color in shales (Potter et al, 1980:Fig. 1.25).

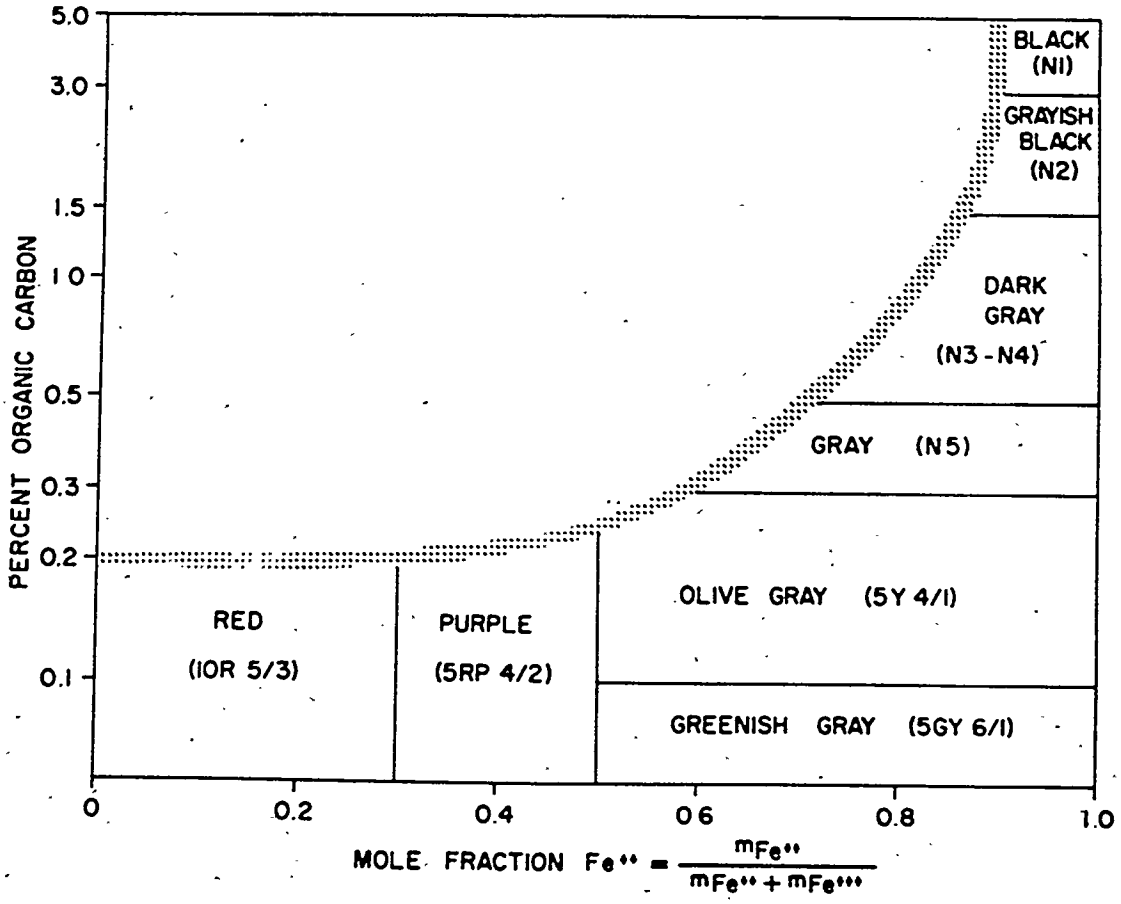

Figure 1.25 Suggested relationship of shale color to carbon content and oxidation state of iron. The mole fraction is used to indicate the proportion of the total iron that is in the +2 state and m represents the number of moles of iron per gram of rock. Finer subdivisions of color are possible, but are difficult to reproduce. Colors determined on wet samples in natural light.

Figure 3. Illustrated core characteristics.

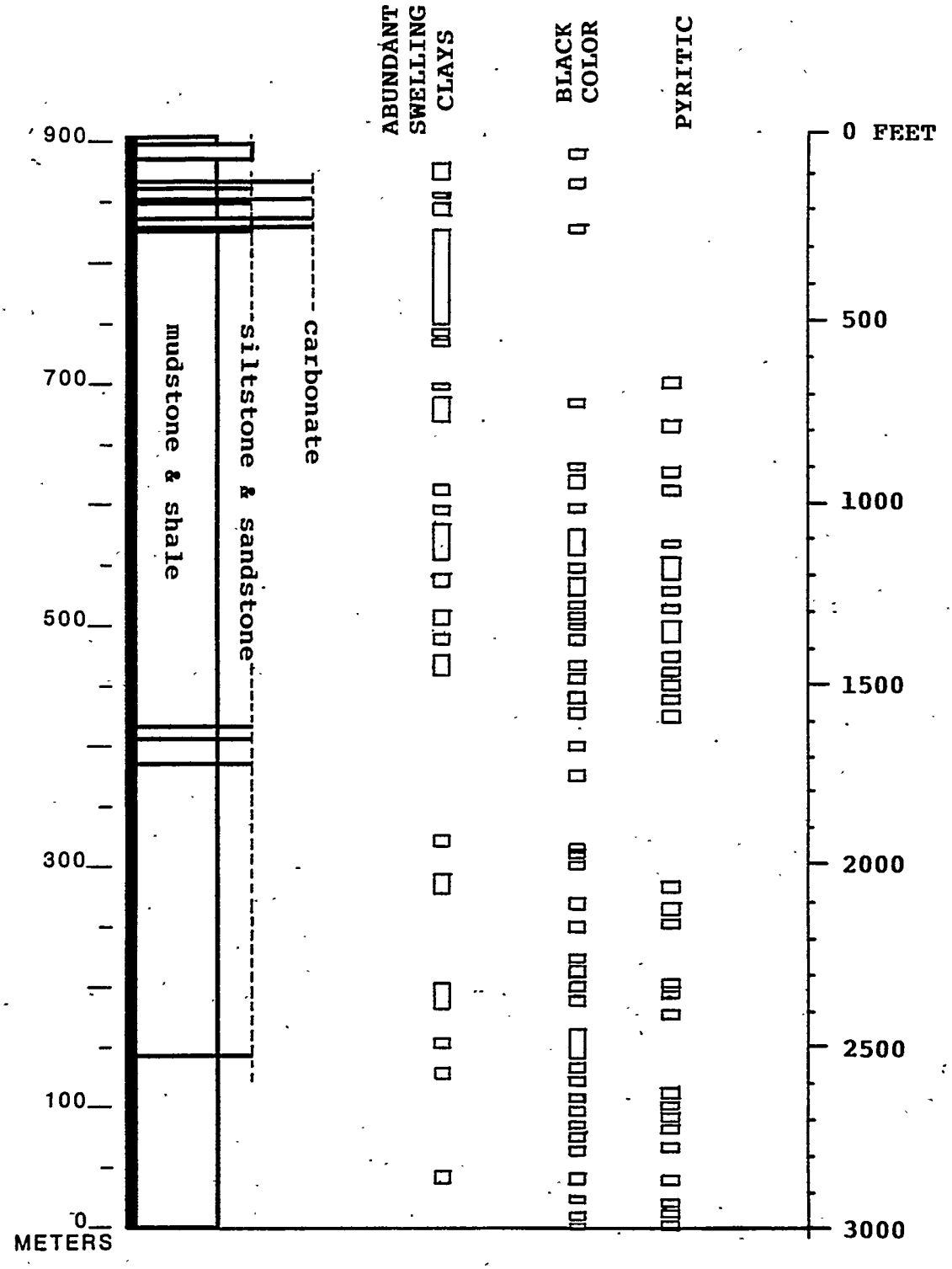

Appendix A. List of samples collected for this study. Consisting of copies of sample removal forms from the U.S.G.S. Mercury Core Library: eight (8) pages.

• Donna M. Herring • P.O. Box 13652, Reno NV 89507-3652 • (702) 786-5620 •

FILE

SAMPLE REMOVAL FORM

HOLE NUMBER: UE17e DATE: 14 January 93

SELECTED BY WHOM: D. Herring Flanigan FOR WHOM: P. Cashman / UNR

PURPOSE: Geologic study / testing RECEIVING LAB: UNR

SAMPLE TYPE	SAMPLE INTERVAL	SAMPLE TYPE	SAMPLE INTERVAL
Waxed core	2523.8-2524.7	Dry core	2654.0-2654.5
	2903.1-2904.2		2691.7-2692.2
	1662.4-1662.9		2871.5-2872.0
			2902.4-2902.9
			2224.8-2225.0
			2158.0-2158.4
			2092.5-2092.6
			1985.5-1986.0
			1962.5-1963.0
			1662.0-1662.4
			1660.0-1660.5
			1560.2-1560.4

How taken from DC/CL

Hand carry

Ship (~~Instructions~~ on back)

Number & Type container(s)

D. Herring Flanigan

7/90

15 core

FILE DF NRS/UE17e

SAMPLE REMOVAL FORM

HOLE NUMBER: UE17e DATE: 4 January 93

SELECTED BY WHOM: D. Herring Flanigan FOR WHOM: P. Cashman / UNR

PURPOSE: Geologic study/testing RECEIVING LAB: UNR

SAMPLE TYPE	SAMPLE INTERVAL	SAMPLE TYPE	SAMPLE INTERVAL
Dry core chips	2495.0'		
"	2585.0'		

How taken from DC/CL

(Hand carry) by J.H. Trexler

Ship (Instructions on back)

Number & Type container(s)

D.H.F. Flanigan

7/90

2 chip

Donna

FILE

SAMPLE REMOVAL FORM NTS/UE17e

HOLE NUMBER: UE17e DATE: 19 Feb 93

SELECTED BY WHOM: Donna Herring FOR WHOM: UNR-YMP/Cashman

PURPOSE: Geologic examination RECEIVING LAB: UNR

SAMPLE TYPE	INTERVAL	SAMPLE TYPE	INTERVAL
Dry core chips	2901.4	Dry core chips	1735.4
"	2834.5	"	1697.3
"	2360.0	"	1626.7
"	2346.0	Core segment (dry)	1584.0-1584.5
"	2316.0	Dry core chips	2492.0
"	2295.0	"	2453.8
"	2270.5	"	2420.1
"	2241.0	"	1596.0
"	2061.1	"	1549.0
"	2029.5	Core segment (dry)	21.0-21.5
"	1947.2	"	35.8-36.0
"	1901.7	"	66.2-66.7
"	1847.9	"	108.0-108.1
"	1809.2	"	119.0-119.6
"	1765.1	"	1793.0-1793.4

How taken from DC/CL

Hand carry

Ship (Instructions on back) Please ship to Cashman/UNR

Number & Type container(s)

7/90

23 chip + 7 core

Donna

SAMPLE REMOVAL FORM

FILE

HOLE NUMBER: UE17e DATE: 19 Feb 93

SELECTED BY WHOM: Donna Herring FOR WHOM: UNR-YMP/Cashman

PURPOSE: Geologic examination RECEIVING LAB: UNR

SAMPLE TYPE	INTERVAL	SAMPLE TYPE	INTERVAL
Dry core chips	14.1	Dry core chips	179.0
	44.0		189.0
	51.8		192.8
	82.7		202.5
	102.9		205.9
	111.5		218.5
	114.4		213.5
	117.0		226.0
	121.0	Dry core Segments	246.5-246.8
	121.5		223.8-224.4
	136.4		215.9-216.3
	142.0		210.5-211.0
	145.0		162.6-162.8
	148.0		140.5-141.0
	156.5		127.5-128.0

How taken from DC/CL

Hand carry

Ship (Instructions on back) Please ship to Cashman/UNR

Number & Type container(s)

7/90

23 chip + 7 core

SAMPLE REMOVAL FORM ~~NTS/UE17e~~ FILE

HOLE NUMBER: UE 17e DATE: 19Feb93

SELECTED BY WHOM: Donna Herring FOR WHOM: UNR-YMP/Cashman

PURPOSE: Geologic examination RECEIVING LAB: UNR

SAMPLE TYPE	INTERVAL	SAMPLE TYPE	INTERVAL
Dry core chips	2775.7	Dry core chips	597.0
	2272		616.0
	2099		633.0
	2205 ~~2286~~		664.0
	232.0		677.0
	240.0		698.0
	242.5		800.0
	252.5		860.5
	266.6		
	324.5		
	338.2		
	515.0		
	535.3		
	564.5		
	587.0		

How taken from DC/CL

Hand carry

Ship (Instructions on back)

Number & Type container(s)

7/90

23 chip

SAMPLE REMOVAL FORM

NTS/UE17e well file

HOLE NUMBER: UE 17e DATE: 9/23/93

SELECTED BY WHOM: D. Herring FOR WHOM: UNR

PURPOSE: geologic analysis RECEIVING LAB: UNR

SAMPLE TYPE	SAMPLE INTERVAL	SAMPLE TYPE	SAMPLE INTERVAL
chip	494.5	"	1281.5
"	507.7	"	1300.5 - 1300.7
"	301.4	"	1339.0
"	905.5	"	(x)
"	970.0	"	494.5
"	995.0 - 995.2	"	801.4
"	996.0	"	911.2
"	1050.5	"	993.4
"	1094.6	"	1003.3
"	1105.8	"	1040.4
"	1122.0	"	1041.5
"	1128.8	"	1043.5
"	1198.8	"	1105.8
"	1222.0	"	1122.0
"	1260.1	"	1198.8

How taken from DC/CL

Hand carry

Ship (Instructions on back)

Number & Type container(s)

7/90

29 chip

SAMPLE REMOVAL FORM

HOLE NUMBER: UE 17e DATE: 9/23/93 NTS/UE17e with G.G.

SELECTED BY WHOM: D. Hoffman + P Cashman FOR WHOM: UNR

PURPOSE: geologic analyses RECEIVING LAB: UNR

SAMPLE TYPE	INTERVAL	SAMPLE TYPE	INTERVAL
core	701.0 - 701.4	chips	1153.5 - 1154.7
"	706.0 - 706.6	"	1338.2 - 1339.0
"	751.1 - 751.5	"	1033.5 (F.)
"	1030 - 1030.5	"	1034.5
"	1224.2 - 1224.5	core (waxed)	1250.5 - 1251.6
"	1325.8 - 1326.0	chips	1223.0
"	1391.0 - 1391.5	"	1360.1
"	1401.0 - 1401.3	"	1281.5
"	1522.0 - 1522.5	"	1300.5
"	1655.5 - 1659.0	"	1364.3
chips	507.7 - 508.2		
"	970.0 - 971.4		
"	997.4 - 998.0		
"	1128.0 - 1128.8		
"	1145.3 - 1146.3		

How taken from DC/CL

Hand carry

Ship (Instructions on back)

Number & Type container(s)

7/90

11 core + 14 chips

SAMPLE REMOVAL FORM

HOLE NUMBER: UE 17e DATE: 9/23/93

SELECTED BY WHOM: D. Herring FOR WHOM: UNR

PURPOSE: TOC analysis RECEIVING LAB: C. Barker, USGS

SAMPLE TYPE	SAMPLE INTERVAL	SAMPLE TYPE	SAMPLE INTERVAL
core chip	905.5		
"	1003.3		
"	993.4		
"	1026.5 (TAI)		
"	1050.5 (TAI)		
"	1105.8		
"	1193.8		
"	1300.5		
"	1281.5		
"	1364.3		

How taken from DC/CL

Hand carry

Ship (Instructions on back)

Number & Type container(s)

7/90

Appendix B. Core description notes: twenty-five (25) pages. Most abbreviations confirm to American Stratigraphic standards.

• Donna M. Herring • P.O. Box 13652, Reno NV 89507-3652 • (702) 786-5620 •

DONNA HERRING FLANIGAN

"Rite in the Rain"
WEATHERPROOF

TRANSIT

NOTEBOOK NO. 301

UE17e

a product of

J. L. DARLING CORPORATION
TACOMA, WASHINGTON 98421 U.S.A.

POSTAGE GARUNTEED
RETURN TO:

D.M. Herring
P.O. Box 13652
Reno NV 89507
(702) 786-5620

UNR - Yucca Mtn. Project
Pat Cashman, P.I.

Core description + review NTS: UE17e

Samples described water-wet
GSA Rock Color Chart color terms

Many intervals have missing section sampled by previous workers; distinctive beds may have been previously sampled to extinction.

Plastic bags w/masking tape labels/closures are not meant as permanent closures/ID.

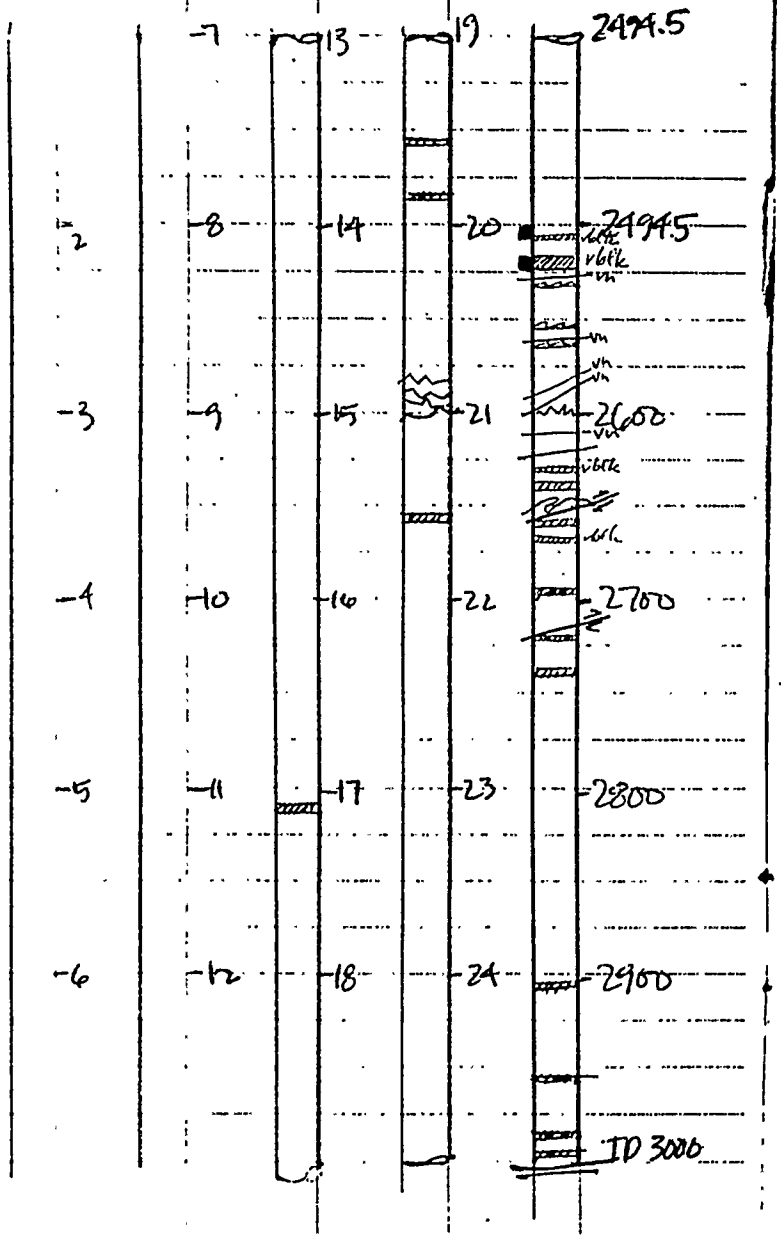

First recon. 2494.5 - 3000.0 (TD)
(fracs not measured, just estimated)

2494.5 - 2502.2 No clip exceeds 10cm, 5mm vblg
2ns to 30cm, broken mstly 80hz, mdst sh, blk, hd

2502.2 - 2513 Indurated, bkn mstly, 80hz,
2 fracs w/in 20° vert; sh, mdst blk - vdkgy, hd

2513 - 2514 Sh intrv, sh fm bkh - vdkgy

* LNR spld 2514.5 - 2520.0

2514 - 2526 Indurated, mdst, com fracs @ v45°,
vblk section @ 2516, @ 2523 - 23.8

* Spl WAXED CORE 2523.8 - 2524.7 ?

2526 - 2527 Bkn, mdst vdl, wh vns < 3mm
w/slks + 5m dkgrd xls (dol?)

2527 - 2530.5 Mod ind, bkn, fracs @ 45°
+ 80hz, thn sft zn @ 2529 w/healed
fracs @ 45°; sh, mdst vdkgy/mdkgy

2530.5 - 2531 Ripple lam, gtz slt, com + starved,
disturbed fr6 sft sdl, fracd & bdg (even and
slumped surfs). Slt lam 1-2mm, 5m 3mm w/vvthd
hd blk sh 2-3mm, lam; slt bds dec to 1 bd
per 3 fcm sh divn sth; sh blk hd mdst

Major slickensided zones:

2873-74 sltwd pol vbl
2812-31 bdg-pln slks (?)
2758 abnt slks
2719 fltd vns, abnt slks
2714 flt, brec, slk
2618-54 lateral slks
2558-75 sm slks, various directions
2531 sltwd, abnt slks, multiple dirs
2526 slks w/dfnd dbl vls
2055-1896 abnt slks
1704 vbl w/pol slks vert+ various dirs

[above from examinations of footage
2494-3000 and 1610-2237]

2531-2533 AA, sltwcvd w/abnt polished slks in multiple directions; intrbdd sh less indurated, occ splitting-papery vbl l.p., sft lam 4-6cm apt
2533-2536.5 Sh, vdkgy-blk, blm sm fg com silky feel, sm pencily-splitting, wh rthy ctg sm fracs (kaolin?), occ slks w/sft gn calc mnrl, occ assg arbky(?) lam ≤2mm w/slks, occ sft lam
2536.5-2547 Ind, scttrs to 5mm, fracs 86+2, blk hd sh+ mjst
2547-2551.5 Sh, mjst blk, blky conchoidal vbl, sft zn 2550-50.5, silky feel l.p.
2551.5-2557 Sh, mdst hd blk, fracs/5mm w/slks com @45°
2557-2558.5 Sh, mdst hd blk, blky conchoid vbl
2558.5-2575.5 Sh, vdk gy-blk, fin splitting-papery, mstly vbl, sm slks var directions, gtz vns (rpl lam?) to 2cm @ 2558.5, @ 2566; tr vert/disturbed ? wh vns @ 2564
2575.5-2618.4 Sh, mdst blk, hd, wh frac flg sm fracs near 75°; sm conch vbl @ 2593.5-2594; tr pyr; sm wh bds(?vns) ≤1cm w/pol slks @ 2612-13.4
2618.4-2675 Sh, blk, sm vdkgy, fiss-ppry, sm blky mjst l.p.; sm sltwt fracs w/pavly wh rthy ctg, sm slks lateral along 30° planes + var other directions;

Classic examples, "typical" lithologies:

Box 62 496.2-499.7 Sh, lblk to gy-blk, papery lam, steep bdg, xctg thn uns

Box 76 593.3-601.0 Mdst, slty, gy-blk, obsc bdg, xctg uns, short crshd zn

[vblk = flat, (rtng) black] [vdk gy = gray, vry blk]

extrmly splintry zns @2636-37, @2645-45.5, @2667-68, @2671-72; vblk intvls @2628-29, @2639-40, @2640.5-41.5 (mdst), @2655.5-565, @2669-70; wh uns @2621-25 vsft thn vert ?, @2628.5 ≤2mm scratches w/probe (bdg) pwdr'd off

add HCl, recumbent fld apparat upslp:

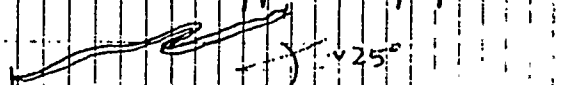

@2650 ≤1.5mm, blu, scr w/pr6 (bdg); @2654-54.5 uns vslkd lateral invmt along planes curved + sbvrt, slks on uns of yellowish-gy (yel-gy) to dk yel-org sft mineral AA to 2mm thk w/intvls of blk mdst; @2654.5-55 convolute uns dk yel-gy, anhy lt-gy, gtz dk yel-org

* crosscutg sft slty bds ≤4mm + lam mgy gtz w/abnt vert/sbvrt fracs fld w/wh anhy; hld 'ftt' w/1-2cm offset. @2661.5 wh-dk yel org gtz (crackle ripple bases?) w/slks both sides, @70° f. w/core; @2669.5, as @2612 wh gtz uns w/brnate? chlorite? sbhz, slks + pyr, Smular dol uns w/gtz @2664-2665.5. Pyr lam @2621.5, vr dissem pyr 2626 nr 2675-2926 Mdst, vdk gy-blk, carn rbl, Sm fiss zns ≤1.5mm @2686.5-87, 2713.5-

-2721, 2728-2731, 2732-32.5,
2735.5-36, 2790-91, 2791.5-92,
2795-96.8, 2817-18.5, 2833-37.5,
2839-40, 2867.5-69, 2880-82, 2893-97.3,
2899-2901, 2913-15.5. Com sclss on
belg-plin (??) fracs @45°-60°; sm steep sclss,
com ppl; wh uns cc + dol @ 2683.5 upsclss;
vscat thn-vthn wh uns anhy to 2713.5;
un dol, wh to yel-gy sil dol wavy even bdd
2mm @ 2698.5, 2702.5, 2709.5; Similar
but unsegy ≤1.5mm + discontin @ 2705.5,
2712.5, 2713. Vblk sh 2691-92. At 2713.8,
Filtd + brec sclss, irregular dol, gy, ong ≤2cm
w/yel-gy-vlt gy grz uns ≤1.5cm in unlst
mtx ⇒ n-vscl calc; alt ripples ?; vert hz orient
Abdt sclss 2717-19.5, filtd uns ≤3mm dol +
Sm cc in unlst mtx.
Wispy uns dol 2722. Vblk unlst 2724-
2725.7; 2729-2730 splotchy brec
w/gn mmcl (chlorite?) + wh rthy mm sm sclss
Vblk unlst 2743-44.8; unsegy dol uns
@ 2746, 2749.5. Anhy frac flg @ ~60° thru out,
2748-50 occ. Abdt sclss + ppl
2758-59. Thin uns lt-gy + yel-gy dol ≤1cm

unr vert. Calcite fill wh tension gashes ~60°
@ 2807.5.
2812 (identical to 2713) 2.5cm pol slks
bounded uns dol + sm cc w/vert + hz uns
Bdg-pln slks (sm pol) 1.5-6cm apart,
2812-2831; rthy crushed zn 2832-35.5,
w/2 wh uns qtz. Com bdg-pln slks less
regular to 2862.
Vus lt col + disturbed, wispy l.p. 2857.5-
2858, sm @ 2859, 2859.5.
Rthy frac ctgs, wh, ltgn @ 2862.5,
2868-69, 2871.5-72, uns dol vert + hz
(as @ 2812 + 2713.5) 5cm thk @ 2872.
Sheared polished rock sm wh uns/ctgs
2873-2874.
Wh rthy ctgs on slks com 2879-2882
Thk lt-wgy + dk yelomg uns dol, slt calc,
1-2cm convolute + blk sloz common
2888-2892, selcd l.p.
Wh uns anhy, slt calc com cyclics 2899-2901.
Vbelt mdst 2902.4-2903
Thk qtz vn wh ~3cm (real ripple?) @ 2914.5
Vbelt 2956-57
Wispy lt-wgy laminated + anhy

Vblk mdst 2985.5 - 2983 - 2984.5,
+ 2995.5 - 2996

New core layout: NEW CORE LAYOUT
Working upsection from 2237.5
gy sh - blk
Mdst, 2237.5 - 2167, shly-pencilly mx
@ 2226 - 2226.5
Dol/sil conv vns 2224.8, 2221 - 11.5
Vblk 2158.0 - 2158.8

Brec mdst - sh, vdk gy - blk, sm kaolin
on frac, sm pol sclts, sm dol/sil vns
2167 - 2077

2077 - 2055 Mdst, vdk gy - blk, hd, fract,
sm vns 2055 - 2059.5

2055 - 1896 Rbl of fm - hd fiss - blky sh,
hd mdst, vdk gy - blk, abnt sclts, sm vns,
Occ comp zn to 20cm; Vblk + mtrln
1984 - 1986; 1962 - 1964.5. Convoluted vns
1901 - 1902 conv

1896 - 1677 Mdst vdkgy - blk, hd, com fracs. Crushed zn 1868 - 1869 w/ slt ush vns + blebs, occ vthn slt/fss zns; slt zn; 1849.7 - 1845.5, 1837 - 37.5 w/ brec wh matx dol + cc; unsppy vns dol + cc 1834 - 49; slt zn 1827 - 29.5, slt vbl 1782.2 - 83, slt zn 1767.5 - 1761, 1755.5 - 58,

* Poss dol lam (conv // bdg) 1734.5 - 35.5

Rbl mdst ppy 1714.5 - 16.4

Blk - vblk umblen mdst 1713 - 1709

Rbl w/ pol slks 1704.5 - 1706, vert + various

Thk umblen mdst 1697.2 - 1703.5

1677 - 1669.0 Crushed dkgy - vdkgy slt + mdst w/ wh blebs kaolin, wh vns dol + cc

1669.0 - 1663.5 fract slkd mdst, sm w/ slt xbds (nv) + cc wh tension cracks flgs

1663.5 - 1657.4 Porous dolomitic xbdd slt gpl-gy, dkgy gpl sets to 2cm nearly vertical (85°e) grdg down to interlam slt + mdst (blk - vblk)

1657.4 - 1610.5 Mdst vdkgy, slt lam @

Slt lam @1625A - 1627 w/ weak ld fracs/flts

NEW CORE LAYOUT 2237 - ~~2494~~ 2383'

2237.5 - 2241.3 Mdst, blk, hd; sm pol slks vert; @38.8 vn, wh-yell grn w/ brec mdst incl; vn is calc + dol

2241.3 - 2265 Mdst, blk, sft-fm, rthy; silty l.p.; slks dull, com; sm coring-induced (?) vertical fracs; sm slks have sft grn mineral HCl reactive. Bdg 40-60° avg, guess bry sft + dk lam (blk-dk grn-md grn)

Partially ~~brk~~ @2251

Vbrec + ~~brecc~~ com slks 2257 - 2265; incl sl vert + flutes; slks have cc ctg.

Sm vsft silty sh ady 1.5cm cc vn — vn blk

2265 - 2321.8 Mdst, blk, fm-hd, lam @ ~60° bdg. Pol slk @ ~80° @ 2268. Rthy, crshd zn 2269 - 2274.5 w/ pol slks w/ multiple unmnt. blk kaolin (? vsft mcalc) Bdg-plu splitting (?) near 45°, 2314 - 2318

2321.8 - 2383.0 Mdst-sh, blk-dgy blk, sft-fm, fissile + partially l.p.; Com splitting sl horiz

[fm, slwd zn mdst 2286 - 2302]

+ sb parallel ≈45° com sb horiz slks
dull-polished. 5cm vns ≤3cm wh to pale yell
orng, multi-mineral w/brec under mcl;
wh qtz w/dol pale yell orng irreg blebs - these
fract w/cc flg. 5cm rec'd qtz-sl/slt wh
bds ≤1cm, faintly ripple-forms, fld fracs
1 bdg, pale yell orng dol flg. sb horiz
~~strae~~ strae btm surface, four or more
lateral +/or oblique slick sets on top surf.
@2340 | lam line vns sbvert wispy white
cc and gn-gy silica (some + diff vns have
cc+sil), com dissem + minute clusters
pyr. @2345.5-46.2.
Pen dilly zn 2370-2381, com sb horiz slks,
thn wh-pale yell orng vfgr cc sb horiz vns.

NEW CORE LAYOUT 1496.6-1610.5

1496.6-1535.2 Mdst, blk-gy-blk, sl-fm.
Pen dilly 1498.5-1499.5. Com dull slks w/gn +
wh mins (kaolin + bruc?), com dilation vns
≤3mm, mostly ≤1mm, quhy. Incl zn
1504-1510.5 | shrd zn w/sbvert cc + dolic cc wh vns
[pyr-burrows(?) @1507.2]

@ 1549:

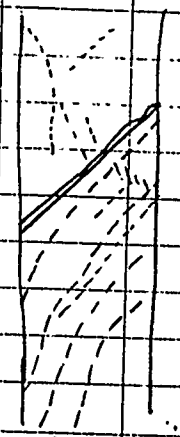

-- anhy
= qtz
-- obsc poss bdg

1514.5-1521.4 w/pol slks, sl vert @ 1520.
Abnt anhy vns @ 1534, conjugate (?) in part.
1535.2-1610.9 Mdst, blk to gy-blk, fm-hd, (sm vert-sl vert slks, com pol w/kaolin + brec (?). Com sl vert slks w/optical mvmt up
Wh dol + dolicrc vns @ 1561 sl vert + slkd-sided. Com vns 1556-58 + 1568-69;
@ 1568 vert/sl vert slk w/lateral mvmt
Bdg-pln parallel (?) pol slks @ 1569, 1571, 1579-80.
Vns wh + pale yell ang qtz, sm w/anhy brec inclusions @ 1578.5-79 + 1582.0-82.5, 1587-1588, 1594-84.5, 1595.7
@ 1584-84.5, thin gen silica: qtz xls w/ yell-brng matx

Slks generally sm,
v blk 1601.5-1603; fm-vf 1603-04

NEW CORE LAYOUT 2383.0-2494.5
2383.0-2446 Mdst, blk (sm gy blk), hd; sm bdg-pln splitting 40-60°. Sm anhy vns @ 2402.5-2403, bdg-pln // (?), sm w/slks

RECON: TOP of HOLE:
Top of hole, gtst has shelly debris, incl bracks(?), fusiliids(?), corals(?)(finger corals). Debris becomes less common, burrows pick up, then down into barren shale. Ls has burrows, slt has burrows, then down into barren sh.
What does this say about oxygen/energy?

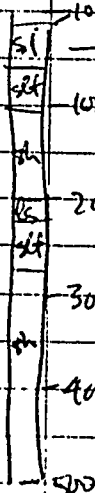

w-dff H=2½+. @ 2401.5, dol sm (?) w/tryglothrix (?) bdng one side; mass pale yell orng intr w/rr ish gtz blebs
2416-2434 Mdst+sh, sft-fm, splntry, com, rbl com, blk to gy blk. Shrd 2425-26 sm ?bdg-pln ll; ?bdg-pln ll splitting 2426-2428. Vbelz 2430.5-2431.
2434-2456 Mdst+sh, blk, fm-hd, splntry, l.p., sm rr slks (?bdg-pln ll?), rblk, l.p., vsplntry 2441.5-2450.3 + 2453.5-2454.8
2456-2490 Mdst, blk-vblk, sm rr bdg-pln (?) pt35; H2O absorp @ 2477. Shrd 2490-
2490-2491.5 Shrd sm prl slks splntry blk mdst+sh; dol vrs calc+pale yell orng sgrd/ compacted ≠ 3cm, each max 1cm
2491.5-2494.5 Sh, blk, sft-fm, splntry, rare siltstone slk w/bruite(?). H2O absorp com. Slks w/rr min sm bdg-pln(?) 2493.8-2494.1

NEW CORE LAYOUT 100-406 2-
10.0-21.0 Sh, dkly yell-brn, Fe-stn ~~of~~ on abnt fracs, sft-fm, blky splty @ 16.5 +

9.0-17.5, blkish zns dskish yell-brn to brn-blk

~~19.6-23.6 (?) Xbedsg~~

21.0-21.5 (mssg 21.5-22.6) Sltst, vfoss, vcalc
crudely bdd ≈25-30°, flaser echin frags - poss
ldeut arms + col; fibrous brach segs); prob fucoid.
Foss are calc, rarely recrzd, com lam sltst.
Sltst wthr dk dskish yell brn
22.6-23.5 Sltst/Sltst, vcalc, brec, no rec foss,
cc fracflg w/inds in fracs; cc wthr; dk yell brn
wthr w/ish speckled appearance; poss stylo
23.5-32.5 Shn + mdst, dskish yell brn, brec, incl
wxdd sd to fd size - clut? transl wthr pale elk
Bdg 30-35° com lam shn, one 2cm bd vdk reel sltst.
32.5-33.0 Sdst/Sltst reckd, calc, dkishy yell brn,
brec v.p., one vn has terminated xls - flourite?
(no dt even pdrd cold HCl) (not hex); no recog
foss, bdg 30-35° [33.0-33.7 mssg + poss stylo.
33.7-34.3 Sltst, dk-dskish yell brn, hd, calc,
grdd foss + burrowed. Sl vert vns cc
34.6-37.5 Sltst/Vlnk sh ptgs), lams + grdd i.p.,
blkish shly, lam + nunbds, dskish yell brn
sltstn wthr w/cc foss (bash of thin btm shells)
stnd w/klm.
39.5-44.5 Poraceia zn, klm stnd dayish Sltst,

incl zn 39.0-44.4 w/ hd bds(?)
to 4cm sl/l fracs (+? stylos?)
44.5-48.0 Sh, dusky yell brn, blky i.p., occ
sltst ≤1.5cm, fracd - prob equiv above
"hd beds"; sm blk ptgs
48.0-65.5 Mdst+sh, crushed, brec, dism stnd
to 60.0 Then gybl-rthy brec
65.5-114.8 Mdst+sh, gybl-blk, blky-pbty
rbl, sm brec; sm wh ctgs fracs, rr sltst
stks; -fn unlist 76 102.5-105.5
+108.5-110.0 + 110.5-111.8(+) vsbly sltstr
114.1-115.5 Dol, speckld ungy-dkgy, hd, blky,
rbl, occ bds, com fos debris to mdl size;
sltst dk + trans wh qtz, ↓ to wkdd,
flty in cgelly-mdkgy dol mtx (slicvole);
40-50% sd-slt by volume + ins ost;
Sd is bimodal fU + fL; fossis dissolvd
completely; tr mdkgy clay. Base of
unit has 1-1.5cm thk sh-mdstt pbty,
fm, velty, mdkgy, calc/dol.
115.5-120.5 Sltst, calc/dol, mass (bottom 6
prob), wispy + blky dkgy clay lams rr vsr ooze;
tr thn shell debris 1-3mm, bothic slt-prob
clst, also blk-mdkgy Minute pyr com.

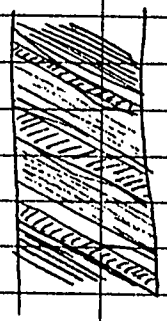

slt/st
sh
dk gtz

Dk elongate blebs more clay-rich, have crude orient ~60°. Com ptgs @ ~60° w/calc
Kaolin ctgs - pass sm slip sm faces (?)
Btm 2ft shown bdg w/clg burrows; bdg lam ~30-40° burrows to 3cm
120.5-126.5 slt/st, lam mltgy + brnblk-gnblk, hd, blky. Mltgy lam = gtz slt ~3% w/tr dol wh mtx. Brnblk-gnblk lam ~5-30% = lithic slt - cht, dk mins, about ppr cm layers; smoky gtz ?, clay min minor mtx. Cc uns thn, sbvert. Abnt xbds, sets to 2cm, gross bdg 25-30° (?) top 2ft; minor micro channel fill + starved ripples next ft, Then lam w/sm small burrows to 1mm
126.5-131.7 slt/st + sh, slt/st bdg to 1.5cm, com rd-brn stn; variably banded slt/st/clay gtz slt/st + sd/dk sh, tr burrows, sm gtz micro channel fill. Top stn 50% + slt/st, grdg downsctn to hd lam slty sh
133.0-140.5 Sh, sft-fm vslty, bvec i.p., ind i.p., ind. is banded Mgy/blk, w/lighter zns vslty
140.5-142.0 Dol, lmy, vsdy + slty, abnt calc foss debris; speckled mdkgy + dusky blk, blky splty, hard

mdkgy

142.0-155.4 Sltst, f-vfgr, hd, massive-flat lam, com stylo. Qtz dom, clay mtx, blk grns, com Fe Sh

155.4-156.6 Sltst, lam-xbdd (lo x-sc scale), dk gry-sft + clay-rich lams; ltgy-mdkgy

156.6-162.0 Sh + mdst-vdkgy-blk, lam H_2O sens i.p., bndd + ind i.p. - fiss + slks, sl vert plu, oblique slip

162.0-170.0 Mdst + sltst, sdy i.p., lam + sm-sc xbdd i.p., burrowed (small scale) i.p.; Sh ptgs vdkgy, also blk splts; dips ~30°

170.0-207.0 Sh, dk gry-mdkgy, most H_2O sens, sdy, bxes. Sltst-bds to 1 cm thk @ 184.5-184.6, 190.8-191.2, 192.5-193, 198-198.3; vfgr, sm rdstn, dips ~30°; start vr vfgr sdy lam. Sh v H_2O sens 201.5-204.0

208.6-212.3 Sltst, hd, mdkgy, blocky i.p., rcalc, abnt cc foss

212.3-227.5 Sltst, hd, sdy, abnt sdy ptgs, blocky, ltgy-mdkgy; sm incl clgs dusky blck thn sltst; thn bdd

660.0-665.0 slty hd mdst mod frg dissem pyr
768 - 782 com lam ex fol
Com pyr nod 763-764, 771-772, nbdd 773-776, com 790-796 (end of ex) esp. nod bdg

sltst, bumwood, w/ss 214.5-216.3,
~~232.5-2~~
227.6 - 232.6 mssv
232.6 - 242.0 slt + sltst, lam blk + lt gy,
sm burrows
242.0 slt, vdky, H2O seus
NO TIME! Abbreviated recon:
Sltst + Grac ~~33~~ 287-301
H2O seus ~~thy~~ slt/mdst 242-564, slt 442-449
Hd mdst 564-576
H2O seus slt, 576-582
582-896.6 mdst, mod thy hd blk, md bgy
Sburd 583-589
Sfr 589-590
Sfr 603.5-603.5, 604.5-605
Sburd + sfr 611.5-612.5, 628.3-629.5
Sfr/sburd 651.4-660.0, 665.0-675
Fm, H2O seus in 675-694, 700-776
Sburd 693-700, 776.1-780
Fm 776-820
Sburd 820-825, 835-845, 848-870, Fm
856-857
Hd mdst 857-896
796-811 horiz bdg?

~~233.5-2~~

242-896 recon to date, chips spl only
896-1496, 700-748 not yet scan

700.5-748.0 Mdst, gy-blk, lt-fin, slty
Vns w/stks 705.0-708.4, @713.0, 724.7-734.0,
738.0-739.0. Mud cake 704-705, 747-748.
V slty + pr 722.0-724.7, 734.5-736
Rdom ppr fn bd (dstf) in slty sli pr gy-blk
zn 741.7-746.5

20 Sep 93
NEW CORE LAYOUT

896.6-963.0 Mdst, blk-v dk gy, fin-lam, H2O seps i.p.
*abnt dist bdg in mdst paint @ a/60°. Rr vns
wh w/pale yel along cvgs, dol + gyp, to 2mm poss
sub// bdg (?), com blkn/dest to 4mm. Rr vns wh wisps
thru to 1mm, soft; under 30x lt gyish-yel-gn,
unrec wood eff HCl, vit; dissol HCl liberates
clr frags gyp (?), one etched tab pt vn:
(930.8) gyish mass
rsid clusters clr, xls, non-cb/eff clay veneer
cb mtx dissol out 2mm
clr bladed soft min vit (rr acic residue in HCl+yel gyn)
Sm rdom blebs more mic (?), prob fn dissm pyr, (blades grew into void)
blebs rr, irreg to 2cm elongate oval inclus. esp 945-955
Fracs com 60-90°, 1-6 cm apart. *
Olive blk 911.1-912.6, fn lam blkn
*Rr vnlty stks subvert to 60°
963.0-990.0 Crushed + partly healed bdg/healed zone,
mdst sft-fm, v calc, mdl gry (v sol H2O to
m blkish gy mud; v eff cold HCl (*), abnt
wh vns + prob rextzd nvpls (?) to 1.5 cm fnd
+ slvd. Less calc, lt-fm, not slvd @ 981.7-
986.0 v pron thn wh vns subvert sm w/stks pol.

* rsid acic mod rare-com, also wit lt apple-gn tab xls rare-com

990.0- ~~1029~~ 1029.0 Mdst, gy blk to mgy blk, rr calc, blky, com vns wh calc + ncalc (along steep bdg?) Crushed + shrd, stks (pol i.p.) mod calc @996.8-1001.5? spkd by others - missing 3 or 4 ft, prob rbl; @1023.5-1024.5. Crsh + shr ncalc @1021.5-1022.5. Blk mdst H2O, mod dissag 1003.3 - 1004.0.

1029.0 - 1071.5 Mdst rbl + healed rbl, mass shrd + crshd. 1034 - 1058 vpor + com calc; com wispy thn vns to 1.5mm, sft wh off cold HCl (frag, traces/dec clay + chlor(?)) 1032.0 - 1034.2 cvs xhv sheared, mullions near 70°, vns transl-wh cc + dol, sm dol dk yel org to gy org, incl near edges vns

1051 - 1064 abdt wh ctgs kaolin on stks + fracs, sm w/chlor(?)

1071.5 - 1125.0 Mdst, gy blk - blk, hd, shrd, vns com, com pol stks var orient, sm dissem slt

Zn 1081.0 - 1083.0 incl dist/crshd/fraicd cc + dol vns, sm frags 2 - 10cm hd mdst w/cc dil vns, in mdst sft gy blk mdst - vH2O sol yields gy-blk mud. @1091.1 blebs slt pk brn to 2.5cm; ~~cast~~ thn bds dk dish brn near 60° (rr; + ½cm) @1089.0

Shly ptg, H2O sens @ 1105.5 - 1106.0 vblk. Shly, ptg sft w/cc vns wispy, sft @ 1106.5 - 1107.5, blk. Com pol stks w/kao, var orient @1114.9 - 1125.0

TH pyr @ 1110.0

Mdst, thn-sft, blk, gy blk @ 1100.4 - 1100.6, 1121.6 - 1125.0

1125.0 - 1134.2 Sh, gy blk, H2O sol sens, slky, v thn dny, sm pol stks

Crshd + bld (i.p.) 1129.3 - 1134.2, w/v calc vns (// bdg?) to 1cm com pinch out, shattered, sm shtr frags dissagg

1134.2 - 1152.2 Mdst, gy blk, fin-bd, rr thn sft + zns dist bds, 1137.5 - 1140.0 reddish mod brn, hd, also blebs, bdg in 40°, H2O sens i.p. esp sft zns + mod brn bnt intervals. Shrd on @1140.0, max 3cm, wh + gy org dol cc, one shear face incl wh kaolin + clay ds + frags to 2mm

1152.2 - 1155.5 Sh, gy-blk, papery, spltg ip, sft, shrd along dol cc vn @1152.4 ≤ 3mm, H2O sens, slt slftg.

1155.5 - 1182.0 Mdst, gy-blk - blk, fin-bd, rr thn crshd zns bec sft. Zn dist bdg, hd, gy-brn + dusky yell brn in 60° @1168.5 - 1168.7 w/sft crshd Zn for mtx pr below kaolin; hd beds to ≤ 1cm w/v thn dil vns calc-kaolin (?) (analog?), one bd includes tektite body pyr 1.6mm × 3.5cm

1182.0 - 1185.0 Shly mdst, crushed gy-blk, thn-sft, sm wh crshd dol thn vns, dmt H2O sens

1185.0 - 1294.0 Mdst, gy-blk to blk, v thn-bd,

vsli calc i.p. nr 1260

1185.0-1208.5 slty, sli-mod H2O sans, sm prgny & splty wet, blk w/wh rr clay, uns to 2mm shrd, com mod bn hd zns dust, rr vert elongated blebs.
* Hd uns dol 2-3mm wh+dk yell ong, shrd, @1195.4, @1198.0, @1263.0, @1250.5, @1267.0-68.0, @1270.0-67.0
Sli-mod H2O sans, blk, fin rr mod bn blebs, prgny por exhd wet @1198.0-1200.0, @1201.5-1206.1, bec vslty + gy-blk 1208.5-1221.0.
Crushed zns 1206.1-1208.5, 1234.0-1236.8, 1250.0-1247
* Lg uns wh+dk yell ong dol 5mm+, shrd, var dot dil frags @1224.5, @1250.5-1251.8, @1253.0-1253.3, 1260.0-1269.0,
Blk sh, slty dny, prgnly, sheen @1222.0-1223.0
Mdst wh clay on pol sfcs @1248.5-1250.5, @1268.0-1270.0, @1306.0-1310.5
V blk frags @1222.0-1223.0 sh, fm, sli slty; @1257-1262.0 mdst, fm, slty; @1285.0-1286.0 mdst blky hd, v slty
prgr zns @1193.3-1195 along blebs + rr bn blg; @1198.0-1197.0 dissem fn; @1233.5-1237.0 dissem fn @1254.5 mod 1.2×3cm; @1257.0-1258.5 fn dissem; @1260.7-1262.6-1263.5 dissem fn; @1276.0 bn bl fn lam <50°, @1279.0-1285.1 sm dissem + rdbn blg ≤1cm ≥70°; @1288.0-1289.5 dissem fn

1294.0-1308.1 Mdst + slty wackst, gy-blk & blk, sli slty. Blk 1299.5-1302.0 fm-sft mdst + slty wackst, mod H2O sat i.p. v H2O sat 1298-1301. Crushed 1300.2-1303.5. Pol sfcs w/wh clay @1306-1308.4 rr vert. sli por
1310.8-1335.5 Mdst, blk, sm gy-blk, fm-hd, sli-mod calc, Str Crshd zns 1318.8-1319.5, 1324.5-1325.0. Vugs only 1-2 per 6x core, mstly sfcd. Com dissem pyr throughout; sm gy-blk blg thin wispy stringers, 2-4°. Sm pyr mod dist blds
1335.5-1371.0 Mdst fm-hd gy-blk, dk blk, sli calc i.p., whole interval shrd/sfcd/und w/wh + org debris, wh clay
Mud calc + pyr 1350.5-1351.5, 1351.9-1352.8. Pprg, splty, v. H2O sat 1363.5-1365.1, 1367-1367.7
1371.0-1406.7/1406.7-1413.7 Stmpld (away/ext & rr warped) Mdst, dkgy + blk, olv-blk, hd, slty, mod calc
Por + vcalc 1372-1373 (anhdrk)
Thin ≤5mm slty blds com 1387-1394 v dist prob sft-sed flow folds + micro flts
Fctd uns 1394.4, 1395.5, 1401.5, 1403-1406 rr vert x pol

~~1425.8~~ (1416.7-1420.0 dbse)

1413.7 - ~~1416.7~~ (1406.7-1413.7 dbse) Mdst, gy-blk, lnd, pvr l.p., slty. Shrd vns @ 1425.2

Bdd pyr mod @ 1416.2

1425.8 - 1449.0 Mdst, blk, fm-lnd gy-blk, slt-mod calc, H2O sens mod, pyr mod @ 1448, 1448.8

1449.0 - 1463.0 Mdst, slty, blk, gy-blk, slt-mod calc, sft-fm; vH2O sens 1449-1457.5, 1458.5-1459, 1459.5-1461.5; pyr mod 1455.5

1463.0 - 1476.4 Mdst, blk, gy-blk, sft-fm, H2O sens 1465.0-1475.8 v, 1476.2-1478.5 v, 1477.5-1481.5 mod-v, 1485.0-1491.5 mod-v

Pyr mod 1476.5

Wispy bdg 1478.0-1478.5

Fract, shrd vns 1470-1470.5

Thin section depths 12 March 93

*	21.2	2692.1
	21.5	2902.1
	35.9	
	66.3	Picked parallel to any
*	108.0	evident true dip in
*	119.3	most cases. Some picked
	127.8	for paragenesis. Some
*	141.1	too indistinct or rubbly
*	162.7	to tell dip.
*	210.6	
	216.0	* RUSH REQUEST
	216.2	
	224.0	
	224.2	
*	246.6	
*	1560.3	
*	1584.2	
*	1660.3	
	1793.1	
	1793.3	
	2092.5	
	2158.2	
	2523.9	

Drg core segments:
- 970 - 971.4 (conodonts)
- 9950 - 995.2
- 997.4 - 998.0 rubble (conodonts)
- 1224.2 - 1224.5 (petrol vns, xcts)
- 1153.5 - 1154.7 (conodonts)
- 1145.3 - 1146.3 (")
- 801.4 - 801.5 (split for XRD-dry)
- 1300.5 - 1300.7 (split: TOC/XRD/dry)
- 1128.0 - 1128.8 (conodonts)
- 1325.8 - 1326.0 (petrography)
- 751.1 - 751.5 (petrography)

Chip samples for later microscopic examination:

					1281.5
					1128.8
					1046.4
2775.7	2901.4	800.0	1549.0	205.9	1043.5
2272.0	2834.5	860.5	14.1	28.5	1041.5
2099.0	2360.0	44.1	44.0	213.5	1364.3
220.5	2346.0	44.0	51.8	226.0	1339.0
232.0	2316.0	51.8	82.7		567.7
240.0	2295.0	82.7	102.9	911.2	
242.5	2270.5	102.9	111.5	905.5	
252.5	2241.0	111.5	114.4	1603.3 top	
266.6	2061.1	114.4	117.0	993.4	
324.5	2029.5	117.0	121.0	1026.5	
338.2	1947.2	121.0	121.5	1033.8	
515.0	1901.7	121.5	136.4	1050.5	
535.3	1847.9	136.4	142.0	1071.6	
564.5	1801.2	142.0	145.0	1105.8	
587.0	1765.1	145.0	148.0	1122.0	
597.0	1735.4	148.0	156.5	1198.8	
616.0	1697.3	156.5	179.0	12226	
633.0	1626.7	179.0	189.0	996.0	
664.0	2492.0	189.0	192.8	970.0	
677.0	2420.1	192.8	202.5	494.5	
698.0	1596.0	202.5		1034.5	

* = want to thin-section
⊛ = sent for thin section

Thin core segments:

- ⊛ 158.4-158.5 Qtz-in-qtz vn
- ⊛ 21.0-21.5 Sltst, s/about cc foss
- ⊛ 35.8-36.0 Sltst w/abnt cc foss, shly
- ⊛ 66.2-66.7 Mdst
- ⊛ 108.0-108.1 Sh, H2O sens
- ⊛ 119.0-119.6 Sltst/fsd, burrowed + bndd
- ⊛ 793.0-793.4 Mdst w/fsd: bioturb?
- ⊛ 127.5-128.0 Mdst+Sh, bndd, red/grn
- ⊛ 140.5-141.0 Sltst, v foss/fsly, slty LS/Dol
- ⊛ 162.6-162.8 Sltst+Sh, eruptive burrow
- ⊛ 210.5-211.0 Sltst, calc foss, bioturb
- ⊛ 223.8-224.4 Sltst, chps sltst, bioturb
- ⊛ 246.5-246.8 Mdst, Sh below Sltst
- ⊛ 215.9-216.3 Sltst, bioturb

Conodont samples:

- 970.0-971 ft (rubble/dry core; viable sh/mdst)
- 978-998.0
- 1153.5-1154.7 sltst fsm, Sh, dry core

X = not sent for thin section
3/12/93

SAMPLES

Waxed core - slice for sedimentology; TOC

⊛ 2523.8 - 2524.7
⊛ 2903.1 - 2904.2
⊛ 1662.4 - 1662.9 flaser sds

Dry core

2654.0 - 2654.5 papery slt+mdst : TOC
⊛ 2691.7 - 2692.2 " : TOC
2871.5 - 2872.0 ", sltst : TOC
⊛ 2902.4 - 2902.9 ", bdg-plu fracs : sed
⊛ 2224.8 - 2225 vns : min + sed
⊛ 2158.0 - 2158.4 blk mdst : TOC + sed
⊛ * 2092.5 - 2092.6 " :
* 1985.5 - 1986.0 vblk slt : TOC
1962.5 - 1963.0 vblk slt : TOC
⊛ * 1662.0 - 1662.4 flaser beds : sed
⊛ 1660.0 - 1660.5 slt/mdst intrlam : sed/str
⊛ 1560.2 - 1560.4 lower vns : sed/str

Appendix C. X-ray diffraction studies. Including copies of the machine charts, tables of percentages, and discussion by Dr. W.A. Pryor of the results: nineteen (19) pages.

Wayne A. Pryor & Associates, Inc.
consulting geologist

455 Fairview Place, Cincinnati, Ohio 45219 • 513/241-6270

May 21, 1993

Donna M. Herring
Consulting Geologist
P.O. Box 13652
Reno, Nevada 89507

Re: UE17e core sample Clay Mineral and Bulk Mineral Analyses

Donna,

Attached are the results of the clay mineral and bulk mineral analyses of the UE17e core samples and Olinghouse Fault Gouge sample.

1) - Fault Gouge sample analyses indicate that the gouge is composed entirely of amorphous silica (opalline silica) that is diagenetic in origin and is probably not useful in precisely dating the faulting.

2) - The Mississippian Eleana Formation mudrocks are composed of nearly equal parts of clay minerals (20-54%) and quartz (31-42%) with minor amounts of the feldspar microcline, and trace amounts of goethite. The deeper mudstones (samples 677.0', 2,270.5', and 2,901.4') are slightly less clay mineral-rich and contain minor amounts of pyrophyllite (a talc-like metamorphic phyllosilicate often found in schists).

The clay mineral fraction of the Mississippian Eleana Formation mudstones is dominated by interlayered Illite/Smectite and is the predominant swelling clay mineral in the mudstones. Interlayered Chlorite/Kaolinite is present in the upper samples (111.5' and 202.5') in nearly equal amounts with the Illite/Smectite, but is replaced by Chlorite, in diminishing amounts with increase in depth. Pyrophyllite is present at and below a depth of at least 677.0, in minor amounts.

No Zeolites or other diagenetic minerals were observed.

Interpretation

The Illite/Smectite clay minerals suggest the possibility of a volcanic origin for some of the clays, but is not unequivocal. Illite/Smectite clays are responsible for the swelling character-

istics of the Ele[illegible]a Formation mudstones.

The change from a Chlorite/Kaolinite to Chlorite and the presence of Pyrophyllite in the lower samples is probably provenance controlled and suggests a shift in provenance and that a metamorphic rock source played a part in the origins of the lower parts of the Eleana Formation mudstones. This vertical variation in clay mineral composition may prove useful for stratigraphically subdividing the Eleana Formation. More closely spaced sample analyses may be necessary and may show other mineralogical variations that are stratigraphically controlled.

The minor variations in bulk mineral or clay mineral compositions should have no significant influence on the wire log signatures.

Wayne A. Pryor

Wayne A. Pryor
Consulting Geologist and
Certified Petroleum Geologist #2303

MINERALOGY UE17e CORE SAMPLES

Bulk Mineral and Clay Mineral analyses were acquired using a Siemans D500 Diffractometer (CuK Alpha Radiation). Clay Mineral assemblages were analyzed in air-dried and glycolated conditions. Compositional percentages were calculated using the Biscaye Method (Biscaye, 1965). The percentage values are relative and accurate only to a ± 5-10% level.

BULK MINERAL ANALYSIS

Sample	Composition
Olinghouse Fault Gouge	Amorphous Silica - 100%
UE17e - 111.5′	Clay minerals ---- 45.2% Quartz ---------- 33.9% Microcline ------- 14.4% Goethite --------- 6.5%
UE17e - 202.5′	Clay minerals ---- 43.7% Quartz ---------- 40.2% Microcline ------- 16.1%
UE17e - 338.3′	Clay minerals ---- 54.3% Quartz ---------- 31.5% Microcline ------- 9.4% Goethite --------- 4.8%
UE17e - 667.0′	Clay minerals ---- 24.2% Quartz ---------- 41.8% Microcline ------- 10.2% Goethite --------- 15.6% Pyrophyllite ----- 8.2%
UE17e - 2,270.5′	Clay minerals ---- 23.0% Quartz ---------- 35.0% Microcline ------- 13.0% Goethite --------- 13.0% Pyrophyllite ----- 16.0%
UE17e - 2901.4′	Clay minerals ---- 20.0% Quartz ---------- 40.5% Microcline ------- 20.7% Goethite --------- 5.5% Pyrophyllite ----- 13.3%

CLAY MINERAL ANALYSES

Sample	Composition	
Olinghouse Fault Gouge	Chlorite --------	Trace
UE17e - 111.5′	Illite/Smectite ----	68.0%
	Chlorite/Kaolinite -	31.9%
UE17e - 202.5′	Illite/Smectite ----	46.1%
	Chlorite/Kaolinite -	53.9%
UE17e - 338.3%	Illite/Smectite ----	48.3%
	Chlorite ----------	51.7%
UE17e - 677.0′	Illite/Smectite ----	48.1%
	Chlorite ----------	48.4%
	Pyrophyllite -------	3.5%
UE17e - 2,270.5′	Illite/Smectite ----	45.7%
	Chlorite ----------	38.0%
	Pyrophyllite -------	16.3%
UE17e - 2,901.4′	Illite/Smectite ----	88.0%
	Chlorite ----------	6.2%
	Pyrophyllite -------	5.8%

Wayne A. Pryor & Associates, Inc.

consulting geologist

455 Fairview Place, Cincinnati, Ohio 45219 • 513/241-6270

September 13, 1993

Donna M. Herring
Consulting Geoogist
P.O. Box 13652
Reno, Nevada 89507

Dear Donna,

Not to worry Donna, I understand the inability of university purchasing department to pay their bills on time or at all.

Enclosed are the two sets of X-ray diffraction records of the UE17e drill hole samples and the Olinhouse Fault gouge sample.

Set A - Clay mineral analyses

Set B - Bulk mineral analyses

I would be pleased to run more analyses for you, just call, or send the samples. Again I can turn them around for you at a fairly rapid rate and at competative prices.

Sincerely,

Wayne

Wayne A. Pryor

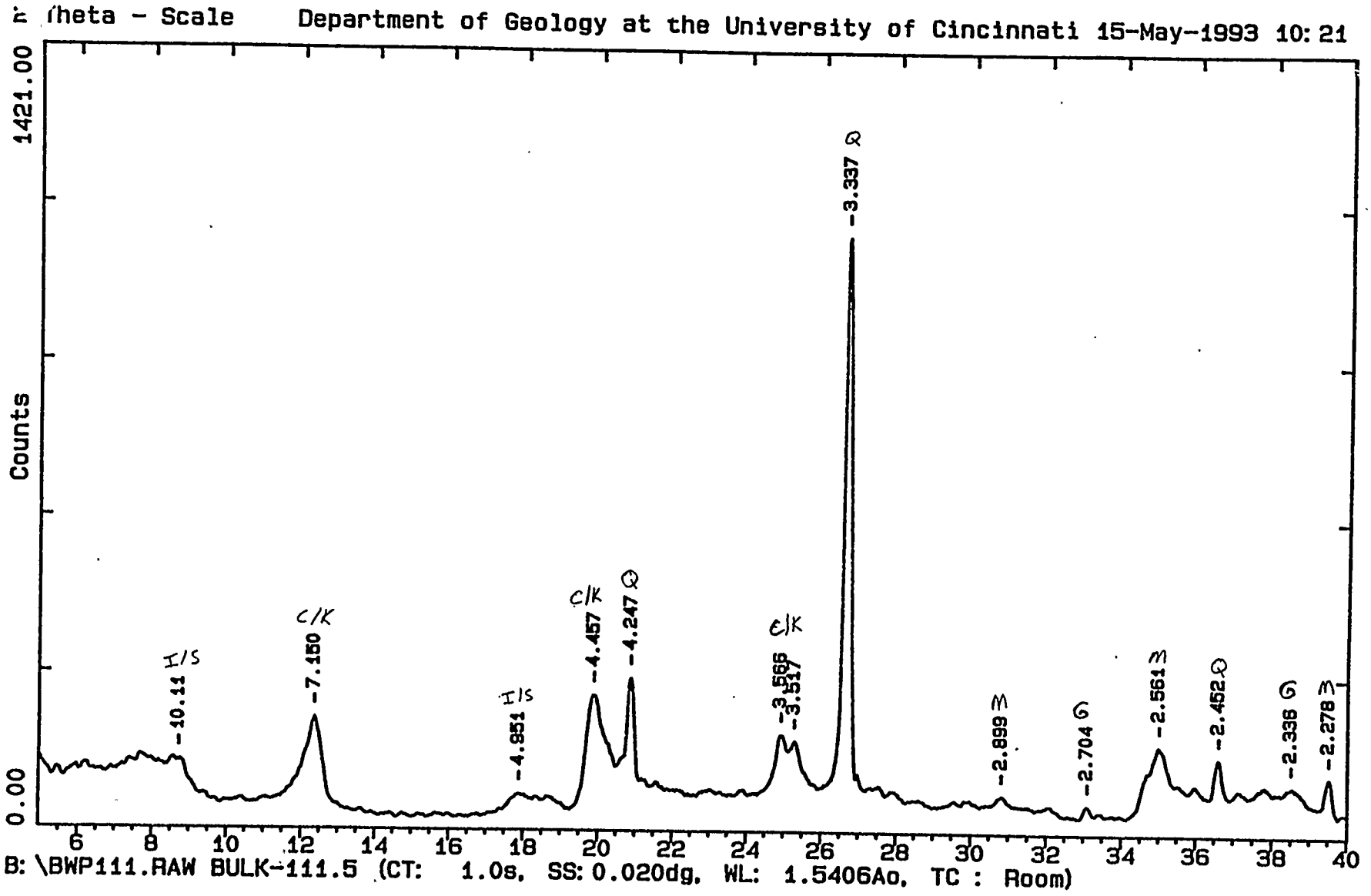

B

I/S = Illite / Smectite

C/K = Chlorite / Kaolinite

Q = Quartz

G = Goethite

M = Mineral

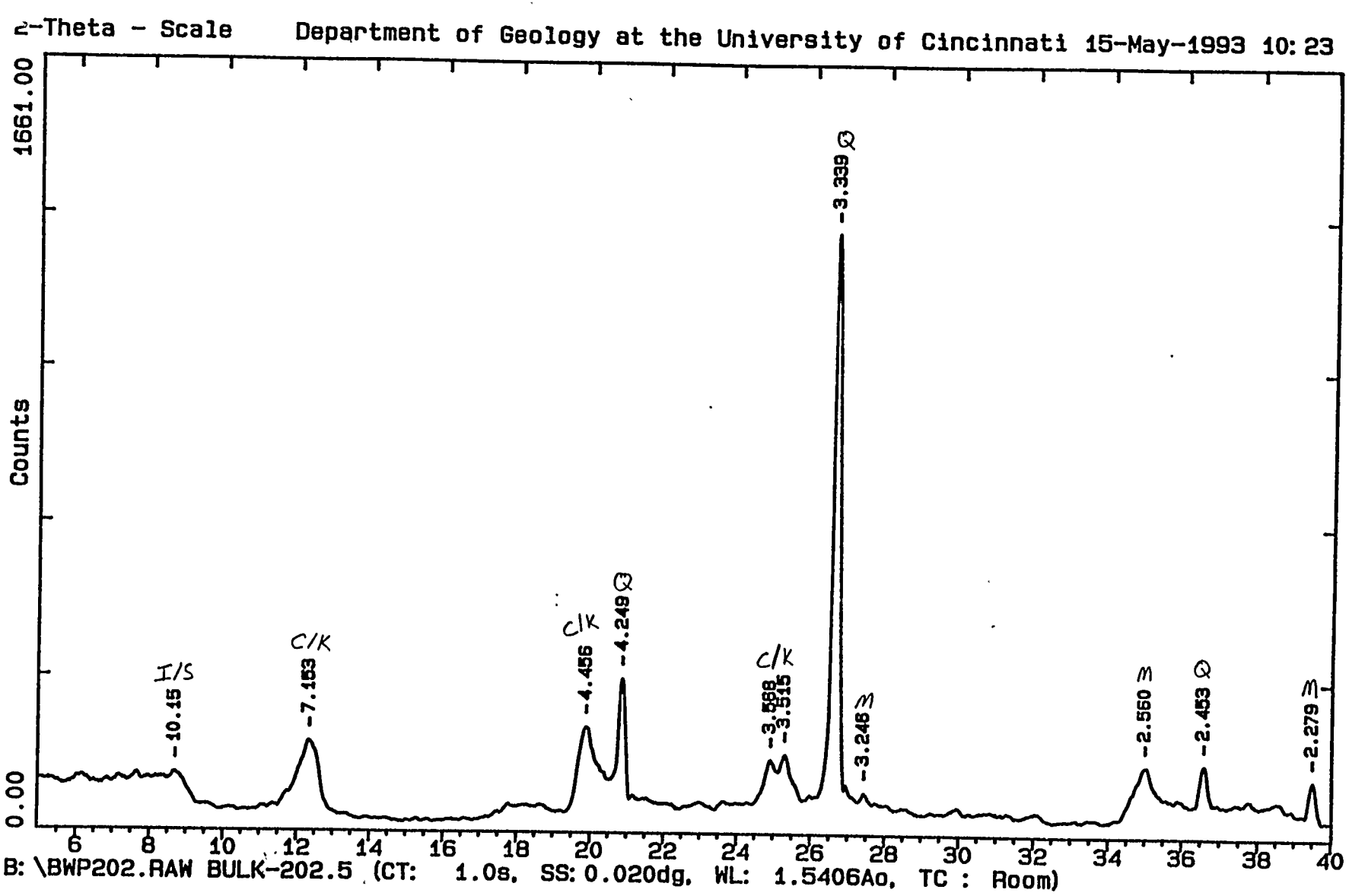
2-Theta - Scale
Department of Geology at the University of Cincinnati 15-May-1993 10:23
1661.00
Counts
0.00
I/S
-10.15
C/K
-7.153
C/K
-4.456
-4.249 Q
C/K
-3.588
-3.515
-3.339 Q
-3.248 M
-2.560 M
-2.453 Q
-2.279 M
6 8 10 12 14 16 18 20 22 24 26 28 30 32 34 36 38 40
B: \BWP202.RAW BULK-202.5 (CT: 1.0s, SS: 0.020dg, WL: 1.5406Ao, TC : Room)

15

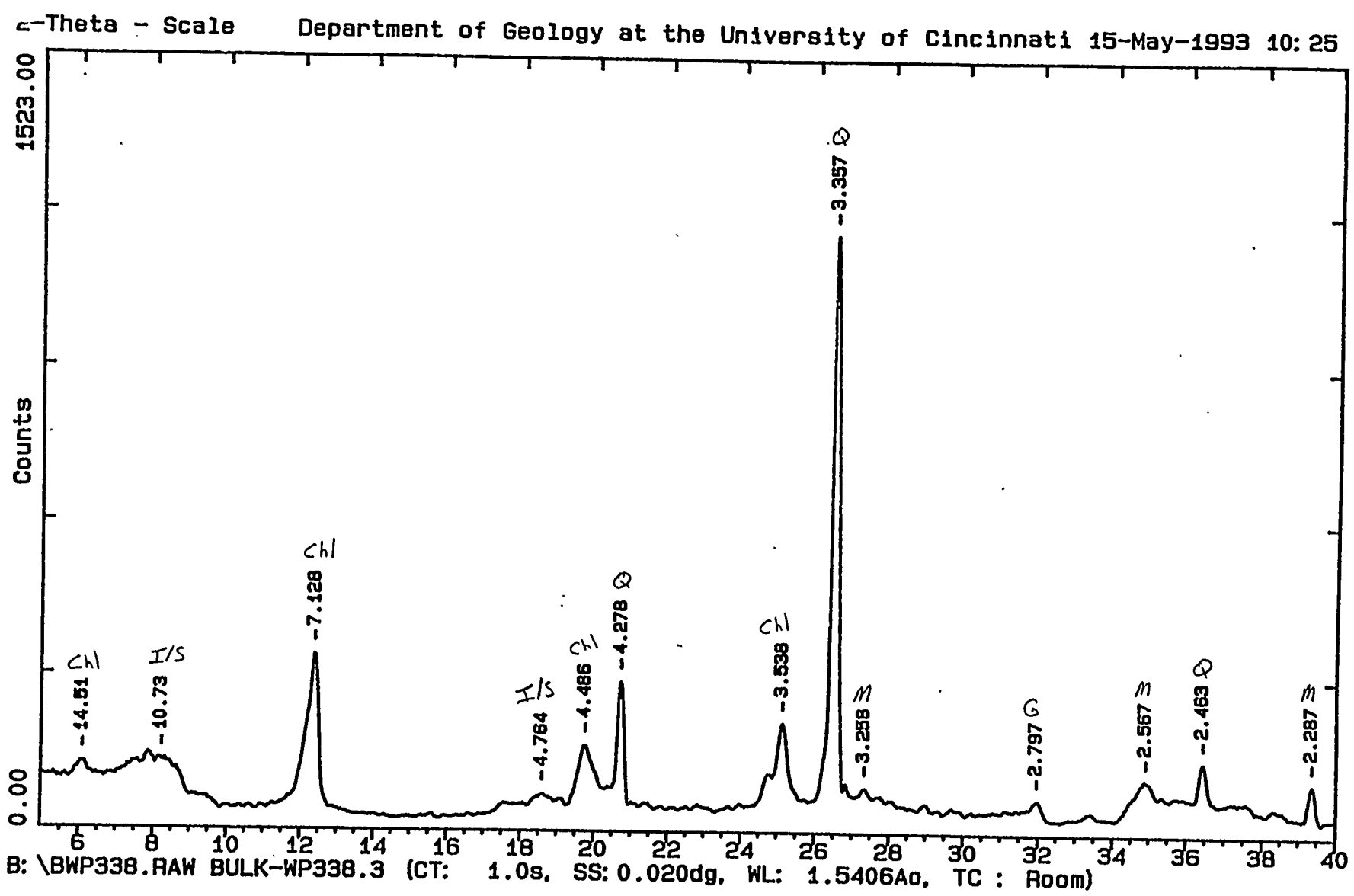

Chl = Chlorite

B

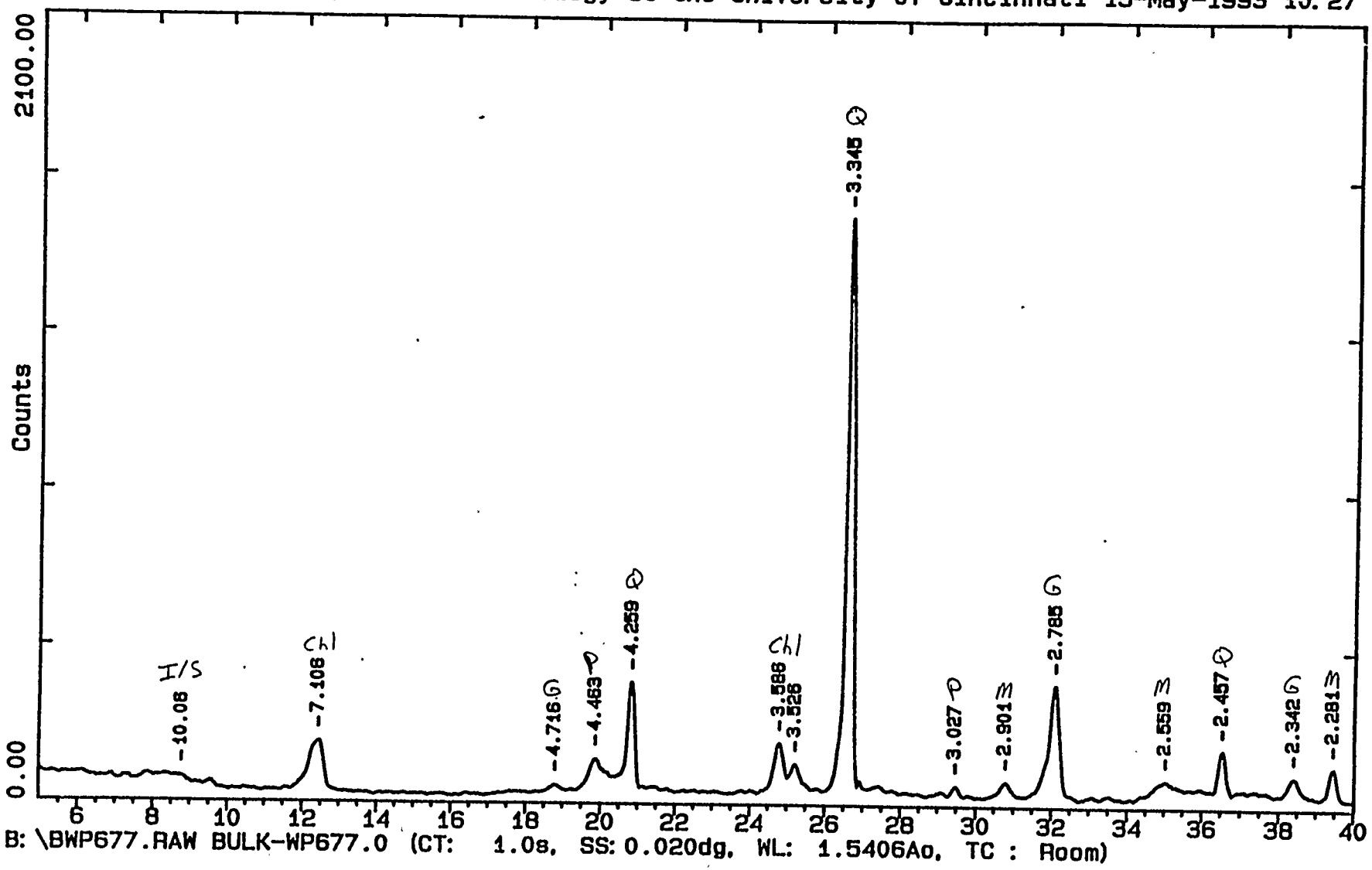

P = Pyrophyllite

R

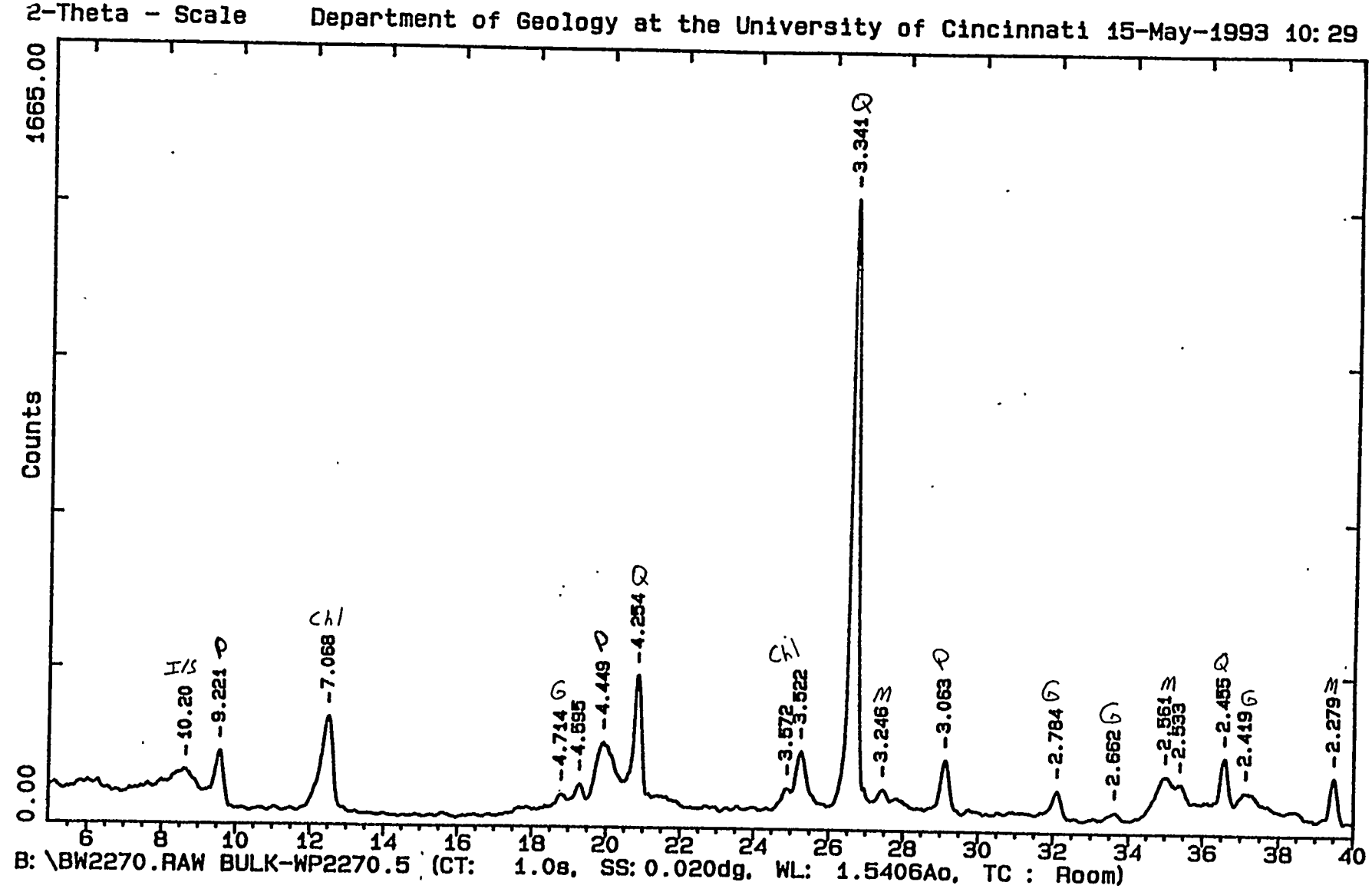
2-Theta - Scale
Department of Geology at the University of Cincinnati 15-May-1993 10:29
1665.00
Counts
0.00
I/S
-10.20
-9.221 P
Chl
-7.068
-4.714 G
-4.595
-4.449 P
-4.254 Q
Chl
-3.572
-3.522
-3.341 Q
-3.246 M
-3.063 P
-2.784 G
-2.662 G
-2.561 M
-2.533
-2.455 Q
-2.419 G
-2.279 M
6 8 10 12 14 16 18 20 22 24 26 28 30 32 34 36 38 40
B: \BW2270.RAW BULK-WP2270.5 (CT: 1.0s, SS: 0.020dg, WL: 1.5406Ao, TC : Room)

B

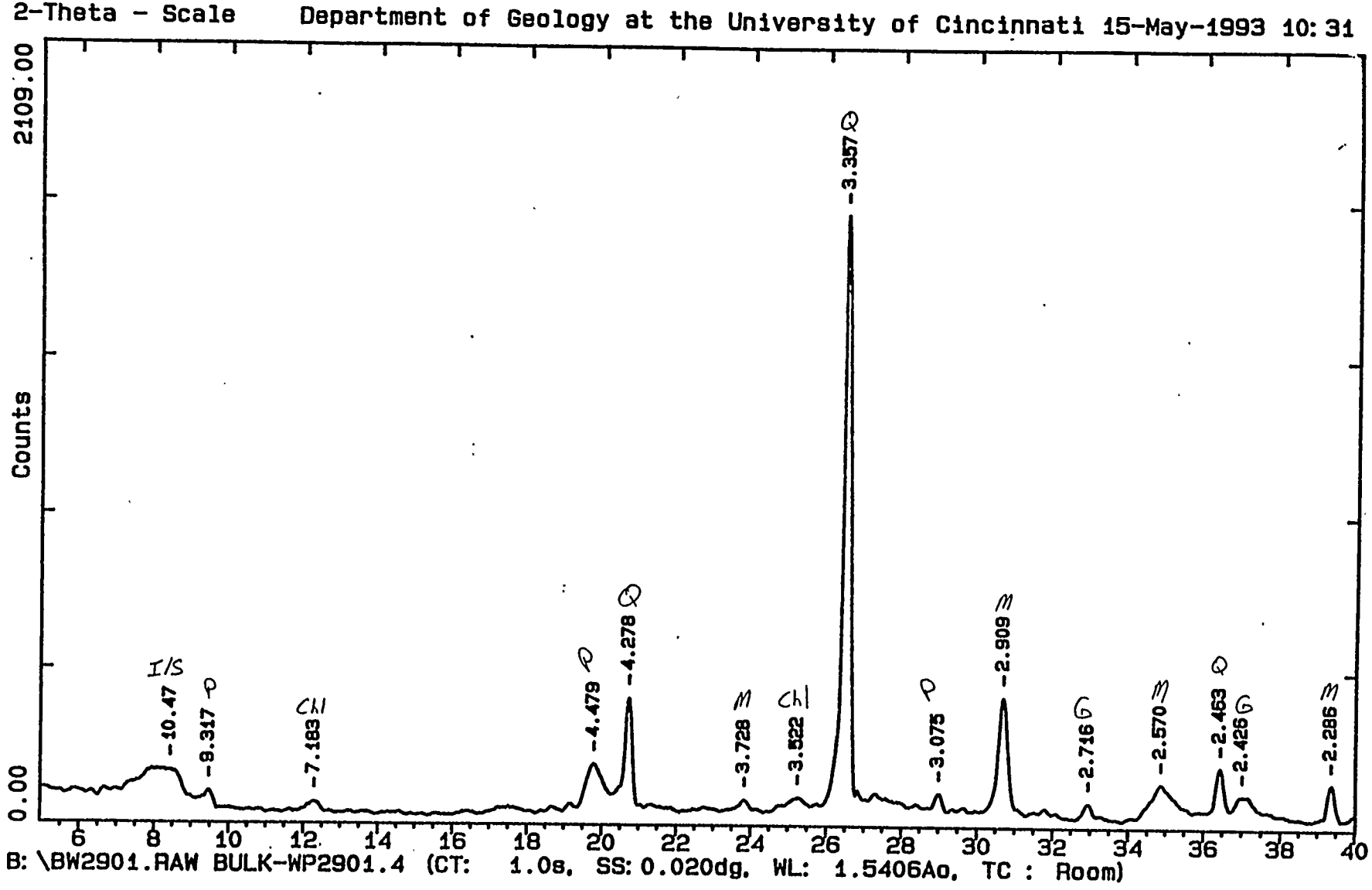
2-Theta - Scale
Department of Geology at the University of Cincinnati 15-May-1993 10:31
2109.00
Counts
0.00
I/S
-10.47
-9.317
Chl
-7.183
-4.479
-4.278
-3.728
Chl
-3.522
-3.357
-3.075
-2.909
-2.716
-2.570
-2.463
-2.426
-2.286
6 8 10 12 14 16 18 20 22 24 26 28 30 32 34 36 38 40
B: \BW2901.RAW BULK-WP2901.4 (CT: 1.0s, SS: 0.020dg, WL: 1.5406Ao, TC : Room)

B

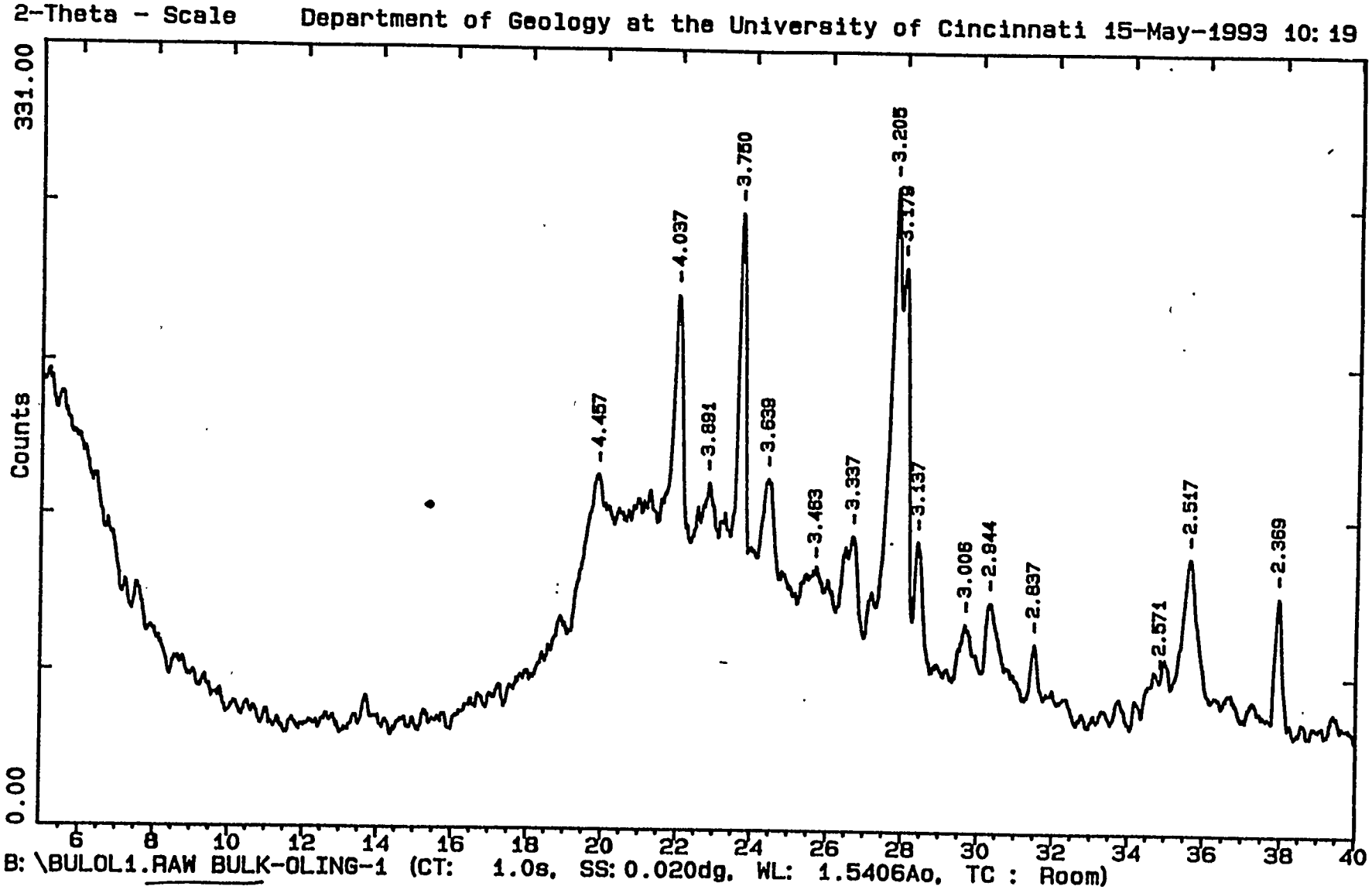
2-Theta - Scale
Department of Geology at the University of Cincinnati 15-May-1993 10:19
331.00
Counts
0.00
-4.457
-4.037
-3.891
-3.750
-3.638
-3.463
-3.337
-3.205
-3.179
-3.137
-3.006
-2.844
-2.837
2.571
-2.517
-2.369
6
8
10
12
14
16
18
20
22
24
26
28
30
32
34
36
38
40
B: \BULOL1.RAW BULK-OLING-1 (CT: 1.0s, SS: 0.020dg, WL: 1.5406Ao, TC : Room)

B

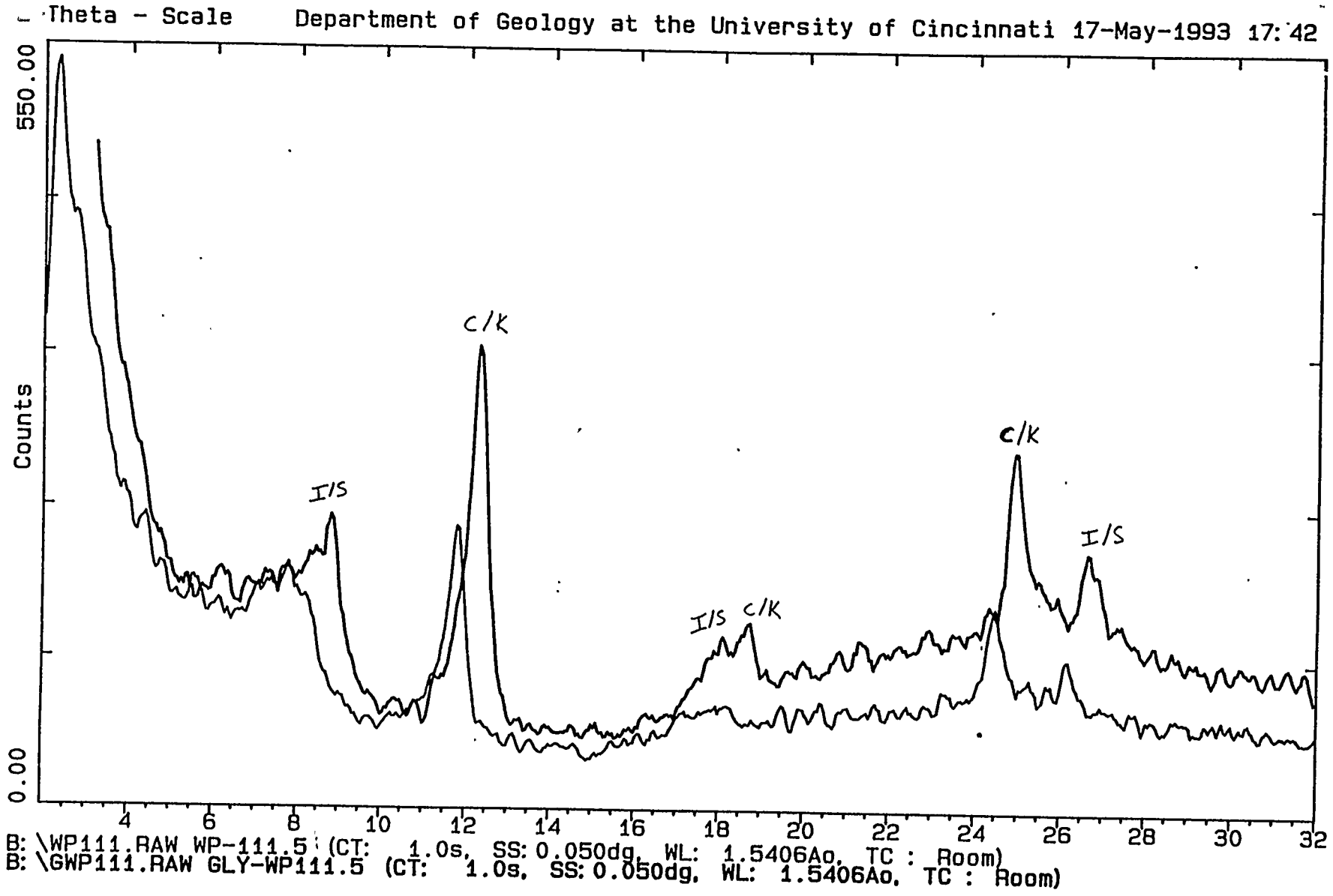

A

Blue line is glycolated.

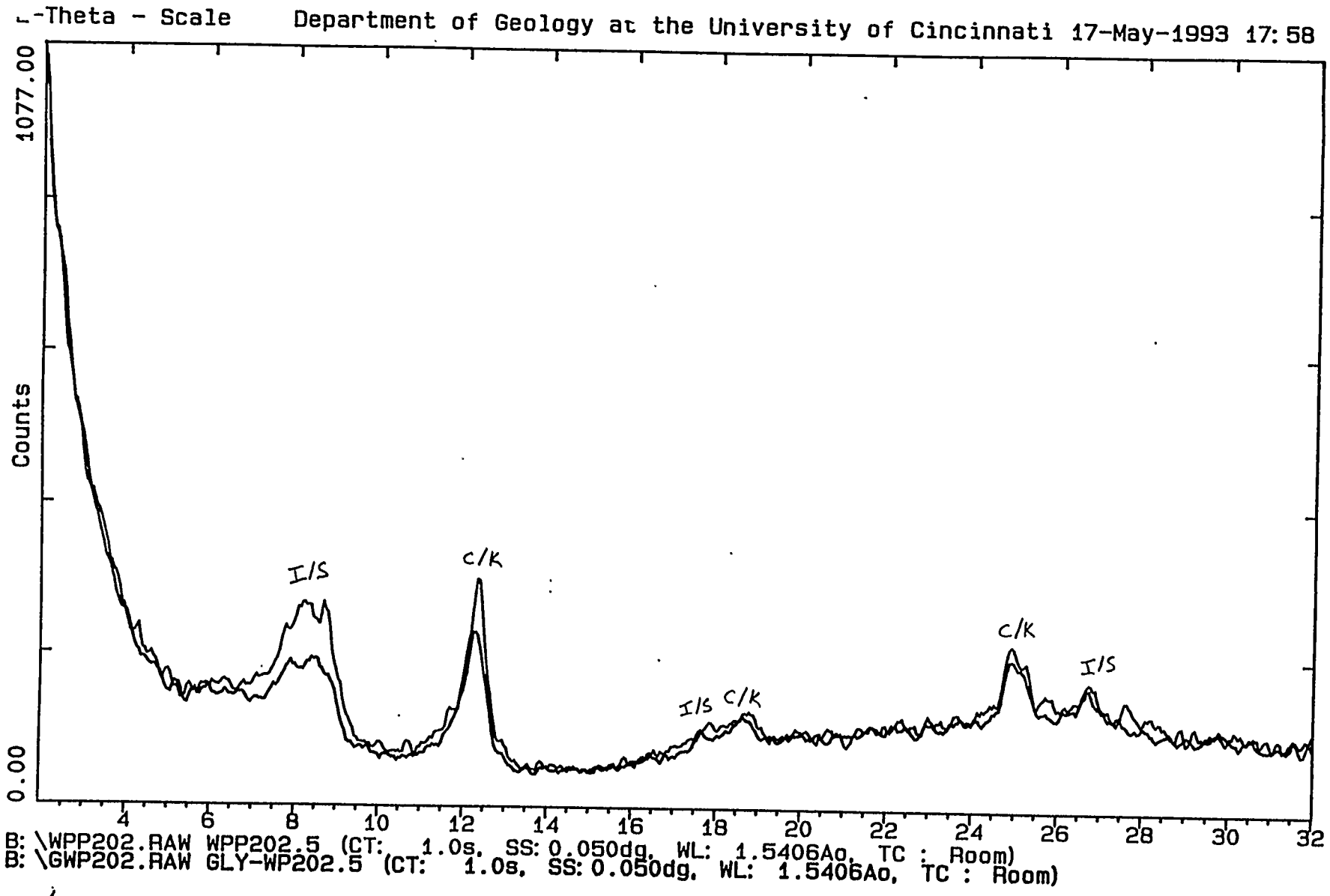
Department of Geology at the University of Cincinnati 17-May-1993 17:58
Theta - Scale
1077.00
Counts
0.00
I/S
C/K
I/S C/K
C/K
I/S
4
6
8
10
12
14
16
18
20
22
24
26
28
30
32
B: \WPP202.RAW WPP202.5 (CT: 1.0s, SS: 0.050dg, WL: 1.5406Ao, TC : Room)
B: \GWP202.RAW GLY-WP202.5 (CT: 1.0s, SS: 0.050dg, WL: 1.5406Ao, TC : Room)

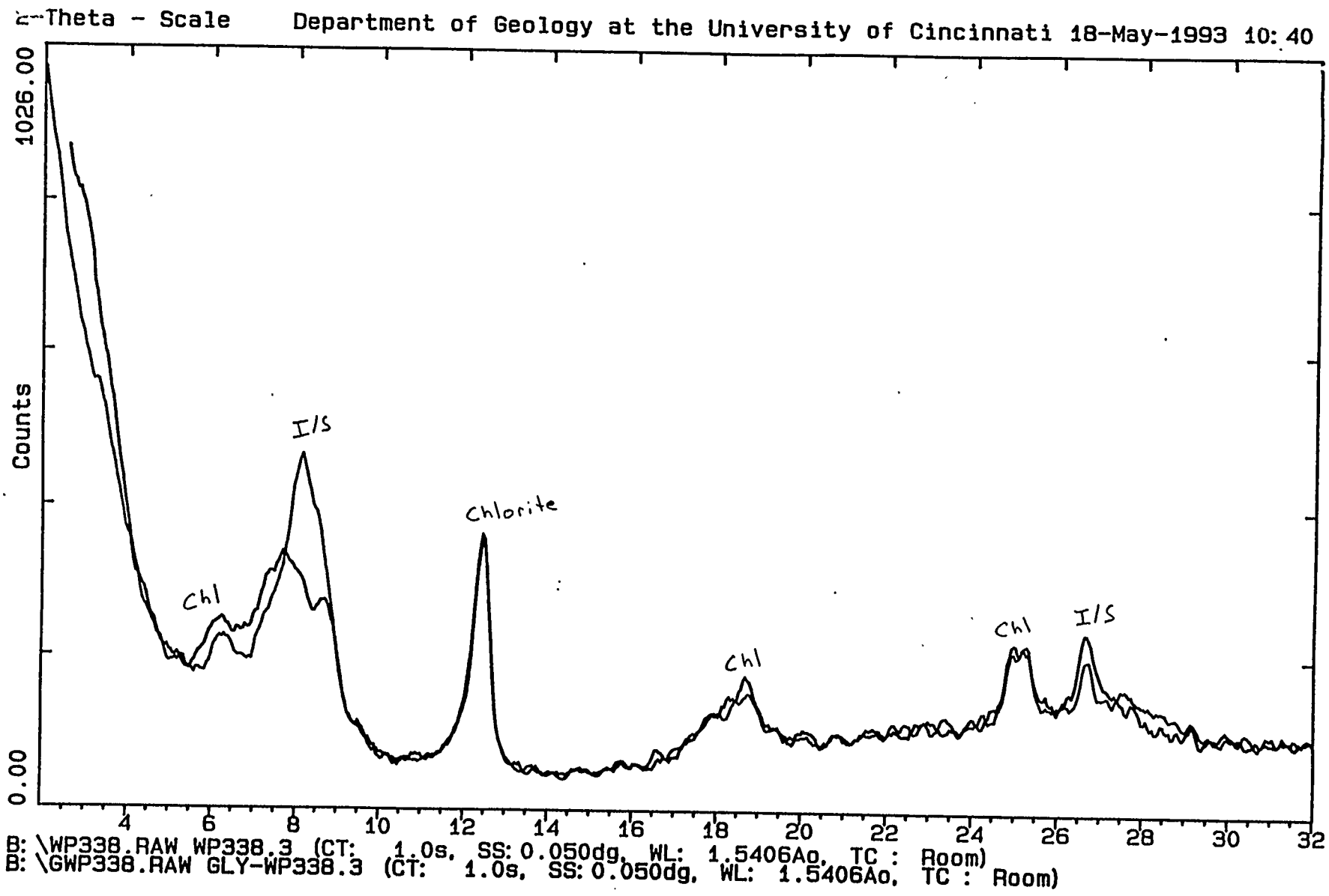
2-Theta - Scale
Department of Geology at the University of Cincinnati 18-May-1993 10:40
1026.00
0.00
Counts
I/S
Chlorite
Chl
Chl
Chl
I/S
4
6
8
10
12
14
16
18
20
22
24
26
28
30
32
B:\WP338.RAW WP338.3 (CT: 1.0s, SS: 0.050dg, WL: 1.5406Ao, TC : Room)
B:\GWP338.RAW GLY-WP338.3 (CT: 1.0s, SS: 0.050dg, WL: 1.5406Ao, TC : Room)

A

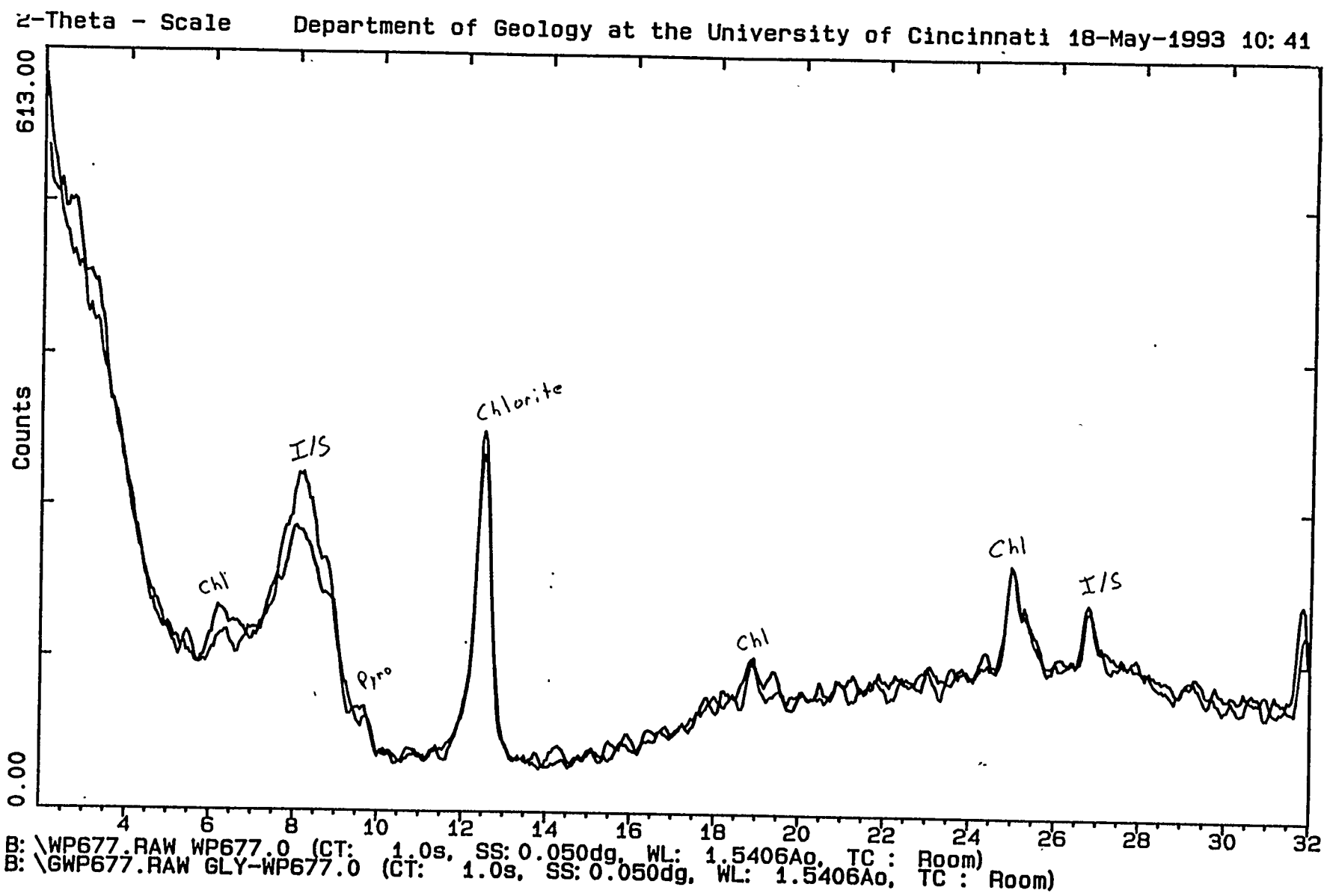
2-Theta - Scale
Department of Geology at the University of Cincinnati 18-May-1993 10:41
613.00
Counts
0.00
Chl
I/S
Pyro
Chlorite
Chl
Chl
I/S
4
6
8
10
12
14
16
18
20
22
24
26
28
30
32
B: \WP677.RAW WP677.0 (CT: 1.0s, SS: 0.050dg, WL: 1.5406Ao, TC : Room)
B: \GWP677.RAW GLY-WP677.0 (CT: 1.0s, SS: 0.050dg, WL: 1.5406Ao, TC : Room)

A

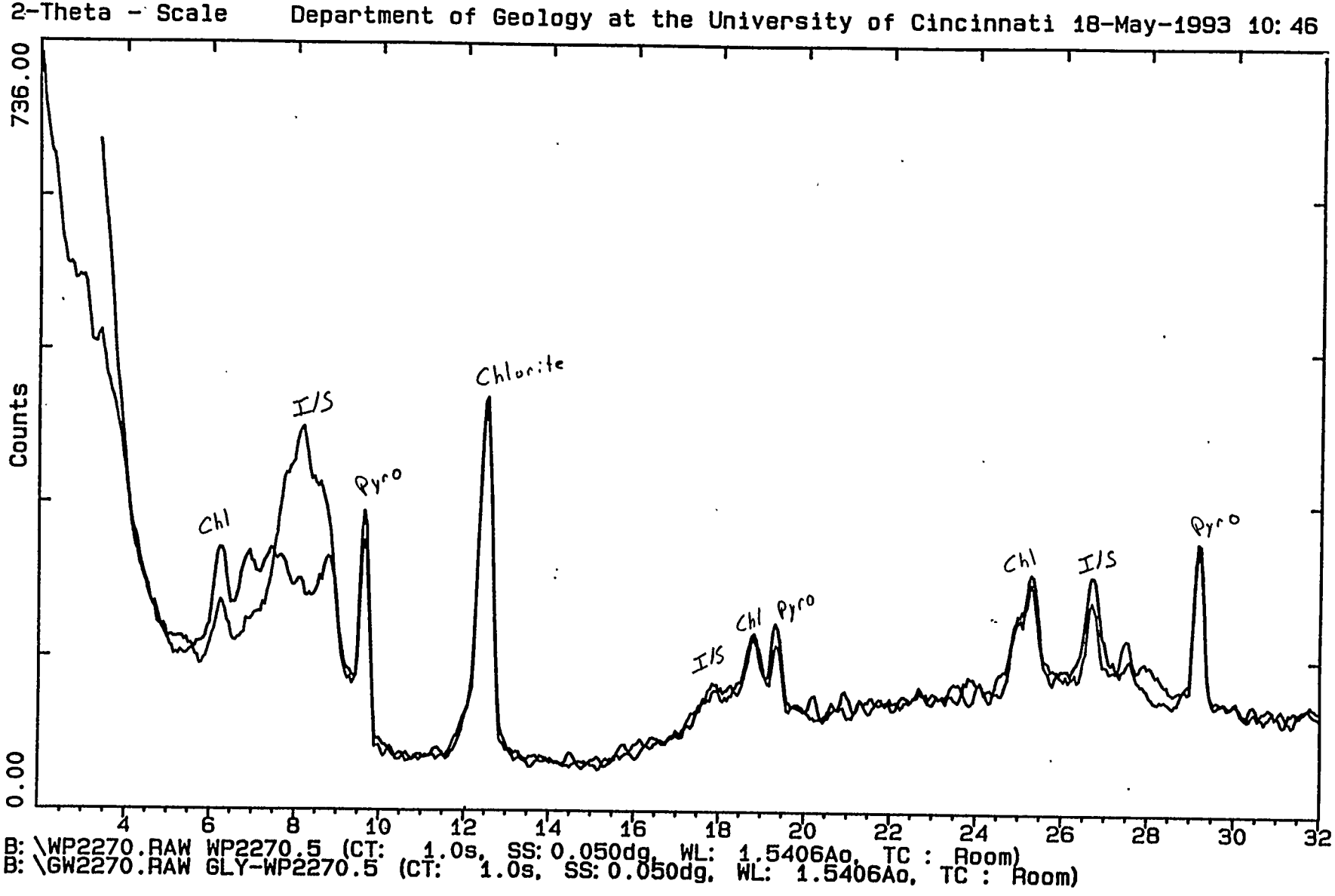
2-Theta - Scale
Department of Geology at the University of Cincinnati 18-May-1993 10:46
736.00
Counts
0.00
Chl
I/S
Pyro
Chlorite
I/S
Chl
Pyro
Chl
I/S
Pyro
4
6
8
10
12
14
16
18
20
22
24
26
28
30
32
B: \WP2270.RAW WP2270.5 (CT: 1.0s, SS: 0.050dg, WL: 1.5406Ao, TC : Room)
B: \GW2270.RAW GLY-WP2270.5 (CT: 1.0s, SS: 0.050dg, WL: 1.5406Ao, TC : Room)

A

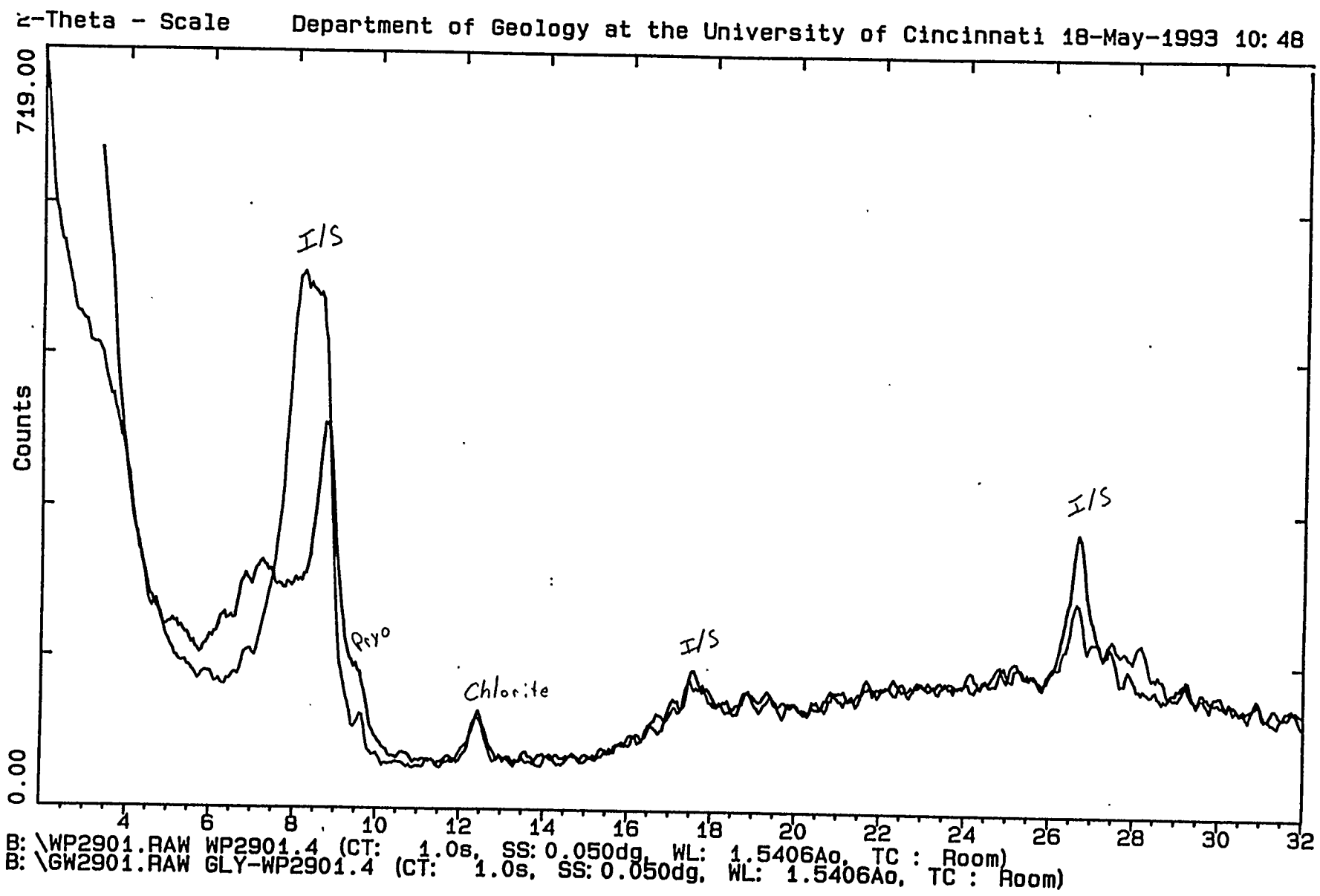
2-Theta - Scale
Department of Geology at the University of Cincinnati 18-May-1993 10:48
719.00
Counts
0.00
I/S
Pyro
Chlorite
I/S
I/S
4
6
8
10
12
14
16
18
20
22
24
26
28
30
32
B:\WP2901.RAW WP2901.4 (CT: 1.0s, SS: 0.050dg, WL: 1.5406Ao, TC : Room)
B:\GW2901.RAW GLY-WP2901.4 (CT: 1.0s, SS: 0.050dg, WL: 1.5406Ao, TC : Room)

A

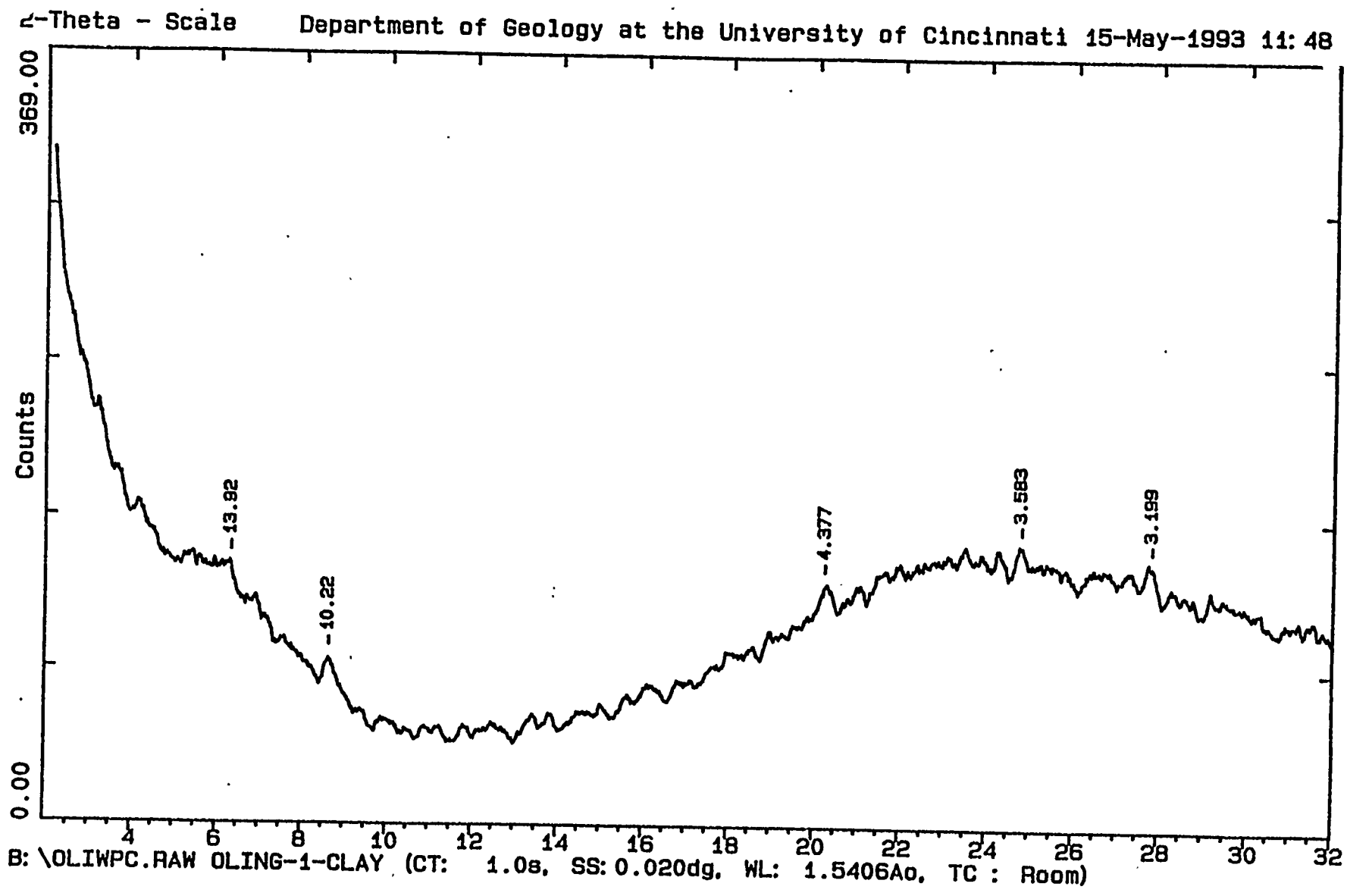
2-Theta - Scale
Department of Geology at the University of Cincinnati 15-May-1993 11:48
369.00
Counts
0.00
13.82
10.22
4.377
3.583
3.199
4
6
8
10
12
14
16
18
20
22
24
26
28
30
32
B:\OLIWPC.RAW OLING-1-CLAY (CT: 1.0s, SS: 0.020dg, WL: 1.5406Ao, TC : Room)

A

PETROLEUM DRILL HOLES IN NEVADA
NEAR THE NEVADA TEST SITE

EXECUTIVE SUMMARY

Twenty-four petroleum tests have been drilled near the Nevada Test Site, thirteen of which had shows of oil and/or gas. Shows occurred in Paleozoic and Tertiary rocks, with lithologies including sedimentary rocks and volcanics. Potential Paleozoic hydrocarbon source rocks penetrated in two boreholes were within the oil window. Potential Tertiary hydrocarbon source rocks were penetrated in two holes. Richness of source rocks and maturity of source rocks, particularly north and east of the NTS, are favorable for the nearby production of liquid hydrocarbons. Volume of source rocks and heterogeneity of source rock maturity are presently unstudied.

INTRODUCTION AND METHODS

The wellfiles of the Nevada Bureau of Mines & Geology were searched for hydrocarbon indicators in boreholes of petroleum and geothermal tests in the Nevada Test Site (NTS) area. The nearest oil field, Grant Canyon Field in Railroad Valley, Nye County, is approximately 84 miles from the NTS. Wells included in the summary are: all those within twenty miles of the NTS; in the absence of a well within the 20-mile limit in a particular direction, those wells nearest the NTS within about 75 miles of the NTS in that direction; where the nearest well(s) in a given direction had incomplete wellfiles, the next nearest

• Donna M. Herring • P.O. Box 13652, Reno NV 89507-3652 • (702) 786-5620 •

well(s) within about 75 miles of the NTS were also summarized. Well logs were not evaluated, and well cuttings were not examined. Known bibliographic references which mentioned these wells were consulted, but an exhaustive search of the literature was not made.

Twenty-four petroleum tests have been drilled within the boundaries noted above. One of these holes has been subsequently re-entered, with no new hole drilled, and one has a pending application for re-entry and deepening. Five geothermal tests are permitted, with no apparent move to drill.

DISCUSSION: HYDROCARBON INDICATORS

Based on existing State wellfiles, hydrocarbon indicators occurring in the boreholes include (see Table 1 and Map 1): A) shows, including two cases of minor undocumented production, of oil or gas in 13 of the 24 holes; and, B) penetrations of hydrocarbon source rocks and/or potential source rocks in five holes, with a possible penetration in a sixth hole. Appendix A includes discussion of individual boreholes.

Oil shows occur in Paleozoic and Tertiary rocks including carbonates, sandstones and volcanics; gas shows occur in Paleozoic and Tertiary rocks including carbonates, shales, sandstones and volcanics. Wells with shows occur to the east, west, south and north of the NTS. Limited oil production was reported from probable Permian rocks (carbonates?) in the Lichtenwalter & Turpin No.1 Turpin (Permit No.51). Gas apparently caused a rig fire, and has apparently been intermittently produced, at the Fish Lake Oil Co. Coaldale Well (Permit No.ES3), though this gas is probably biogenic and not catagenetic.

Organic maturity and/or richness information is available for rocks ranging in age from Cambrian to Tertiary and

penetrated in 8 holes. Available analyses of the Mississippian Chainman (and from a "Mississippian Eleana" penetration which is probably Chainman) indicate the Total Organic Carbon (TOC) ranges from 0.06% to 2.77% (poor to excellent), and maturity values range from early oil window to overmature. Available analyses of Tertiary source rocks in two holes were 0.77-1.3% TOC; maturity data were unavailable from one hole with sampling depth below 7000', and data indicate immaturity at a sample depth of 700' in the second hole.

DISCUSSION: SIGNIFICANCE OF SHOWS AND ANALYSES

Oil and gas shows in boreholes drilled in producing valleys in Nevada are relatively common. A cursory examination of Nevada Bureau of Mines and Geology Bulletin 104, Plate 1, indicates that shows in dry holes in Railroad Valley (the primary producing area in Nevada) probably do not occur at a greater rate than about 50%. As noted above, the show rate is 13 of 24, over 50%, in the area summarized for this report. Statistically-accurate analysis of show rates in producing versus non-producing areas in Nevada has not been done. A qualitative comparison of specific hydrocarbon show character in area boreholes is required to accurately relate NTS area shows to Railroad Valley area shows.

Two holes in the summary area had Paleozoic source rock analyses very favorable for nearby generation of hydrocarbons: American Quasar No.19-1 Adobe Federal (Permit No.270), and Apache No.10-14 Warm Springs Federal (Permit No.310). Chainman and/or Eleana samples were above the 0.5% TOC threshold and within the oil window. No information is available as to volume of source rock penetrated in these holes; examination of drill cuttings would be required to determine source rock thickness.

A third hole, Maxus No.22-1 Hi-Lo (Permit No.612), encountered a significant thickness of apparently organic, black calcareous Chainman. Public information does not indicate particularly rich TOC, however, the sampled interval was not the most promising, and hydrothermal alteration in the Paleozoic section of this hole is pervasive through a 1000' interval. Such an extensive hydrothermal event would probably have matured and expelled the majority of kerogen in the area, leaving the source rock depleted.

The BTA No.1 Stone Cabin may have penetrated Chainman Formation, but no tops were reported and no analyses are available.

Two holes had TOC values above the 0.5% threshold in Tertiary rocks: Nevada Oil & Minerals No.1 V.R.S. (Permit No.146; TOC to 0.77%, 7050-7100') and Felderhoff No.5-1 Felderhoff-Federal (Permit No.605; TOC 1.3% at 700'). No maturity data are available for the Nevada Oil & Minerals hole, and the No.5-1 Felderhoff-Federal sample was immature.

Maturity and richness of Paleozoic source rocks north and east of the NTS, as indicated by the American Quasar, Apache and Maxus holes discussed above, appear favorable for the nearby production of liquid hydrocarbons. Richness of Tertiary source rocks is promising, but additional data on maturity and extent is required. Volume of both Paleozoic and Tertiary source rocks is unknown; study of drill cuttings is required to determine volume.

CONCLUSIONS

Twenty-four tests for petroleum have been drilled near the NTS, over half of which had shows of oil and/or gas. Shows occurred in Paleozoic and Tertiary rocks, with lithologies including carbonates, sandstones, shales and volcanics. Minor

production of oil was reported from Permian rocks (probable carbonates), and minor production of gas was reported from Tertiary rocks (probable sandstones).

Potential Paleozoic hydrocarbon source rocks were within the oil window where penetrated in two boreholes. Potential Tertiary hydrocarbon source rocks were penetrated in two holes. Richness and maturity of Paleozoic source rocks, particularly north and east of the NTS, are favorable for the nearby production of liquid hydrocarbons. Volume of Paleozoic and Tertiary source rocks, and heterogeneity of source rock maturity, are presently unstudied.

Donna M. Herring
Petroleum Geologist
(D.M.H. Flanigan)

• Donna M. Herring • P.O. Box 13652, Reno NV 89507-3652 • (702) 786-5620 •

County	Per	Operator	Well No.	
Clark	344	Jayhawk Exploration	No.1	Federal-Inc
Clark	51	Lichtenwalter, S.J. & Turpin, C.M.	No.1	
Clark	462	Sun Exploration & Production	No.1	Blue Diar
Clark	39	Tri-State Oil Exploration Co.	No.1	Miskell
Esmeralda	ES1	California Excelsior Co.	No.1	M
Esmeralda	ES2	Fish Lake Merger Oil Co.	No.1	
Esmeralda	ES3	Fish Lake Oil Co.		Co
Esmeralda	131	Monte Cristo Oil Co.	No.1	Wi
Esmeralda	146	Nevada Oil & Minerals Inc.	No.1	
Esmeralda	238	Wright Exploration	No.26-1	
Lincoln	270	American Quasar Petroleum	No.19-1	Ac
Lincoln	470	Amoco Production	No.1	Ga
Lincoln	95	Gulf Oil Corp.	No.1	Nevada
Lincoln	612	Maxus Energy Co.	No.22-1	
Lincoln	524	Maxus Energy Co.	No.6-1	Moore McCorr
Nye	302	Apache Corp.	No.24-13	Hot Cr
Nye	310	Apache Corp.	No.10-14	Warm Spr
Nye	456	BTA Oil Producers	No.1	
Nye	457	BTA Oil Producers	No.2	
Nye	606	Felderhoff Production Co.	No.25-1	Felderl
Nye	605	Felderhoff Production Co.	No.5-1	Felderl
Nye	NOS	Lehwald, Charles H.	No.5-1	Smith Federa
Nye	571	Myjo Oil Corp.	No.1	
Nye	115	Pan American Petroleum Corp.	No.1	U.S.A.
Nye	645	Southwest Oil & Gas	No.1	Coffe
Nye	280	Supron Energy Corp.	No.1	Lea

TABLE 1. Nevada Test Site Area Drill Holes

Listed alphabetically by County, Operator, Well Name and Well Number. "Per" is Permit Number; Appendix A presents wells in alpha-numeric order by Permit Number. "GEOCHEMISTRY" in Hydrocarbon Information column means source rock richness and/or maturity data are available in wellfile and discussed in Appendix A.

Well Name	Twp	Rge.	Hydrocarbon Information
lian Springs	17S	57E	GAS show in shale, possible Paleozoic.
Turpin	20S	59E	OIL show/very minor production in Permian.
ıond Federal	21S	59E	GAS & OIL trace, in Bird Spring & Monte Cristo.
-Government	21S	56E	OIL trace in Permian.
lcNett Ranch	1S	36E	None reported.
	1S	36E	None reported, no information.
aldale Well	2N	37E	GAS in Tertiary, probable biogenic.
liam Wright	5N	37E	OIL & GAS shows, Tertiary lakebeds & fractured volcanics.
V.R.S.	1S	36E	GAS & OIL trace, Tertiary shales; GEOCHEMISTRY.
Federal	1N	38E	None reported, no information.
lobe Federal	2N	60E	None reported; 3 DST's; GEOCHEMISTRY.
arden Valley	2N	57E	None.
a-Federal CM	1S	60E	None reported; one DST.
Hi-Lo	7S	58E	None; GEOCHEMISTRY.
nack Federal	7S	58E	OIL & GAS traces, Devonian; GEOCHEMISTRY.
reek Federal	8N	50E	GAS & OIL shows in volcanics; GEOCHEMISTRY.
ings Federal	4N	50E	GAS show in volcanics; GEOCHEMISTRY.
Stone Cabin	5N	48E	GAS trace in Paleozoics; 2 DST's.
Stone Cabin	6N	47E	None reported; one DST.
noff-Federal	15S	49E	Gas trace in Paleozoic; GEOCHEMISTRY.
noff-Federal	16S	50E	GAS trace in Paleozoic; GEOCHEMISTRY.
l (Re-entry)	16S	50E	(not yet re-entered)
Coffer	10S	48E	Possible trace hydrocarbon in volcanics.
Pan American	3N	54E	None reported.
r (Re-entry)	10S	48E	(re-entry unsucessful)
se F-30-4-55	4N	55E	None reported, no information.

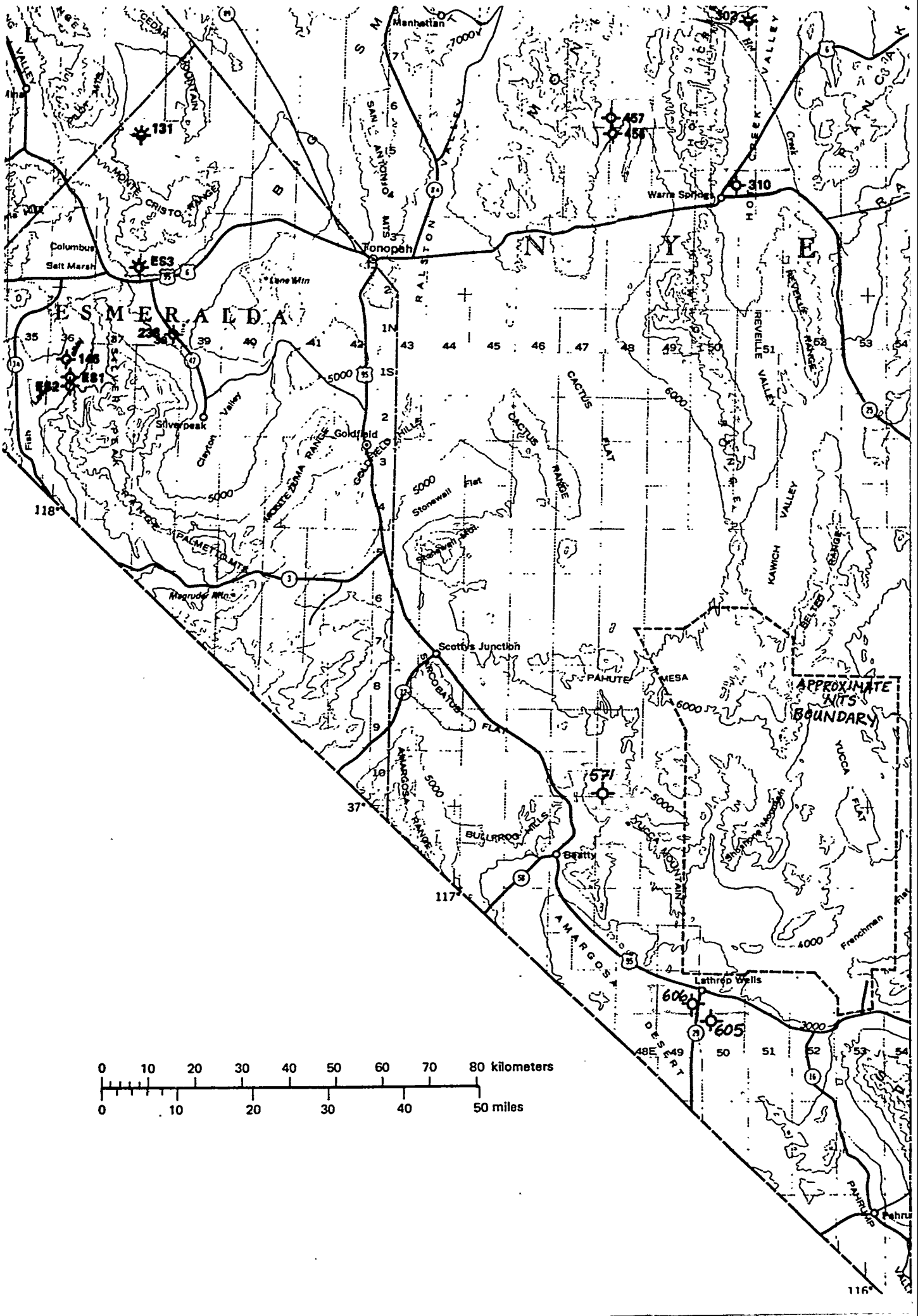
ESMERALDA
NYE
Manhattan
Tonopah
Warm Springs
Columbus
Salt Marsh
Silverpeak
Goldfield
Scotty's Junction
Beatty
Lathrop Wells
Pahrump
APPROXIMATE NTS BOUNDARY
PAHUTE MESA
AMARGOSA DESERT
131
ES3
145
ES1
ES2
457
458
310
302
571
606
605
0 10 20 30 40 50 60 70 80 kilometers
0 10 20 30 40 50 miles

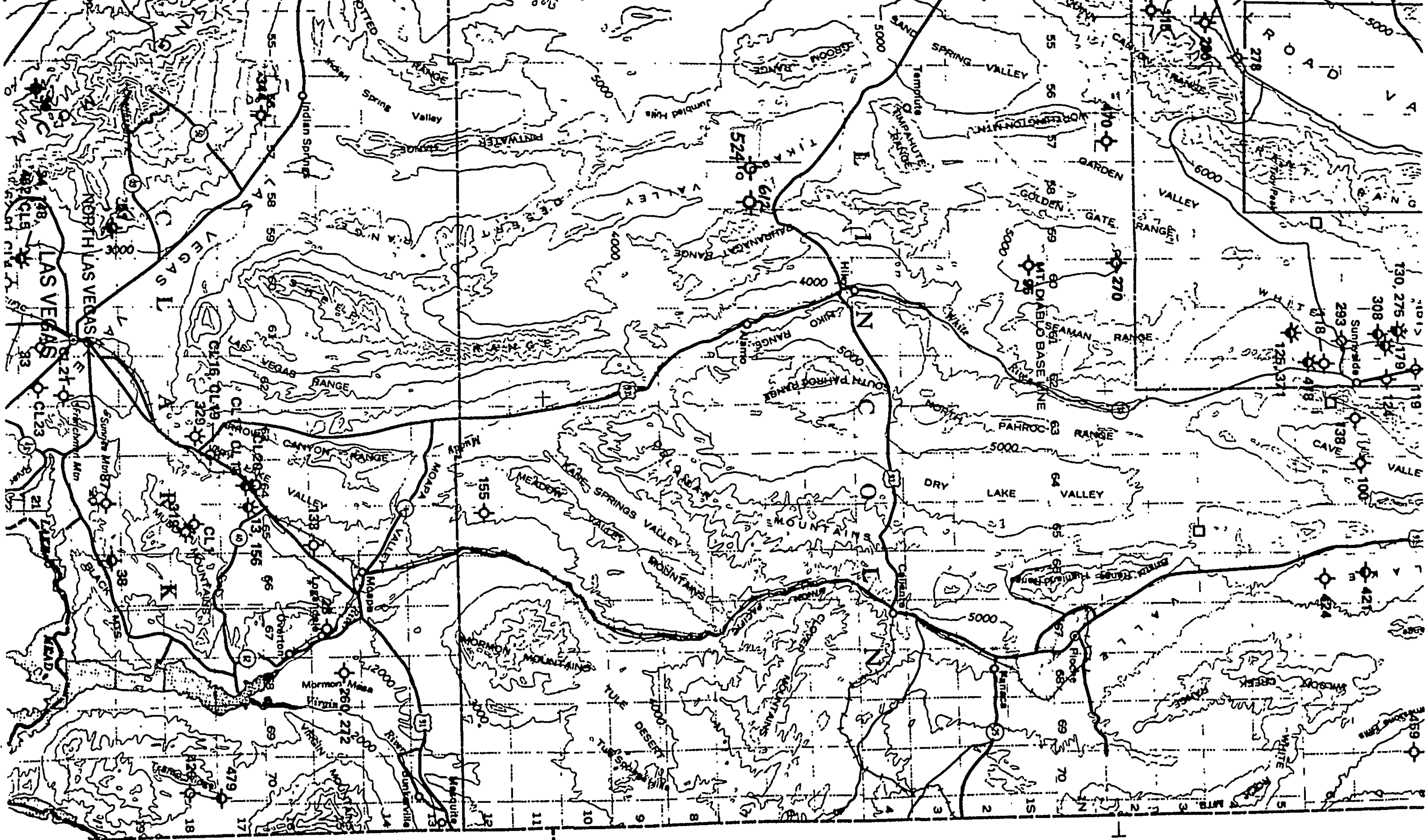

MAP 1. Nevada Test Site Area Drill Holes

Located with dry hole symbols and identified by Permit Number. Base map is Nevada Bureau of Mines and Geology Bulletin 104, Plate 1.

APPENDIX A. Nevada Test Site Area Drill Holes

Listed alpha-numerically by Permit Number.

Twp. = township
Rge. = range
DST = drill stem test
C1 = methane
C2 = ethane
TOC = total organic carbon
CAI = conodont alteration index
TAI = thermal alteration index of kerogen
Ro = vitrinite reflectance
Tmax = pyrolysis maximum yield temperature
Standard abbreviations of lithology and geologic period.

Permit:	ES1
County:	Esmeralda
Type:	P&A
Operator:	California Excelsior Co.
Well No.:	No.1
Well Name:	McNett Ranch
Year:	1920
Footage:	
Location:	unkn
Sec.:	27
Twp.:	1S
Rge.:	36E
Depth:	488'

Shows: None reported.

DSTs: None

Remarks: Completed for water, flowing 500 gpm.

Permit:	ES2
County:	Esmeralda
Type:	P&A
Operator:	Fish Lake Merger Oil Co.
Well No.:	No.1
Well Name:	
Year:	1923
Footage:	
Location:	Center
Sec.:	34
Twp.:	1S
Rge.:	36E
Depth:	1447'

Shows: None reported.

DSTs: None

Remarks: None

Permit:	ES3
County:	Esmeralda
Type:	P&A
Operator:	Fish Lake Oil Co.
Well No.:	
Well Name:	Coaldale Well
Year:	1925
Footage:	
Location:	unkn
Sec.:	12
Twp.:	2N
Rge.:	37E
Depth:	5218'

Shows: "Gas pockets" reported, causing rig fire. Probably biogenic gas; well was spud in Columbia Marsh.

DSTs: None

Remarks: Reported capable of producing "small quantities of gas" in 1957.

Permit:	NOS
County:	Nye
Type:	NYD
Operator:	Lehwald, Charles H.
Well No.:	No.5-1
Well Name:	Smith Federal (Re-entry)
Year:	0
Footage:	1845 FSL, 1980 FEL
Location:	SW/NW
Sec.:	5
Twp.:	16S
Rge.:	50E
Depth:	PTD 5000'

Shows: Not yet re-entered.

DSTs: Not yet re-entered.

Remarks: Re-entry of Felderhoff No.5-1 Felderhoff-Federal; not yet re-entered.

Permit:	39
County:	Clark
Type:	P&A
Operator:	Tri-State Oil Exploration Co.
Well No.:	No.1
Well Name:	Miskell-Government
Year:	1959
Footage:	1800 FNL, 1370 FEL
Location:	NE/SW/NE
Sec.:	22
Twp.:	21S
Rge.:	56E
Depth:	2602'

Shows: Minor oil in Permian carbonates.

DSTs: None.

Remarks: Spud to TD in Permian Bird Spring Group.

Permit:	51
County:	Clark
Type:	P&A
Operator:	Lichtenwalter, S.J. & Turpin, C.M.
Well No.:	No.1
Well Name:	Turpin
Year:	1961
Footage:	
Location:	NW/SE/NE
Sec.:	4
Twp.:	20S
Rge.:	59E
Depth:	1725'

Shows: Oil shows in probable Permian rocks. Reported that after acidizing, well flowed "about 1/3 barrel oil per hour of high gravity oil" from a depth of 810'.

DSTs: None

Remarks: No record of production; application to abandon in October 1965 not accepted by U.S.G.S., no other details available.

Permit:	95
County:	Lincoln
Type:	P&A
Operator:	Gulf Oil Corp.
Well No.:	No.1
Well Name:	Nevada-Federal CM
Year:	1966
Footage:	660 FNL, 660 FWL
Location:	NW/NW
Sec.:	17
Twp.:	1S
Rge.:	60E
Depth:	2434'

Shows: None reported.

DSTs: 2110-2143' DST #1, formation not reported, recovered mud cut fresh water, no shows.

Remarks: None

Permit:	115
County:	Nye
Type:	P&A
Operator:	Pan American Petroleum Corp.
Well No.:	No.1
Well Name:	U.S.A. Pan American
Year:	1968
Footage:	163 FNL, 239 FWL
Location:	NW/NW/NW
Sec.:	36
Twp.:	3N
Rge.:	54E
Depth:	8355'

Shows: None reported.

DSTs: None reported.

Remarks: Reported volcanics from surface to TD.

• Donna M. Herring • P.O. Box 13652, Reno NV 89507-3652 • (702) 786-5620 •

Permit:	131
County:	Esmeralda
Type:	P&A
Operator:	Monte Cristo Oil Co.
Well No.:	No.1
Well Name:	William Wright
Year:	1971
Footage:	
Location:	NE/NW/SE
Sec.:	12
Twp.:	5N
Rge.:	37E
Depth:	4776'

Shows: Oil and gas variously reported: oil & gas in "lakebeds" 3002-3018', and in fractured volcanics 3562-3572'. Oil shows also reported @3640' and @4657'.

DSTs: None

Remarks: Wm. Wright drilled in 1N-38E eight years later, in 1979. BHT 156 degrees F.

Permit:	146
County:	Esmeralda
Type:	P&A
Operator:	Nevada Oil & Minerals Inc.
Well No.:	No.1
Well Name:	V.R.S.
Year:	1970
Footage:	
Location:	NW/NW/NW
Sec.:	16
Twp.:	1S
Rge.:	36E
Depth:	9178'

Shows: Mudlog shows scattered minor traces cut flourescence, with total gas to 10 units, in Tertiary shales.

DSTs: None

Remarks: Source rock geochemistry in file: in 1980, P.C. van de Camp sampled Tertiary shale 7050-7100' (TOC 0.77%), and 7400-7430' (TOC 0.37%).

Permit:	238
County:	Esmeralda
Type:	P&A
Operator:	Wright Exploration
Well No.:	No.26-1
Well Name:	Federal
Year:	1979
Footage:	
Location:	SW/NE
Sec.:	26
Twp.:	1N
Rge.:	38E
Depth:	5666'

Shows: None reported.

DSTs: None.

Remarks: None

• Donna M. Herring • P.O. Box 13652, Reno NV 89507-3652 • (702) 786-5620 •

Permit:	270
County:	Lincoln
Type:	P&A
Operator:	American Quasar Petroleum
Well No.:	No.19-1
Well Name:	Adobe Federal
Year:	1979
Footage:	1980 FSL, 1980 FWL
Location:	NE/SW
Sec.:	19
Twp.:	2N
Rge.:	60E
Depth:	7706'

Shows: None reported.

DSTs: 2661-2716' DST #1, valley fill, recovered mud and fresh water.
4605-4766' DST #2, volcanics, recovered fresh water.
7500-7706' DST #3, Miss. Joana Limestone, recovered mud cut fresh water.

Remarks: Source rock geochemistry in Chainman Shale, data for Marathon Oil by Robertson Research: TOC 1.08% @6825' with Ro 1.29 and TAI 3-; TOC 2.77% @7400' with Ro 1.19 and TAI 3-; further details available in wellfile.
Geochemical data by Ehni Enterprises/DGSI in Chainman: TOC 0.71-1.20% @6780-7170' with Tmax 432-448C; TOC 1.61-4.49% @7200-7460' with Tmax 445-441C; Ro 1.18 @6910-6920', Ro 1.35(?) @7250-7260', Ro 1.27 @7450-7460'. TAI 3- by T. Hutter for Ehni/DGSI samples #97 and #108, no depth given.

Permit:	280
County:	Nye
Type:	P&A
Operator:	Supron Energy Corp.
Well No.:	No.1
Well Name:	Lease F-30-4-55
Year:	1980
Footage:	1980 FEL, 660 FNL
Location:	NW/NE
Sec.:	30
Twp.:	4N
Rge.:	55E
Depth:	8347'

Shows: None reported.

DSTs: None reported.

Remarks: No completion report filed.

Permit:	302
County:	Nye
Type:	P&A
Operator:	Apache Corp.
Well No.:	No.24-13
Well Name:	Hot Creek Federal
Year:	1981
Footage:	500 FSL, 650 FWL
Location:	SW/SW
Sec.:	24
Twp.:	8N
Rge.:	50E
Depth:	11,028'

Shows: Gas minor while drilling in volcanics, scattered @8890-9148'.
Dead oil in flow test samples (see DST section).

DSTs: Seven failed DST's, one valid test on DST #5.
7400-8600' DST #5, recovered 1443 ft mud in pipe, 2400cc mud in sample chamber with Rm 1.0 @60F and Cl 9000ppm.
Four flow tests, with dead oil and gas in tests #3 & #4.
7001-9563' FT#3, volcanics, included kick to 8 units C1, dead oil in sample fluid.
7001-9563' FT#4, volcanics, gas maximum 31 total units, 28

Remarks: BHT 375F @8842.53 from flow test.
Source rock geochemistry by Ehni/DGSI: "Ls/dol/mbl" @9750-10360' had TOC 0.03-0.12%, probable Devonian; "Ls/dol/mbl" @10440-11060' had TOC 0.06-0.17%, probable Joana.

Permit:	310
County:	Nye
Type:	P&A
Operator:	Apache Corp.
Well No.:	No.10-14
Well Name:	Warm Springs Federal
Year:	1981
Footage:	660FSL, 1980 FWL
Location:	SE/SW
Sec.:	10
Twp.:	4N
Rge.:	50E
Depth:	9180'

Shows: Total gas increased from less than one unit to average 10 units, all C1, in volcanics 4560-5260'.

DSTs: None

Remarks: Reported tops: valley fill at surface, Miss Eleana Formation @8770'.

Source rock geochemistry by Ehni Enterprises/DGSI: siltstone, conglomerate, limestone and shale @8780-9170 had TOC ranging from 0.06 to 0.66%. Sample 9000-9010' had 0.66% TOC, Tmax 450C, Ro 1.56; sample 9120-9130' had TOC 0.54%, invalid Tmax, Ro 1.53.

Permit:	344
County:	Clark
Type:	P&A
Operator:	Jayhawk Exploration
Well No.:	No.1
Well Name:	Federal-Indian Springs
Year:	1982
Footage:	673 FNL, 660 FEL
Location:	NE/NE
Sec.:	6
Twp.:	17S
Rge.:	57E
Depth:	5583'

Shows: Gas show 3590-3600' total 25 units C1, in slow-drilling shale.

DSTs: None reported.

Remarks: Drilled overbalanced. NBMG has drill cuttings 67-5520', missing bottom 63'. No formation tops reported. Gas show in thin red-brown micaceous shale interbed in grey and green siltstone unit.

Permit:	456
County:	Nye
Type:	P&A
Operator:	BTA Oil Producers
Well No.:	No.1
Well Name:	Stone Cabin
Year:	1986
Footage:	1850 FNL, 1530 FWL
Location:	NW/SE/NW
Sec.:	6
Twp.:	5N
Rge.:	48E
Depth:	9815'

Shows: Total gas 2 units, trace C2, at top Paleozoics.

DSTs: 5255-5300' DST #1, volcanics, failed.
5244-5300' DST #2, volcanics, recovered 180 ft mud.

Remarks: Possible penetration of Chainman below volcanics and carbonates.

• Donna M. Herring • P.O. Box 13652, Reno NV 89507-3652 • (702) 786-5620 •

Permit:	457
County:	Nye
Type:	P&A
Operator:	BTA Oil Producers
Well No.:	No.2
Well Name:	Stone Cabin
Year:	1986
Footage:	1910 FNL, 330 FEL
Location:	NE/SE/NE
Sec.:	25
Twp.:	6N
Rge.:	47E
Depth:	1184'

Shows: None reported.

DSTs: 1157-1184' DST #1, volcanics, recovered 833 ft mud, mud cut water and fresh water.

Remarks: None

• Donna M. Herring • P.O. Box 13652, Reno NV 89507-3652 • (702) 786-5620 •

Permit:	462
County:	Clark
Type:	P&A
Operator:	Sun Exploration & Production
Well No.:	No.1
Well Name:	Blue Diamond Federal
Year:	1986
Footage:	279 FSL, 128 FEL
Location:	SE/SE
Sec.:	25
Twp.:	21S
Rge.:	59E
Depth:	6220'

Shows: Mudlogger's report includes only trace total gas, no oil. Two DST's were run apparently to test porosity in the Miss-Penn. Bird Spring Fm. and Miss. Monte Cristo Fm.; DST #1 in Bird Spring had trace gas, DST #2 in Monte Cristo may have had trace oil (see details below).

DSTs: 3577-3611' DST#1, recovered 1100 ft fresh water cut mud, sample chamber had trace gas and 2000cc water.
4966-5044' DST#2, recovered filtrate and mud cut water; a geochemical analysis of recovered fluids indicates traces of oil not noted in the field report.

Remarks: Lost circulation @5912', and drilled blind losing 4446 barrels of mud to 6220' (TD). Other lost circulation zones, all in Monte Cristo, @4859' (75'), 5452' (30 bbl), 5494' (75 bbl), 5731' (350 bbl), and 5876' (280 bbl).

Tops reported:

Triassic Moenkopi	Surface
Permian Kaibab	790'
Permian Toroweap	1070'
Permian Supai	1350'
Miss-Penn Bird Spg	2694'
Miss Monte Cristo	4000'
(TD Monte Cristo @6220')	

Slight deviation in the hole essentially from spud, averaging 2 degrees, maximum 4 degrees. Mud weight 8.9 to 9.2.

Permit:	470
County:	Lincoln
Type:	P&A
Operator:	Amoco Production
Well No.:	No.1
Well Name:	Garden Valley
Year:	1986
Footage:	1947 FSL, 2310 FWL
Location:	NE/SW
Sec.:	27
Twp.:	2N
Rge.:	57E
Depth:	6401'

Shows: None.

DSTs: None

Remarks: Tops from mudlog: volcanics 3140', Miss. Joana 5925, jasperoid 6035', Dev. dolomite (?) 6200.

Permit:	524
County:	Lincoln
Type:	P&A
Operator:	Maxus Energy Co.
Well No.:	No.6-1
Well Name:	Moore McCormack Federal
Year:	1987
Footage:	1790 FSL, 40 FEL
Location:	NE/NE
Sec.:	6
Twp.:	7S
Rge.:	58E
Depth:	7798'

Shows: Gas to 8 units total, including C2, in Devonian carbonate immediately under volcanics. Gas rose to 10 units average, all C1, 7300-7798'(TD). Devonian also included trace to rare pinpoint dead oil stain and carbonaceous material scattered throughout.

DSTs: None

Remarks: Reported tops: valley fill at surface, volcanics 2734', Paleozoic 4828', Simonson ?, Sevy 7647'. Published tops estimated from graphic: Dev Guilmette 4828', Dev Simonson 5500', Dev Sevy 7300' or 7480', fault cut with top Ord Eureka 7646'.

Maturity data by Maxus published: intra-volcanic sediment TAI 3- near 4700'; Guilmette TAI 3 near 4900'; Guilmette TAI 3+, Tmax 412-307C, Ro 1.6, near 5400'; Simonson Tmax 270C near 5600'; Simonson Tmax 438C near 7300'; Eureka TAI 3+, Tmax 347-301C, Ro 2.31, near 7700'.

Richness and maturity data from USGS OFR93-186: TOC 0.2%, Tmax 340C, in Devonian dolomite @5490-5520', where mudlog reports no shows; TOC 0.27%, Tmax 335C in Devonian dolomite 7500-7530' where mudlog reports dolomite "arg/carb i.p.".

Permit:	571
County:	Nye
Type:	P&A
Operator:	Myjo Oil Corp.
Well No.:	No.1
Well Name:	Coffer
Year:	1991
Footage:	2061 FSL, 741 FEL
Location:	NE/SE
Sec.:	31
Twp.:	10S
Rge.:	48E
Depth:	3877'

Shows: Reported possible hydrocarbon, with third-party analysis "negative"; no other details. Drilled without hotwire or chromatograph.

DSTs: None.

Remarks: Drilled without geolograph. Reported tops: alluvium at surface, various volcanics beginning at 830'.

Permit:	605
County:	Nye
Type:	P&A
Operator:	Felderhoff Production Co.
Well No.:	No.5-1
Well Name:	Felderhoff-Federal
Year:	1991
Footage:	1980 FNL, 660 FWL
Location:	SW/NW
Sec.:	5
Twp.:	16S
Rge.:	50E
Depth:	1468'

Shows: Trace gas in dolomite @1260-1330', including trace C2.

DSTs: None.

Remarks: Reported tops: volcanics @347', Tertiary gravel @505', Cambrian dolomite @1300'.

Harris et al, 1992, reported "dense carbonates"; "thermally unaltered icthyoliths" recovered with pyritized freshwater ostracodes @850-940', 1060-1100' and 1200-1300'. Nonmarine palynomorphs @1110-1190'. Cuttings TOC 1.3% and immature @700'; other cuttings TOC <0.4.

Permit:	606
County:	Nye
Type:	P&A
Operator:	Felderhoff Production Co.
Well No.:	No.25-1
Well Name:	Felderhoff-Federal
Year:	1991
Footage:	1845 FSL, 1980 FEL
Location:	NW/SE
Sec.:	25
Twp.:	15S
Rge.:	49E
Depth:	5000'

Shows: Trace gas scattered 2210-2830', all C1.

DSTs: None

Remarks: Reported tops: basalt 343', Tertiary gravel 518', Cambrian dolomite 2000'. Alternative reported top Paleozoic 2192'.
Harris et al, 1992, reported overturned Cambrian and Ordovician, with Ord conodonts 3460-5000', CAI 5; cuttings 3000-4300' TOC <0.12%.

Permit:	612
County:	Lincoln
Type:	P&A
Operator:	Maxus Energy Co.
Well No.:	No.22-1
Well Name:	Hi-Lo
Year:	1991
Footage:	1664 FNL, 1785 FWL
Location:	NW/SE/NW
Sec.:	1
Twp.:	7S
Rge.:	58E
Depth:	5215'

Shows: None

DSTs: None

Remarks: Rotary sidewall core @4953. Tops: Ord Ely Springs Dol 1898', major fault 3320', Penn Ely Ls 3340', Miss Chainman Sh 3398', Paleozoic metasediments 4332', Camb Prospect Mtn Qtzt 4907.

Maturity data by Maxus and Nevada Bureau of Mines and Geology published, with Ordovician to Silurian CAI 4.0 @2210-2250', Chainman TOC 0.06% and Tmax 360C @3410-3710, Chainman palynology TAI 4 @3420-4370', Chainman Tmax 430C @3430-3440', Chainman Tmax 333C @3670-3680', Joana to Chainman conodonts CAI 2.0 @4150-4200'.

Permit:	645
County:	Nye
Type:	Drlg
Operator:	Southwest Oil & Gas
Well No.:	No.1
Well Name:	Coffer (Re-entry)
Year:	1993
Footage:	2061 FSL, 741 FEL
Location:	NE/SE
Sec.:	31
Twp.:	10S
Rge.:	48E
Depth:	PTD 6000'

Shows: Re-entered, but suspended operations before drilling out last plug; no new hole.

DSTs: None.

Remarks: Re-entered but suspended before drilling any new hole. Operator probably in bankruptcy.

• Donna M. Herring • P.O. Box 13652, Reno NV 89507-3652 • (702) 786-5620 •